EXPERIMENTAL EVALUATION OF OZONE FORMING POTENTIALS OF MOTOR VEHICLE EMISSIONS

Final Report to

California Air Resources Board
Contract No. 95-903

South Coast Air Quality Management District
Contract No 95073/Project 4, Phase 2

by
W. P. L. Carter, M. Smith, D. Luo,
I. L. Malkina, T. J. Truex, and J. M. Norbeck

May 14, 1999

College of Engineering,
Center for Environmental Research and Technology
University of California, Riverside, CA 92521

ABSTRACT

Quantitative evaluations of air quality impacts from vehicle emissions are based on the assumptions that all the important reactive species in the exhaust have been identified and quantified, and that the air quality models accurately represent how their atmospheric reactions affect ozone production. To provide data to test this, environmental chamber experiments were carried out with exhaust from ten different fuel-vehicle combinations. These include exhausts from vehicles fueled by LPG, M100, M85, CNG, and diesel, and from five vehicles employing Phase 2 reformulated gasoline (RFG), representing a range of mileages, types, and pollution levels. Baseline FTP tests and speciation analyses were carried out for all vehicles studied but diesel, and the conditions of the environmental chamber experiments were characterized so their data could be used for model evaluation. The chamber experiments consisted of irradiations of the exhausts themselves, "incremental reactivity" experiments with the exhaust added to two different surrogate VOC - NO_x mixtures simulating conditions of photochemical smog, and irradiations of synthetic exhaust mixtures designed to simulate the experiments with the actual exhausts. Two different methods were used to transfer the diluted exhausts from the vehicle to the chamber, one using a mini-diluter system with a long sample line, and the other using a Teflon transfer bag. The transfer bag was used for most of this project because of evidence for formaldehyde loss when the long sample lines were employed.

Although some characterization problems and model discrepancies were observed, the results of most of the experiments with LPG, M100, M85, CNG and RFG exhausts were consistent with results of experiments using synthetic exhausts derived to represent them, and were generally consistent with model predictions. The major exception to this was the one experiment with diesel exhaust, where a complete analysis was not conducted and where it was clear that the major reactive species have not been identified. The results with the other exhausts indicate that the major constituents contributing to their ozone impacts have probably been identified, and that current chemical mechanisms are reasonably successful in predicting these impacts. There was no evidence for a contribution of nitrites or other contaminates or artifacts to the reactivities of any of these exhausts. There was some evidence, albeit inconclusive, that the model may be underpredicting the ozone impacts of some of the constituents of exhausts from the two highest mileage RFG-fueled vehicles in some experiments. This would require further studies with other vehicles before any conclusions can be made. However, the model gave reasonably good simulations of effects of adding these to realistic ambient VOC - NO_x mixtures, as was the case for all the other exhausts for which complete analyses were conducted.

ACKNOWLEDGMENTS AND DISCLAIMER

TABLE OF CONTENTS

LIST OF TABLES

LIST OF FIGURES

LIST OF ACRONYMS

Acronym	Meaning
AL	CE-CERT's Analytical Laboratory (where the detailed speciated exhaust analyses are carried out.)
APL	CE-CERT's Atmospheric Processes Laboratory (where the environmental chamber experiments are carried out)
CARB	California Air Resources Board
CE-CERT	College of Engineering-Center for Environmental Research and Technology
CFR	Code of Federal Regulations
CO	carbon monoxide
CO_2	carbon dioxide
CVD	constant volume diluter
CVS	constant volume sampler
DNPH	2,4-dinitrophenylhydrazine
DTC	dividable Teflon environmental chamber
FFV	flexible fuel vehicle
FID	flame ionization detector
FTP	Federal Test Procedure
GC	gas chromatography
HPLC	high performance liquid chromatography
LC	liquid chromatography
LPG	liquefied petroleum gas
M85	15% gasoline and 85% methanol
M100	100% methanol fuel
MIR	maximum incremental reactivity
mph	miles per hour
NMHC	non-methane hydrocarbon
NMOG	non-methane organic carbon gas
NO_x	oxides of nitrogen
OMHCE	organic material hydrocarbon equivalent
PAN	peroxyacetyl nitrate
RAF	reactivity adjustment factors
RFG	Reformulated Gasoline
ROG	reactive organic gases
SAPRC	Statewide Air Pollution Research Center
SCAQMD	South Coast Air Quality Management District
SCFH	standard cubic feet per hour
TAC	Toxic air contaminant
THC	total hydrocarbons
TLEV	transitional low-emissions vehicle
VERL	CE-CERT's Vehicle Emissions Research Laboratory
VOC	volatile organic carbon gases

EXECUTIVE SUMMARY

Background and Objectives

To account for the lower reactivity of alternative fuel exhaust, the California Air Resources Board (CARB) has established emission standards that use "reactivity adjustment factors" (RAFs) to adjust the non-methane organic gases (NMOG) mass emission rate for the different ozone formation potentials of the chemical species in the exhaust. Reactivity factors have been developed over the years on the basis of chemical mechanisms for volatile organic compounds (VOC) and nitrogen oxides (NO_x). These mechanisms are used in airshed models and are the primary means for assessing the effects of alternative fuels on air quality. The validity of such evaluations rest on the assumptions that all the important reactive species in the exhaust have been identified and quantified, and that the chemical mechanisms used in the model accurately represent how their atmospheric reactions affect ozone production.

The objective of this program is to provide data to test whether all of the important reactive species in vehicle exhausts using selected fuels have been identified, and whether current chemical models can predict the amount of ozone and other oxidants formed when the exhaust is irradiated. The approach involved conducting environmental chamber experiments using diluted exhaust from conventional and alternative fueled vehicles, and also with known mixtures designed to represent the compounds identified in these exhaust samples. The vehicle emissions were characterized using FTP tests with speciated analyses, and with complete speciated analyses of the exhausts injected into the chamber. The chamber experiments were conducted under sufficiently well characterized conditions so that the results can be simulated with models to determine whether they are consistent with the predictions of chemical mechanisms used to predict ozone impacts in the atmosphere. The exhaust and synthetic exhaust experiments were carried out in conjunction with an array of control and characterization experiments to characterize the chamber and light source effects as needed for model evaluation. The results of the experiments were compared with the predictions of an updated version of the chemical mechanism used predict the RAFs incorporated in the CARB vehicle emissions regulations.

A comparison of the results of synthetic and "actual" exhaust experiments was used to evaluate whether the important reactive species in the exhaust have been identified. Comparison of the NO oxidized, ozone formed and radical levels in the chamber experiments with those predicted by the model was

performed to evaluate our level of understanding of which exhaust components are contributing to the reactivity, and the reliability of model predictions of reactivity in the atmosphere.

LPG Exhaust Evaluation

The vehicle emissions testing and exhaust sampling was carried out in the College of Engineering Center for Environmental Research and Technology (CE-CERT)'s Vehicle Emissions Research Laboratory (VERL). The VERL utilizes a Burke E. Porter 48-inch single-roll, electric chassis dynamometer coupled with a Pierburg CVS and analytical system. Speciated analyses of the hydrocarbons and oxygenates in the exhausts were carried out according to the Auto/Oil Phase II protocol using GC/FID and HPLC analysis. The Federal Test Procedure (FTP) tests were carried out using the protocol in the Code of Federal Regulations (CFR).

The tests used to produce and collect the exhausts for the chamber experiments were carried out separately from the FTP tests. To obtain a useful measure of the effects of the VOCs present in the exhaust mixtures on ozone formation and other measures of air pollution, it is necessary to introduce a sufficient amount of exhaust VOCs in the chamber to yield a measurable effect. Therefore, most chamber experiments utilized cold-start exhausts to provide the largest amount of exhaust VOC for chamber testing. The typical procedure was to gradually accelerate the vehicle to 40 mph from a cold start condition, followed immediately by sampling for ~30 seconds once steady state operation was achieved.

Two different procedures were used to transfer the exhaust from the vehicle to the chamber during the course of this program. During the first phase, a mini-diluter system was used to dilute the exhaust and transfer it to the chamber laboratory, with the dilution being such that the humidity was no more than 50% RH at ambient temperature. Tests with a M100 vehicle indicated that there may be loss of formaldehyde on the sample line during this procedure, so this was not used for the second phase. During the second phase the exhaust was injected into a Teflon transfer bag (again diluted so the humidity was less than 50% at ambient temperature), which was then moved to the chamber laboratory for injection into the chamber. In both cases, analyses were made both of the raw exhaust, and of the diluted exhaust in the transfer line or the transfer bag prior to injecting the exhaust into the chamber.

The chamber experiments were carried out using CE-CERT's dual-mode Dividable Teflon Chamber (DTC). This consists of two ~5000-liter FEP Teflon reaction bags surrounded by blacklights. Two types of experiments were carried out using exhausts or synthetic exhaust mixtures: one where the exhaust (or the

mixture of VOCs and NO_x designed to simulate the exhaust) was irradiated by itself, and the other where the exhausts or synthetic exahusts were evaluated in "incremental reactivity" experiments. In those experiments, the exhaust was added to a "surrogate" reactive organic gas (ROG) - NO_x mixture, to measure the incremental effect of the exhaust (or synthetic exhaust) addition. Two types of ROG surrogates were used to simulate the effects of ambient VOCs in the incremental reactivity experiments. A simple 3-component "mini-surrogate" was employed because it was found to be highly sensitive to the effects of added VOCs, and in particular their effects on the overall radical levels (an important factor affecting a compounds Maximum Incremental Reactivity [MIR]). In addition, a more complex 8-component "full surrogate" designed to represent more closely the VOCs present in polluted urban atmospheres, was also employed. Experiments with mechanism evaluation and VOC reactivity assessment indicate that experiments with these two surrogates provide good tests of different aspects of a VOC's mechanism which affect ozone formation. The incremental reactivity experiments were carried out with the NO_x levels the same in both the both the "base case" and the added exhaust reaction mixtures, to assess the effects of the exhaust VOCs only.

The results of the experiments were compared with the predictions of model calculations using an updated version of the Statewide Air Pollution Research Center (SAPRC) chemical mechanism that was recently developed for the CARB. An earlier version of this mechanism was utilized to calculate the MIR scale that was used to derive the RAFs in the CARB vehicle regulations. The updates incorporate improvements to mechanisms for aromatics, alkenes, and other VOCs resulting from more recent laboratory and environmental chamber studies, which will be utilized for developing updated versions of the MIR scale (and RAFs) which are under development.

Vehicles Studied

The ten fuel-vehicle combinations studied in this program are summarized in Table EX-1. The results of the FTP tests are also summarized for those vehicles that were tested. The table shows that vehicle test matrix employed in this study includes a diverse cross section of late model and intermediate age alternative fuel and conventional fuel vehicles. These vehicles are all equipped with closed loop feedback and catalytic converters and show a range of restorative and preventative maintenance. The mass emission rates are similarly diverse with transitional low-emissions vehicle (TLEV) certified vehicles tested with older malfunctioning super emitters. Therefore, they provide a varied set of exhaust types for reactivity evaluation in the environmental chamber experiments.

Table EX-1.   Summary of fuel-vehicle combinations studied and FTP results.

Vehicle Description	Fuel	Odometer at start	FTP Emissions (mg/mile)				
			NMHC	MeOH	HCHO	CO	NOx
Retrofitted 1989 Plymouth Reliant. 2.2-liter, 4-cylinder engine.	LPG	29,600	1,080	-	-	18,170	163
1993 Ford Taurus Flexible Fuel Vehicle. 3.0-liter, 6-cylinder engine.	M100	38,100	181	335	21	1,793	206
1997 Ford Taurus OEM Flexible Fuel Vehicle. 3.0-liter, 6-cylinder engine.	M85	6,890	71	247	17	1,149	103
1991 Ford Ranger PU. Dedicated retrofit CNG.	CNG	17,800	42	0	5	3,591	498
1997 Ford Taurus OEM Flexible Fuel Vehicle. 3.0-liter, 6-cylinder engine.	RFG	13,600	(Not tested. Lowest VOC, NOx and CO in chamber experiments than all the other vehicles tested.)				
1991 Dodge Sprit. OEM Flexible Fuel Vehicle. 2.5-liter 4 cylinder engine	RFG	14,300	107	11	3	2,373	184
1994 Chevrolet Suburban C1500 2 wheel drive. 5.7-liter V8 engine	RFG	58,000	350	0	3	7,930	540
1984 Toyota PU. 2.4-liter engine.	RFG	227,000	2,080	-	-	6,220	1,670
1988 Accord 2.0-liter 4 cylinder engine	RFG	150,000	190	-	-	5,900	740
1984 Mercedes Benz 300D. 3.0-liter, 5 cylinder turbocharged diesel	RFD	170,000	(Not tested)				

Results and Conclusions

LPG Reactivity

The species accounting for the reactivity of cold-start exhaust from the LPG vehicle were found to be CO, propane, isobutane, n-butane, ethylene, and propene. There are apparently no undetected compounds significantly affecting the reactivity of the cold-start LPG exhaust, because experiments with synthetic exhausts made up with these compounds in the appropriate proportions with NO_x gave essentially the same results. The model performed reasonably well in simulating the results of the LPG experiments. This is expected, because the main contributors to LPG reactivity are simple compounds whose mechanisms are believed to be reasonably well understood, and which have been individually evaluated previously using chamber data.

Based on these results, we can conclude that we understand the compounds and mechanisms accounting for the ozone impacts of the cold-start exhaust from this type of LPG-fueled vehicle. Although the mass emission rates of the LPG vehicle tested were higher than the appropriate emission standard would indicate, the hydrocarbon profiles found in this study are consistent with previous work and indicate the results should be representative of LPG vehicles in general.

M100 and M85 Reactivity

The species accounting for the reactivity of the cold-start M100 emissions were, as expected, methanol and formaldehyde. Methanol and formaldehyde were also found to be the only species measured in high enough levels to contribute significantly to the reactivity of the cold-start M85 exhausts as well. No significant differences were observed in incremental reactivity experiments between actual cold-start M100 and M85 exhaust and the methanol/formaldehyde/NO_x mixtures designed to simulate them. This indicates that there are probably no significant contributors to M100 and M85's reactivity which are not being detected, and that the hydrocarbons from at least the M85 vehicle used in this study do not contribute measurable to the cold-start exhaust reactivity. In no case was there any evidence for any contribution of methyl nitrite to M100's reactivity, which, if it were significant, would be apparent in the initial NO oxidation rate.

The results of the model simulations of the M100 reactivity experiments gave similar results with the synthetic M100 and M85 exhausts as the actual exhausts, providing further support to our conclusion that the observed methanol and formaldehyde are the main contributors to M100's reactivity, and that undetected compounds do not play a significant role. The simulations also did not indicate large significant

biases in the model, though some inconsistencies were observed. These inconsistencies appeared to be due to problems with the models ability to simulate any experiments with formaldehyde or methanol, regardless of whether they are in synthetic mixtures or in actual exhausts. In particular, the model had a slight but consistent biases towards underprediction of reactivity of formaldehyde in this chamber, and overprediction of reactivity of methanol or methanol with formaldehyde when irradiated in the absence of other VOCs. (Note that this overprediction in the simulations of the methanol-containing systems cannot be attributed to formation of methyl nitrite, since the presence of methyl nitrite in the model simulation would make the overprediction even worse.) These biases were essentially the same when simulating actual M100 or M85 exhausts as when simulating synthetic methanol with formaldehyde - NO_x mixtures. On the other hand, the model simulated the incremental effects of adding the exhausts or methanol with formaldehyde mixtures to photochemical smog surrogate mixtures without any apparent consistent biases. The reasons for these biases in the simulations of experiments with methanol and/or formaldehyde in the absence of other pollutants is and may be due to problems with chamber characterization, since the atmospheric reactions of these compounds are believed to be reasonably well established. If this is the case, the experiments with the more realistic mixtures appear to be less sensitive to this characterization problem. In any case, the results of the reactivity experiments suggest that the model will probably perform reasonably well in simulating the reactivities of methanol exhausts in the atmosphere.

CNG Reactivity

The only species detected in the cold-start CNG exhausts studied in this program at levels sufficient to affect ozone formation were NO_x, CO, and formaldehyde. The levels of methane and other hydrocarbons detected in these exhausts were insufficient to significantly affect predicted reactivity. Although essentially no O_3 formation occurs when the exhaust is irradiated by itself, the CO and formaldehyde levels in the cold start CNG exhausts were sufficient to have a measurable (and positive) effect on NO oxidation and O_3 formation when added to smog surrogate VOC - NO_x mixtures. Essentially the same results were obtained in experiments using CO and formaldehyde mixtures at the same levels as measured in the CNG exhaust experiments, and the results were consistent with model predictions. This indicates that CO and formaldehyde are indeed the major species accounting for CNG reactivity. Significantly less reactivity was observed when formaldehyde was omitted from the synthetic CNG mixtures, indicating that the formaldehyde in CNG exhaust makes a non-negligible contribution to its reactivity, at least in the chamber experiments.

RFG Reactivity

The five RFG-fueled vehicles used in this program represented a variety of vehicle types, mileages, and NO_x and VOC pollutant levels, and thus provided a good survey of cold-start exhausts from gasoline-fueled vehicles. The VOC levels in the cold-start exhaust of the cleanest of the vehicles studied, a low-mileage 1997 Ford Taurus, were too low for the chamber experiments to provide a very precise measurement of the VOC reactivity, but the chamber data were useful in confirming that the overall reactivity was indeed as low as indicated by the exhaust analysis and the model predictions. In particular, the experiments with the 1997 Ford Taurus indicated there were no unmeasured species in the cold-start exhaust contributing significantly to its reactivity. The other four vehicles studied had sufficiently high VOC levels to permit quantitative reactivity measurements to be obtained from the environmental chamber data.

The cold-start exhausts from these other four vehicles were found to significantly enhance rates of NO oxidation and O_3 formation when added to ambient surrogate - NO_x mixtures, and to measurably increase integrated OH radical levels. Experiments using synthetic RFG exhaust mixtures, derived by lumping VOCs of similar types and reactivities together and using a single compound to represent each VOC type, gave very similar results as the experiments with the actual exhausts. This indicates that representing the complex exhaust mixtures by simpler synthetic mixtures, with reactivity weighting based on relative MIR values to account for differences among individual VOCs of the various types, gives reasonably good approximations of the overall effects of the exhausts on NO oxidation, ozone formation, and overall radical levels in the environmental chamber experiments. More significantly, this also indicates that, as with the LPG, methanol-containing and CNG exhausts discussed above, there is no significant contribution to reactivity caused by undetected compounds in the exhaust, and that the exhaust analyses methods currently employed for RFG exhausts are accounting for the major components causing their reactivities.

The model performed reasonably well in simulating most of the actual and synthetic RFG exhaust experiments. The results of all the synthetic exhaust experiments were simulated without significant consistent bias, as were the results of the experiments using the actual exhausts from the moderately low VOC 1991 Dodge Spirit used for reproducibility studies in our laboratories, and from the relatively high VOC Chevrolet Suburban. Thus for these two vehicles (and also for the 1997 Taurus, where both the model and the experiment indicated low reactivity), the model is able to satisfactorily account for the reactivities of their cold-start exhausts. For the older, higher mileage 1988 Honda Accord and 1984 Toyota pickup, the

model performed reasonably well in simulating the experiments with the exhausts alone or when the exhaust was added to a mixture representative to VOCs measured in ambient air, but the model somewhat underpredicted the effect of the exhaust on NO oxidation and O_3 formation when added to a simpler mini-surrogate - NO_x mixture. This is despite the fact that, for the Accord at least, the synthetic exhaust had about the same effect on the mini-surrogate as the actual exhaust, and the model simulated the mini-surrogate with synthetic Accord exhaust run reasonably well. It may be that there is a constituent of these exhausts which is not well represented by the model and is better represented by the model for the compound used in the synthetic exhaust to represent it. However, more replicate experiments with these vehicles, and experiments with other relatively high mileage, in-use vehicles would be needed to determine if this is a consistent problem, or just a problem with the characterization of the two experiments involved, which were not replicated. However, even for these vehicles the model performs in simulating the exhaust reactivity in the experiments with the more realistic surrogate, indicating that it probably will also in simulating the effects of these and the other RFG exhausts in the atmosphere.

Diesel Reactivity

The exploratory experiment carried out with a high-mileage 1984 diesel sedan indicate that the cold-start exhaust from this vehicle can significantly enhance NO oxidation and O_3 formation rates and also measurably increase integrated OH radical levels. However, the species accounting for this reactivity have not been accounted for. It is clearly not due to light hydrocarbons such as $C_{\leq}10$ alkenes, olefins, or aromatics, or $C_{\leq}3$ oxygenates such as formaldehyde and acetaldehyde, levels of these compounds in the chamber was either below the detection limits or too small to significantly affect the results. It is clear that chamber experiments need to be carried out with more comprehensive analyses before we can assess whether we can understand the factors accounting for the reactivities of diesel exhausts.

Overall Conclusions

Although some experimental and model evaluation problems were encountered as indicated above, we believe that overall this program has been successful in achieving its objective. Environmental chamber data which are sufficiently well characterized for model evaluation were obtained using exhausts from a variety of fuels and vehicle types. Incremental reactivity experiments were found to be particularly useful in providing reactivity evaluation data, especially for the lower reactivity exhausts or exhausts with low ROG/NO_x ratios. In most cases the results of the experiments with the exhausts were consistent with model predictions, and consistent with results of experiments using synthetic exhausts derived from mixtures of compounds measured in the actual exhausts. This indicates that in most cases the major exhaust constituents

which contributes to the ozone impacts of these exhausts have probably been identified, and that current chemical mechanisms are reasonably successful in predicting the impacts of these species on ozone. The major exception noted in this study was diesel, where it was clear that the major reactive species have not been identified. There was also some evidence, albeit inconclusive, that the model is underpredicting the ozone impacts of some of the constituents of exhausts from the two high-mileage, in-use RFG-fueled vehicles which were studied. In addition, problems were encountered in the models ability to simulate experiments containing formaldehyde or formaldehyde with methanol which affected the evaluation of the model for the methanol-containing fuels. However, the model successfully predicted the incremental effects of methanol-containing exhausts to surrogate mixtures simulating ambient environments. This was the case for most of the other exhaust studied as well.

INTRODUCTION

Background and Statement of the Problem

Over the past two decades, there has been a considerable effort in the United States to develop and introduce alternatives to gasoline and diesel as transportation fuels. The introduction of alternative fuels is considered by many to be an important component in the implementation of air quality improvement plans. The benefits of alternative fuel vehicles for air quality are related both to an anticipated decrease in the mass emission rate and a decrease in the atmospheric reactivity of the exhaust gas components. To account for the lower reactivity of alternative fuel exhaust, the California Air Resources Board (CARB) has established reactivity-based emission standards. Such standards use "reactivity adjustment factors" (RAFs) to adjust the non-methane organic carbon gas (NMOG) mass emission rate for the different ozone formation potentials of the chemical species in the exhaust. Reactivity factors have been developed over the years on the basis of chemical mechanisms for volatile organic carbon (VOC) and nitrogen oxides (NO_x). These mechanisms are used in airshed models and are the primary means for assessing the effects of alternative fuels on air quality. The validity of such evaluations rest on the assumptions that all the important reactive species in the exhaust have been identified and quantified, and that the chemical mechanisms used in the model accurately represent how their atmospheric reactions affect ozone production.

There is a need for further validation of these assumptions. Conducting environmental chamber experiments involving irradiation of actual vehicle emissions and determining whether the formation of ozone and other secondary pollutants is consistent with model predictions is one way of testing these assumptions. A limited number of environmental chamber experiments involving automobile exhaust have been carried out (Jeffries et al., 1985a,b; Kelly, 1994; Kleindienst et al., 1994), and some have been used to a limited extent for model evaluation (Carter and Lurmann, 1990, 1991). However, most of the previous experiments involving automobile exhaust have not been sufficiently well characterized for model evaluation, or have not used current state-of-the-art methods for speciated vehicle emissions analysis. In addition, if the model is not successful in simulating the results of an irradiated exhaust experiment, one does not know whether the problem is with the identification and quantification of the reactive species present, the gas-phase chemical mechanism for the species, or the representation in the model of important chamber and light source characteristics. Furthermore, a successful model simulation of such an experiment does not by itself provide convincing evidence that we adequately understand the system, since there is always the possibility that errors in the exhaust speciation might be masked by compensating errors in the chemical mechanism or the model for chamber conditions.

1

One approach for identifying the source of unsuccessful model simulations or for assuring that successful simulations are not due to compensating errors is to conduct the exhaust experiments in conjunction with control experiments where uncertainties can be either removed or systematically evaluated. For example, uncertainties in VOC speciation can be eliminated by conducting experiments with synthetically prepared known mixtures of the compounds measured in the exhaust. If different results are obtained in the experiment with the actual exhaust and the mixture of compounds believed to be present in the exhaust, there is evidence for the presence of an unidentified reactive compound that is affecting the results. If the model cannot successfully simulate the results of the experiments with the known mixture, there is evidence of a lack of understanding of the chemical mechanism of the identified species, or there is an incorrect representation of chamber or light source effects. Experiments with single compounds or other control and characterization runs then can be used to separately evaluate whether the chamber and light source effects are being represented correctly. If the experiments with the actual and synthetic exhaust mixtures give similar results, and if the model can successfully simulate these experiments and appropriate control and characterization runs carried out under the same conditions, there is fairly strong evidence that the important compounds present in the exhaust have been correctly identified and the model correctly predicts their atmospheric impact.

Objectives

The overall objective of this program is to provide data to test whether all of the important reactive species in vehicle exhausts using selected fuels have been identified, and whether current chemical models can predict the amount of ozone and other oxidants formed when the exhaust is irradiated. The approach involves conducting environmental chamber experiments using diluted exhaust from conventional and alternative fueled vehicles, and also with known mixtures designed to represent the compounds identified in these exhaust samples. The experiments are conducted under sufficiently well characterized conditions to allow model testing, and in conjunction with the array of control and characterization experiments to characterize chamber and light source effects. A comparison of the results of synthetic and "actual" exhaust experiments is used as evidence that the important reactive species in the exhaust have been identified. Comparison of the ozone and other oxidants formed in the chamber experiments with those predicted by the model is used as evidence of the level of understanding of which exhaust components are contributing to the reactivity.

METHODS

Summary of Overall Approach

This project was carried out in two phases, both of which are discussed in this report. The first phase consisted of experiments with an a vehicle fueled by LPG and preliminary experiments with an M100 vehicle. During this phase, a dilution flow system was used to transfer the exhaust from the vehicle to the chamber. The second phase consisted of more definitive experiments with M100 vehicles, experiments with vehicles fueled with M85 and CNG, and several vehicles using Phase II reformulated gasoline (RFG). The latter included a relatively new, low polluting vehicle, the vehicle used at CE-CERT for reproducibility tests, and several in-use vehicles of various mileages and types. The general approach used in both phases was as follows:

1. Procure the subject vehicles and conduct baseline emission testing with speciation of the vehicle exhaust to determine the concentrations and emission rates of important reactive species. This information is used for determination of the dilution ratios and conditions required for introduction of the vehicle exhaust into the smog chamber. The initial experiments were carried out with LPG and M100 vehicles, since their exhausts are the simplest mixtures to characterize chemically and were expected to have sufficient reactivity for useful chamber experiments. Experiments with the lower reactivity CNG exhausts or the more chemically complex M85 and RFG exhausts were carried out during Phase 2, when the procedures were better characterized and refined.

2. Develop a vehicle exhaust dilution and transfer system for the introduction of diluted exhaust into the smog chamber. This system is required to provide exhaust at a dilution ratio suitable for smog chamber experiments, not introduce additional reactive species other than those present in the vehicle exhaust, or cause significant losses of reactive species. The system must have provisions for analysis of all reactive species present in the diluted exhaust as they are being introduced into the smog chamber. The Phase I experiments utilized a dilution system to transfer the exhausts from the vehicle to the chamber via long Teflon lines, but it was found that this method may have caused non-negligible losses of formaldehyde during the transfer. Therefore, the Phase II experiments utilized a transfer bag to eliminate the loss of formaldehyde.

3. Utilizing the developed dilution system, introduce vehicle exhaust into the smog chamber under well characterized conditions with speciation of the diluted exhaust mixture and conduct reactivity assessment experiments. Somewhat different procedures were used in the two phases, as indicated above.

4. Conduct environmental chamber experiments both with the exhaust in the absence of other reactants, and with the exhausts added to "surrogate" reactive organic - NO_x mixtures designed to represent photochemical smog.

3

5. Conduct similar environmental chamber experiments using known synthetic or synthetic mixtures designed to represent the vehicle exhausts which were studied. Compare the results from the synthetic and "actual" exhaust mixtures to assess whether all important reactive species have been identified, and to assess whether the model can simulate the atmospheric reactivities of the mixtures.

6. Conduct control and characterization experiments necessary to characterize the experimental data for model simulations. This includes measuring light intensity and carrying out characterization experiments sensitive to various types of wall effects, such as the chamber radical source.

7. Compare the experimental reactivity results with model predictions to determine whether the model can simulate levels of ozone and other oxidants formed in these experiments.

Details of the technical approaches used in both phases of this project are given in the following sections.

Vehicle Procurement and Baseline Emissions Testing

The vehicles and fuel-vehicle combinations employed in this study are summarized on Table 1. As indicated above, they included vehicles fueled with LPG, CNG, M100 (100% methanol), M85 (85% methanol, 15% Phase II gasoline), RFG (California Phase II reformulated gasoline) and diesel 2. The following procedures were carried out for each of the vehicles listed in Table 1, with the exception of the diesel Mercedes. The diesel vehicle was used in only one preliminary and exploratory chamber experiment, and was not otherwise characterized.

The CNG and propane vehicles were tested with the in-tank fuel as delivered. The M100 was obtained from a commercial fuel and chemical distributor, while the RFG was obtained from the University Fleet Services. The fuel used on M85 flexible fuel vehicles was splash-blended using M100 and RFG. A results of the M85 test fuel analysis indicated an API Gravity of 48.3, a RVP of 7.05 psi, and the following components (in vol %): Olefins: 0.222; Aromatics: 3.07; Methanol: 87.2; Paraffins: 1.27; Benzene: 0.091; MTBE: 1.35. As indicated on Table 1, the M100, M85 and RFG vehicles were subjected to a fuel drain and fill preconditioning sequence as outlined in the Auto/Oil protocol (Siegel et. al., 1993).

Baseline emission testing was performed on each vehicle in CE-CERT's Vehicle Emissions Research Laboratory (VERL) in accordance with the light duty vehicle Federal Test Procedure as stated in the Code of Federal Regulations [CFR 1997]. Each vehicle was tested over the Urban Dynamometer Driving Schedule of the Federal Test Procedure (FTP) using the protocol outlined in the Code of Federal Regulations (CFR), Title 40, Part 86, Subpart B. The VERL utilizes a Burke E. Porter 48-inch single-roll, electric chassis dynamometer coupled with a Pierburg CVS and analytical system. In addition to measurement of THC, CH4, CO, CO_2, and NO_x, sampling and analyses for carbonyls and oxygenates were

Table 1.   Characteristics of vehicles and fuels used in this program.

Designation in Report	Description	Fuel	Odometer at Start	Procured From	Comments
LPG	Retrofitted 1989 Plymouth Reliant. 2.2-liter, 4-cylinder engine.	LPG	29,600	SCAQMD	Used with fuel as delivered. Used in Phase I study.
M100	1993 Ford Taurus Flexible Fuel Vehicle. Can be operated on M100 and M85 as well as gasoline. 3.0-liter, 6-cylinder engine.	M100	38,100 (Phase 2)	SCAQMD	Preconditioned by two sequences of fuel drain and fill with RFG (to 40% tank capacity), followed by driving over the LA-4 cycle or CFR equivalent, prior to testing. Same vehicle used for both Phase I and Phase II study.
M85	1997 Ford Taurus OEM Flexible Fuel Vehicle. 3.0-liter, 6-cylinder engine.	M85	6,890	UC Riverside Fleet	Preconditioned by two sequences of fuel drain and fill with M85 (to 40% tank capacity), followed by driving over the LA-4 cycle or CFR equivalent, prior to testing. This and all subsequent vehicles used in Phase II study.
CNG	1991 Ford Ranger PU. Dedicated retrofit CNG.	CNG	17,800	UC Riverside Fleet	Used with fuel as delivered. Preconditioned by driving over the LA-4 cycle, prior to testing.
Taurus	1997 Ford Taurus OEM Flexible Fuel Vehicle. 3.0-liter, 6-cylinder engine.	RFG	13,600	Enterprise Rent A Car	Preconditioned by two sequences of fuel drain and fill with RFG (to 40% tank capacity), followed by driving over the LA-4 cycle or CFR equivalent, prior to testing.
Rep Car	1991 Dodge Sprint. OEM Flexible Fuel Vehicle. 2.5-liter 4 cylinder engine	RFG	14,300	CE-CERT VERL	VERL Repeatable car used for weekly validation. Driving preparation over the LA-4 cycle or CFR equivalent
Suburban	1994 Chevrolet Suburban C1500 2 wheel drive. 5.7-liter V8 engine	RFG	58,000	UC Riverside Fleet	Preconditioned by two sequences of fuel drain and fill with RFG (to 40% tank capacity), followed by driving over the LA-4 cycle or CFR equivalent, prior to testing.
Toyota	1984 Toyota PU. 2.4-liter	RFG	227,000	Staff Member	Preconditioned by driving over the LA-4 cycle or CFR equivalent, prior to testing.
Honda	1988 Accord 2.0-liter 4 cylinder engine	RFG	150,000	Staff Member	Preconditioned by driving over the LA-4 cycle or CFR equivalent, prior to testing.
Diesel	1984 Mercedes Benz 300D. 3.0-liter, 5 cylinder turbocharged diesel	RFD	170,000	Staff Member	Used in one exploratory experiment only. No baseline emisssions testing or other characterizations carried out.

5

performed on the M100 vehicle. Hydrocarbon speciation results were obtained for the LPG vehicle from bag samples collected during each of the three phases of the FTP.

A Pierburg Impinger Sampling System was used to collect alcohol (e.g., methanol, ethanol, etc.) and carbonyl (e.g., formaldehyde, acetaldehyde, etc.) samples. Two 25-mL midget glass impingers (Ace Glass) containing 15 mL of deionized water were connected in series to capture methanol samples with no more than 10% breakthrough of the total oxygenate sample collected in the second impinger. To minimize evaporative losses of methanol, the impinger was placed in an ice bath at a temperature near 32oF (0°C). The carbonyls were sampled through Waters Sep-Pak Silica cartridges coated with acidified 2,4-dinitrophenylhydrazine (DNPH). Since the carbonyl capture efficiency of the Waters Sep-Pak Silica cartridges is greater than 95%, only one cartridge per phase was needed. The oxygenate and carbonyl were sampled at a flow rate of 1.0 L/min. The sampling flow rates were monitored and controlled using mass flow controllers.

Hydrocarbon analyses following the Auto/Oil Phase II protocol were conducted in CE-CERT's Fuels and Analytical Instrumentation Laboratory (Siegel, et al., 1993). The light hydrocarbons (C1 through C4) were measured using a Hewlett-Packard (HP) 6890 Series GC with a flame ionization detector (FID) maintained to 250oC. A 15 m x 0.53 mm polyethylene glycol pre-column and a 50 m x 0.53 mm Alumina oxide "S" deactivation PLOT column were used for these measurements. A second HP 6890 Series GC with a FID maintained to 300°C was used to measure C5 to C12 hydrocarbons. A 2 m x 0.32 mm deactivated fused silica pre-column and a 60 m x 0.32 mm HP-1 column were used for these hydrocarbon measurements. For both the C1 to C4 and the C5 to C12 hydrocarbons a 5 mL stainless steel sample loop was conditioned with sample from the GC bag prior to analysis.

Carbonyl samples were analyzed following the Auto/Oil Phase II (Siegel, et al., 1993) using a Shimadzu high performance liquid chromatograph (HPLC) equipped with a SPD-10AV UV-VIS detector. Acetonitrile extracts from the DNPH cartridges were injected into the splitter via the autosampler. A HP 5890 Series II GC with a Wasson ECE O-FID maintained to 250oC and a 60 m DB-1 column were used to measure alcohols. Prior to analyses, the samples were spiked with an internal standard (1 mL of 2-propanol), thoroughly mixed, and transferred to a 1.5 mL liquid chromatograph (LC) vials (and capped) for analysis. These samples were also injected into the splitter via the autosampler.

Vehicle Exhaust Dilution and Transfer Procedures

Phase 1 System and Procedures

The standard Pierburg Constant Volume Sampler (CVS) uses filtered but not purified ambient air as a diluent. As a result, the standard CVS system could not be used for exhaust dilution and transfer to the smog chamber due to concern with the unknown effects of dilution air contaminants on the reactivity experiments. Instead, a modified Pierburg Constant Volume Diluter (CVD) or mini-dilution system was utilized for this purpose. The CVD operates by taking a small fraction of the raw vehicle exhaust (as opposed to the total exhaust in a standard CVS system) and diluting it with a known and constant flow of dilution gas. Since the total flow rates are modest, the diluent gases can be purified nitrogen or air, thus removing concerns about the introduction of background contaminants into the smog chamber. The dilution ratio can be changed by varying either the raw exhaust flow or the dilution gas flow.

A schematic of the Pierburg CVD and associated hardware is presented in Figure 1. This system utilizes a heated metal bellows pump to draw a constant analytical sample from the raw exhaust stream via a heated line. A series of valves can be used to divert a portion of the sample out of the system such that the amount of analytical sample can be varied. Thus, the concentration of the dilute sample and its dilution ratio can be selected. The analytical sample is diluted with purified air in a mixing "T" to lower the dew point temperature of the dilute sample below room temperature, eliminating the need to heat the transfer line. Purified air is used as a diluent to prevent the introduction of background hydrocarbons which could affect the smog chamber reactivity experiments. Aadco purified air was selected as the sample diluent to be consistent with the air used in the smog chamber. Aadco purified air is produced by scrubbing hydrocarbons except for methane and CO from ambient air.

Immediately downstream of the mixing "T," sampling lines are connected to draw a portion of the dilute sample into a black Tedlar bag for speciated hydrocarbon analysis, carbonyl and alcohol sample collection using DNPH cartridges and water impingers, and second-by-second analysis of the exhaust emissions using the Pierburg exhaust gas analyzer bench. The raw exhaust was also continuously analyzed with the Pierburg exhaust gas analytical bench to monitor the exhaust gas dilution ratio. The remainder of the sample is transferred to the smog chamber via a 1/2 inch Teflon line approximately 150 feet long. Teflon tubing and fittings were used downstream of the dilution point to minimize exposure of reactive components to surfaces which can catalyze reaction or lead to losses due to adsorption. All samples collected for smog chamber experiments were obtained at a speed of 45 mph with a sampling period of approximately 3 minutes. The constant speed was necessary to provide a relatively constant ratio between

7
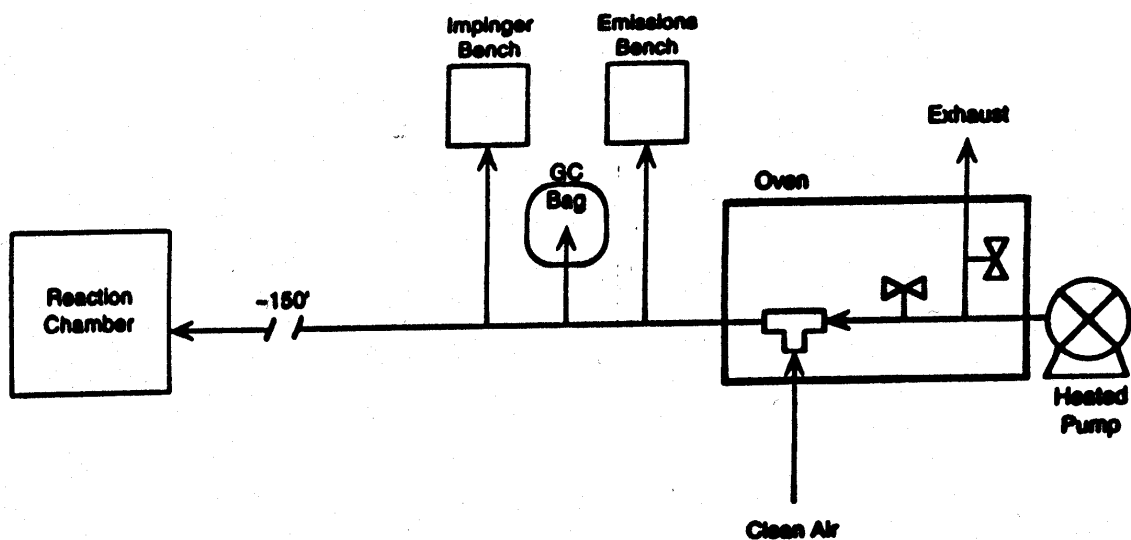
Figure 1.   Pierburg CVD Sampling System.

the exhaust sample and dilution air flows so dilute exhaust concentrations would not change. Speed was maintained by setting the cruise control once the driver had reached the operating speed. The deviation observed from this set speed was within ± 1 mph.

Vehicles were soaked for a period between 12 and 36 hours at a temperature of $70\pm4^{o}F$ before each test. Prior to sampling, the vehicle was accelerated to 45 mph from a "cold start" condition; thus, the emissions sampled usually included a cold-start component prior to the engine warm-up and catalyst light-off. Preliminary experiments were also conducted where exhaust samples were collected during hot-stabilized operation at 45 mph constant speed. It was found, however, that the emission levels under hot stabilized operation were too low to provide a concentration of reactive species for meaningful smog chamber analysis.

Phase 2 System and Procedures
As discussed later, it was subsequently concluded that formaldehyde losses in the long sample line to the chamber may be non-negligible. For this reason, this sampling method was modified for Phase 2 of the project. Some associated procedures were modified as well. These are discussed in this section.

8

The new transfer system used exhaust back pressure by means of a sampling manifold and adjustable restriction plate to divert raw vehicle exhaust into a transfer vessel filled with purified air. The transfer vessel consisted of a ~500-liter FTP Teflon bag inside a plastic and plexiglas airtight container which can either be pressurized to force the contents out of the vessel, or partially evacuated to fill the vessel, in both cases without having to pass the raw or diluted exhaust through a pump. A schematic of this system is presented in Figure 2. In order to reduce exhaust contamination and entrainment of soluble hydrocarbons, a small diameter heated stainless steel line of minimum length was used. All connections to the vehicle and transfer vessel are constructed of stainless steel or other non-reactive materials. The transfer vessel consists of a 750-liter semi ridged polyethylene container in which a Tedlar bag is fitted to sample inlet and exhaust ports.

The revised transfer bag system was developed to reduce the possibility of formaldehyde loss in the sampling lines, as may have occurred during the previous M100 experiments. Measurement of exhaust constituents, both in the transfer bag and directly from the vehicle were conducted using CE-CERT Vehicle Emissions Research Laboratory analytical equipment before, during and after vehicle testing. Due to test cycle length and impinger bench sampling rate limitations, alcohol and carbonyl sampling were taken from the transfer vessel immediately following each test run.

Prior to each test sequence for a given vehicle and fuel combination, the vehicle was prepared in accordance with the Federal Test Procedure. In addition to the fuel change each vehicle was subjected to an LA4 test cycle on the Vehicle Emissions Research Laboratory 48" chassis dynamometer. Upon completion of the preparation cycle, the vehicle was stored in a climate controlled environment in accordance with Title 40 Part 86 of the Code of Federal Regulations. In order to maximize the number of smog chamber tests, some baseline FTP test results were obtained from other concurrent programs employing the same vehicle and fuel combinations.

The new transfer system required a revision of the cycle used in the previous experiments in response to operator safety issues, as well as simplifying the measurement of the vehicle exhaust. Previously, exhaust transfer was performed continuously during the three-minute cycle using a Pierburg mini-dilution system. In this earlier configuration, no additional personnel were required in the dynamometer cell during testing. In the current experiments, the transfer process requires two additional technicians inside the test cell at the exhaust outlet to monitor and control the introduction of raw exhaust into the transfer vessel. The risk during the transfer process to the technicians was due to working in close proximity, < 2 ft. to the drive wheels and the dynamometer rolls. In response to this problem, the maximum
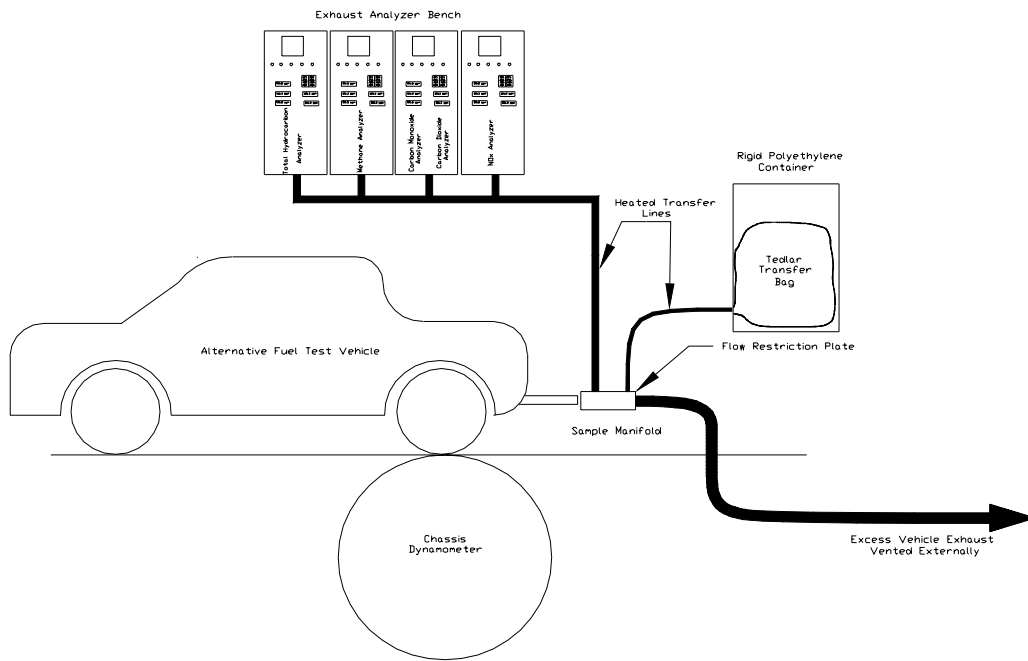
Figure 2.   Schematic of vehicle exhaust sampling system for the Phase 2 environmental chamber experiments.

cycle speed was reduced, and all drive components were carefully inspected and all debris was removed from the drive wheels.

The cycle employed for the smog chamber experiments was a timed steady state test. The test itself consists of a gradual acceleration of 1.33 mph/s (0 to 40 mph in 30 seconds) to 40-mph followed by steady state operation. During the steady state period, the test technicians manually attach the heated sample line to the transfer vessel. The limitations of the sample transfer vessel are restricted to concentration and relative humidity of the mixture of dilutant and raw vehicle exhaust. The objective for each test was to achieve a dilutant to exhaust ratio not less than 10:1 in the transfer vessel, and or a relative humidity of less than 50% at 68 to 75 degrees F. Since sampling duration is a function of fuel type, emission certification level, engine displacement and exhaust system integrity, multiple iterations were required for some vehicles to obtain sufficient quantities of exhaust in the transfer vessel. In the current phase, the average exhaust transfer duration for all vehicle and fuel tests was approximately 45 seconds.

Before sample transfer, the transfer vessel was prepared by flushing it with Aadco purified air overnight and then evacuated using a vacuum pump. The bag was filled with Aadco air at a known flow rate

10

as measured by a dry gas flow meter. Typically the volume of air in the bag was approximately 350-450 liters. The initial concentration of carbon monoxide in the bag was measured, since the Aadco system employed did not completely remove CO. This background CO amount could then be used to determine the amount of exhaust CO added to the bag. The bag was then moved to the vehicle emissions laboratory for exhaust transfer.

During sample transfer, simultaneous measurement of vehicle exhaust was taken directly from the sampling manifold and transferred by heated line, maintained at 131 °C, to the Pierburg Exhaust Analyzers. Second by second measurements for THC, CH4, CO, CO_2 and NO_x were recorded for post test analysis to determine the dilution ratio. After each test the transfer vessel containing diluted exhaust was attached directly to the Pierburg Exhaust Analyzers and sampled for not less than 30 seconds. Due to the short test duration and low maximum sampling rate of the Pierburg Alcohol and Carbonyl Impinger System, simultaneous measurement during the transfer process was not possible. In order to obtain satisfactory measurement of these compounds it was necessary to sample directly from the transfer vessel after each test for a period of 15 minutes. Sampling for speciated hydrocarbon analysis was taken directly from the transfer vessel after each test using a Pyrex syringe. Each sample was subjected to analysis in accordance with the Auto/Oil Phase II protocol at CE-CERT's Fuels and Analytical Instrumentation Laboratory.

The transfer vessel was moved to the environmental chamber laboratory for injection of its contents into the chamber. In the surrogate with exhaust experiments, the VOC components of the surrogate were injected into both sides of the chamber and mixed prior to the exhaust injection. The transfer vessel was attached to a port on Side A of the chamber using 2" vacuum cleaner tubing, and its contents were forced into the chamber by pressurizing the container around the vessel. In the experiments where the exhaust was injected into both sides of the chamber, the ports connecting the sides were open, and the contents of the two sides were exchanged and well mixed before the sides were separated by closing the ports connecting them. In the experiments where exhaust was only on one side, the ports connecting the sides were closed prior to the exhaust injection. (The design of the environmental chamber is discussed in the following section.) If necessary, NO_x was injected in the non-exhaust side or separately to both sides to yield the desired concentration of NO_x equally on both sides. Additional injections were made into individual sides, as appropriate (see tabulation of experiments).

Environmental Chamber Experiments

    General Approach

        The objectives of the environmental chamber experiments were to determine whether the effects of the exhaust mixtures on various manifestations of photochemical smog formation were consistent with model predictions, and to determine whether similar results are obtained in experiments employing synthetic mixtures of the compounds found to be present in the exhausts. Several different types of experiments were employed to determine the effects of the actual and synthetic exhaust mixtures on NO oxidation, ozone formation, OH radical levels as measured by VOC consumption rates, and formation of formaldehyde, PAN and other products. The chamber employed was the Dividable Teflon Chamber (DTC) and is described below. This chamber is irradiated with fluorescent blacklights and is designed to allow for simultaneous irradiation of two different mixtures in each of its "sides," and described in more detail below. The following types of experiments were carried out:

        Exhaust Experiments. These consisted of diluted vehicle exhaust, or a mixture simulating diluted vehicle exhaust, without any other added reactants. This is the most straightforward and sensitive method for model evaluation for more reactive exhaust mixtures. However, it is less useful for low-reactivity or low-VOC exhaust mixtures because very little ozone is formed, and because the NO oxidation rates in experiments with low-reactivity VOCs can be sensitive to chamber effects, particularly the chamber radical source, which tends to enhance the NO oxidation rates to varying degrees. It is also not a realistic representation of ambient conditions under which ozone is formed, because of the high NO_x levels.

        Exhaust with Formaldehyde Experiments. Some experiments with LPG exhaust were carried out with formaldehyde added to increase the reactivity of the mixture. Model calculations show that ozone formation and NO oxidation rates in experiments where formaldehyde is added to the exhaust mixture can be highly sensitive to the level and characteristics of the low-reactivity species such as those in LPG exhausts. Thus, such experiments provide a chemically simple and sensitive method to test whether the model is adequately representing these low-reactivity compounds. Typically, these experiments were carried out simultaneously with the exhaust-only runs; both sides of the dual chamber are filled with the exhaust mixture, and then formaldehyde is injected into one side only.

        Incremental Reactivity Experiments. An incremental reactivity experiment consists of determining the effect of a compound or mixture on NO oxidation, ozone formation, and other photochemical smog manifestations when added to a reactive organic gas (ROG) - NO_x surrogate simulating ambient pollution.

Such experiments can be carried out using different ROG mixtures and ROG/NO$_x$ ratios to assess the effects of the compounds or mixtures under varying conditions. The experiment with only the ROG surrogate and NO$_x$ is referred to as the "base case" run, and the experiment where the test compound or mixture was added to the base ROG and NO$_x$ reactions is referred to as the "test" run. Because of the dual design of the DTC, the base case and test runs were carried out simultaneously, with the base case reactants on one side, and the base case with added exhaust VOCs (the test run) on the other. Generally, the surrogate ROG components were added to both sides of the dual chamber, the exhaust (which includes NO$_x$ as well as VOCs) was added to one side, and varying amounts of NO$_x$ were added to each side to equalize the NO$_x$ levels on both sides. Two types of incremental reactivity experiments were conducted, as follows.

Mini-Surrogate Incremental Reactivity Experiments. The mini-surrogate incremental reactivity experiments employ a highly simplified mixture of only three VOCs (ethene, n-hexane, and m-xylene) to represent ambient ROGs, and a relatively low ROG/NO$_x$ ratio. This type of mini-surrogate reactivity experiment has been extensively employed in our experimental studies of incremental reactivities of a wide variety of individual VOCs (Carter et al., 1993a). It provides a more sensitive test of effects of many types of mechanism differences (particularly those involving radical initiation or termination) than experiments employing more complex and realistic ROG surrogates (Carter et al, 1995a). The low ROG/NO$_x$ ratio is designed to represent chemical conditions where ozone is most sensitive to VOC additions, which is designed to represent the conditions used to develop the "Maximum Incremental Reactivity" (MIR) scale (Carter, 1994).

Full Surrogate Incremental Reactivity Experiments. For most of the exhausts studied, an additional type of incremental reactivity experiment was carried using an 8-component mixture to provide a more realistic representation of the VOCs present in ambient air, and using somewhat higher ROG/NO$_x$ ratios. While a less sensitive test of some aspects of the mechanism, experiments with a more representative ROG surrogate represent conditions more closely resembling the atmosphere. The ROG surrogate was the same as the 8-component "lumped molecule" surrogate as used in our previous study (Carter et al., 1995a), and consists of n-butane, n-octane, ethene, propene, trans-2-butene, toluene, m-xylene, and formaldehyde. Calculations have indicated that use of this 8-component mixture will give essentially the same results in incremental reactivity experiments as use of actual ambient mixtures (Carter et al., 1995a).

Characterization and Control Experiments. Additional experiments were carried out to assure data consistency and quality, and to characterize the conditions of the runs for use in modeling. For example, actinometry runs were conducted periodically to measure light intensity; n-butane-NO$_x$ and CO-NO$_x$ runs

were conducted to assess chamber effects on radical initiation processes (the "chamber radical source"); and replicate propene-NO_x runs were conducted to assure consistency of conditions and results. The results of these experiments are summarized in the chronological listings of the experiments carried out, and where relevant in the modeling methods section.

Environmental Chamber Employed

The Dividable Teflon Chamber (DTC) consists of two ~5000-liter 2-mil heat-sealed FEP Teflon reaction bags located adjacent to each other and fitted inside an 8-foot cubic framework. A schematic of this chamber is shown in Figure 3. Two diametrically opposed banks of 32 Sylvania 40-W BL blacklights are the light source (Carter et al, 1995a,b). Only half of the blacklights are normally used, though 75% of the lights were used in some experiments because of the continual decline of light intensity over time (see discussion below). The unused blacklights are covered with an aluminum sheet and used to bring the chamber up to the temperature it will encounter during the irradiation. To initiate the irradiation, the uncovered lights are turned on and the covered ones are turned off simultaneously. Four air blowers located in the bottom of the chamber are used to cool the blacklights as well as mix the contents of the chamber.

The DTC is designed to allow simultaneous irradiations of the base case and the test experiments under the same reaction conditions. The two reactor bags (side A and side B) are interconnected with two ports, each with a box fan, which rapidly exchange their contents to assure that base case reactant concentrations are identical within each side. The ports connecting the two reactors can then be closed to allow separate injections on each side, and separate monitoring of each. Individual fans are located in each of the reaction bags to rapidly mix the reactants separately introduced into each chamber.

Experimental Procedures

The reaction bags were flushed with dry purified air (Aadco model 737) for 14 hours (6pm-8am) on the nights before experiments. Continuous monitors for ozone, nitrogen oxides, formaldehyde, and carbon monoxide were connected prior to reactant injection to measure background concentrations. The reactants were injected as described below (see also Carter et al, 1993a, 1995b,c). The common reactants were injected in both sides simultaneously using a three-way (one inlet and two outlets connected to side A and B respectively) bulb of 2 liters in the injection line and were well mixed before the chamber was divided. The contents of each side were blown into the other using two box fans located between them. Mixing fans were used to mix the reactants in the chamber during the injection period, but these were turned off prior to the irradiation. The sides were then separated by closing the ports which connected them, after turning all the fans off to allow their pressures to equalize. Reactants for specific sides (the test

14
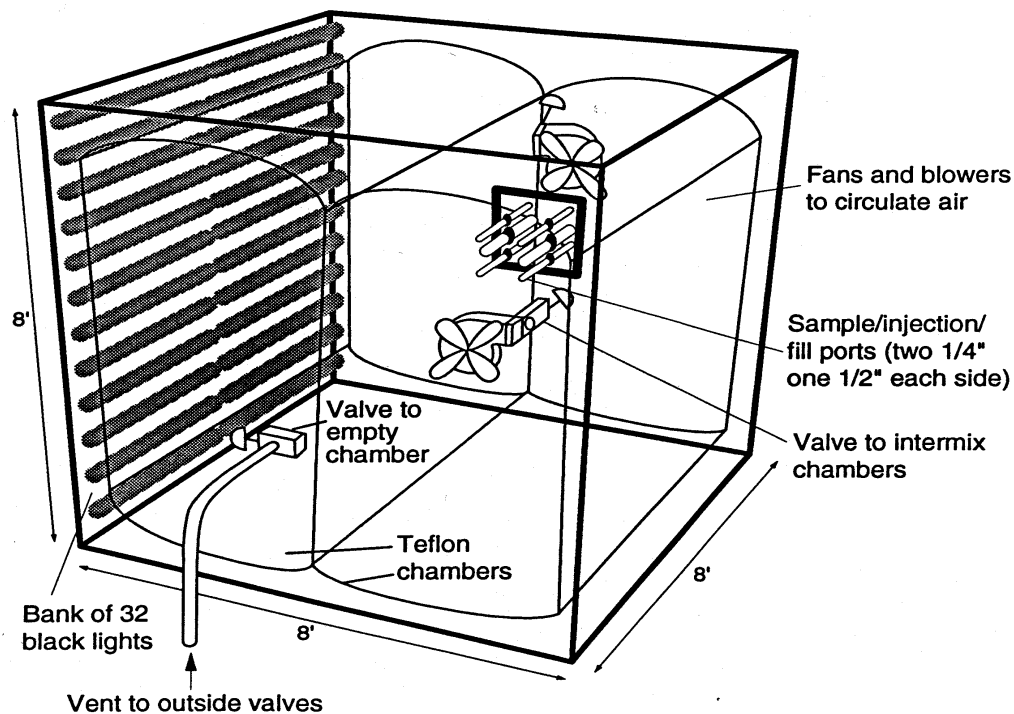
Figure 3.   Schematic of the environmental chamber used in this study.

compound in the case of reactivity experiments) were injected and mixed. The irradiation began by turning on the lights and proceeded for 6 hours. After the run, the contents of the chambers were emptied by allowing the bag to collapse, and then the chambers were flushed with purified air.

The NO and NO_2 were prepared for injection using a high vacuum rack. Known pressures of NO, measured with MKS Baratron capacitance manometers, were expanded into Pyrex bulbs with known volumes, which were then filled with nitrogen (for NO) or oxygen (for NO_2). The contents of the bulbs were then flushed into the chamber with purified air. The other gas reactants were prepared for injection either using a high vacuum rack or gas-tight syringes whose amounts were calculated. The gas reactants in a gas-tight syringe was usually diluted to 100 mL with nitrogen in a syringe. The volatile liquid reactants were injected, using a micro syringe, into a 1-liter Pyrex bulb equipped with stopcocks on each end and a port for the injection of the liquid. The port was then closed and one end of the bulb was attached to the injection port of the chamber and the other to a dry air source. The stopcocks were then opened, and the contents of the bulb were flushed into the chamber with a combination of dry air and heat gun for approximately 5

15

minutes. Formaldehyde was prepared for injection on a vacuum rack by heating paraformaldehyde and collecting it in a trap immersed in liquid nitrogen. A bulb was filled with formaldehyde by removing the liquid nitrogen from the trap until the desired pressure was attained. The bulb was then closed and detached from the vacuum system and its contents were flushed into the chamber with dry air (from the Aadco system) through the injection port.

Exhaust Injection: Phase 1

The LPG or M100 vehicle exhaust was introduced into the chamber by connecting the outlet of mini-dilution system as described above. The outlet flow was approximately 160-200 standard cubic feet per hour (SCFH) and the injection amount was controlled by the injection time, approximately 3 minutes. A "tee" with equal 4-foot-long Teflon tubes was used between the exhaust outlet and chamber when the exhaust was introduced into both sides. When only one side was being filled, the other line of the "tee" was vented. The mixing fans were turned on during the injection.

Exhaust Injection: Phase 2

The transfer vessel was moved from the VERL to the environmental chamber laboratory for injection of its contents into the chamber. In the surrogate with exhaust experiments, the VOC components of the surrogate were injected into both sides of the chamber and mixed, prior to the exhaust injection into the chamber. The transfer vessel was attached to a port on one side of the chamber using 2 inch non-reactive PVC tubing, and its contents were forced into the chamber by pressuring the container around the vessel. The airflow into the vessel as well as the sample flow into the chamber was controlled by an adjustable vent which controlled the amount of pressurization. The amount injected to the chamber depended on the type of experiment. In experiments where the exhaust was injected into both chamber sides, the ports connecting the sides were open, and the contents of the two sides were exchanged and mixed before they were separated by closing the ports connecting them. In the experiments where exhaust was only on one side, the ports connecting the sides were closed prior to the exhaust injection. The typical injection time for the entire bag was approximately 2 to 3 minutes. In reactivity experiments, NO_x was generally injected in the non-exhaust side or separately to both sides to yield the desired of NO_x equally on both sides. Additional injections were made into individual sides, as appropriate (see tabulation of experiments)

Analytical Methods

Continuous analyzers were connected directly to the chamber using PFA Teflon tubing. The sampling lines from each side of the chamber were connected to PFA Teflon solenoid valves, which

16

switched from side to side every 10 minutes, so the instruments alternately collected data from each side. A chemiluminescent analyzer was used for nitrogen oxides (Thermoenvironmental model 42), a UV phototometric for ozone (Dasibi model 1003 AH), and a gas correlation IR analyzer for carbon monoxide (Thermoenvironmental model 48). An automated wet chemical method based on fluorometric measurement was set up to sample for formaldehyde (Carter et al, 1995c; Dasgupta et al. 1988, 1990). The output of these instruments, along with that from the temperature sensors, was attached to a computer data acquisition system, which recorded the data at 10-minute intervals for ozone, NO and temperature (and at 20 minutes for formaldehyde), using 30-second averaging times. This yielded a sampling interval of 20 minutes for taking data from each side.

The NO_x and CO analyzers were calibrated with a certified compressed gas source and using a CSI model 1700 gas-phase dilution system prior to each chamber experiment. The NO_2 converter efficiency check was carried out in regular intervals. The ozone analyzer was calibrated with a transfer standard ozone analyze at intervals of three months and was checked daily with CSI ozone generator (set to 400 ppb). The details are discussed elsewhere (Carter et al, 1995c).

Organic reactants other than formaldehyde were measured by gas chromatography with FID detectors as described elsewhere (Carter et al., 1993a, 1995c). GC samples were taken for analysis at intervals from 20 minutes to 30 minutes either using 100 mL gas-tight glass syringes or by collecting the 100 mL sample from the chamber onto Tenax-GC solid adsorbent cartridge. These samples were taken from ports directly connected to the chamber after injection and before irradiation and at regular intervals after irradiation. The contents of the syringe were flushed through a 2 mL or 3 mL stainless steel or 1/8 inch Teflon tube loop and subsequently injected onto the column by turning a gas sample valve. The light hydrocarbons (C2 through C4) were analyzed using a 30 m x 0.53 mm megabore gas-solid alumina column. The others (C5 through C10, including aromatics) were analyzed using a 15 m x 0.53 mm megabore DB-5 (5% phenyl-methylpolysiloxane) column. A 30 m x 0.53 mm megabore DB-WAX (polyethylene Glycol) column was used for the measurement of alcohols.

The calibrations for the GC analyses for most compounds were carried out by sampling from chambers into which known amounts of the reactants were injected, as described previously (Carter et al, 1995c). For the gaseous compounds such as those identified in these exhausts, samples for injection were prepared using the vacuum rack. The chamber volume was determined by measuring the CO concentration in chamber into which known amount of CO was injected using vacuum rack system.

Chamber Characterization

Three thermocouples were used to monitor the chamber temperature. One each was located in each of the sample lines on each side of the chamber that were used for the continuous analyzers. The third was in the chamber enclosure itself, outside the reaction bags. Temperatures in these experiments typically were 21-25°C. The light intensity in the DTC chamber was monitored by periodic NO_2 actinometry experiments utilizing the quartz tube method of Zafonte et al (1977), with the data analysis method modified as discussed by Carter et al (1995c). The results of these experiments were tracked over time in this chamber since it was first constructed in early 1994. The spectrum of the blacklight light source has been found not to vary significantly with time, and the general blacklight spectrum recommended by Carter et al (1995c) was used when modeling these blacklight chamber experiments. The light characterization results, and how they were used to characterize the experiments for modeling, are discussed in more detail later in this report.

The dilution of the DTC chamber due to sampling is expected to be small because the flexible reactions bags can collapse as sample is withdrawn for analysis. However, some dilution occurs with the age of reaction bags because of small leaks. Information concerning dilution in an experiment can be obtained from relative rates of decay of added VOCs, which react with OH radicals with differing rate constants (Carter et al., 1993a; 1995c). Most experiments had a more reactive compound such as m-xylene and n-octane present either as a reactant or added in trace amounts to monitor OH radical levels. Trace amounts (~0.1 ppm) of n-butane were added to some experiments as needed to provide a less reactive compound for the purposes of the monitoring dilution. In addition, specific dilution check experiments were conducted by preparing chambers with high concentrations of carbon monoxide (~20 ppm) and monitoring the concentration for several days. The dilution rates were found to be minor during the course of these experiments, typically ranging from being too low to measure to ~0.5% per hour.

Modeling Methods

General Atmospheric Photooxidation Mechanism

The chemical mechanism used in the environmental chamber and atmospheric model simulations in this study is given in Appendix A to this report. This mechanism is based on that documented by Carter (1990), with a number of updates as discussed below. It can explicitly represent a large number of different types of organic compounds, but it lumps together species reacting with similar rate constants and mechanisms in atmospheric simulations, and it uses a condensed representation for many of the reactive organic products. The reactions of inorganics, CO, formaldehyde, acetaldehyde, peroxyacetyl nitrate (PAN), propionaldehyde, peroxypropionyl nitrate, glyoxal and its PAN analog, methylglyoxal, and several other

product compounds are represented explicitly. In addition, the reactions of unknown photoreactive products formed in the reactions of aromatic hydrocarbons are represented by a model species "AFG2," whose yields and photolysis parameters are adjusted to minimize the discrepancies between model simulations and results of environmental chamber experiments. A chemical operator approach is used to represent peroxy radical reactions, as discussed in detail by Carter (1990). Generalized reactions with variable rate constants and product yields are used to represent the primary emitted alkane, alkene, aromatic and other VOCs (with rate constants and product yields appropriate for the individual compounds being represented in each simulation). Most of the higher molecular weight oxygenated product species are represented using the "surrogate species" approach, where simpler molecules such as propionaldehyde or 2-butanone are used to represent the reactions of higher molecular weight analogues that are assumed to react similarly. The tables in Appendix A list reactions used for all VOCs represented in the simulations in this work.

The mechanism of Carter (1990) was updated several times prior to this work. A number of changes were made to account for new kinetic and mechanistic information for certain classes of compounds as described by Carter et. al. (1993b) and Carter (1995). Further modifications to the uncertain portions of the mechanisms for the aromatic hydrocarbons were made to satisfactorily simulate results of experiments carried out using differing light sources (Carter et al. 1997). The latest version of the general mechanism is discussed by Carter et al. (1997). The most significant updates from the perspective of this report concerned improvements in the representation of the higher alkenes based on results of laboratory studies and chamber experiments (Carter, 1995), and representations of the aromatic hydrocarbons based on results of chamber experiments with differing light sources (Carter et al, 1997).

Environmental Chamber Simulations

The ability of the chemical mechanisms to appropriately simulate the observed effects of the actual and synthetic exhaust mixtures on ozone formation and other measures of photochemical smog was evaluated by conducting model simulations of the individual chamber experiments from this study. This required including in the model appropriate representations of chamber-dependent effects such as wall reactions and characteristics of the light source in the model. The methods used are based on those discussed in detail by Carter and Lurmann (1990, 1991), updated as discussed by Carter et al (1995b,c; 1997). The photolysis rates were derived from results of NO_2 actinometry experiments and direct measurements of the spectra of the light source. (See below for a discussion of how the photolysis rates were derived for these specific experiments.) In the case of the blacklights used in the DTC, the spectrum was assumed to be constant and the blacklight spectrum given by Carter et al (1995b,c) was employed. The thermal rate constants were calculated using the temperatures measured during the experiments, with the

small variations in temperature with time during the experiment being taken into account. The computer programs and modeling methods employed are discussed in more detail elsewhere (Carter et al, 1995c). The specific values of the chamber-dependent parameters used in the model simulations of the experiments for this study are given in Table A-4 in Appendix A.

The individual organic compounds were represented explicitly using the reactions given in Appendix A when conducting the model simulations of all the chamber experiments except for those containing RFG exhausts. Because RFG exhausts are highly complex mixtures of many organics, it is not practical to represent each as a separate model species. For those runs, the individual compounds which could be resolved and monitored separately using the GC instruments in the chamber lab (which included the base case surrogate components in the incremental reactivity experiments) were represented explicitly, but the other species measured in the exhaust, whose concentrations were derived from analyses of the exhaust transfer bag after applying the transfer bag / chamber dilution ratio (see below), were represented using a lumped parameter approach which is similar to the representation of VOC emissions in EKMA simulations (e.g., see Carter, 1993b). The specific lumping approach is as follows:

Represented explicitly: Formaldehyde, acetaldehyde, acetone, isoprene, isobutane

Represented with lumped parameter approach, with the rate constant and product yield parameters adjusted based on the compounds being represented:

AAR1:	Alkanes, aromatics, and other non-alkene, non-carbonyl compounds which react only with OH radicals, and whose OH rate constants are less than 5 x 10^3 ppm^{-1} min^{-1}, weighed by OH reactivity using IntOH = 50 ppt-min (Carter, 1993).
AAR2:	As above, but for compounds with OH rate constants between 5 x 10^3 and 1 x 10^4 ppm^{-1} min^{-1}, each compound weighed equally
AAR3:	As above, but for compounds with OH rate constants between 1 x 10^4 and 2 x 10^4 ppm^{-1} min^{-1}, each compound weighed equally
AAR4:	As above, but for compounds with OH rate constants higher than 2 x 10^4 ppm^{-1} min^{-1}, each compound weighed equally.
OLE1:	Alkenes and other compounds which react non-negligibly with O_3 and NO_3, with OH rate constants less than 2 x 10^4 ppm^{-1} min^{-1}, each compound weighed equally (primarily ethene).
OLE2:	As above, but for compounds with OH rate constants between 2 and 6 x 10^4 ppm^{-1} min^{-1}, each compound weighed equally (primarily terminal alkenes).

OLE3   As above, but for compounds with OH rate constants higher than 6 x 10^4 ppm^{-1} min^{-1}, each compound weighed equally (primarily internal alkenes).

Represented using "lumped molecule" approach, with the model species representing the individual compounds on a mole-per-mole basis without parameter adjustment.

RCHO: Propionaldehyde and higher aldehydes

MEK: Methylethyl ketone and higher ketones

BALD: Benzaldehyde and tolualdehyde

Table A-2 in Appendix A includes the explicit reactions of each of the compounds detected in the LPG exhausts which were represented using the lumped parameter approach. The rate constants and product yields given in these reactions were used to derive the rate constant and product yield parameters for the lumped model species used to represent them in the simulation, based on the relative contribution of each compound to the total mixture being represented by the lumped model species.

Incremental Reactivity Data Analysis Methods

As indicated above, many of the environmental chamber experiments were incremental reactivity runs, which consist of simultaneous irradiation of a "base case" reactive organic gas (ROG) surrogate - NO$_x$ mixture in one of the dual reaction chambers, together with an irradiation, in the other reactor, of the same mixture with a actual or synthetic exhaust mixture added. The latter is referred to as the "test" experiment. The results are analyzed to yield two measures of reactivity: the effects of the added mixtures on the amount of NO reacted plus the amount of ozone formed, and their effects on integrated OH radical levels. The methods for analyzing these data are summarized in this section.

The first measure of reactivity is the effect of the mixture on the change in the quantity ($[O_3]t$-$[NO]_t$)-($[O_3]_0$-$[NO]_0$), which is abbreviated as D(O$_3$-NO) in the subsequent discussion. As discussed elsewhere (e.g., Johnson, 1983; Carter and Atkinson, 1987; Carter and Lurmann, 1990, 1991, Carter et al, 1993a, 1995a,b), this gives a direct measure of the amount of conversion of NO to NO$_2$ by peroxy radicals formed in the photooxidation reactions, which is the process that is directly responsible for ozone formation in the atmosphere. (Johnson calls it "smog produced" or "SP".) The effect of the exhaust mixture is then given by

$$\triangle D(O_3\text{-}NO) = D(O_3\text{-}NO)^{test} - D(O_3\text{-}NO)^{base},$$

the difference between D(O$_3$-NO) in the test experiment and that in the base case side, which is calculated for each hour of the experiment. An estimated uncertainty for $\triangle$ D(O$_3$-NO) is derived based on assuming an

~3% uncertainty or imprecision in the measured D(O$_3$-NO) values. This is consistent with the results of the side equivalency test, where equivalent base case mixtures are irradiated on each side of the chamber.

Note that reactivity relative to D(O$_3$-NO) is essentially the same as reactivity relative to O$_3$ in experiments where O$_3$ levels are high, because under such conditions [NO]$_t^{base}$ ≈ [NO]$_t^{test}$ ≈ 0, so a change D(O$_3$-NO) caused by the test compound is due to the change in O$_3$ alone. However, D(O$_3$-NO) reactivity has the advantage that it provides a useful measure of the effect of the VOC on processes responsible for O$_3$ formation even in experiments where O$_3$ formation is suppressed by relatively high NO levels.

The second measure of reactivity is the effect of the VOC on integrated hydroxyl (OH) radical concentrations in the experiment, which is abbreviated as "IntOH" in the subsequent discussion. This is an important factor affecting reactivity because radical levels affect how rapidly all VOCs present, including the base ROG components, react to form ozone. If a compound is present in the experiment which reacts primarily with OH radicals, then the IntOH at time t can be estimated from:

$$IntOH_t = \int_0^t [OH]_\tau \, d\tau = \frac{\ln \left(\dfrac{[tracer]_0}{[tracer]_t} \right) - D\,t}{KOH^{tracer}} \, , \tag{II}$$

where [tracer]$_0$ and [tracer]$_t$ are the initial and time=t concentrations of the tracer compound, KOH^{tracer} its OH rate constant, and D is the dilution rate in the experiments. The latter was found to be small and was neglected in our analysis. The concentration of tracer at each hourly interval was determined by linear interpolation of the experimentally measured values. m-Xylene was used as the OH tracer in these experiments because it is a surrogate component present in all experiments, its OH rate constant is known (the value used was 2.36x10^{-11} cm^3 molec^{-1} s^{-1} [Atkinson, 1989]), and it reacts relatively rapidly.

The effect of the exhaust mixture on OH radicals can thus be measured by Δ IntOH, which is the difference between the IntOH measured in the test experiment and the IntOH measured in the base case run. The results are reported for each hour in units of 10^6 min. The uncertainties in IntOH and Δ IntOH are estimated based on assuming an ~2% imprecision in the measurements of the m-xylene concentrations. This is consistent with the observed precision of results of replicate analyses of this compound.

RESULTS AND DISCUSSION

Baseline Emissions Characterization

The major characteristics and fuels for the vehicles studied in this project have been summarized in Table 1, above. Emissions characterization using the Federal Test Procedure (FTP) was carried out for all these vehicles except for the diesel Mercedes, and detailed hydrocarbon and oxygenate speciation was carried out during most of these tests. The results of these FTP baseline emissions tests are summarized in Table 2, and the detailed speciation results associated with these tests, for those cases where such measurements were made, are given in Table B-1 in Appendix B. These data are discussed below for the various vehicles which were tested.

LPG Vehicle

As indicated in Table 1, the LPG tests were carried out using a retrofitted 1989 Plymouth Reliant, and two FTP tests were carried out using this vehicle. The results on Table 2 show that the NMHC and CO emission levels from the LPG vehicle are substantially higher than the 1989 vehicle certification standards of 0.39 g/mi NMHC and 7.0 g/mi CO. The results are, however, comparable with those found in other studies showing that the quality of a conversion or conversion kit can have a substantial impact on the emission performance of LPG vehicles. Earlier studies by the California Air Resources Board (CARB) of in-use converted LPG vehicles found higher CO and NMOG emissions for these vehicles when compared with unconverted gasoline vehicles (CARB, 1992). Investigation of the conversion equipment in the CARB study showed that, in some cases, the systems had been improperly installed and/or maintained. For the purposes of this study, these high emission rates do not affect the objectives and are, indeed, useful in providing high enough concentrations for the smog chamber experiments.

Hydrocarbon speciation gas chromatography (GC) was conducted on each of the two FTPs to obtain a hydrocarbon profile for the vehicle, and the results are shown on Table B-1 in Appendix B. Note that no oxygenate analyses were carried out during these tests. The ratio of NMHC determined by the GC compared to that determined by the analyzer bench FID was 0.97 and 1.02 for the two FTPs, showing excellent recovery in the speciation studies. The GC analyses were able to identify >90% of the NMHCs present in the exhaust. The remaining 10% of the species observed were compounds not identified in the Auto/Oil protocol.

Table 2.Summary of FTP results on vehicles used in this program.

Vehicle	FTP Emissions							
Desig.	NOx	CO	CO2	THC	NMHC	CH4	MeOH	HCHO
			(grams/mile)				(mg/mile)	
Alternative Fueled Vehicles								
LPG	0.15	17.2	236	1.05	0.89	0.16		
	0.18	19.1	257	1.11	0.95	0.16		
M100	0.17	2.5	341	0.07		0.01	551	22.0
	0.21	1.8	363	0.21	0.18	0.01	335	20.9
M85	0.05	0.6	379	0.08	0.07	0.00	114	9.7
	0.16	1.7	376	0.09	0.07	0.02	379	25.2
CNG	0.50	3.6	368	0.77	0.04	0.74	0.0	5.3
RFG Fueled Vehicles								
Rep Car	0.18	2.4	415	0.18	0.11	0.03	11.0	3.1
Suburban	0.53	7.7	625	0.40	0.33	0.07	0.0	3.1
	0.55	8.1	617	0.44	0.37	0.07		
Toyota	1.67	6.2	410	2.14	2.08	0.06		
Honda	0.74	5.9	349	0.24	0.19	0.05		

As has been observed previously for LPG-fueled vehicles, the light-end species account for >85% of the total hydrocarbons identified, with the majority being C1-C4 hydrocarbons. Unreacted propane accounts for >60% of the total hydrocarbon emissions. Generally, the species profile for the two runs agree very well, although there are some differences seen in the ethane and butane profiles between the two runs. This may hve resulted from slight differences in fuel composition since there was a refueling between these runs. Test No. 9605005 was run with the fuel present in the vehicle as received from the SCAQMD, while Test No. 9605011 was run after refueling at a local Riverside LPG station. An analysis was run of this fuel showing it to contain 0.4% methane, 3.0% ethane, and 1.5% butane in addition to propane. Unfortunately, no analyses were performed on the original fuel as obtained from the SCAQMD

M100 Vehicle

The 1993 Ford Taurus FFV used during Phase I of this project was recruited for the Phase II testing (see Table 1). The vehicle is an original equipment manufacturer (OEM) flexible fuel conversion capable of operating on a range of RFG and Methanol up to 85% (M85). Prior testing on M85 and RFG indicate this vehicle provided repeatable emission test results; however, no replicate baseline testing was performed on M100. Since the normal operation of the vehicle does not include the use of M100 or neat methanol, the manufacturer was contacted to insure that vehicle testing on M100 would not result in temporary or sustained performance degradation.

The baseline emission rate for organic material hydrocarbon equivalent (OMHCE) exceeded the standard by 44%; (CARB,1994) however, the majority is attributable to raw methanol in Phase 1 of the FTP. Previous workers (Gabele, 1990) have shown that the organic material hydrocarbon equivalent (OMHCE) emissions of flex-fuel vehicles are relatively unaffected by the fuel methanol content, but the fuel type does strongly influence the composition of the organic material. These studies have shown that as the methanol content increases from 25 to 50 to 85 to 100%, the hydrocarbon content of the exhaust drops dramatically with a corresponding increase in methanol and formaldehyde emissions. The emission rates for CO, CO2 and NO_x are below the standard and are comparable to that found in other late model M85 vehicles. Table 2 shows that the total NO_x, CO, and total hydrocarbon results were comparable, though there is a discrepancy in the formaldehyde and methanol data. Our results, presented in Table 2, are consistent with these previous findings.

While separate FTP tests were conducted with this vehicle during both phases, detailed hydrocarbon speciation measurements were performed during the second test only. In the second phase, the speciated hydrocarbon to integrated FTP THC recovery acceptance criteria for methanol fueled vehicles is similar to that outlined in the Auto/Oil Protocol. A target acceptance of >85% recovery or <5ppm difference between GC and THC FID was achieved for both hot stabilized segments of the FTP. The deviation observed during the cold start phase exceeded the acceptance criteria by 0.11 ppm; however, this is not sufficient to invalidate the test and is within an acceptable range for characterization. The FTP weighted mass emission rate by group indicates that normal alkanes account for 46% of the mass recovered followed by alkenes>branched alkanes>aromatic hydrocarbons>cyclo-alkanes. Unidentified compounds account for less than 1% of the mass recovered. A detailed list of the species identified is provided in Table B-1.

The emission rate of toxic air contaminants (TACs) accounts for less than 6% of the total species

identified and is predominated by formaldehyde emissions at 21 mg/mi. The ozone forming potential (MIR)[1] is 431.4 mg O_3/mi with the specific reactivity of 1.11 gm O_3/gm NMOG which is consistent with the lower reactivity of methanol powered vehicles found in other studies. (Black 1995)

M85 Vehicle

The 1997 Ford Taurus FFV was acquired from UC Riverside Fleet and was utilized for M85 testing. The vehicle is a late model, low mileage (~6900 miles) OEM flexible fuel conversion capable of operating on a range of RFG and methanol up to 85% (M85). The vehicle had recently been placed in service and was operated exclusively on RFG prior to testing. The vehicle is California certified to an alternative fuel TLEV standard for 1997 model year vehicles.

The hydrocarbon certification standard for alternative fuel low emission vehicles is in terms NMOG. The weighted mass emission rate of NMOG by GC exceeds the transition low emission standard (0.125 g/mi) by 32%. The emissions of CO, 0.6g/mi, were significantly below the certification standard of 3.4 g/mi. Emissions of NO_x at 0.05 g/mi, were similarly lower than the standard 0.4 g/mi. Integrated hydrocarbon emissions as measured by the CVS system indicate that hot stabilized emissions were below the ambient background of 1.5-1.7 ppm for Phase 2 of the FTP. This phenomenon has been observed on several occasions with late model low emitting vehicles. Pre and post bag analysis zero span checks indicated the instrumentation was functioning properly and the test was valid. The weighted mass hydrocarbon profile indicates that slightly greater than half of the total, is attributed to methanol which is evolved during Phase 1 of the FTP.

The speciated hydrocarbon profile indicates that methane accounts for 31% of the non methanol hydrocarbons collected. The remaining predominant constituents include in decreasing order of abundance butane > toluene > ethene > m&p-xylene > 2-methylbutane and benzene. These constituents account for 58% of the identified compounds. The distribution according to compound group indicates that normal alkanes account for 46% followed by aromatics>branched alkanes and alkenes. The remaining constituent

---

[1] The MIR's given in conjunction with the FTP tests are those used in the CARB Clean Fuels/Low Emissions Vehicle regulations (CARB, 1993), based on the data of Carter (1994). Note that these differ slightly from MIR's calculated using the updated mechanism utilized when modeling the chamber experiments, as discussed in conjunction with the results of the chamber experiments. The earlier MIR and specific reactivity numbers from Carter (1994) are used in the discussion of the FTP data rather than the updated values to be consistent with the measures of ozone formation potential currently used in conjunction with such data.

groups, cyclo alkanes, alkynes, ethers, and unknowns comprise less than 4% of the total mass identified. The emission rates for aldehydes and ketones are below approximately 40% below the M100 vehicle tested; however this may be a function of the lower vehicle mileage and the more stringent standard to which the vehicle was certified. This profile is similar to that observed in other late model M85 vehicles and does not deviate substantially from the chamber profiles with the exception that a larger percentage of unknowns are present in the chamber experiments. (Clean Fleet,1995)

The mass emission rate of toxic air contaminants is 12.2 mg/mi which is approximately half of that found in the M100 vehicle tested. The profile is similar to the M100 vehicle, with the majority comprised of formaldehyde accounting for 76% of the mass collected followed by acetaldehyde>benzene and 1,3 butadiene. The ozone forming potential was determined to be 255.7 mg O_3/mi with the specific reactivity of 1.53 gO_3/g NMOG identified. The predominant contributors can be traced to the oxygenates formaldehyde> methanol> and the aromatic hydrocarbons and alkynes.

CNG Vehicle

The vehicle used for CNG testing was a 1991 Ford Ranger Pickup that was configured for dedicated CNG use. This vehicle was tested previously in other programs and found to be repeatable within a range of $\pm 10\%$ for THC, NMHC and NO_x. The deviation for CO and CO2 from test to test is slightly greater, but within a range of $\pm 15\%$. The FTP results are summarized in Table 2, and the results of the speciated analyses are given in Appendix B. They indicate that both THC and NO_x emission rates exceed the certification standards by 88% and 25% respectively. Examination of the emission rate of NMHC indicates the bulk of the THC measured is comprised of methane. The ratio between the emission rates for THC and NMHC are consistent from phase to phase with that observed in other CNG vehicles where the elevated emission rate for THC and relatively low NMHC emissions are consistent with that found in other gaseous fuel retrofit conversions, where the conversion kit can have a substantial impact on the emission performance of these vehicles.

Full hydrocarbon speciation was not performed during the baseline tests due to the low inherent reactivity of the fuel. However, sampling for oxygenates was included. Problems in recovery prohibited the determination of a methanol emission rate. The emission rate for aldehydes were greatest for formaldehyde>acrolein>acetaldehyde and no measurable ketones were recovered. Prior test data on gaseous fuel vehicles indicates the emission rates of methanol, ethanol are at or below detection limits. The emission rates of air toxics, benzene, formaldehyde, acetaldehyde and 1,3-butadiene are (with the exception of

formaldehyde) substantially lower than those obtained for equivalent vehicles operating on either methanol or gasoline and are consistent with that reported elsewhere. (Black, 1995)

RFG Vehicles
1991 Dodge Spirit

The test matrix for the RFG vehicles included two late model low mileage and two older high mileage vehicles. The first vehicle tested was a fuel injected 1991 Dodge Spirit FFV. This vehicle is a pre-production OEM M85 conversion which is in service as the CE-CERT VERL repeatable correlation vehicle or "Rep Car". The FTP weighted mass emission rates are well below CARB 93-94 certification standards for NMHC, CO and NO_x and are consistent with the mean and standard deviation observed in routine correlation exercises performed by VERL. The recovery rate between integrated and speciated mass emission rate for the FTP is above the 90% and or less than 3 ppm targets set for gasoline vehicles as outlined in the Auto/Oil protocol. The speciated hydrocarbon profile for the identified compounds indicates that methane accounts for the largest constituent in both the baseline and chamber tests. The remaining constituents are comprised of the remaining normal alkanes> aromatics >branched alkanes> alkenes. The remaining unidentified compounds account for 1% of the total mass recovered. The resultant ozone forming potential (MIR) was determined to be 484 mg O_3/mi with a corresponding specific reactivity of 2.82 g O_3/ g NMOG. The species profile is predominated by aromatic hydrocarbons and alkenes each accounting for 36% of the total profile. The remaining segment is comprised of branched alkenes > aromatic oxygenates > alkynes each contributing approximately 8% of the total identified.

The emission rate of toxic air contaminants is lower than that observed in the methanol vehicles by a factor which ranges from 1.5 for the M85 vehicle and to 2.6 for the M100 vehicle. It should be noted that the upper limit is consistent with the average observed in older M85 FFV in service. (Norbeck et al, 1998) The species profile indicates that benzene emissions are the highest of the TACs at 3.9 mg/mi followed by formaldehyde, 3.12 mg/mi and acetaldehyde and 1,3 butadiene each account for less than 1 mg/mi.

1994 Chevrolet Suburban

The second late model vehicle included in the test matrix a 1994 ½ ton two wheel drive Chevrolet Suburban. This vehicle is equipped with a fuel injected 5.7 liter V8 engine which is operated on RFG exclusively and is certified to the secondary light duty truck chassis standard. This vehicle is assigned to CE-CERT and has been routinely used in other vehicle emission programs. The vehicle has demonstrated an integrated emission rate that is consistant with that observed in both previous tests and other late model, full size, light duty trucks. The FTP weighted mass emission rate is below the secondary certification

standard, 0.5 g/mi NMHC, 9.0 g/mi CO and 1.0 g/mi NOx, for all regulated emissions. A second test baseline test was performed without hydrocarbon speciation and the integrated results are equivalent within a range of 10%.

The recovery rate between integrated and speciated mass emission rate for the FTP is above the 90% and or less than 3 ppm targets set for gasoline vehicles as outlined in the Auto/Oil protocol. The speciation profile indicates roughly equivalent apportionment between branched alkanes > aromatic hydrocarbons > alkenes. The recovery of normal alkanes account for 33% of the mass with the leading constituent being methane > butane > pentane > hexane. The leading aromatic hydrocarbons include toluene > benzene > m&p-xylene > o-xylene, each accounting for 3% total mass identified The distribution of alkenes has a larger range with ethene (6%) > 1-butene(3%)>propene (2%) of the total mass identified. The emission rate of toxic air contaminents were the lowest recorded for the vehicles tested at 4.48 mg/mi. Formaldehyde emissions account the largest constituent, accounting for 70% of the TACs. Those compounds not identified in the Auto/Oil protocol account for slightly greater than 2% of the total mass recovered.

The ozone forming potential and specific reactivity (MIR) as determined from the speciation profile is 1,018.4 mg O3 /mi with a corresponding specific reactivity of 2.83 g O3 / g NMOG. The species profile is predominated by the alkenes and aromatic hydrocarbons which account for 72% of the formation potential. The primary contributors (Ethene > 1-butene > propene) account for 39% of the total formation profile.

1988 Honda Accord

The final two vehicles were added to the matrix after the Phase II testing had been completed. The vehicles were selected based on their representativeness of the on road fleet and high in service mileage accumulations. The 1988 Honda Accord, with a 2.0 liter 4 cylinder engine, is a high mileage example which has had routine maintenance performed during the course of its in service operation. The vehicle was equipped with the original catalytic converter and emission control system. It was tested using the in-tank RFG obtained within the South Coast Air Basin from a retail vendor. The vehicle was preconditioned over a roadway preparation cycle in accordance with the CFR. Following the preconditioning cycle the vehicle was baseline tested over the FTP. The exhaust was not sampled for NMOG speciation during the FTP tests, though speciation was carried out in conjunction with the chamber experiments.

The FTP integrated NMHC mass emissions rate was 41% below the certification standard while the

CO was only 15% below standard. The emission rate for NO_x exceeded the standard by 6%. The overall emission profile is consistent with a vehicle whose emission control components are providing the signs of deterioration or failure.

1984 Toyota Pickup

The final vehicle tested was a 1984 Toyota Pickup equipped with the original 2.4 liter 4-cylinder engine. The detailed vehicle maintenance history of the vehicle was not available; however, during the course of ownership, a range of restorative maintenance had been performed. The vehicle was tested with the original equipment catalytic converter and corresponding emission control equipment. The vehicle was tested on the in tank RFG obtained from the Temecula, California area from a retail vendor. The vehicle was preconditioned over a roadway preparation cycle in accordance with the CFR. Following the preconditioning cycle the vehicle was baseline tested over the FTP. The exhaust was not sampled for NMOG speciation during the FTP tests, though speciation analyses were carried out in conjunction with the chamber experiments.

The FTP integrated mass emissions exceeded the certification standard for THC and NMHC by a factor of 5, while NO_x emissions exceeded the standard by a factor of 4.2. CO emissions were slightly below the standard, however the overall emissions would place this vehicle in a high to super emitter category. This is despite the fact that the vehicle was recently tested and passed the bi-annual BAR 90 smog check, after unplugging the EGR line.

Summary

The vehicle test matrix employed in this study includes a diverse cross section of late model and intermediate age alternative fuel and conventional fuel vehicles. These vehicles are all equipped with catalytic converters and show a range of restorative and preventative maintenance. The mass emission rates are similarly diverse with TLEV certified vehicles tested with older malfunctioning super emitters. Therefore, they provide a varied set of exhaust types for reactivity evaluation in the environmental chamber experiments.

Environmental Chamber Experiments

Approximately 140 environmental chamber experiments were carried out for this program. These include characterization and control runs to determine chamber-dependent parameters needed for model simulations and to assure data validity and consistency of results with previous experiments, methanol and aldehyde control runs to evaluate the ability for the model to simulate reactions of these important alcohol

fuel constituents, runs with actual exhaust using the vehicles discussed in the previous sections, and runs with synthetic exhaust mixtures designed to simulate the experiments carried out with the actual exhausts. A chronological listing of all these experiments, including the title, date, description, and a brief summary of the results, including results of model simulations where applicable, are given in Appendix C to this report. The following sections discuss in detail the results of the various types of experiments, beginning with a discussion of the characterization and control runs, followed by a discussion of the runs with each of the individual fuel types and vehicles.

Characterization and Control Experiments
Light Intensity Measurements

As indicated above, the light intensity in these experiments was monitored by conducting periodic NO_2 actinometry experiments using the quartz tube method of Zafonte et al (1977), modified as discussed by Carter et al (1995c). During the course of this program, three different reaction bags (designated Bags 2 through 4) were employed, with the light bank employed being changed when Bag 2 was replaced by Bag 3. The results of all the NO_2 actinometry experiments carried out using these bags, up to the time of the beginning of the preparation of this report, are plotted against DTC run number in Figure 4. Note that this includes actinometry runs carried out for other programs as well as this, which are not listed on Table 3. Note that most experiments were carried out using 50% lights, but this was not the case for all actinometry runs. To place these data on a common basis, the runs at light intensities other than 50% are adjusted by the appropriate factor to make them comparable, as indicated in the figure legend. The lines through the points show the linear least squares fits which were used to assign NO_2 photolysis rates to the various experimental runs for modeling, given their run number. The two sets of lines refer to assignments based on differing assumptions concerning the validity of the actinometry results between DTC610 and DTC646, as discussed below.

If no changes to the chamber or lights are made, there is generally a continual slow decline in light intensity due to the aging of the lamps. When Bag 3 was installed the light banks used were also changed, with less aged, and therefore brighter, lights being used. The lights were not changed subsequent to this, and a ~20% decrease in the apparent NO_2 photolysis ates around the time of DTC600 is difficult to rationalize. The lights were not changed when Bag 3 was replaced, but during that time we started carrying out experiments using 75% light intensity, in an attempt to make the lighting conditions for the synthetic exhaust runs more comparable to those when the exhaust runs they were duplicating were carried out. This was done by using some lights from both of the light banks. The actinometry results (adjusted for differences in % lights) did not change significantly when the bag and lighting procedure was changed.

31

Figure 4.   Plots of results of NO2 actinometry experiments against run number.
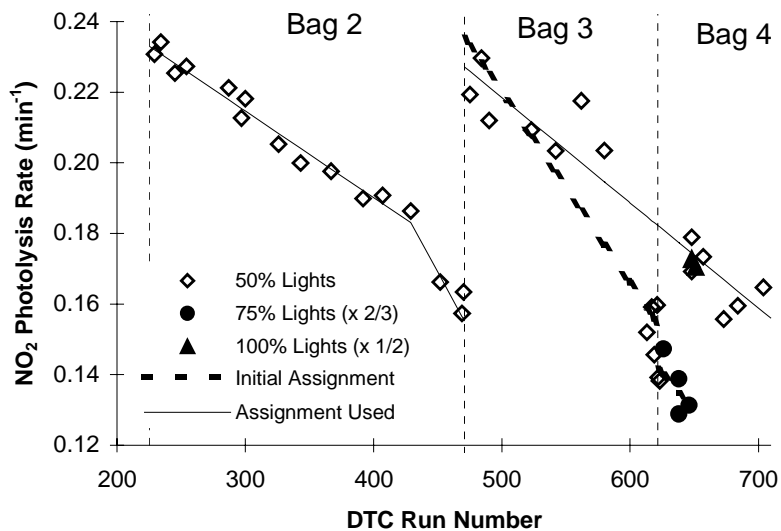
Figure 5.   Plots of ozone formed and NO oxidized in the standard replicate mini-surrogate experiments against the assigned NO2 photolysis rates.
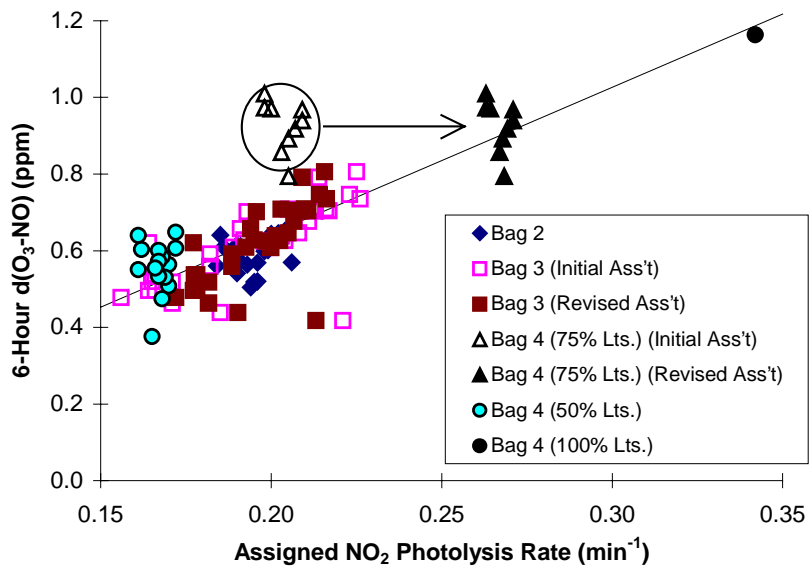
This suggests that the bag and light bank changes did not significantly affect the overall light intensity on a per-light basis. Note that by this time, both light banks were about equally aged.

However, if the data from the NO_2 actinometry experiments carried out between DTC610 and DTC646 are used as the basis for assigning the NO_2 photolysis rates for the experiments (i.e., the assignments shown as the dashed lines on the figures), it was found that the model significantly overpredicted the O_3 formation and NO oxidation rates in the experiments carried out during this period using 75% lights. This is despite the fact that the model fits the data with no apparent biases for similar runs carried out at different times. In particular, a large number of replicate standard mini-surrogate - NO_x experiments were carried out in conjunction with incremental reactivity experiments for this and other programs, and model simulations predict that the final amount of O_3 formed and NO oxidized, or $D(O_3\text{-}NO)$ (see discussion of this quantity above) will be relatively sensitive to the light intensity assumed. Figure 5 shows the 6-hour $D(O_3\text{-}NO)$ data for all the standard mini-surrogate experiments carried out since the beginning of this program (including runs carried out for other programs), plotted against the assigned NO_2 photolysis rates. This shows that the 6-hour $D(O_3\text{-}NO)$ is indeed correlated with the assigned NO_2 photolysis rates. However, the results of the experiments carried out with 75% lights do not agree with this correlation if the results of the associated NO_2 actinometry experiments are used to derive their NO_2 photolysis rates. This can be seen by looking at the "Bag 4 (75% Lts.) (Initial Ass't)" points on the figure.

Once the problem with modeling the 75% lights runs was recognized, it was decided to go back to the lighting configuration previously employed. Therefore, the light banks were changed back to the configuration that permitted use of 50% (and 100%) lights. At that time, it was found that the quartz tube was positioned where it might be shaded by some of the reaction bag supports (it was normally positioned between the two reaction bags), though it did not seem like this should have a large effect. During this period the lights were also cleaned of dust, which was not done when the bags were changed previously. Subsequently, NO_2 actinometry experiments were carried out at both 50% and 100% light intensity, and all subsequent experimental runs were carried out using 50% lights. The only exception was one standard mini-surrogate run carried out using 100% lights to provide more data on the effect of light intensity on mini-surrogate results.

Figure 4 shows that the changes made when reconfiguring the lights banks from 75% back to 50 or 100% capability resulted in a increase in the measured NO_2 photolysis rates, to a level which fit the trend defined carried out in Bag 3 prior to the sudden decrease around the time of DTC600. If it is assumed that the low actinometry numbers between DTC600 and DTC648 are in error (perhaps due to the obstruction of

the quartz tube actinometer with the reaction bag framework) and those data are rejected, then the other data in both bags are fit well by the same line, shown as the solid lines on the plots in Figure 4. If those lines are then used to derive the NO_2 photolysis rates for the 75% light mini-surrogate experiments, then their $D(O_3-NO)$ results become consistent with the results of the experiments at the other light intensities, as shown by the "(Revised Ass't)" points on Figure 5. Note that the results of the one 100% lights mini-surrogate experiment is also entirely consistent with results of the other experiments, which together suggest an approximately linear dependence of $D(O_3-NO)$ on the light intensity.

Based on these results, we conclude that it is probable that the actinometry experiments between DTC600 and DTC648 may be anomalously low, and thus their data should not be used for deriving light intensity assignments for modeling. Therefore, the light intensities used when modeling all Bag 3 and Bag 4 runs in this program were derived using the line fits which ignored these data, shown as the solid lines on Figure 4. This yielded consistent results when modeling the full data base of experiments carried out in these reaction bags. However, the reason for the apparently anomalous results of these actinometry runs has not been definitively established.

Chamber Effects Characterization

The other chamber characterization experiments consisted of n-butane - NO_x or CO - NO_x experiments to measure the chamber radical source, ozone dark decay experiments to measure losses of O_3 on the walls, pure air irradiations to measure background effects, and standard propene - NO_x experiments to test for side equivalency and for comparison with results of similar runs in this and other chambers. The purposes and methods for analyzing the data for these experiments have been discussed previously (Carter et al, 1995c, and references therein), and the major results of these experiments are given with the run summaries in Appendix C.

As noted in Appendix C, the results of most of these experiments are within the normal range, and consistent with the predictions of the standard chamber model. The only significant exception was that during the first set of experiments for Phase 2 (runs DTC545-616) which employed Bag #3, the chamber radical source, as determined by modeling the n-butane - NO_x and CO - NO_x experiments, was ~33% higher on Side A than on Side B. This may have been due to the fact that during that period the injection ports were such that the exhausts could only be injected into Side A. This had only a relatively small effect on results of the incremental reactivity experiments, as discussed in the following section. The radical sources in Bags 2 and 4 were essentially the same on both sides, and within the normal range. The chamber dependent

34

parameters used when modeling the chamber experiments for this program took these results into account, and are given in Table A-4 in Appendix A.

Side Equivalency Tests

Since a number of experiments for this program involved determining the effects of adding exhausts or synthetic exhausts to standard ambient surrogate - NO_x experiments, an important control experiment is to determine if differences are found if nothing is added to the standard experiment. Therefore, a number of "side equivalency tests" were carried out in which the same surrogate - NO_x mixture was simultaneously irradiated in both sides of the chamber. These were carried out periodically during Phase 2 of this program to assess the current state of the chamber. Six such experiments were conducted using the standard mini-surrogate experiment (which is expected to be the most sensitive to background effects since it is generally more sensitive to added VOCs (Carter et al, 1995c), and one such experiment used the full surrogate. The conditions and major results of these experiments are summarized in Table 3, and the concentration vs. time plots for $D(O_3-NO)$, difference in $D(O_3-NO)$, m-xylene, and difference in IntOH (which is calculated from the m-xylene data as discussed above) are shown on Figures 6 and 7. Results of model calculations are also shown on these figures.

It can be seen from Figures 6 and 7 that excellent side equivalency was obtained in all experiments except for the mini-surrogate run DTC590 and the full surrogate run DTC616. Both of those experiments were carried out around the latter period when Bag 3 was in use, when the n-butane runs indicated a ~33% higher radical source on Side A. However, even for those experiments the side differences were small compared to the effects of adding most of the exhausts or synthetic exhausts, as shown in the subsequent sections, and good side equivalency was obtained for m-xylene consumption and therefore calculated IntOH. The model, which incorporated the differences in radical source as indicated by the n-butane runs (see Table A-4) predicted the side differences for the full surrogate experiment very well, but slightly underpredicted the side differences for the mini-surrogate run DTC590. However, even in that case the difference was small enough that it should not significantly affect conclusions concerning the ability of the model to simulate effects of added exhaust mixtures to these experiments.

Figures 6 and 7 also show that there is some variability in the ability of the model to simulate $D(O_3-NO)$ formation and m-xylene consumption in these standard surrogate experiments, with the model somewhat underpredicting $D(O_3-NO)$ formation and m-xylene consumption rates in about half the mini-surrogate experiments, and somewhat overpredicting the $D(O_3-NO)$ in the full surrogate run. This is the usual level of variability observed when modeling these types of the experiments, and can also be seen in

Table 3.   Summary of conditions of side equivalency tests and aldehyde or methanol test runs.

Type / Run	$k(NO_2+ h\upsilon)$ (min^{-1})	Initial concentrations (ppm)				Base ROG (ppmC)	Data Plots
		NO	NO2	Aldehyde	Methanol		
Mini-Surrogate - NOx Side Equivalency Tests							
DTC570A	0.20	0.26	0.10			5.70	Fig 6
DTC590A	0.19	0.32	0.10			6.07	6
DTC627A	0.27	0.27	0.10			5.71	6
DTC645A	0.26	0.32	0.11			5.76	6
DTC649A	0.17	0.29	0.08			5.84	7
DTC668A	0.17	0.27	0.10			5.67	7
Full Surrogate - NOx Side Equivalency Tests							
DTC616A	0.18	0.38	0.42			3.93	7
Formaldehyde - NOx							
DTC387A	0.19	0.20	0.06	0.44			8
DTC630A	0.27	0.15	0.08	0.46			8
Mini-Surrogate + Formaldehyde							
DTC631B	0.27	0.25	0.12	0.27		5.80	10
DTC653A (a)	0.35	0.26	0.07	0.28		5.89	10
Methanol - NOx							
DTC382A	0.20	0.06	0.01		14.35		11
DTC561B	0.20	0.14	0.06		5.19		11
DTC579A	0.20	0.20	0.08		5.50		11
Methanol + Formaldehyde - NOx							
DTC379A (b)	0.20	0.06	0.01	0.07	13.58		12
DTC561A	0.20	0.14	0.06	0.21	4.99		12
DTC579B	0.20	0.20	0.08	0.26	5.66		12
Acetaldehyde NOx							
DTC387B	0.19	0.19	0.06	0.44			9
DTC630B	0.27	0.15	0.08	0.71			9

(a) Carried out with 100% lights (twice normal light intensity).

(b) Intended to duplicate M100 exhaust run DTC374 based on erroneous methanol analysis.

| DTC570 MINI-SURROGATE | DTC590 MINI-SURROGATE | DTC627 MINI-SURROGATE | DTC645 MINI-SURROGATE |

d(O₃-NO) (ppm)

Difference in d(O₃-NO)

m-Xylene (ppm)

Difference in IntOH

- □ **Side A Data**
- — **Side A Model**
- — **Side B Model or Model Difference**
- ◆ **Side B Data or B Data - A Data**
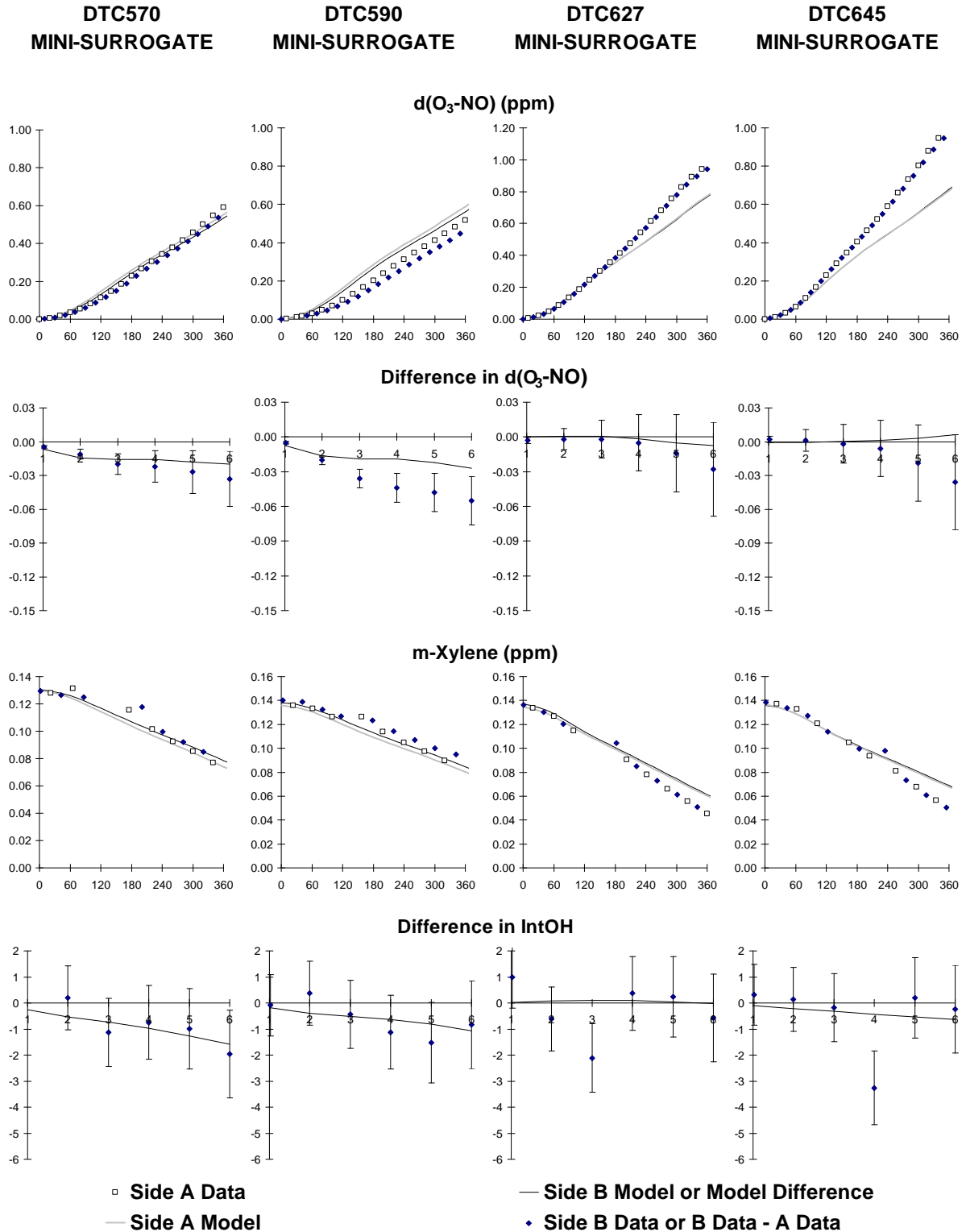
Figure 6.   Plots of selected results of the mini-surrogate side comparison test experiments DTC570 though DTC645.

37

DTC649
MINI-SURROGATE

DTC668
MINI-SURROGATE

DTC616
FULL SURROGATE

d(O$_3$-NO) (ppm)

Difference in d(O$_3$-NO)

m-Xylene (ppm)

Difference in IntOH

□ Side A Data
— Side A Model

— Side B Model or Model Difference
♦ Side B Data or B Data - A Data

Figure 7.   Plots of selected results of the mini-surrogate side comparison test
experiments DTC649 and DTC668 and the full surrogate side comparison
test experiment DTC616.

38

the simulation of the base case side in the added exhaust experiments discussed in the following sections. This variability in model performance can be attributed to uncertainties or variabilities in chamber characterization and uncertainties in measured initial reactant concentrations. Note that these relatively small discrepancies should cancel out when evaluating how well the model can predict side-by-side differences caused by adding exhaust mixtures, since if (for example) it overpredicts on the base side it would be expected to overpredict by about the same amount on the added exhaust side, if there is no problem with the model for the exhaust mixture itself.

Methanol and Aldehyde Model Evaluation Tests

Methanol and formaldehyde are important components of M100 and M85 exhausts, and it is useful to evaluate how well the model can simulate experiments with those compounds alone (or together) as a part of an evaluation of how well the model can simulate reactivities of those exhausts. For that reason, several VOC - NO_x experiments with formaldehyde, methanol, and methanol + formaldehyde, and several formaldehyde incremental reactivity experiments were carried out in conjunction with the evaluations of M100 and M85 exhausts for this program. Acetaldehyde - NO_x control runs were also carried out at the same time as the formaldehyde runs to evaluate whether any model inconsistencies may be the same for both of these photoreactive compounds. In addition, the formaldehyde incremental reactivity experiments were carried out at different light intensities to evaluate how well the model could predict the reactivity of this photoreactive compounds at different light intensities, as well as to obtain mini-surrogate data at 100% lights (see discussion above). The conditions and major results of these experiments are summarized on Table 3, and experimental and calculated concentration-time plots for the major measured species are given on Figures 8-12.

The results of the formaldehyde - NO_x and the simultaneous acetaldehyde - NO_2 experiments are shown on Figures 8 and 9. Note that one experiment was carried out during Phase 1 of the program while the other was carried out about two years later, during Phase 2. The model was found to somewhat underpredict the observed O_3 formation and NO oxidation rates, though to a somewhat greater extent on the first experiment than on the second. On the other hand, the simultaneous acetaldehyde - NO_2 experiments were reasonably well simulated. The somewhat greater discrepancies in the simulations of the formaldehyde runs may be due to uncertainties in characterizing the initial formaldehyde level, since in both experiments the measured formaldehyde levels are higher than the model prediction after the lights are turned on. (The initial formaldehyde concentrations are determined by the pre measurements made before the lights were turned on, which are not shown on the figure.) However, the discrepancy for run DTC630A was relatively small.
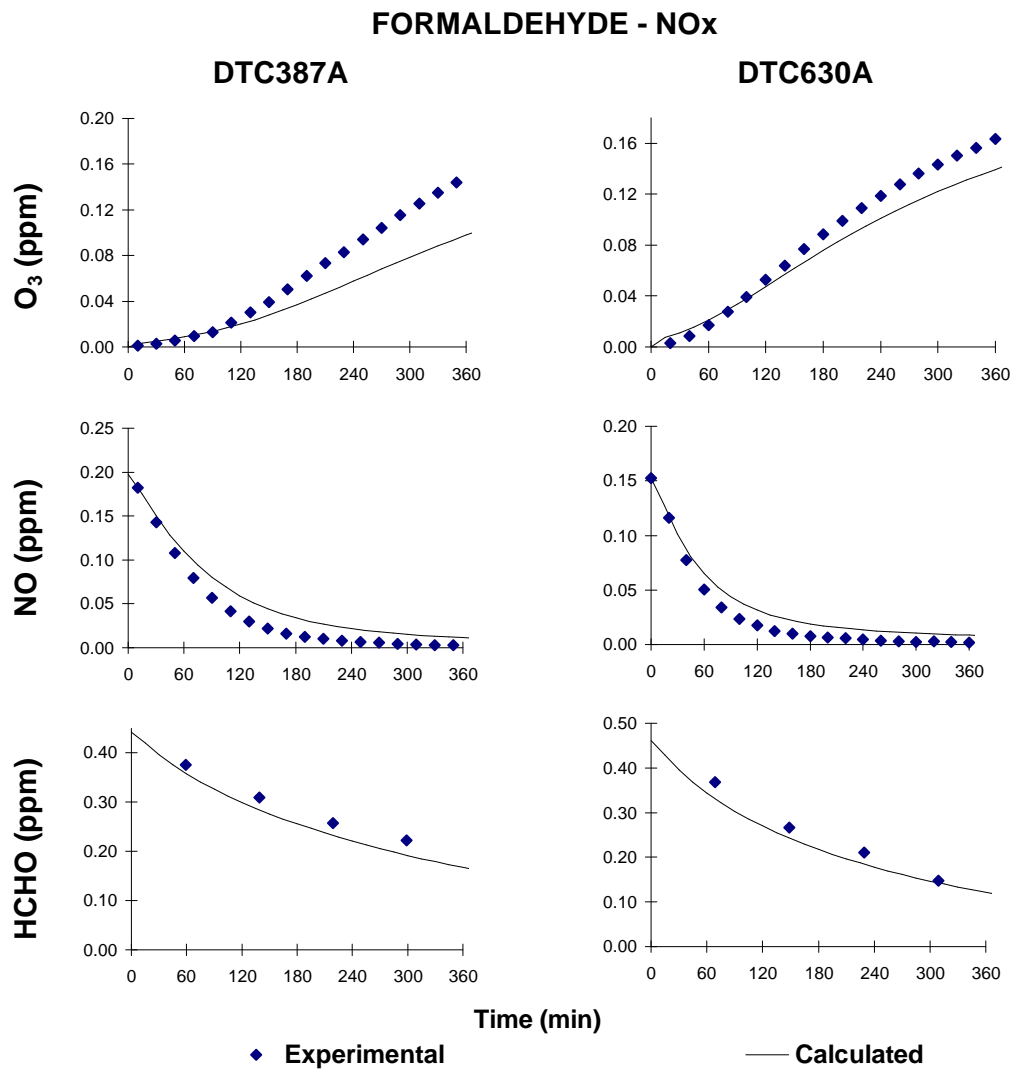
Figure 8.   Experimental and calculated concentration-time plots for selected species in the formaldehyde - NO$_x$ runs.
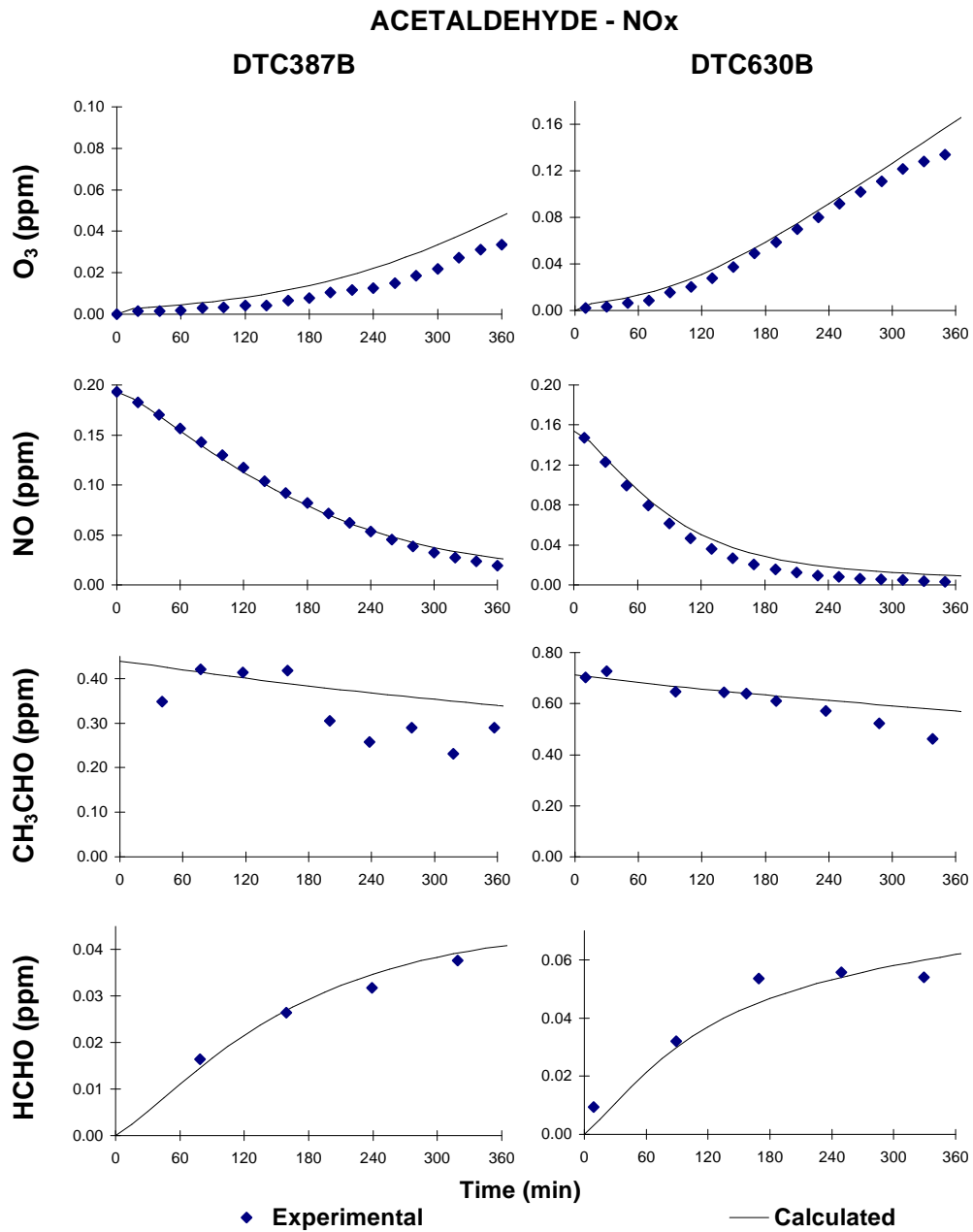
ACETALDEHYDE - NOx

Figure 9.   Experimental and calculated concentration-time plots for selected species in the acetaldehyde - NO$_x$ runs.
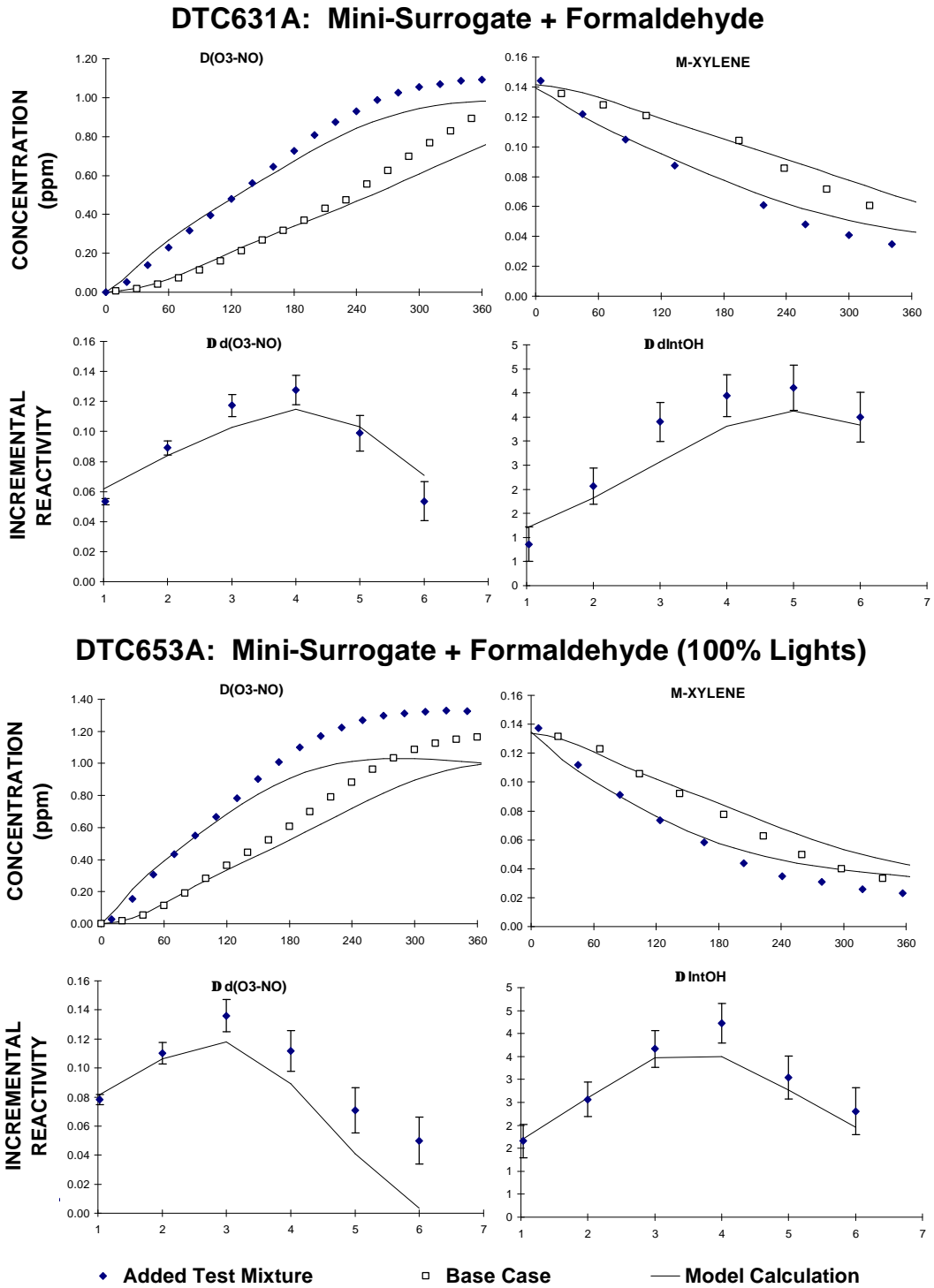
Figure 10.   Experimental and calculated results of incremental reactivity experiments with formaldehyde.
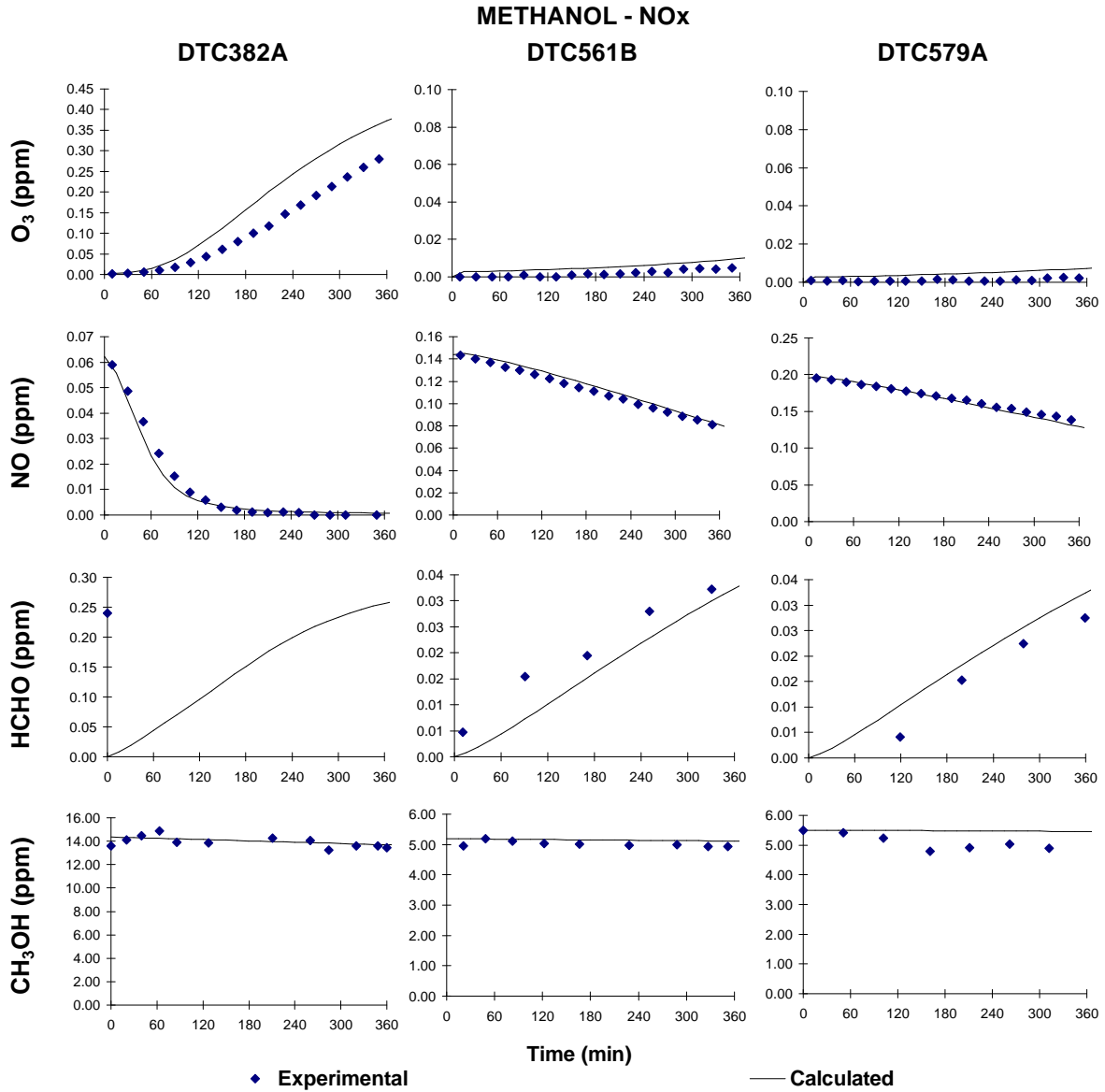
METHANOL - NOx

Figure 11.   Experimental and calculated concentration-time plots for selected species in the methanol - NOx runs.

METHANOL + FORMALDEHYDE - NOx
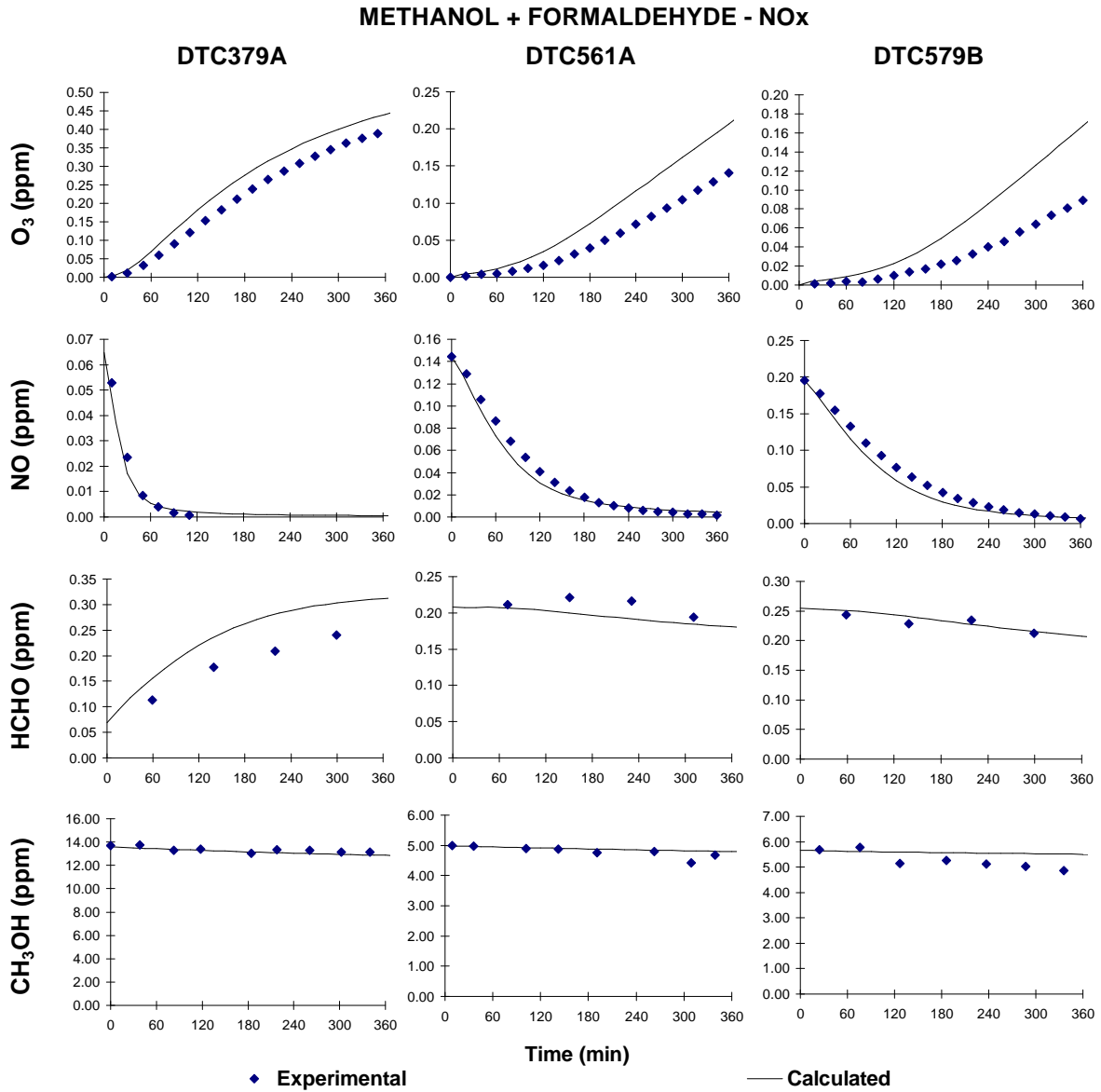
Figure 12.   Experimental and calculated concentration-time plots for selected species in the methanol + formaldehyde - NO$_x$ runs.

The results of the mini-surrogate with formaldehyde incremental reactivity experiments are shown on Figure 10. In both cases, the model somewhat underpredicted the reactivity of the base case experiment, but gave a reasonably good simulation of the effect of added formaldehyde. There may be a slight tendency to underpredict $D(O_3$-NO) and IntOH incremental reactivities, which is consistent with the tendency towards underprediction observed in the formaldehyde - NO_2 experiments. However, this reactivity underprediction may also be related to the tendency to underpredict the base case experiment.

It is interesting to note that the model underpredicts the maximum ozone in the 100% lights experiment to a greater extent than the usual run-to-run variability in model performance in simulating this type of run. This may suggest a problem with the ability of the base mechanism in predicting light intensity effects for this surrogate. This in turn suggests a possible problem in the mechanism for m-xylene, the most reactive component of the surrogate that also has the most uncertain mechanism. However, more data are needed before this can be evaluated further, and this issue is somewhat beyond the scope of this particular study.

Figure 11 shows the results of the methanol - NO_x experiments. The amount of methanol added in the latter two of those runs was too small for appreciable ozone to form, but the model simulated reasonably well the rate of NO oxidation and also the rate of formaldehyde formation from methanol. The amount of methanol added in the first run was enough for ozone formation to occur, which the model slightly overpredicted. There were no valid data on formaldehyde formation in this experiment, so the model performance in this regard could not be evaluated.

Figure 12 shows the results of the three methanol with formaldehyde experiments that were not designed specifically to be synthetic methanol exhaust runs (or were designed to be represent these exhausts based on what subsequently was found to be invalid data). In all three cases there was a tendency of the model to overpredict O_3, though the discrepancy was not large in terms of absolute amounts of ozone formed. This is despite the fact that the model somewhat underpredicted the ozone in the formaldehyde - NO_x runs but consistent with the tendency to overpredict in the methanol only runs. Although this discrepancy is not large, it should be borne in mind when evaluating the results of the experiments with M100 and M85 exhausts.

Evaluation of LPG Exhaust

Exhaust Injection Procedures and Analyses

All the experiments with LPG exhaust were carried out during Phase 1, and thus used the flow dilution system to transfer the exhaust to the chamber. To obtain a relatively constant dilution ratio during sampling, these tests were run under 45 mph steady-state conditions. The dilution ratio in the CVD system was set to provide a diluted exhaust sample with approximately 50% relative humidity at ambient temperature to avoid water condensation in the sample transfer line.

As shown in the run listing in Appendix C, a total of nine vehicle emission runs were performed with transfer of LPG exhaust to the smog chamber. In the initial vehicle runs (DTC339, DTC340, DTC342, and DTC344), the diluted exhaust was sampled with the vehicle in fully warmed-up, hot-stabilized condition. Under these conditions, it was found that the only significant VOC present was propane. Subsequent testing showed that sampling from a cold-start condition resulted in the presence of non-negligible amounts of ethene and propene with an observed increase in the NO oxidation rate and ozone formation. The revised test protocol involved a cold-start after a 12-36 hour soak followed by a vehicle acceleration to 45 mph. Immediately upon reaching the 45 mph steady-state condition, transfer of the diluted exhaust to the smog chamber was begun together with sampling for analyses.

Table 4 gives the exhaust analysis data for the LPG vehicle runs which were carried out using the cold start procedure. The table compares the hydrocarbon profile measured immediately after the exhaust dilution point (by the CE-CERT Analytical Laboratory) and that measured in the smog chamber after transfer and dilution (by the Atmospheric Processes Laboratory). Since the amount of air initially in the chamber could not be accurately measured, the dilution ratio after mixing exhaust into the smog chamber could not be determined directly. In order to compare the two measurements, the ratio of CO measured by the VERL to that measured in the smog chamber was used to adjust the AL to the APL measurements so that they would be equivalent. CO was used since we did not expect transfer losses from this inert compound. The ratio was typically 24. The results show good agreement for the hydrocarbon profiles obtained at these two sampling locations and methods, indicating there is not a significant loss of reactive species during the transfer to the smog chamber.

As an additional check to see if the transfer method is affecting the reactivity, chamber run DTC355 was performed with the diluted exhaust collected in a Tedlar bag and transferred to the smog chamber

Table 4.   VOC, NOx, and NMHC measurements taken during the environmental chamber experiments employing LPG exhaust.

Vehicle Run No.	5		6		7		8		9 [a]	
Chamber Run No.	DTC348		DTC349		DTC351		DTC354		DTC355	
Analysis [b,c]	VERL	APL	VERL	APL	VERL	APL	VERL	APL	VERL	APL
Hydrocarbons (ppm)										
Methane	0.43	[d]	0.42	[d]	0.39	[d]	[e]	[d]	0.21	[d]
Ethane	0.18	-	0.18	-	0.16	-		-	0.08	-
Ethene	0.90	0.82	0.86	1.00	0.80	0.92		0.08	0.44	0.38
Propane	4.17	4.50	1.37	4.74	3.87	4.35		2.61	1.83	1.59
Propene	0.36	0.36	0.36	0.42	0.33	0.42		0.27	0.18	0.18
Butane	0.16	0.12	0.16	0.16	0.16	0.16		0.08	0.08	0.08
2-Methylpropane	0.16	0.16	0.16	0.16	0.12	0.16		0.08	0.08	0.04
Unknown (ppmC)	0.32		0.30		0.28				0.09	
NMHC (ppmC)	6.25	5.96	6.13	6.48	5.72	6.01		3.12	2.78	2.27
NOx (ppm)	0.29	0.28	0.25	0.34	0.28	0.35	0.18	0.28	0.09	0.08

[a] Exhaust transferred to the chamber using a Tedlar bag
[b] VERL: Hydrocarbon data obtained from the CE-CERT Vehicle Emissions
     Analytical Laboratory analysis of sample collected immediately after vehicle exhaust dilution, with
     concentrations have been corrected for additional dilution which takes place in the smog chamber. Total NMHC
     and NOx data taken from the Vehicle Emissions Research Laboratory analyzer bench, corrected for dilution
     when transferred to the chamber.

[c] APL: Analyses in the environmental chamber using the instrumentation in the chamber laboratory.
[d] Methane analysis of chamber contents not preformed
[e] No analytical laboratory data for this experiment.

without using any pumps or valves. As the results in Table 4 show, this did not have a significant impact on the hydrocarbon species profile.

Table 4 also compares NO_x measured by the VERL emissions bench at the outlet of the mini-diluter and at the smog chamber by the APL. The NO_x measured by the APL was an average of 18% higher while the NMHC measurements were within 25%. The reason for the discrepancy in the NO_x data, which may be slightly outside the uncertainty range in the CO data used for the dilution correction, is not known. Better agreement between the AL and APL NO_x measurements were observed in the M100 experiments, discussed later.

Irradiation Results

The experiments carried out using actual or synthetic LPG exhaust are summarized in Table 5. As indicated there, three types of LPG exhaust runs were carried out: (1) one preliminary run with warm-stabilized LPG exhaust and the mini-surrogate injected in both sides of the chamber for testing the injection method; (2) three incremental reactivity experiments (one with warm-stabilized and two with cold-start LPG exhaust); and (3) three experiments with either cold-start LPG exhaust irradiated by itself on one side of the chamber and exhaust with added formaldehyde irradiated on the other. In addition, two experiments with synthetic cold-start LPG exhaust were carried out to duplicate two of the experiments with actual exhaust, one mini-surrogate reactivity run and one exhaust and exhaust with formaldehyde run. The synthetic LPG exhaust consisted of mixtures of CO, propane, isobutane, n-butane, ethene, and propene in the concentrations observed in the corresponding experiment with the actual exhaust, as indicated on Table 4.

Figure 13 shows concentration-time plots of ozone, NO, propane, propene, formaldehyde and PAN measured in the LPG exhaust chamber experiments, and Figure 14 shows similar results for the LPG exhaust experiment where the transfer bag was used, and for the comparable run with synthetic LPG exhaust. From Figure 13 it can be seen that essentially no ozone was formed in the run with warm-stabilized exhaust (DTC344A), and only relatively slow NO oxidation occurred. No measurable initial olefins were present, and formation of PAN and formaldehyde was insignificant. On the other hand, as shown on Figures 13 and 14, significant ozone formation occurred in the runs with the cold-start exhaust, and measurable amounts of formaldehyde and PAN were generated in the photochemical reactions. This is consistent with the fact that the cold-start emissions not only had significantly higher levels of propane, but also significant levels of ethylene and propene, which have relatively high reactivity. Very similar results were obtained in

48

Table 5.   Summary of experimental runs using actual or synthetic LPG exhaust.

Type / Run	k(NO₂+ hv) (min⁻¹)	NO	NO2	CO	Initial Reactants (ppm) Propane	Isobutane	n-Butane	Ethene	Propene	HCHO	Base ROG (ppmC)	Data Plots Figure
LPG (Warm)												
DTC344A	0.20	0.20	0.05	19	0.70	(a)	(a)	(a)	(a)	(a)	-	3-1
LPG (Cold)												
DTC348B	0.20	0.23	0.04	43	1.44	(a)	0.04	0.41	0.12	(a)	-	3-1
DTC349A	0.20	0.26	0.07	43	1.55	0.04	0.05	0.51	0.15	(a)	-	3-1
DTC355A (b)	0.20	0.08	0.02	21	0.53	0.01	0.02	0.20	0.06	(a)	-	3-2
Synthetic LPG (Cold)												
DTC350A	0.20	0.29	0.08	43	1.65	0.04	0.04	0.52	0.15	(a)	-	3-2
LPG (Warm)+ HCHO												
DTC344B	0.20	0.20	0.05	19	0.69	(a)	(a)	(a)	(a)	0.23	-	3-3
LPG (Cold) + HCHO												
DTC348A	0.20	0.23	0.04	43	1.47	(a)	0.04	0.42	0.12	0.25	-	3-3
DTC349B	0.20	0.27	0.06	43	1.57	0.04	0.05	0.52	0.15	0.23	-	3-3
DTC355B (b)	0.20	0.08	0.02	20	0.52	0.01	0.02	0.19	0.06	0.10	-	3-4
Synthetic LPG (Cold) + HCHO												
DTC350B	0.20	0.29	0.08	43	1.65	0.04	0.04	0.52	0.15	0.17	-	3-4
Mini-Surrogate + LPG (Warm)												
DTC340A	0.21	0.29	0.11	14	1.25	(a)	(a)	0.06	(a)	-	5.5	3-6
Mini-Surrogate + LPG (Cold)												
DTC351B	0.20	0.30	0.07	43	1.43	0.04	0.04	0.48	0.15	0.02	5.5	3-5
DTC354A	0.20	0.27	0.03	36	0.86	0.02	0.03	0.30	0.10	(a)	5.1	3-5
Mini-Surrogate + Synthetic LPG												
DTC352A	0.20	0.28	0.06	43	1.50	0.05	0.05	0.50	0.16	(a)	5.7	3-6

(a) Not detected.
(b) Exhaust injected using transfer bag rather than dilutor.

49
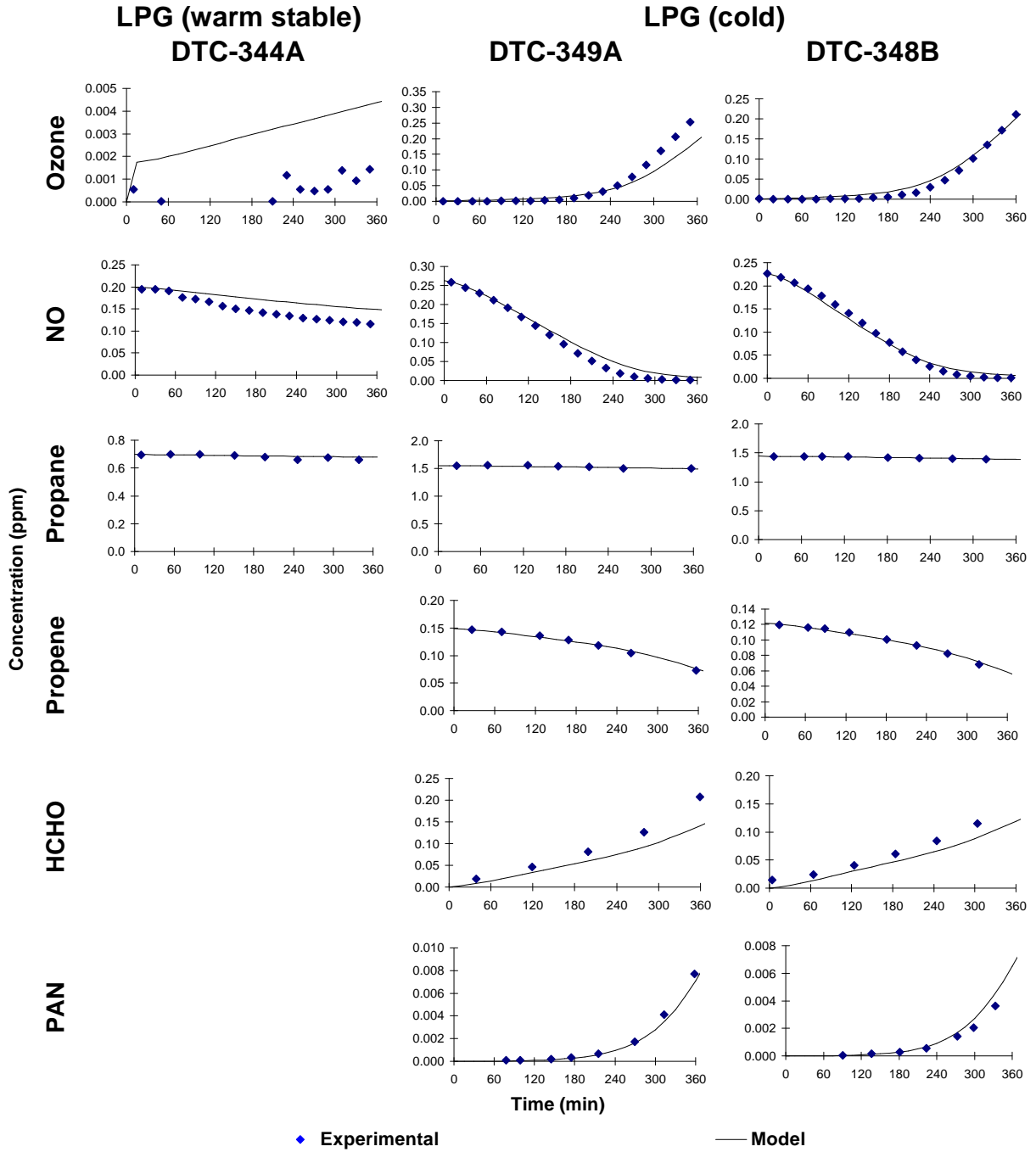
Figure 13.   Experimental and calculated concentration-time profiles for selected species in three LPG exhaust - NOx - air chamber experiments.

50
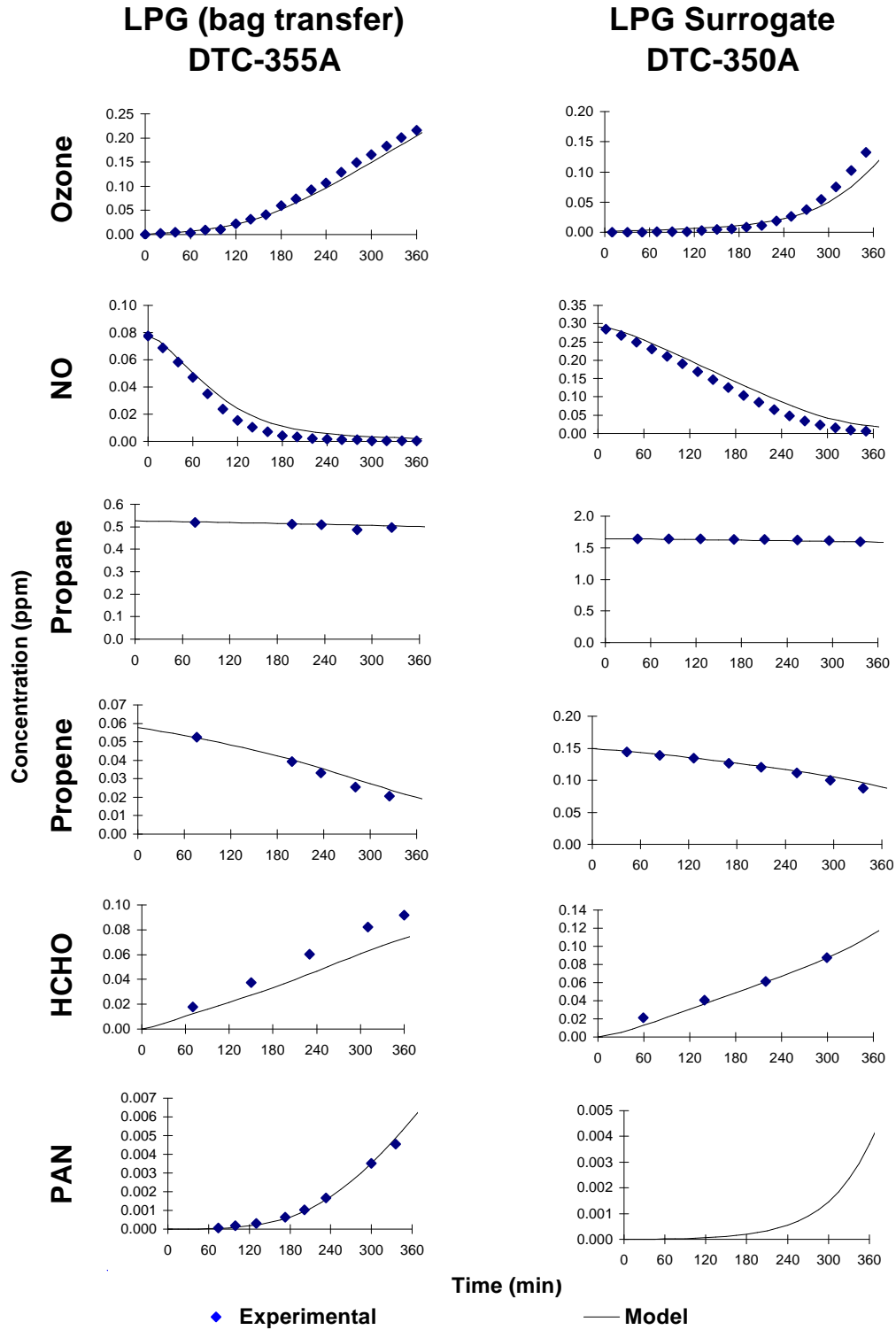
Figure 14.   Experimental and calculated concentration-time profiles for selected species in the LPG exhaust - NOx - air chamber experiment using the bag transfer method, and in the surrogate LPG exhaust - NOx experiment.

all three runs with the cold-start exhaust, indicating relatively reproducible operating conditions of the vehicle.

Figures 15 and 16 show the concentration-time plots for the LPG exhaust with formaldehyde experiments. As can be seen, the presence of the formaldehyde caused a significant increase of the NO oxidation rate in the run with the warm-stabilized exhaust, and an increase in the NO oxidation and O_3 formation rates in the runs with cold-start exhaust. Again, the three experiments using the cold-start exhaust gave very similar results.

Figures 14 and 16 also show the results of the synthetic LPG exhaust and synthetic exhaust with formaldehyde experiments. The results were very similar to the actual LPG exhaust runs they were designed to simulate, with slight differences being attributable to slight differences in initial reactant concentrations. These differences can be taken into account in the model simulations, which are discussed in the following section.

Figures 17 and 18 show the results of the incremental reactivity experiments with the actual and synthetic LPG exhaust mixtures. As discussed above, the data shown are $D(O_3\text{-}NO)$, the sum of O_3 formed and NO oxidized as a function of time for both the base case and the added exhaust sides. Also shown are the change in $D(O_3\text{-}NO)$ caused by adding the exhaust mixture, the m-xylene concentration-time profiles for both sides, and the $\triangle$ IntOH values, giving the effects of the exhausts on integrated OH radical concentrations, which were derived from these m-xylene data. Results of model simulations of these quantities, discussed in the following sections, are also shown.

Figure 17 shows that the addition of the cold-start exhaust has a positive effect on ozone formation, NO oxidation and OH radical levels. The two experiments are good replicates of each other, indicating consistencies in the replicate exhaust injection, as observed with the exhaust-NO_x and exhaust with formaldehyde-NO_x experiments, discussed above. Figure 18 shows that the warm-stabilized LPG exhaust also has a positive effect on NO oxidation and O_3 formation. The effect is much less, as expected based on the lower levels of propane and the absence of detectable olefins. The effect of warm-stabilized exhaust in integrated OH radical levels is too small to detect reliably, but may be slightly positive. Figure 18 also shows that the experiment with the synthetic LPG exhaust mixture (carried out by injecting CO, propane, isobutane, n-butane, ethene, and propene in the levels observed in the experiments shown in Figure 17) gives very similar results in terms of effects on NO oxidation, ozone formation, and OH radical levels. The
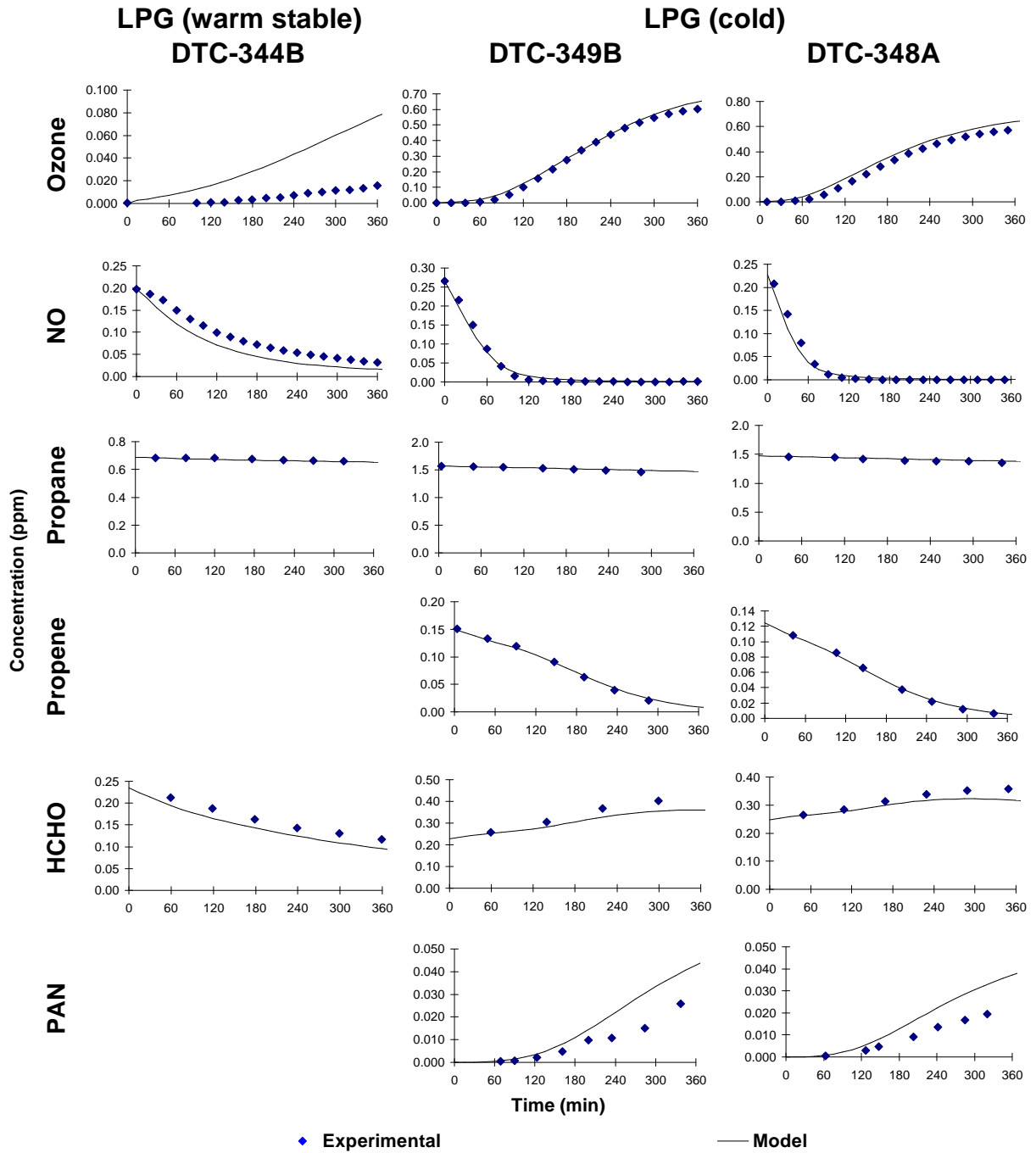
Figure 15.   Experimental and calculated concentration-time profiles for selected species in three LPG exhaust + formaldehyde - NOx - air chamber experiments.

LPG (Cold, bag transfer)
DTC-355A

LPG Surrogate
DTC-350B
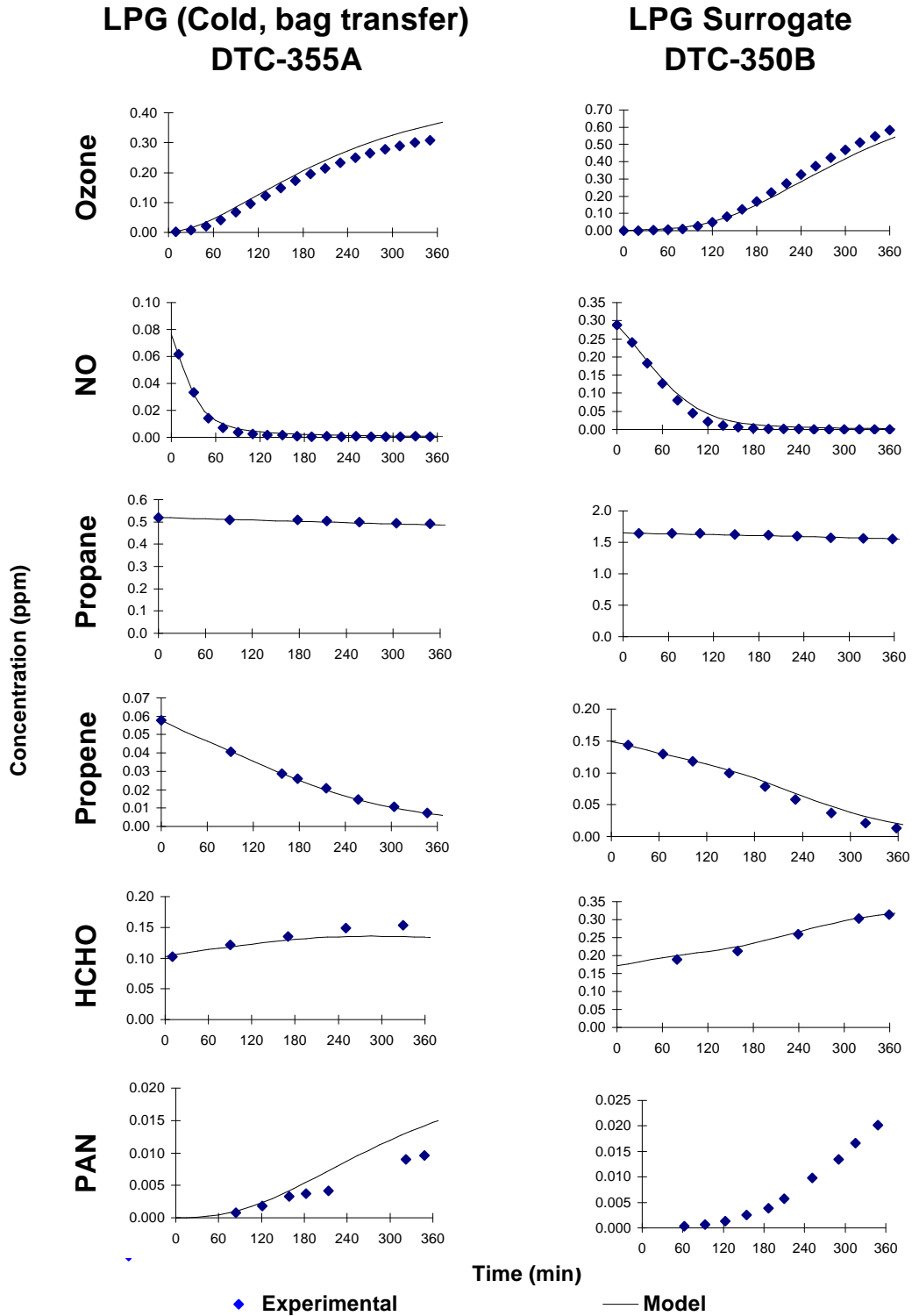
Figure 16. Experimental and calculated concentration-time profiles for selected species in the LPG exhaust + formaldehyde - NOx - air chamber experiment using the bag transfer method, and in the surrogate LPG exhaust + formaldehyde - NOx experiment.

54

DTC351B: LPG Exhaust (cold start)

D(O3-NO)

M-XYLENE

IR d(O3-NO)

IR IntOH
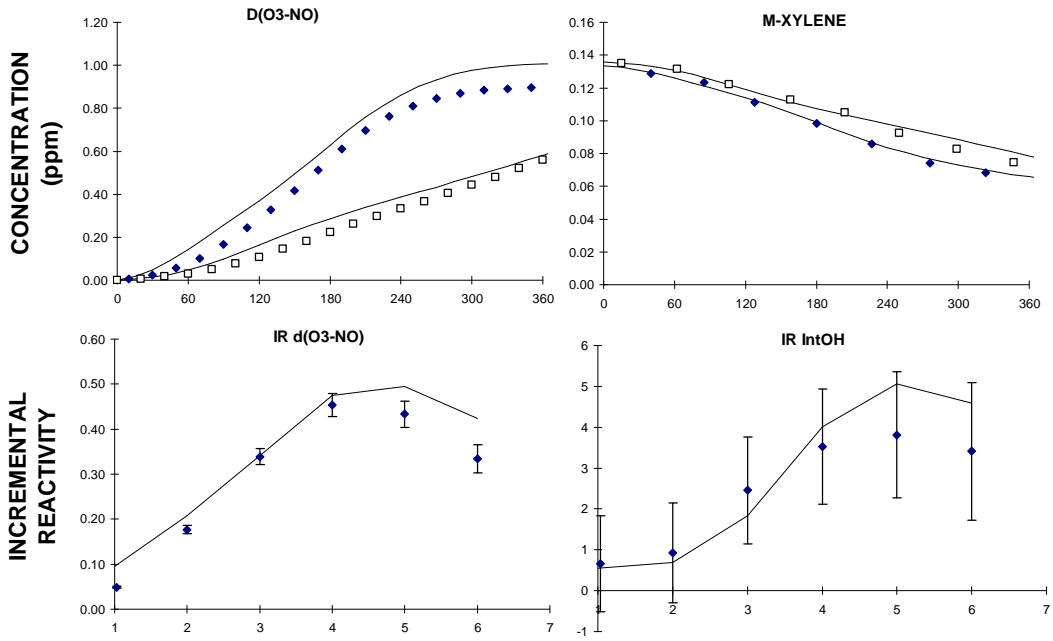
DTC354A: LPG Exhaust (cold start)

D(O3-NO)

M-XYLENE

IR d(O3-NO)

IR IntOH

◆ **Added Test Mixture** □ **Base Case** —— **Model Calculation**
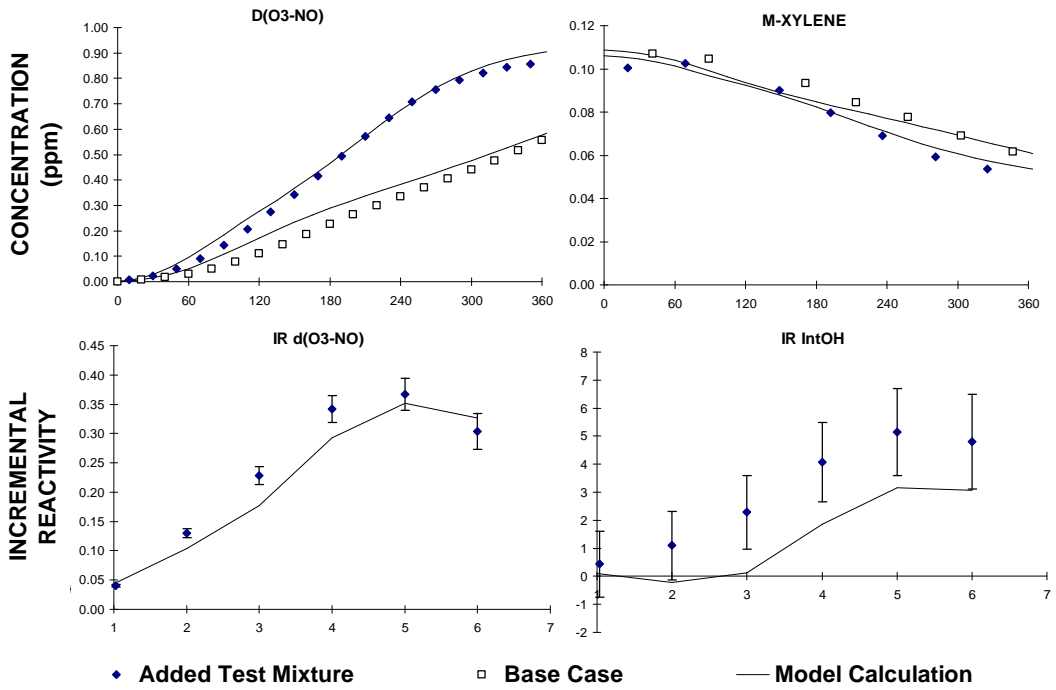
Figure 17.   Experimental and calculated results of incremental reactivity experiments with LPG exhaust.

55
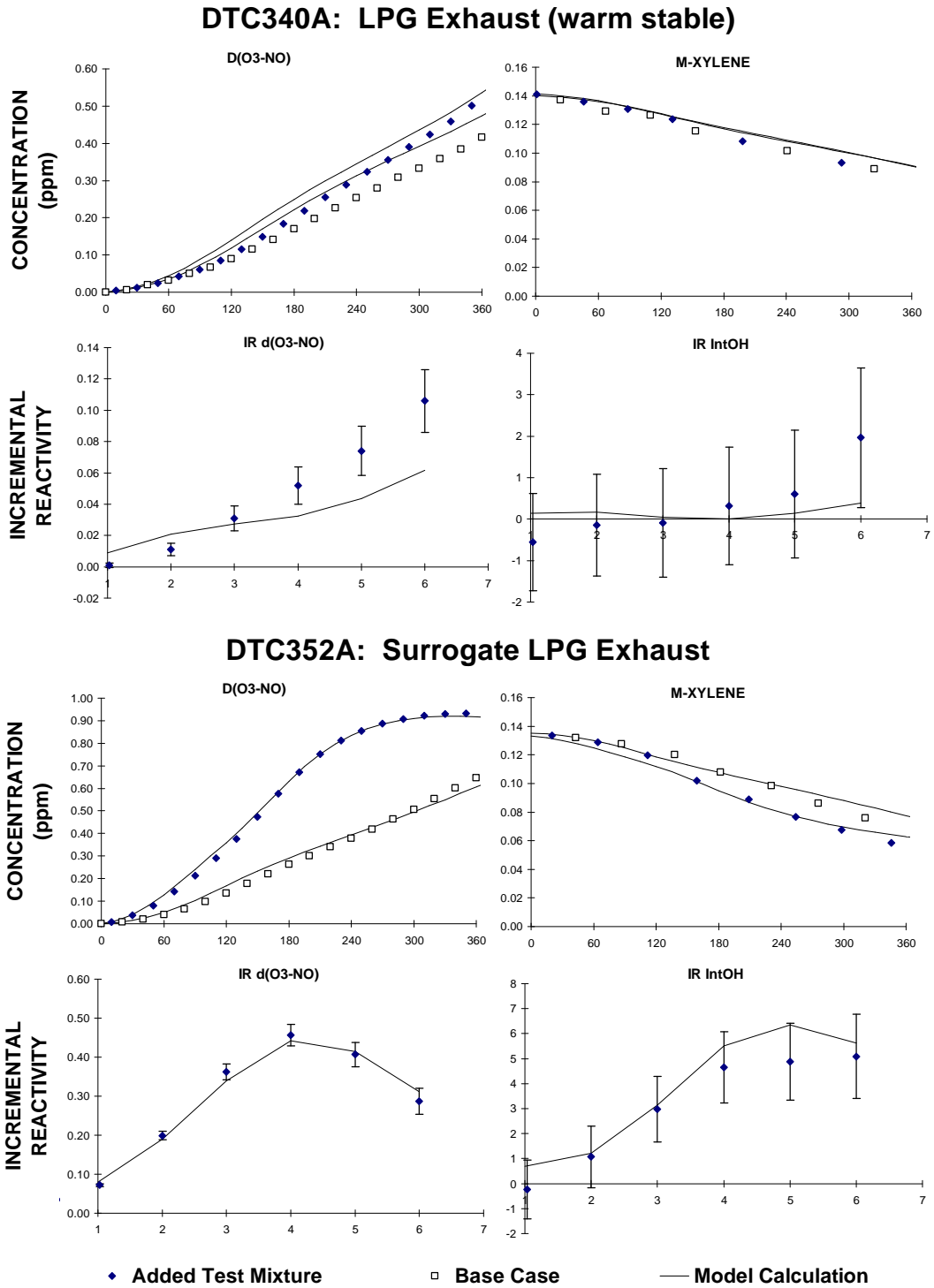
Figure 18. Experimental and calculated results of incremental reactivity experiments with LPG exhaust (warm stable) and surrogate LPG exhaust.

slightly larger effects may be due to small differences in amounts of reactant injections, which can be assessed by comparing experimental results with model predictions.

Model Simulations

One major objective of this study is to assess whether the effects of the exhaust mixtures on O_3 formation and other manifestations of photochemical smog formation are consistent with the predictions of chemical models which are used to predict the effects of exhaust emissions on air quality. The lines on Figures 13 through 18 show the results of the model simulations of the experiments discussed in the previous section. These use the updated SAPRC mechanism discussed previously, and listed in Appendix A. The ability of the model to simulate the experimental results is indicated by how closely the lines calculated by the model agree with the experimental data points.

In most cases the model fits the data reasonably well, considering the variability generally observed when modeling environmental chamber experiments (e.g., see Carter and Lurmann, 1991; Carter et al, 1993a, 1995a,b). The model somewhat overpredicts the NO oxidation rate and thus the onset of O_3 formation in the warm-stabilized exhaust with formaldehyde experiment DTC344B (Figure 3-3), while it tended to underpredict the rate of NO oxidation in the experiment containing only warm-stabilized LPG exhaust, which was carried out at the same time with the same exhaust mixture. The model also somewhat underpredicted the effect of warm-stabilized exhaust addition to the mini-surrogate mixture, as shown on Figure 18. In view of the inconsistencies in the biases of the model performance for the warm-stabilized exhaust, we expect that differences may be due more to uncertainties in characterizing run conditions than problems with the mechanisms for the exhaust components.

The model was able to simulate the effects of the cold-start exhaust experiments on NO oxidation and O_3 formation well in all experiments except for the exhaust-only experiment DTC349A (Figure 13), where it tended to somewhat underpredict the ozone yield. The model was able to simulate the effects of the exhaust mixtures on formaldehyde and PAN formation due to secondary reactions. There were no large differences in model performance in the simulations of the actual exhaust runs and in the simulations of the runs with the synthetic exhaust mixture. This indicates that the slight differences between the actual and synthetic exhaust runs is due to slight differences in reactant concentrations, which are taken into account in the model simulations.

The run where the LPG exhaust was transferred to the chamber using a Teflon bag rather than the mini-diluter cannot be compared directly with the other LPG exhaust runs because the former used lower

reactant concentrations. However, the figures show that the model predictions are as consistent with the results of the bag transfer run as they are with the other runs using the mini-diluter. Thus, there are no differences between these runs that cannot be accounted for. This indicates that there is no unknown artifact due to the transfer method which is being introduced into these runs. This obviously has implications in comparing conditions of these Phase 1 experiments with the Phase 2 runs discussed below, where a transfer bag method was employed.

Evaluation of Methanol Exhausts
M100 Exhaust Injection Procedures and Analyses ─ Phase 1

Experiments employing M100 exhaust were carried out during both phases of this program, both employing the same 1993 Ford Taurus FFV (see above). During Phase 1 the exhaust samples from the M100 vehicle were diluted and transferred to the smog chamber in the same manner as employed for the LPG vehicle, discussed above. As with the LPG vehicle, the testing protocol for the M100 vehicle involved a cold-start after a 12-36 hour soak followed by a vehicle acceleration to 45 mph. Immediately upon reaching the 45 mph steady-state condition, transfer of the diluted exhaust to the smog chamber was begun together with sampling for analyses.

A total of six vehicle runs were performed during Phase 1 where M100 exhaust was transferred to the smog chamber. Table 6 presents emission results measured immediately after the exhaust dilution point (by the CE-CERT VERL Analytical Laboratory) and that measured in the smog chamber after transfer and dilution (by the Atmospheric Process Laboratory). As discussed above, the VERL analytical laboratory results were adjusted by the ratio of the CO concentrations measured immediately after exhaust dilution and that measured in the smog chamber after additional dilution to allow a direct comparison between the two analyses. Results from vehicle runs 1 and 5 (smog chamber runs DTC 372 and DTC 376) are not presented because these runs were aborted due to procedural problems. The results show good agreement for the NO_x analysis results, but the formaldehyde concentrations measured in the smog chamber by APL are substantially lower than those measured immediately after dilution by the VERL analytical laboratory. Subsequent analysis and results of experiments carried out subsequently indicate that the discrepancy is probably due to loss of formaldehyde in the long sample line between the VERL and the chamber. The formaldehyde analysis method used in the APL is considered to be reliable because the amounts measured in the chamber generally agree well with the amounts injected, and the formaldehyde yields in experiments where it is expected as a photochemical product are consistent with predictions of models based on data from other laboratories. The observed rates of O_3 formation and NO oxidation are also consistent with model predictions based on the measured concentrations in the chamber using this method. Better

Table 6.   VOC and NOx measurements taken during the Phase 1 environmental chamber experiments employing M100 exhaust.

Vehicle Run No.	2		3		4		6	
Chamber Run No.	DTC374		DTC375		DTC377		DTC378	
Analysis [a,b]	VERL	APL	VERL	APL	VERL	APL	VERL	APL
Organics (ppm)								
Methanol	[c]	[c]	7.68	8.70	3.18	4.08	3.22	4.10
Formaldehyde	0.92	0.07	0.52	0.15	0.30	0.07	0.33	0.10
CO (ppm)	[d]	3.0	[d]	14.3	[d]	7.3	[d]	5.0
NOx (ppm)	[c]	0.06	0.18	0.18	0.08	0.10	0.10	0.10

[a] VERL: Hydrocarbon data obtained from the CE-CERT Vehicle Emissions Analytical Laboratory analysis of sample collected immediately after vehicle exhaust dilution, with concentrations have been corrected for additional dilution which takes place in the smog chamber. Total NMHC and NOx data taken from the Vehicle Emissions Research Laboratory analyzer bench, corrected for dilution

[b] APL: Analyses in the environmental chamber using the instrumentation in the chamber laboratory.

[c] No valid data available

[d] CO data used to compute dilution, so by definition the VERL value is the same as that measured in the chamber.

agreement between the VERL and APL formaldehyde measurements were obtained in the second phase of the program, as discussed below, though the agreement was still not as close as obtained for other species.

Although the agreement between VERL and the APL methanol analysis is clearly much better than is the case for formaldehyde, the measured concentrations in the VERL laboratory appear to be consistently ~25% higher than those in the APL. The APL has had problems with methanol analysis in the initial experiments, resulting in data from the earlier runs being rejected as unreliable. The analysis was improved after instrument modifications were made, and the amounts of methanol measured in chamber runs where formaldehyde was added as a reactant agreed reasonably well with the amount injected in the subsequent Phase 1 and in most of the Phase 2 experiments.

M100 Exhaust Injection Procedures and Analyses － Phase 2.

During the second phase of the program, the exhaust was transferred from the vehicle to the chamber using a Teflon transfer bag, employing procedures discussed above in the Methods section. All these experiments employed cold start emissions, with the vehicle gradually accelerating to 40 mph in about 30 seconds, followed by steady state operation. Immediately after the vehicle reached steady state, a portion of the exhaust was injected into the transfer bag using a heated sample line, with the pressure from the vehicle forcing the exhaust into the bag. This transfer typically took 30-90 seconds.

Once the transfer bag was filled and mixed, the diluted exhaust in the transfer bag was measured using various methods. Concentrations of CO and NO_x in the transfer bag were measured using VERL instrumentation, and samples were taken for detailed hydrocarbon and oxygenate analysis in the VERL's analytical laboratory. The transfer bag was then moved to the environmental chamber laboratory and its contents (usually most, but sometimes only a portion) were then forced into the chamber by pressurizing the outside of the transfer bag. The diluted exhaust in the chamber was then measured using the various APL instrumentation generally employed with chamber runs.

A total of five experiments employing M100 exhaust were carried out during Phase 2. However, the first run (DTC563) was primarily exploratory in nature, and only limited exhaust and transfer bag measurements were made. Table 7 gives a summary of the major exhaust, transfer bag, and chamber measurements made during the four runs which were more completely characterized. The data shown are corrected for measured background species in the transfer bag, and for background and non-exhaust injections in the chamber, and thus reflect only those species introduced with the exhaust. Detailed hydrocarbon and oxygenate speciated analyses of the exhaust in the transfer bag were carried out for the last two of these runs, and the results are given in Table B-2 in Appendix B. As expected, the only significant reactive VOC species observed in these M100 runs were methanol and formaldehyde.

Table 7 shows that in most cases the various measurements gave consistent dilution ratios in going from the raw exhaust to the transfer bag, and then from the transfer bag to the chamber. Some apparently anomalous dilution ratios were seen in the case of methane and THC measurements in the exhaust and the transfer bag, though the CO and the NO_x data were generally in good agreement. Only one of the M100 runs (DTC588) had both CO and NO_x data in both the chamber and the transfer bag, and the transfer bag/chamber dilution ratios derived from them were in good agreement. Only run (DTC589) had methanol and formaldehyde data in both the transfer bag and the camber. In this case, the dilution ratio obtained with

Table 7.　　　　Summary of exhaust injections and analyses for the Phase 2 M100 exhaust chamber runs.

	DTC564	DTC565	DTC588	DTC589
Exhaust				
Fill Duration (sec)	90	90	34	32
NOx (ppm)	26.6	20.6	31.8	46.1
CO (ppm)	2984	2582	1247	2734
CO2 (%)	14.8	14.8	14.9	14.8
O2 (%)	0.031	0.018	0.054	0.139
THC (ppmC)	355.4	393.4	431.2	801.5
Methane (bench) (ppm)	19.5	19.3	13.4	20.7
Transfer Bag				
NOx (ppm)	2.54	1.12	0.73	1.39
CO (ppm)	-	-	22.66	71.75
CO2 (%)	1.13	0.92	0.38	0.39
THC (ppmC)	28.5	5.8	7.2	17.3
Methane (bench) (ppm)	4.0	1.1	0.08	0.62
Methane (GC) (ppm)	-	-	-	0.87
Methanol (ppm)	-	-	-	65.2
Formaldehyde (ppm)	-	-	-	3.51
Hydrocarbon Speciation Data?	no	no	yes	yes
Aldehyde Speciation Data?	no	no	no	yes
Exhaust/Transfer bag dilution				
Average	<u>12.0</u>	<u>17.3</u>	<u>49.3</u>	<u>37.8</u>
NOx (ppm)	10.5	18.4	43.5	33.2
CO (ppm)	13.1		55.0	38.1
CO2 (%)		16.1	39.2	37.9
THC (ppmC)	12.5	(67.9)	59.6	46.4
Methane (bench)	(4.9)			33.3
Chamber				
Side(s) injected	A	A	A	A+B
NOx	0.131	0.085	0.065	
CO	11.90	9.37	1.75	4.22
Methanol	5.50	4.98	1.64	3.86
Formaldehyde	0.22	0.24	0.20	0.25
Transfer bag / Chamber dilution				
Average	<u>19.4</u>	<u>13.1</u>	<u>12.1</u>	<u>17.0</u>
NOx	19.4	13.1	11.3	
CO			12.9	17.0
Methanol				16.9
Formaldehyde				(14.1)

the methanol data was in excellent agreement with that obtained from the NO_x measurements, and the agreement in the case of the formaldehyde data was within 20%, which is probably within the combined uncertainties of the measurements.

The average dilution ratios for the transfer bag relative to the raw exhaust and for the chamber relative to the transfer bag are also shown on Table 7. The numbers not used in the averages are indicated by parentheses; those that were not used either appeared to be anomalous (in the case of methane in run DTC564) or were judged to have higher uncertainty than the other data (in the case of the formaldehyde measurements).

Note that the initial formaldehyde / methanol ratios in these runs were in the 4-6% range, except for run DTC588, where the ratio was 12%. These can be compared with the same ratio in the Phase 1 M100 experiments, where the ratio obtained with the VERL data were in the 7-10% range, while those measured in the chamber were only around 2%. Thus, the Phase 2 formaldehyde/methanol ratios in the chamber are more consistent with the Phase 1 VERL data than with the Phase 1 chamber data, and is evidence for loss of methanol in the transfer lines during the Phase 1 runs. It is uncertain whether the somewhat lower average formaldehyde/methanol ratio in Phase 2 is due to differences in the exhausts because of the somewhat different operating procedures or to differences in analytical methods. There is no indication of significant formaldehyde loss in the transfer bag, though the possibility of some losses cannot be totally ruled out. However, any formaldehyde losses in the transfer bag must clearly be much less than the apparent formaldehyde losses in the transfer line during Phase 1.

M85 Exhaust Analyses

A total of six experiments employing M85 exhausts were attempted during Phase 2, using essentially the same procedures as employed for the Phase 2 M100 experiments. Of these, one experiment (DTC595) had to be aborted before the irradiation began because of reactant injection errors, but useful data were obtained for the other five experiments. Table 8 gives a summary of the major exhaust, transfer bag, and chamber measurements made during the five M85 experiments which were completed. Detailed hydrocarbon and oxygenate speciated analyses of the exhaust in the transfer bag were carried out for all these runs (including the aborted DTC595), and the results are given in Table B-2 in Appendix B.

As with M100, the only significant reactive VOC species observed in these M85 runs were methanol and formaldehyde. Although some hydrocarbon reactants were observed (see Table B-2), their concentrations in the chamber were low, with the total non-methanol, non-formaldehyde VOC being not significantly greater, and in some cases less, than the formaldehyde alone. In the case of DTC591 and

Table 8.   Summary of exhaust injections and analyses for the M85 exhaust chamber runs.

	DTC591	DTC592	DTC593	DTC594	DTC596
Exhaust					
Fill Duration (sec)	30	30	30	30	~30
NOx (ppm)	60.9	96.1	82.3	107.6	141.7
CO (ppm)	2998	1332	1342.1	802.9	838.8
CO2 (%)	14.8	14.9	14.8	14.9	14.8
O2 (%)	0.115	0.030	0.063	0.119	0.224
THC (ppmC)	678.2	243.4	366.3	387.9	395.5
Methane (bench) (ppm)	21.7	18.6	21.3	21.6	22.7
Transfer Bag					
NOx (ppm)	1.74	3.73	3.45	4.28	6.11
CO (ppm)	68.66	35.46	59.10	14.22	19.46
CO2 (%)	0.35	0.48	0.53	0.51	0.55
THC (ppmC)	12.9	5.8	11.82	9.88	11.12
Methane (bench) (ppm)	0.3	0.4		0.24	1.03
Methane (GC) (ppm)	0.4	0.8	0.75	0.35	0.92
Methanol (ppm)	28.8	18.0	35.5	32.3	40.5
Formaldehyde (ppm)	1.26	0.93	1.25	0.95	1.17
Total VOC - (MeOH + HCHO)	2.45	1.03	0.82	2.13	3.12
Hydrocarbon Speciation Data?	yes	yes	yes	yes	yes
Aldehyde Speciation Data?	yes	yes	yes	yes	yes
Exhaust/Transfer bag dilution					
Average	43.4	34.2	26.4	37.5	32.2
NOx (ppm)	35.0	25.8	23.9	25.1	23.2
CO (ppm)	43.7	37.6	22.7	56.5	43.1
CO2 (%)	42.3	31.1	28.0	29.2	27.0
THC (ppmC)	52.8	42.2	31.0	39.3	35.6
Methane (bench)	(63.8)	(51.6)		(90.1)	(22.1)
Chamber					
Side(s) injected	A	A+B	A	A	A
NOx	0.066	0.123	0.175	0.264	0.196
CO	1.97	1.30	2.83	0.78	0.62
Methanol	1.25	0.458	1.81	1.71	1.39
Formaldehyde	0.092	0.015	0.075	0.086	0.063
Transfer bag / Chamber dilution					
Average	28.0	32.3	20.1	17.8	30.5
NOx	26.3	30.3	19.7	16.2	31.2
CO	34.9	27.3	20.9	18.3	31.2
Methanol	23.0	39.3	19.6	18.9	29.1
Formaldehyde	(13.7)	(60.8)	(16.7)	(11.0)	(18.6)

DTC594, a significant fraction of this hydrocarbon was due to unexpectedly high C_{10+} aromatics peaks observed in the GC analysis, which was subsequently determined to be caused by a contaminated syringe used in the analysis. If these C_{10+} aromatics are excluded, the amount and reactivities of the remaining measured hydrocarbon reactants were sufficiently low that they were not expected to affect the overall reactivity in the experiments. These hydrocarbon reactants were ignored when modeling these experiments and when designing the synthetic M85 exhaust experiments to duplicate the actual exhaust runs.

Results of Chamber Runs

The conditions and major results of the chamber runs using actual and synthetic M100 exhaust are summarized on Table 9, and Table 10 gives a similar summary for the M85 runs. The M100 runs included one with M100 exhaust alone in both sides of the chamber, three with actual M100 exhaust on one side of the chamber and synthetic M100 on the other, and nine incremental reactivity experiments, four using the mini-surrogate with the real exhaust, three using the mini-surrogate with synthetic exhaust, and one each using the full surrogate and real and synthetic exhaust. Experiments with M85 included one run with exhaust in both sides of the chamber, two each of incremental reactivity experiments with the mini-surrogate and the mini-surrogate and with real and synthetic M85 exhaust.

Figures 19-21 show the concentration-time plots for the exhaust-only runs employing actual or synthetic M100 exhaust. Results of model calculations, discussed below, are also shown, though run DTC374 could not be modeled because it was subsequently determined that its methanol measurements were invalid. All runs resulted in complete consumption of NO and non-negligible O_3 formation. Note that the results of the Phase 2 experiments (run DTC588B, DTC563A, and DTC564) were similar to the Phase 1 run (DTC374B), though the Phase 1 run had somewhat less formaldehyde, which as discussed above are attributed to losses on the sample line. Note also that the results of the synthetic M100 run DTC588B were very similar to the results of the actual exhaust run it was designed to duplicate (DTC588A), indicating that the measured methanol and formaldehyde are indeed the major reactants affecting the results. Somewhat more ozone formation was observed in synthetic M100 run DTC563B than in the exhaust run (DTC563A) it was supposed to duplicate, but this can be attributed to a failure to duplicate the reactants exactly. In particular, the synthetic exhaust run had somewhat lower NO_x and considerably more methanol than the actual exhaust run. The higher initial methanol in DTC563B is the reason the formaldehyde is increasing slightly with time in that run, while for the other runs it tends to decrease slightly or stay about the same. The formaldehyde concentrations do not change significantly during these experiments because the formaldehyde being lost due to reaction is partly (or fully) offset by the formaldehyde formed from the photo-oxidation of methanol.

64

Table 9. Summary of experimental runs using actual or synthetic M100 exhaust.

Type / Run	Phase (a)	k(NO$_2$+ hu) (min^{-1})	Initial Reactants (ppm)					Base ROG (ppmC)	Data Plots
			NO	NO2	CO	Methanol	HCHO		
M100 Exhaust Only									
DTC374A,B	1	0.20	0.06	0.00	4.8	(b)	0.07	-	19
DTC563A	2	0.20	0.15	0.05	16.3	4.5	0.17	-	20
DTC564A	2	0.20	0.12	0.01	13.8	5.5	0.22	-	21
DTC588A	2	0.19	0.06	0.00	3.7	1.6	0.16	-	19
Synthetic M100 Exhaust									
DTC563B	2	0.20	0.10	0.03	2.5	7.7	0.16	-	20
DTC564B	2	0.20	0.12	0.03	2.9	5.8	0.22	-	21
DTC588B	3	0.19	0.06	0.00	2.6	1.5	0.20	-	19
Mini-Surrogate + M100									
DTC375A	1	0.20	0.27	0.09	16.3	9.5	0.15	5.28	4-4
DTC377B	1	0.20	0.28	0.08	9.2	4.5	0.07	5.35	4-4
DTC565A	2	0.20	0.27	0.13	11.9	5.0	0.24	5.15	4-6
DTC589A	2	0.19	0.26	0.19	7.1	3.9	0.25	5.67	4-6
Mini-Surrogate + Synthetic M100									
DTC380B	1	0.20	0.26	0.11	2.7	5.4	0.03	5.12	4-5
DTC634A	2	0.27	0.23	0.11	1.9	4.2	0.23	5.57	4-7
DTC658A	2	0.17	0.25	0.13	2.0	3.5	0.25	5.53	4-7
Full Surrogate + M100									
DTC378A	1	0.20	0.21	0.05	6.9	4.5	0.11	3.40	4-4
Full Surrogate + Synthetic M100									
DTC381A	1	0.20	0.19	0.08	2.6	5.7	0.07	3.33	4-5

(a) Indicates whether run carried out during Phase 1 or Phase 2 of this program.

(b) Data Rejected. Probably around 3-4 ppm.

65

Table 10. Summary of experimental runs using actual or synthetic M85 exhaust.

Type / Run	$k(NO_2+ h\nu)$ (min^{-1})	Initial Reactants (ppm)					Base ROG (ppmC)	Data Plots
		NO	NO2	CO	Methanol	HCHO		
M85 Exhaust Only								
DTC592A,B	0.19	0.12	0.01	3.3	0.5	0.01	-	21
Mini-Surrogate + M85								
DTC593A	0.19	0.34	0.11	4.7	1.8	0.08	5.63	4-5
DTC596A	0.19	0.19	0.11	1.8	1.4	0.06	5.68	4-8
Mini-Surrogate + Synthetic M85								
DTC636B	0.27	0.27	0.10	2.6	1.7	0.07	5.59	4-9
DTC670B	0.17	0.30	0.11	1.8	4.8	0.09	5.53	4-9
Full Surrogate + M85								
DTC591A	0.19	0.30	0.05	4.3	1.3	0.18	4.20	4-10
DTC594A	0.19	0.28	0.06	3.0	1.7	0.19	4.17	4-10
Full Surrogate + Synthetic M85								
DTC637A	0.27	0.24	0.06	2.8	1.2	0.16	4.08	4-11
DTC656B	0.17	0.24	0.05	2.3	1.1	0.21	4.24	4-11

M100 EXHAUST

M100 SURROGATE

DTC374A

DTC588A

DTC588B

DATA REJECTED

◆ **Experimental**
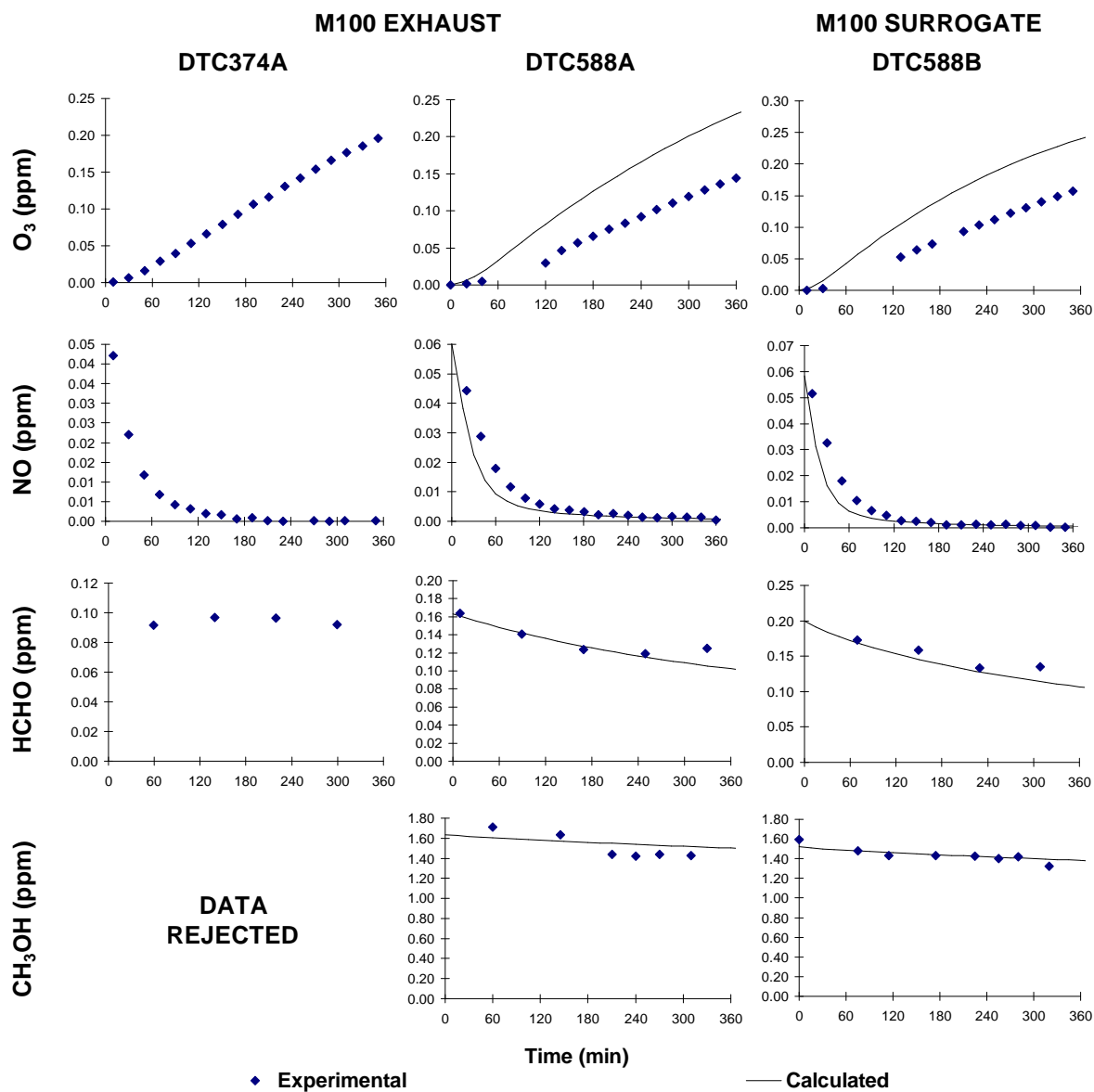
—— **Calculated**

Figure 19.   Experimental and calculated concentration-time plots for selected species in M100 exhaust runs DTC474A and DTC588A and in M100 exhaust surrogate run DTC588B. Note that run DTC374A could not be modeled because of lack of reliable methanol data.

67

M100 EXHAUST

DTC563A

M100 SURROGATE
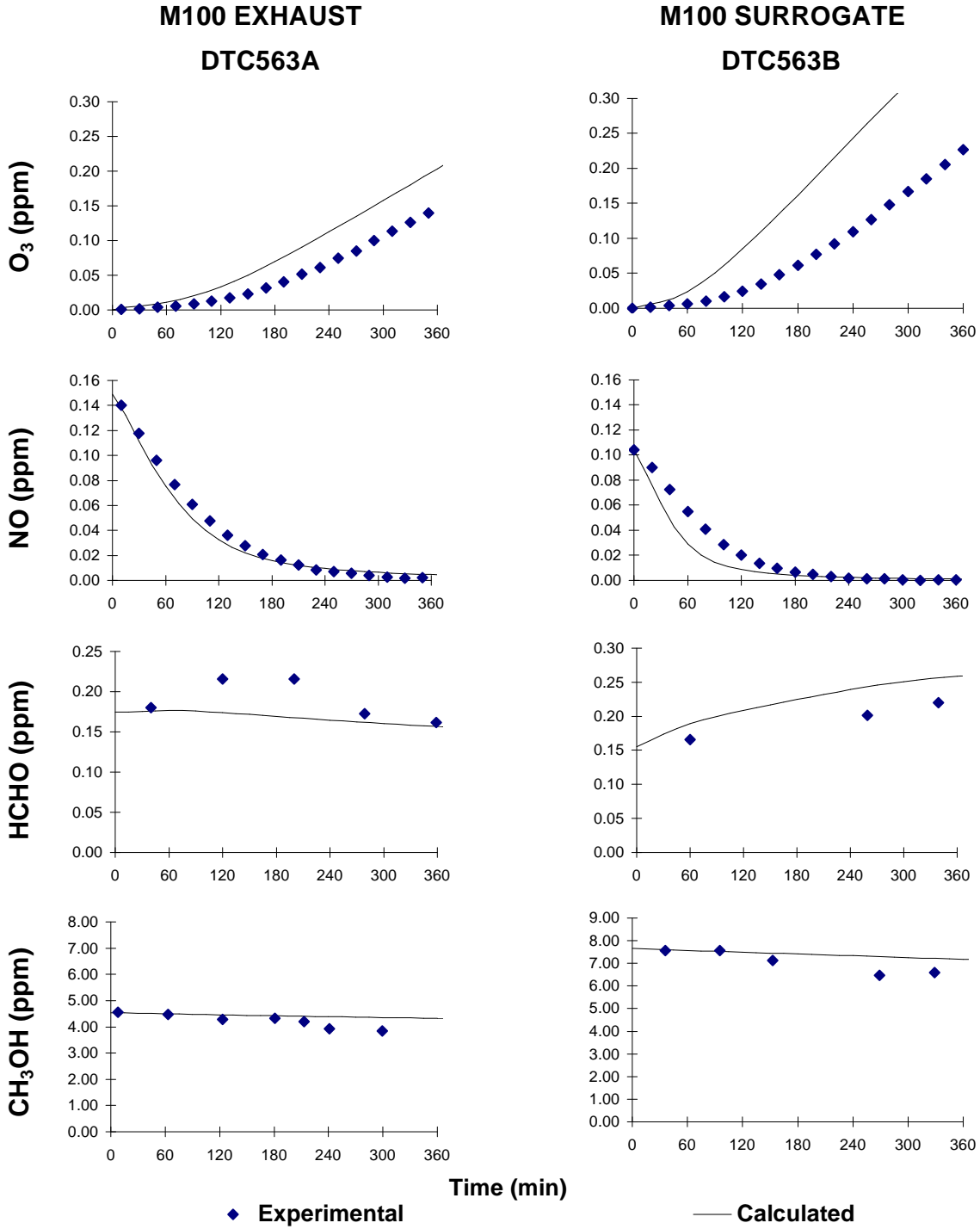
DTC563B

Figure 20. Experimental and calculated concentration-time plots for selected species in M100 exhaust run DTC563A and in M100 exhaust surrogate run DTC563B.

M100 EXHAUST
DTC564A

M100 SURROGATE
DTC564B

M85 EXHAUST
DTC592A
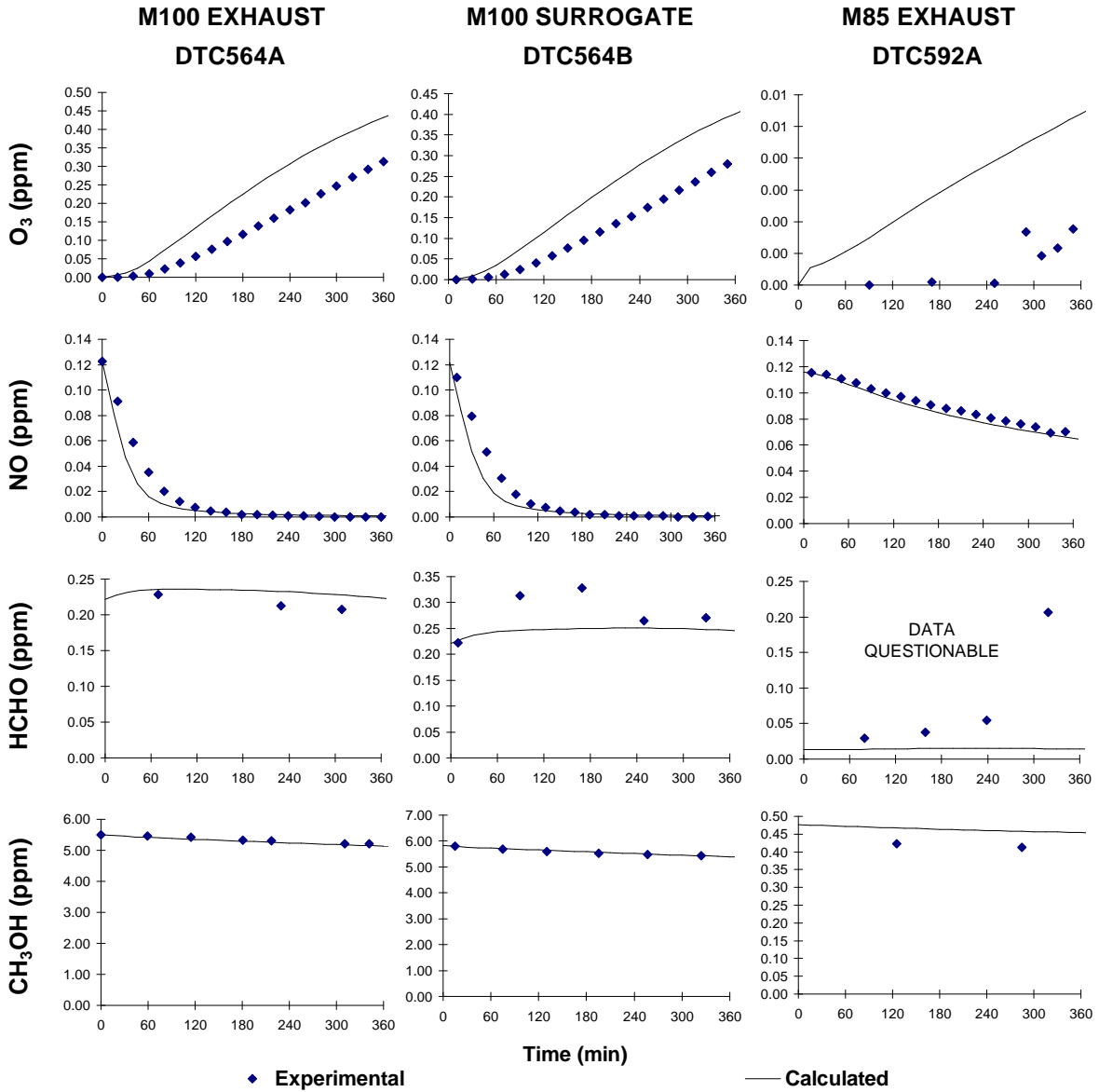
Figure 21. Experimental and calculated concentration-time plots for selected species in M100 exhaust and M100 exhaust surrogate runs DTC563A and DTC563B, and in the M85 exhaust run DTC592A.

69

The data for the one M85 exhaust run (DTC592A) are shown on Figure 21. The relatively low levels of methanol and formaldehyde in the exhaust from that vehicle compared to the NO_x were such that essentially no O_3 formation was observed, and only slow NO oxidation occurred. Because of this, the results are considered not to be particularly useful for model evaluation. Higher levels of methanol and formaldehyde were obtained in the other M85 runs.

Figures 22-25 show the results of the incremental reactivity with the M100 and M85 exhausts, with Figure 22 showing the data from the Phase 1 M100 runs and the other figures showing the Phase 2 data. The methanol exhausts had positive effects on NO oxidation and O_3 formation and also on integrated OH radical levels. The effects were generally larger in the case of the M100 runs compared do those using the M85 vehicle, as expected given the larger amounts of methanol and formaldehyde in the M100 exhausts. However, the amounts of methanol and formaldehyde from the M85 vehicle were sufficient to obtain a useful measure of exhaust reactivity, though the effect was relatively small in the case of the full surrogate with M85 run (bottom plot on Figure 25).

The figures also show the formaldehyde data for the base case and the added exhaust runs. The formaldehyde formation rates in the mini-surrogate with methanol exhaust runs was only slightly higher than the formaldehyde formation in the base case side. This is because the mini-surrogate base case experiment contains significant amounts of ethylene, which reacts to form formaldehyde as its major product. This formaldehyde from ethylene is apparently greater than the formaldehyde from the methanol in the exhausts. In the case of the full surrogate runs, which includes formaldehyde in the base case mixture and has lower amounts of formaldehyde precursors, the formaldehyde formation rates throughout the irradiation are generally much less, but again the formaldehyde formation rates in the added methanol side are not much greater (and sometimes are less) than on the base case side. Thus, reactions of methanol are not a major source of formaldehyde in these surrogate - NO_x systems.

The results of the incremental reactivity experiments with synthetic methanol exhausts are shown on Figures 26-29. In all cases, including M85, the synthetic exhaust mixtures were formulated using only methanol and formaldehyde; other VOCs in the exhausts were assumed to be negligible. The figure caption shows which experiment the synthetic exhaust run was designed to simulate (see also Appendix C), and the extent to which the initial reactants were actually duplicated can be determined from the data in Tables 9 and 10.
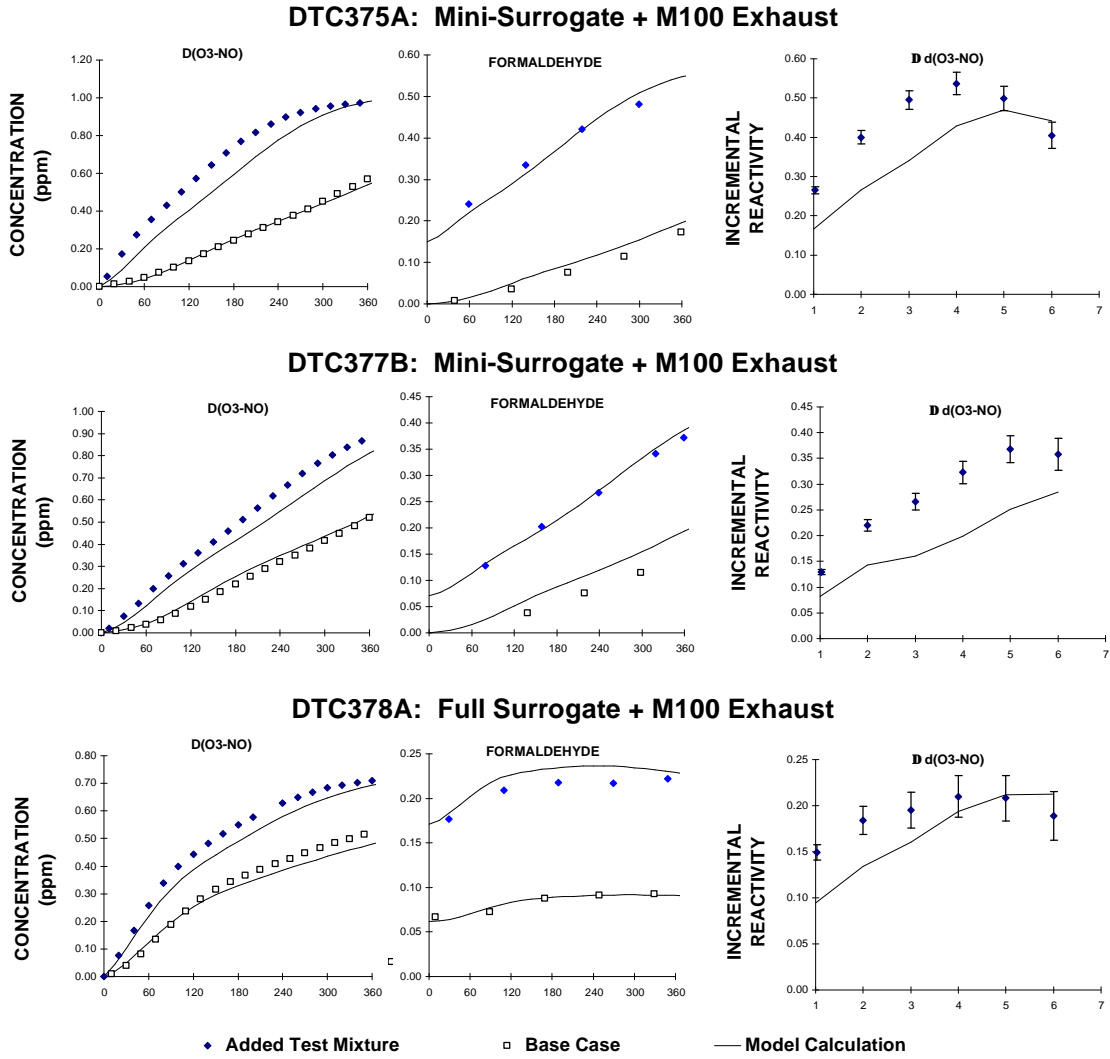
Figure 22.   Experimental and calculated results of the Phase 1 incremental reactivity experiments with M100
exhaust. (No reliable m-xylene or IntOH data available because of analytical problems.)
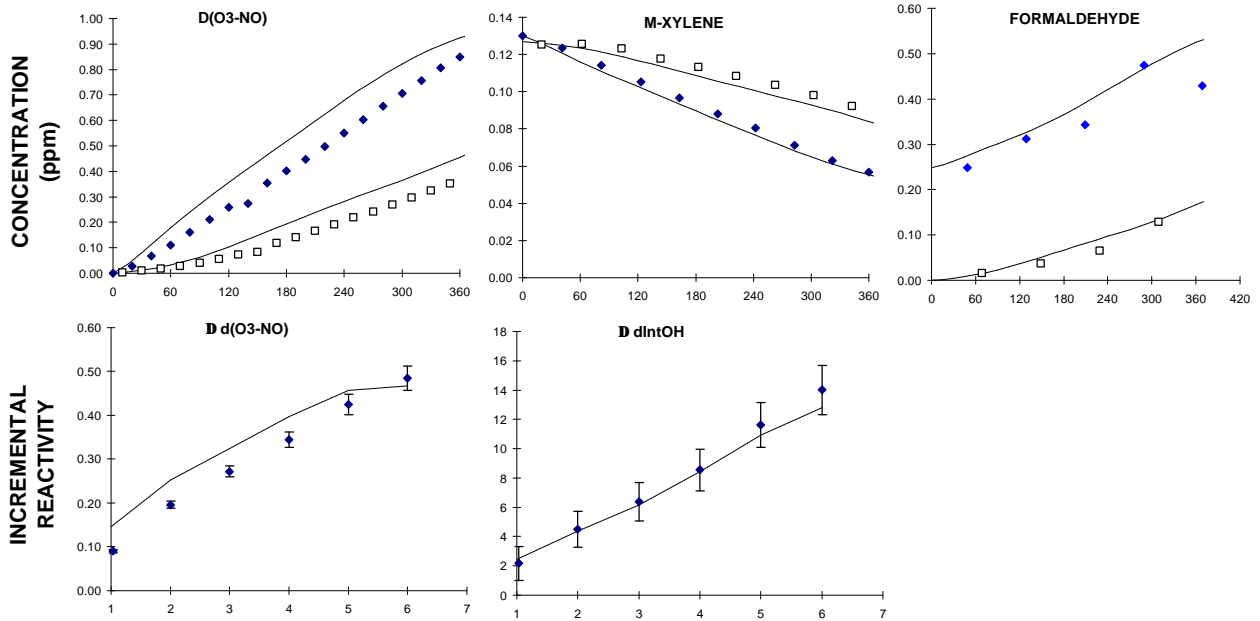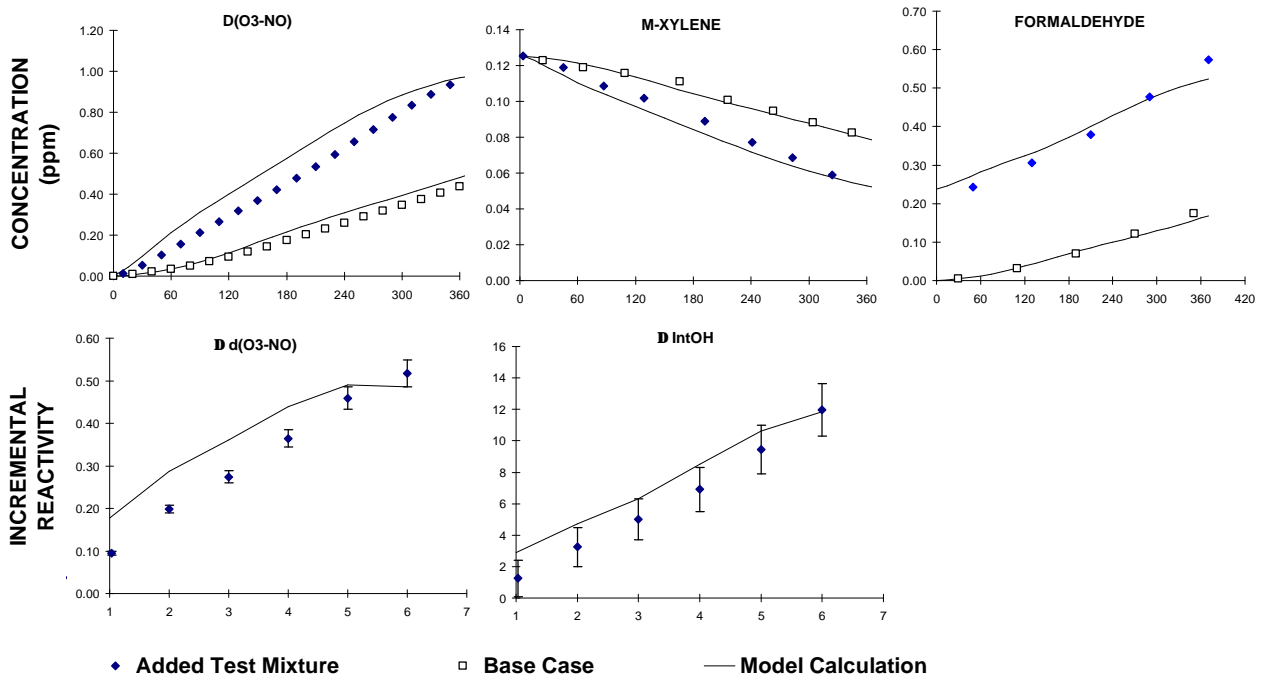
Figure 23.   Experimental and calculated results of the Phase 2 mini-surrogate incremental reactivity experiments with M100 exhaust.

72
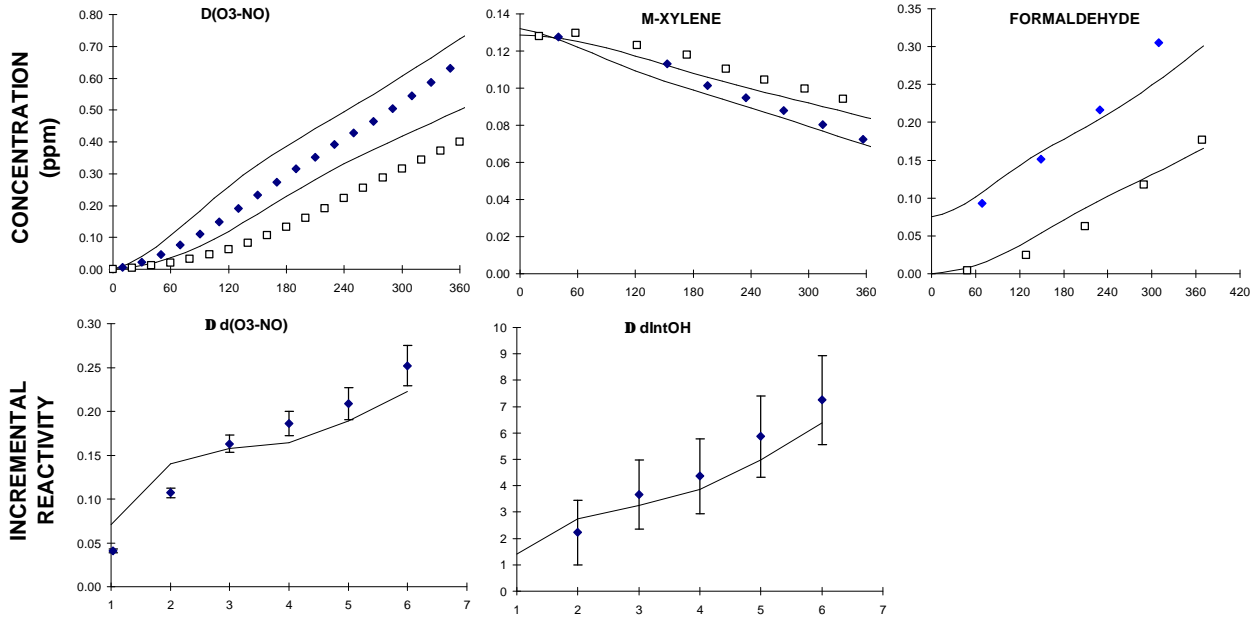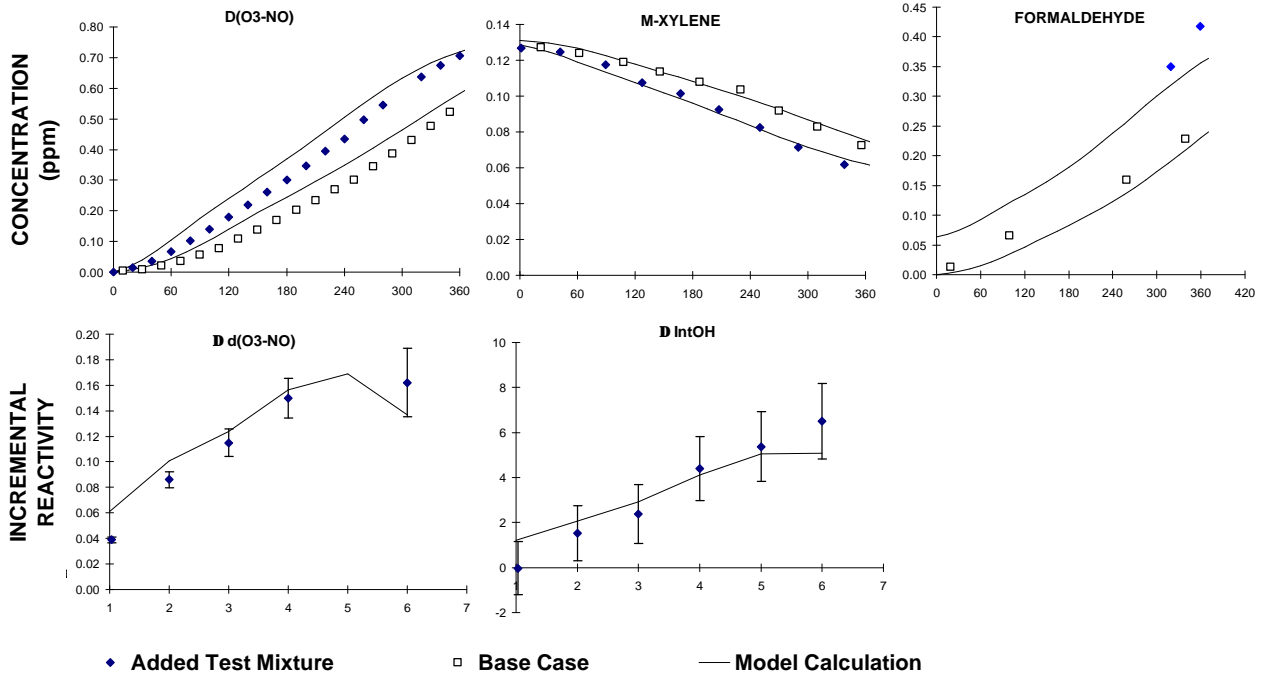
Figure 24. Experimental and calculated results of the mini-surrogate incremental reactivity experiments with M85 exhaust.

DTC591A: Full Surrogate + M100 Exhaust
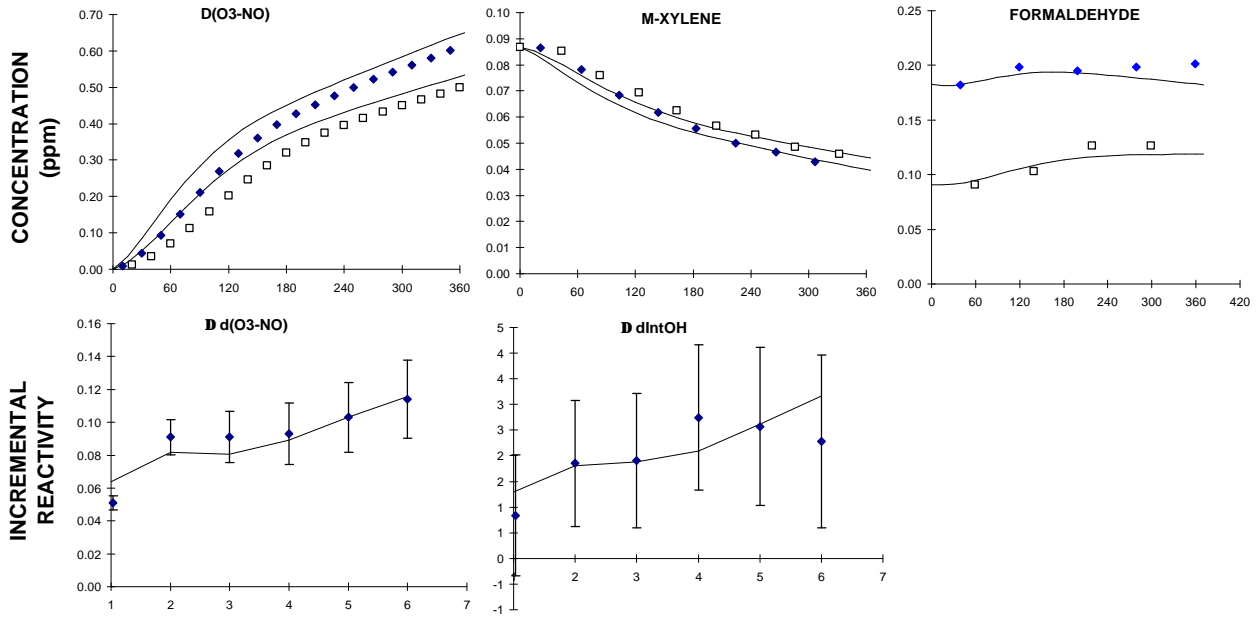
DTC594A: Full Surrogate + M85 Exhaust

♦ **Added Test Mixture**   □ **Base Case**   —— **Model Calculation**
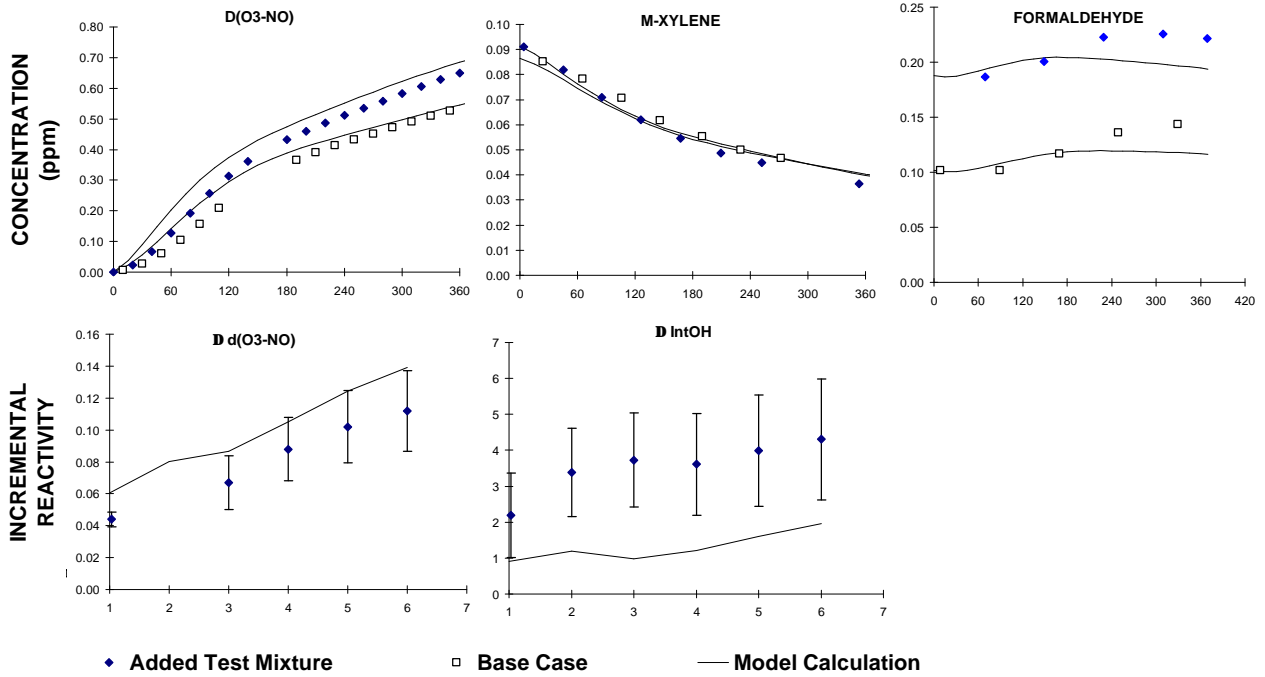
Figure 25.   Experimental and calculated results of the full surrogate incremental reactivity experiments with M100 and M85 exhausts.

74

DTC380B: Mini-Surrogate + Synthetic M100 Exhaust (to duplicate DTC377)
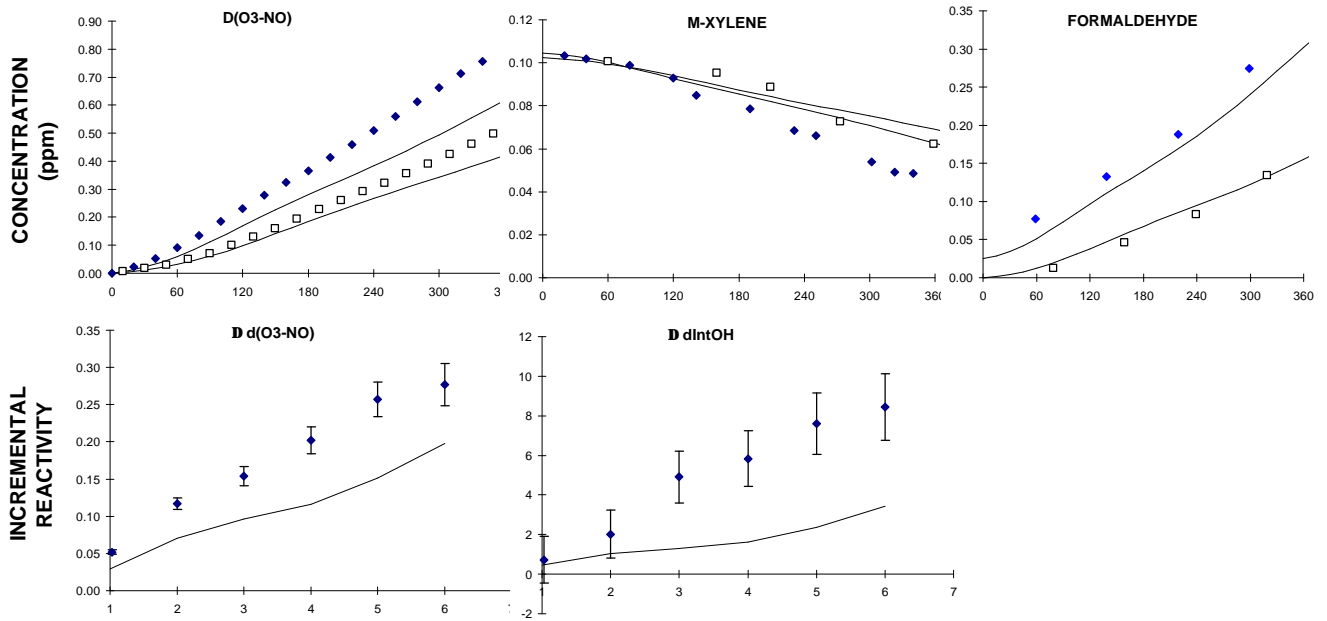
DTC381A: Full Surrogate + Synthetic M100 Exhaust (to duplicate DTC378)

◆ **Added Test Mixture**   □ **Base Case**   —— **Model Calculation**
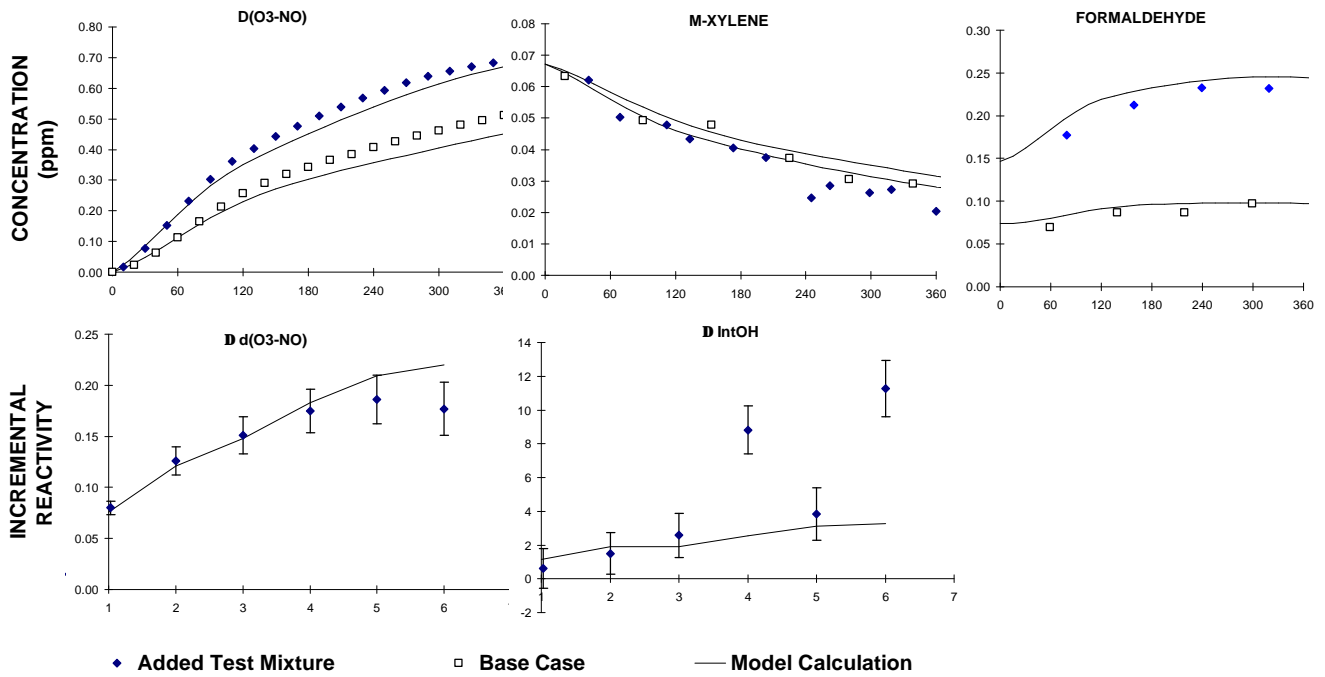
Figure 26.   Experimental and calculated results of the Phase 1 incremental reactivity experiments with synthetic M100 exhaust.
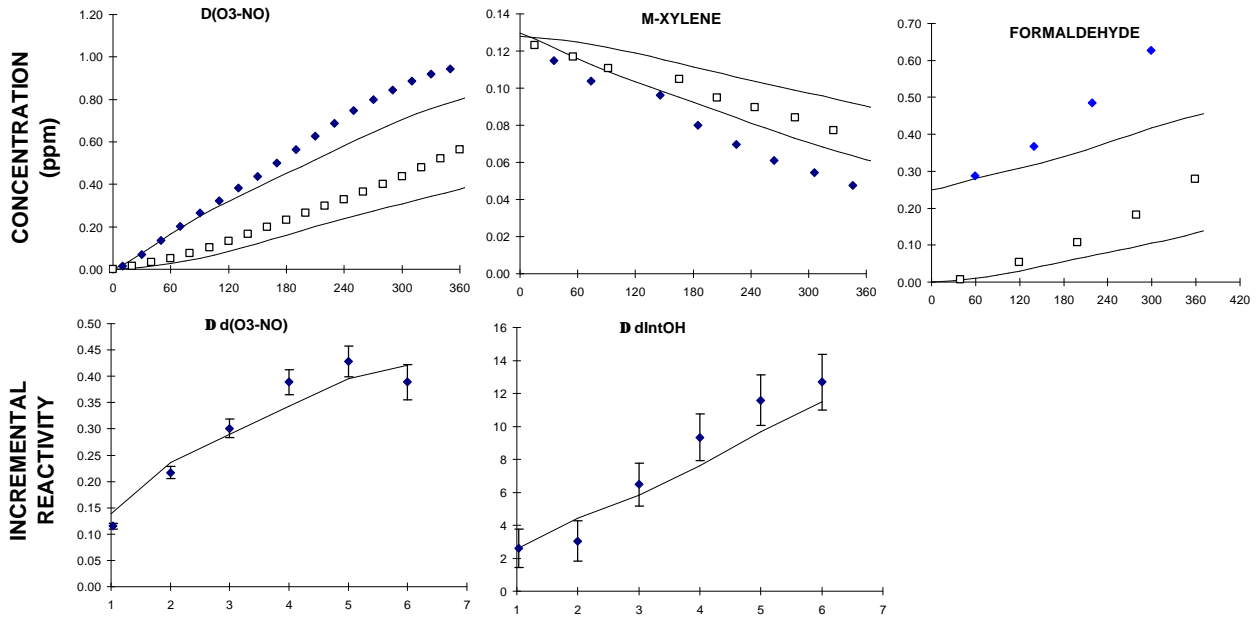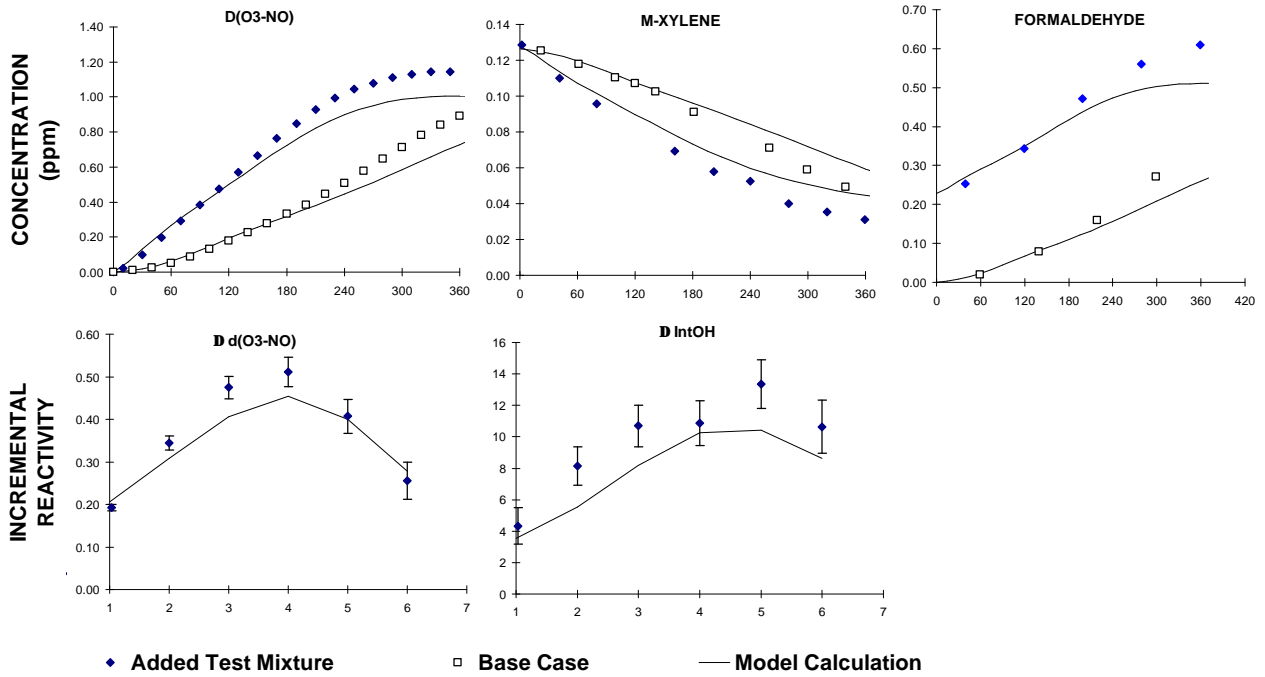
Figure 27.   Experimental and calculated results of Phase 2 mini-surrogate incremental reactivity experiments with synthetic M100 exhaust.
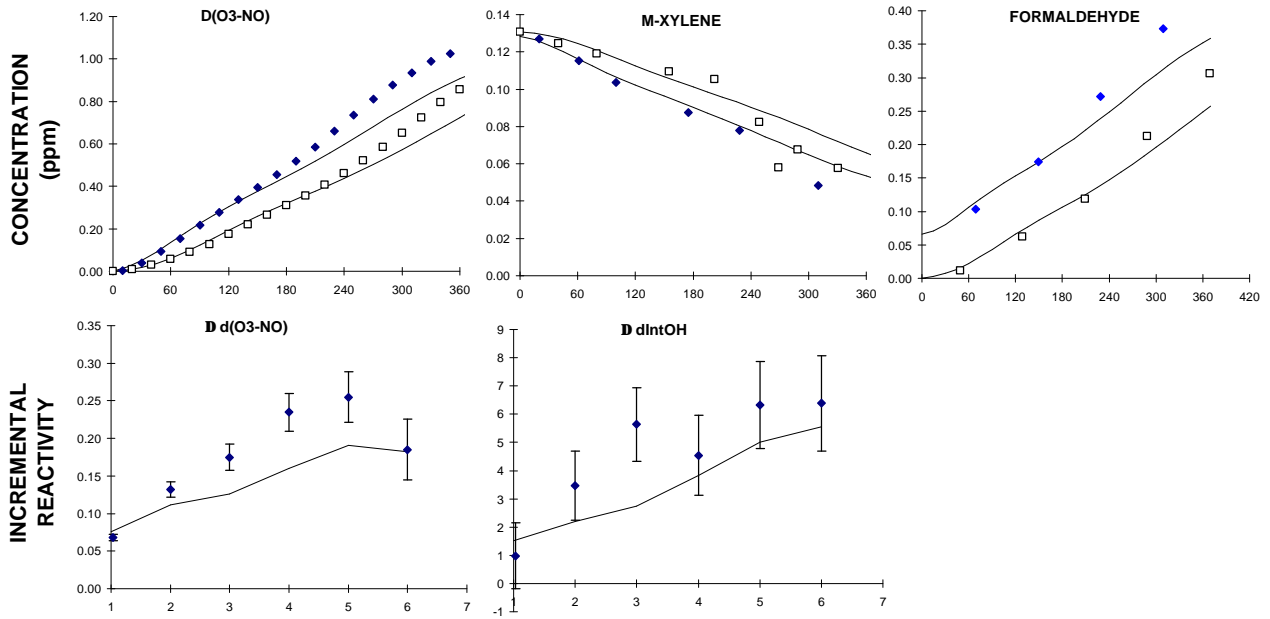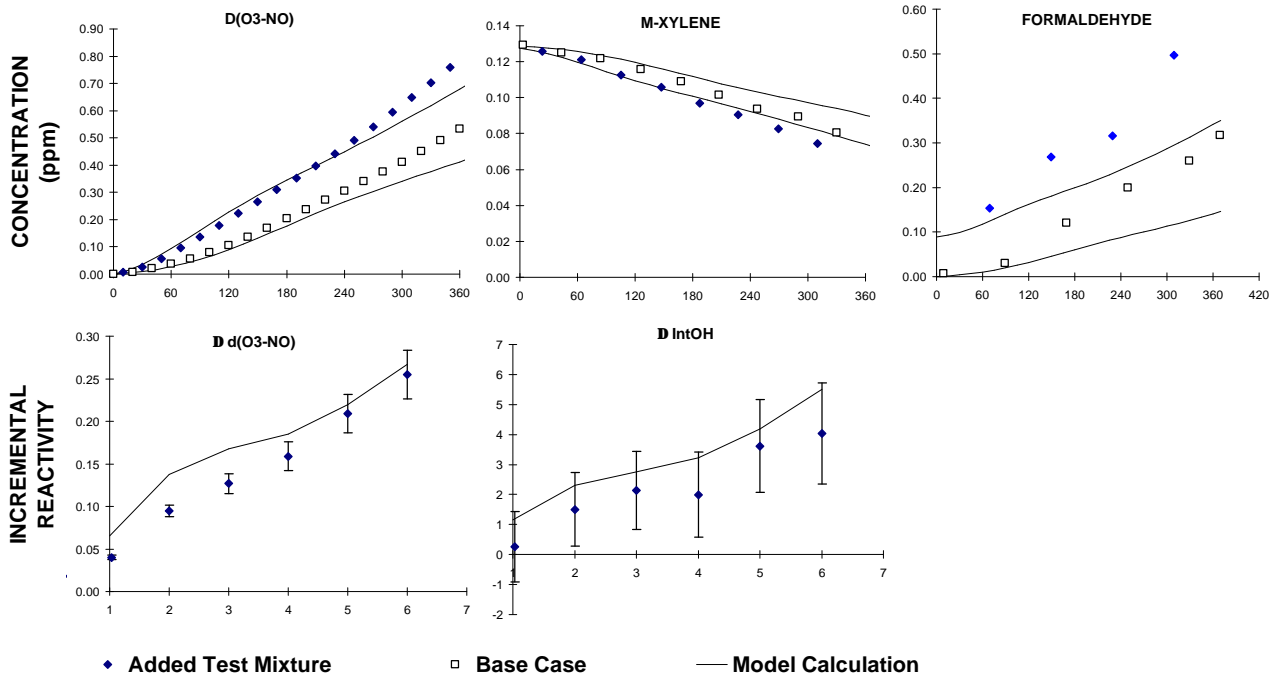
Figure 28.   Experimental and calculated results of the mini-surrogate incremental reactivity experiments with synthetic M85 exhaust.
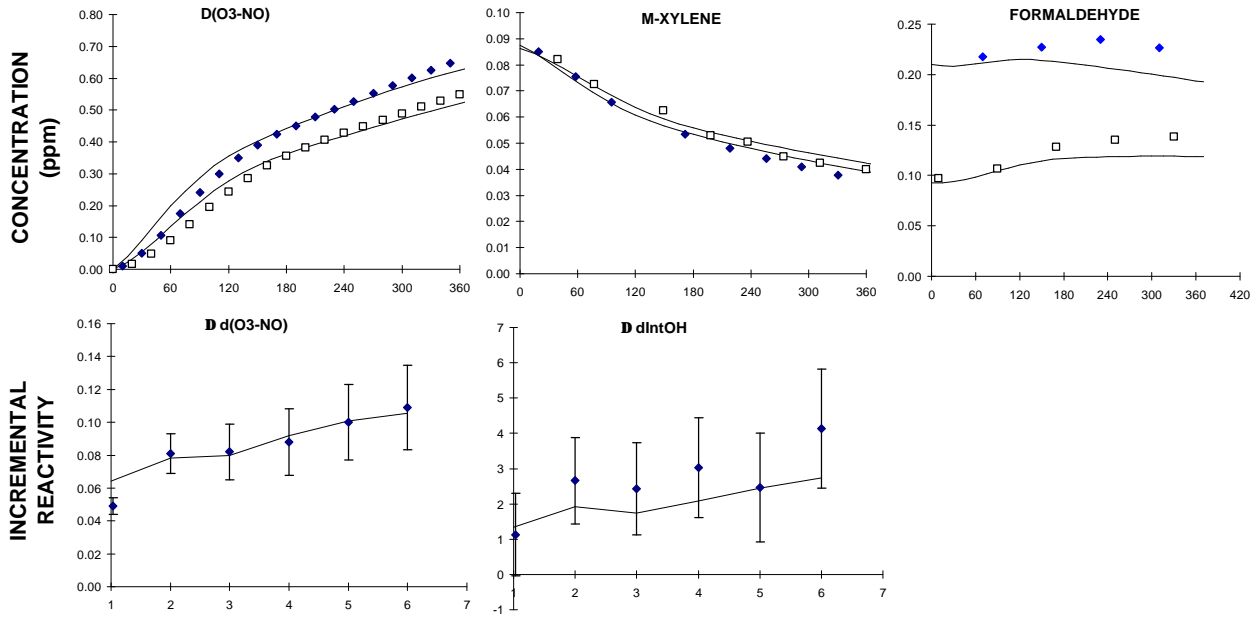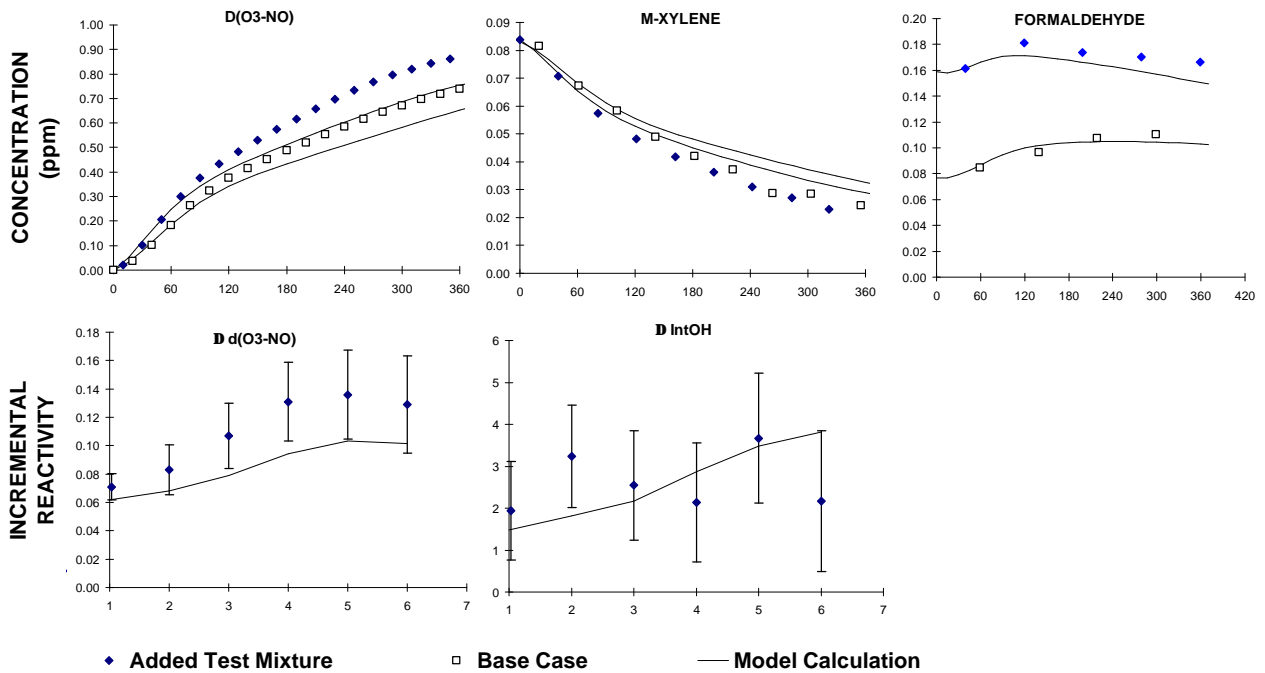
Figure 29. Experimental and calculated results of the full surrogate incremental reactivity experiments with synthetic M100 and M85 exhausts.

Figure 26 shows the two reactivity runs with synthetic exhaust runs carried out during Phase 1, one duplicating a mini-surrogate run and the other duplicating a run with the full surrogate. In both cases the effect of the synthetic methanol and formaldehyde mixture on NO oxidation and O_3 formation was somewhat less than in the exhaust experiment it was intended to duplicate, but in both cases the amount of formaldehyde in the synthetic exhaust run turned out to be about 0.04 ppm lower than in the corresponding exhaust run. On the other hand, the two Phase 2 mini-surrogate runs with synthetic M100 were good duplicates in terms of the amounts of methanol and formaldehyde, and the relative effects of the added synthetic exhausts were reasonably close to those of the runs they were intended to duplicate. The total amount of ozone formation in the synthetic exhaust runs were greater than in the corresponding actual exhaust runs because the light intensity employed was greater. (At the time the synthetic exhaust runs were conducted, it was thought that the light intensity was declining at a more rapid rate than subsequent analysis indicated was likely to be the case, so 75% lights were employed in the synthetic exhaust runs in an attempt to duplicate the conditions of the earlier runs. See the discussion of light characterization, above.) However, the important result in this case is the relative effects of the added exhaust.

Figure 28 shows the results of the mini-surrogate with synthetic M85 experiments. Although both runs were an attempt to duplicate run DTC593 (Figure 24), run DTC636 had higher light intensity and run DTC670, which was carried out later with the light intensity reduced, had much higher initial methanol levels. However, in both cases, the relative effects of synthetic exhaust addition was somewhat less than the relative effect of actual exhaust addition in run DTC593, though not by a large amount. It is interesting to note that the relative effect of synthetic exhaust addition was about the same in run DTC670 as in run DTC636, despite the fact that the former had more than twice as much methanol. This indicates that it is the formaldehyde in the exhaust which is having the much larger effect.

Figure 29 shows the results of the full-surrogate with synthetic M85 exhaust experiments. Both experiments duplicated the reactants in DTC591 reasonably well, though DTC637 had higher light intensity. For these runs, the relative effects of synthetic exhaust addition was reasonably close to the relative effects of actual exhaust addition in the run it was intended to duplicate.

Model Simulations

Figures 19-29 show the results of the model simulations of the actual and synthetic methanol exhaust runs which could be modeled. Figures 19-21 show that the model consistently overpredicted the O_3 formation and NO oxidation rates in the exhaust only and the synthetic exhaust runs, with no significant difference in model performance between actual or synthetic exhaust runs. This is

consistent with the model's consistent tendency to overpredict reactivity in the methanol only runs and in the methanol with formaldehyde mixture runs discussed above (see Figures 11 and 12), but is inconsistent with its tendency to underpredict reactivity in the formaldehyde only runs (see Figure 8). The poor model performance in the case of DTC592 could be attributed to the high sensitivity of such low reactivity runs to variable chamber effects, but the reason for the consistent overpredictions for the other runs is more difficult to rationalize.

On the other hand, Figures 22-29 show that the model has no such consistent bias towards overprediction in the simulations of the relative effects of the real or synthetic methanol exhausts when added to surrogate - NO_x mixtures in incremental reactivity experiments. In most cases, the model performance in simulating the relative effects of exhaust or synthetic exhaust addition is reasonably good, and where there are discrepancies, it tends to be towards *underprediction* of reactivity. Thus the apparent model bias towards overprediction indicated by the exhaust (or synthetic exhaust) only runs is not borne out by the results of the incremental reactivity experiments. It is interesting to note that the runs with non-negligible underprediction by the model are all synthetic exhaust runs; all the runs with actual methanol exhausts are fit reasonably well. However, a majority of the synthetic exhaust runs are also fit reasonably well, and it is more likely that the cases of underprediction are due to characterization problems than to systematic model biases.

Evaluation of CNG Exhaust
Exhaust Injection and Analyses

All of the experiments employing CNG exhaust were carried out during the second phase of the program, using the same procedure as discussed above for the Phase 2 runs with the methanol exhausts. As before, the exhaust was transferred from the vehicle to the chamber using the Teflon transfer bag, and all these experiments employed cold start emissions, with the vehicle gradually accelerating to 40 mph in about 30 seconds, followed by steady state operation, with exhaust being collected for 30-90 seconds. The diluted exhaust in the transfer bag was analyzed using instrumentation in the VERL analytical laboratory prior to being injected into the environmental chamber, where the further diluted exhaust was analyzed using the analytical instrumentation in the chamber laboratory.

A total of six runs with CNG exhaust were carried out. Table 11 gives a summary of the major exhaust, transfer bag, and chamber measurements made during these runs. Reasonably consistent dilution ratios were obtained in most cases when they could be derived using different methods. The exceptions were that the exhaust and transfer bag CO measurements for run DTC 572 were inconsistent with the

exhaust and bag measurements for the other species, and that the transfer bag to chamber dilutions derived from the formaldehyde data were somewhat lower than those derived from the CO data for the two runs where transfer bag formaldehyde measurements were available. It is probable that either the transfer bag or the exhaust CO data for run DTC572 are in error, but it's not clear which is the most likely. The level of agreement for the dilution rates calculated with the formaldehyde data is not out of line with the precision of the measurement of this species. (We tend to suspect that the chamber measurements of the CO are more reliable, based on the general agreements obtained between injected and measured CO in chamber experiments.) Note that if there were loss of formaldehyde between the time it is measured in the transfer bag and the time it is measured in the chamber the dilution ratios calculated using formaldehyde data would tend to be high, which is opposite to what is observed.

The measurements in the chamber indicate that the only detectable CNG exhaust species are NO_x, CO, and low levels of formaldehyde (methane is undoubtedly also present but it is not monitored in the chamber). To determine what other reactants might be present, detailed hydrocarbon and oxygenate speciation analyses were carried out for two of these runs (DTC572 and DTC575), and the data obtained are given in Table B-2 in Appendix B. The speciated analyses indicated that ethane was the major measured NMHC species other than formaldehyde. If ethane and formaldehyde are subtracted off, the remaining NMHC in the transfer bag was only ~0.5 ppmC and <0.1 ppmC in DTC572 and DTC575, respectively, which corresponds to less than 30 ppbC when diluted into the chamber. In terms of VOC reactivity, the only significant measured species in these exhausts were CO and formaldehyde, and these were the only species used when formulating the synthetic exhaust mixtures for the synthetic exhaust experiments.

Results of Chamber Runs

The conditions of the chamber runs carried out using the actual and the synthetic CNG exhausts are summarized on Table 12. Two with actual CO exhaust on one side of the chamber and synthetic CNG on the other, three incremental reactivity experiments with CNG exhaust, three with the mini-surrogate and one with the full surrogate, two synthetic CNG exhaust experiments, each with a surrogate with formaldehyde on one side and without formaldehyde on the other, and two mini-surrogate incremental reactivity experiments with synthetic CNG. As indicated above, the only reactants used to represent the non-NO_x species in the CNG was either CO alone or a mixture of CO and formaldehyde. Although methane is also present, it is calculated not to contribute significantly to the reactivity of the exhausts, so it was not included in the synthetic exhausts. The other hydrocarbons observed in the speciated

81

Table 11. Summary of exhaust injections and analyses for the CNG exhaust chamber runs.

	DTC567	DTC568	DTC569	DTC572	DTC573	DTC575
Exhaust						
Fill Duration (sec)	35	36	~30	37	~30	~30
NOx (ppm)	53.8	54.5	75.9	-	1.7	2.5
CO (ppm)	5570	5591	13543	11335	8286	6078
CO2 (%)	11.3	11.3	9.4	11.0	11.2	11.3
O2 (%)	0.116	0.138	0.310	0.006	0.046	~0
THC (ppmC)	245.4	291.6	665.4	183.3	215.8	206.9
Methane (bench) (ppm)	732.8	816.3	1675.5	550.9	624.9	611.3
Transfer Bag						
NOx (ppm)	2.19	2.68	7.92			
CO (ppm)	189.11	269.93	1315.73	237.46	223.13	322.99
CO2 (%)	0.35	0.51	0.86	0.67		0.58
						19.76
THC (ppmC)	9.7	13.5	36.7	8.3	7.7	11.6
Methane (bench) (ppm)	28.8	35.2	87.3	24.6	22.6	30.7
Methane (GC) (ppm)	-	-	-	28.2	-	37.1
Formaldehyde (ppm)	-	-	-	0.28	-	0.19
Hydrocarbon Speciation Data?	no	no	no	yes	no	yes
Aldehyde Speciation Data?	no	no	no	yes	no	yes
Exhaust/Transfer bag dilution						
Average	<u>27.4</u>	<u>21.6</u>	<u>13.6</u>	<u>20.3</u>	<u>31.0</u>	<u>19.0</u>
NOx (ppm)	24.6	20.3	9.6	-	-	-
CO (ppm)	29.5	20.7	10.3	(47.7)	37.1	18.8
CO2 (%)	32.2	22.1	10.9	16.5	-	19.6
THC (ppmC)	25.2	21.6	18.1	22.0	28.0	17.9
Methane (bench)	25.4	23.2	19.2	22.4	27.7	19.9
Chamber						
Side(s) injected	A	A	A	A	A	A
NOx	0.142	0.108	0.356			0.074
CO	7.14	10.01	42.39	14.32	13.35	19.44
Formaldehyde	-	0.013		0.036	0.041	0.019
Transfer bag / Chamber dilution						
Average	<u>20.9</u>	<u>25.9</u>	<u>26.6</u>	<u>16.6</u>	<u>16.7</u>	<u>16.6</u>
NOx	15.4	24.7	22.2			
CO	26.5	27.0	31.0	16.6	16.7	16.6
Formaldehyde				(7.9)		(10.1)

Table 12.   Summary of experimental runs using actual or synthetic CNG exhaust.

Type / Run	k(NO$_2$+ hν) (min^{-1})	Initial Reactants (ppm)					Base ROG (ppmC)	Data Plots
		NO	NO2	CO	Methane	HCHO		
CNG Exhaust Only								
DTC567A	0.20	0.13	0.01	8.9	1.2	(a)		30
DTC575A	0.20	0.07	0.00	22.5	2.2	0.019		30
Synthetic CNG Exhaust								
DTC567B	0.20	0.13	0.01	8.8	-	(a,b)		30
DTC632A	0.27	0.08	0.01	32.0	-	0.021		31
DTC654B	0.17	0.06	0.00	21.3	-	0.023		31
Synthetic CNG Exhaust without Formaldehyde (CO - NOx)								
DTC575B	0.20	0.07	0.00	21.5	-			30
DTC632B	0.27	0.08	0.01	32.5	-			31
DTC654A	0.17	0.06	0.00	21.2	-			31
Mini-Surrogate + CNG								
DTC568A	0.20	0.37	0.10	12.0	0.9	0.013	5.68	32
DTC569A	0.20	0.33	0.04	44.5	0.7	(a)	5.20	32
DTC572A	0.20	0.29	0.09	16.6	1.7	0.036	4.99	33
Mini-Surrogate + Synthetic CNG								
DTC633B	0.27	0.21	0.11	16.3	-	0.040	5.38	34
DTC655A	0.17	0.23	0.08	16.8	-	0.040	5.51	34
Full Surrogate + CNG								
DTC573A	0.20	0.09	0.04	15.9	1.3	0.041(c)	3.91	33

(a)   No data or data not reliable.
(b)   Formaldehyde not injected
(c)   Not counting formaldehyde in base surrogate mixture.

83

analyses were also too unreactive or too low in concentration to be expected to contribute non-negligibly to the overall exhaust reactivity.

The results of the CNG exhaust and the synthetic CNG exhaust experiments are shown on Figures 30 and 31. Results of model simulations, discussed below, are also shown. DTC567A had relatively high levels of NO compared to the other pollutants, and only a small amount of NO oxidation and essentially no O_3 formation was observed. Since CO and NO_x were the only detectable pollutants in that exhaust experiment (the formaldehyde instrument was not functioning), CO and NO_x was injected on the other side to serve as a synthetic exhaust run. The results were similar, except the NO oxidation rate was somewhat slower than on the actual exhaust side, indicating that there may be other non-negligible reactants present in the exhaust mixture besides CO and NO_x.

Run DTC575A (Figure 30) was more successful in that the ratio of CO and VOC reactants to NO_x was higher, and more rapid NO oxidation and some O_3 formation occurred. On the other side, only CO and NO_x was added to duplicate the conditions of the exhaust run. The rate of NO oxidation was slower on that side, and O_3 formation was minor. Small amounts (~20 ppb) of formaldehyde was observed in the exhaust, but was not added to the synthetic exhaust mixture in run DTC575B. On the other hand, in synthetic CNG exhaust runs DTC632A and DTC654B the ~20 ppb of formaldehyde was included in the mixture, along with the CO. The resulting NO oxidation and ozone formation rates in these runs were much more comparable to the actual exhaust run DTC575A, which these were intended to duplicate. On the other side of both runs, the same CO - NO_2 mixture was used, but without the added formaldehyde. The NO oxidation and O_3 formation was indeed less on those sides, indicating the importance of formaldehyde in contributing to the reactivity of this synthetic CNG exhaust mixture.

Figures 32 and 33 show the results of the four incremental reactivity experiments with CNG exhaust. The formaldehyde data taken during those experiments are also shown. The added CNG exhaust caused a small but measurable increase in NO oxidation and O_3 formation in all runs, with the effect being slightly larger in the mini-surrogate runs than in the run using the full surrogate. The added exhaust slightly increased the integrated OH levels in one of the mini-surrogate runs and slightly decreased it in the full surrogate run, and had too small an effect to measure reliably in the other mini-surrogate runs. The formaldehyde levels were slightly higher in the runs with the added exhaust, but the added exhaust had no significant effect on the formaldehyde formation rates once the irradiations began.
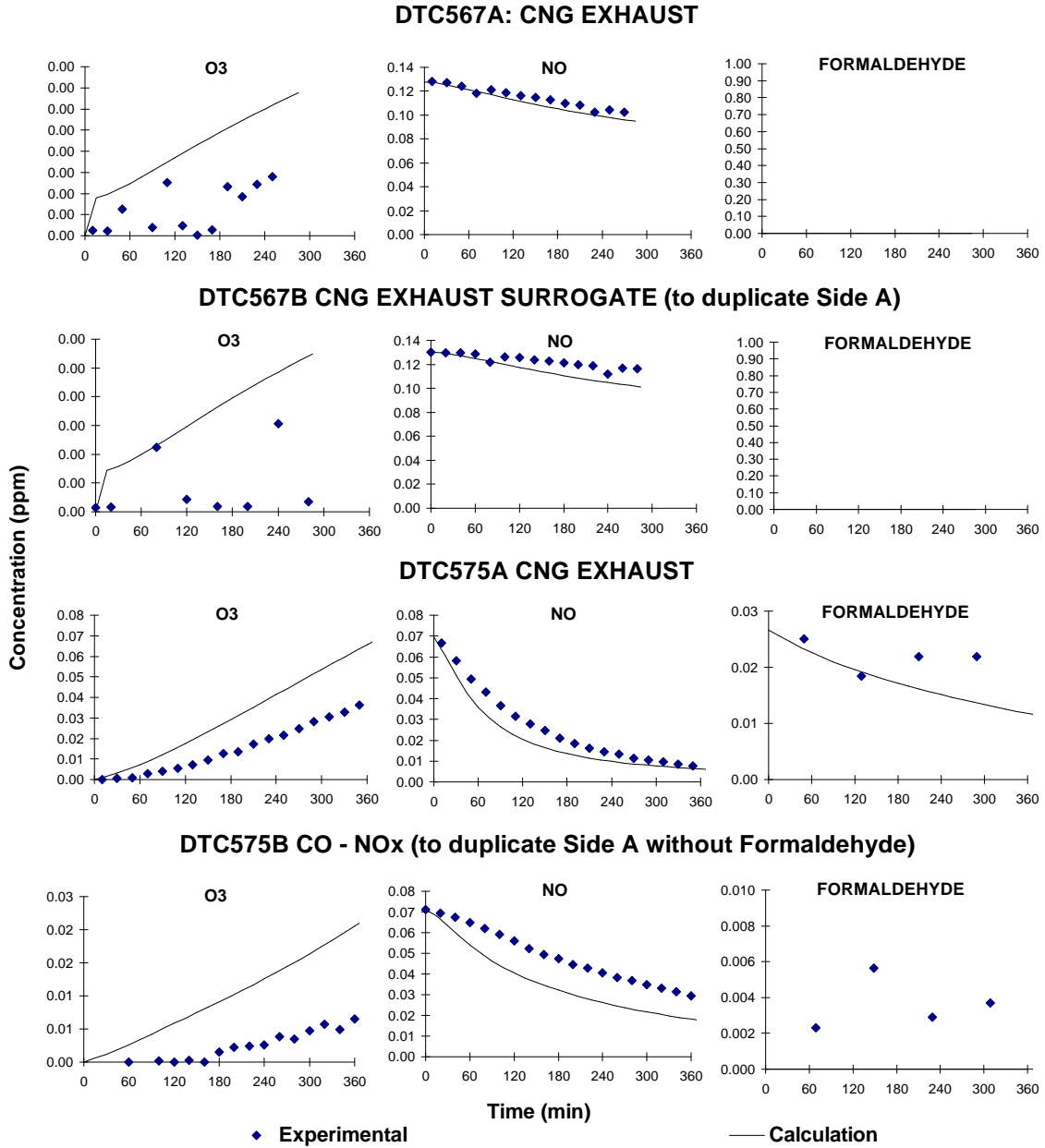
Figure 30.   Experimental and calculated concentration-time plots for ozone, NO, and formaldehyde in the CNG exhaust and surrogate CNG exhaust experiments DTC567 and the CNG exhaust and CO - NOx experiment DTC575.

85

DTC632A: CNG EXHAUST SURROGATE (to duplicate DTC575A)

DTC632B: CO - NOx (to duplicate DTC575A without formaldehyde)

DTC654B: CNG EXHAUST SURROGATE (to duplicate DTC575A)

DTC654A CO - NOx (to duplicate DTC575A without formaldehude)
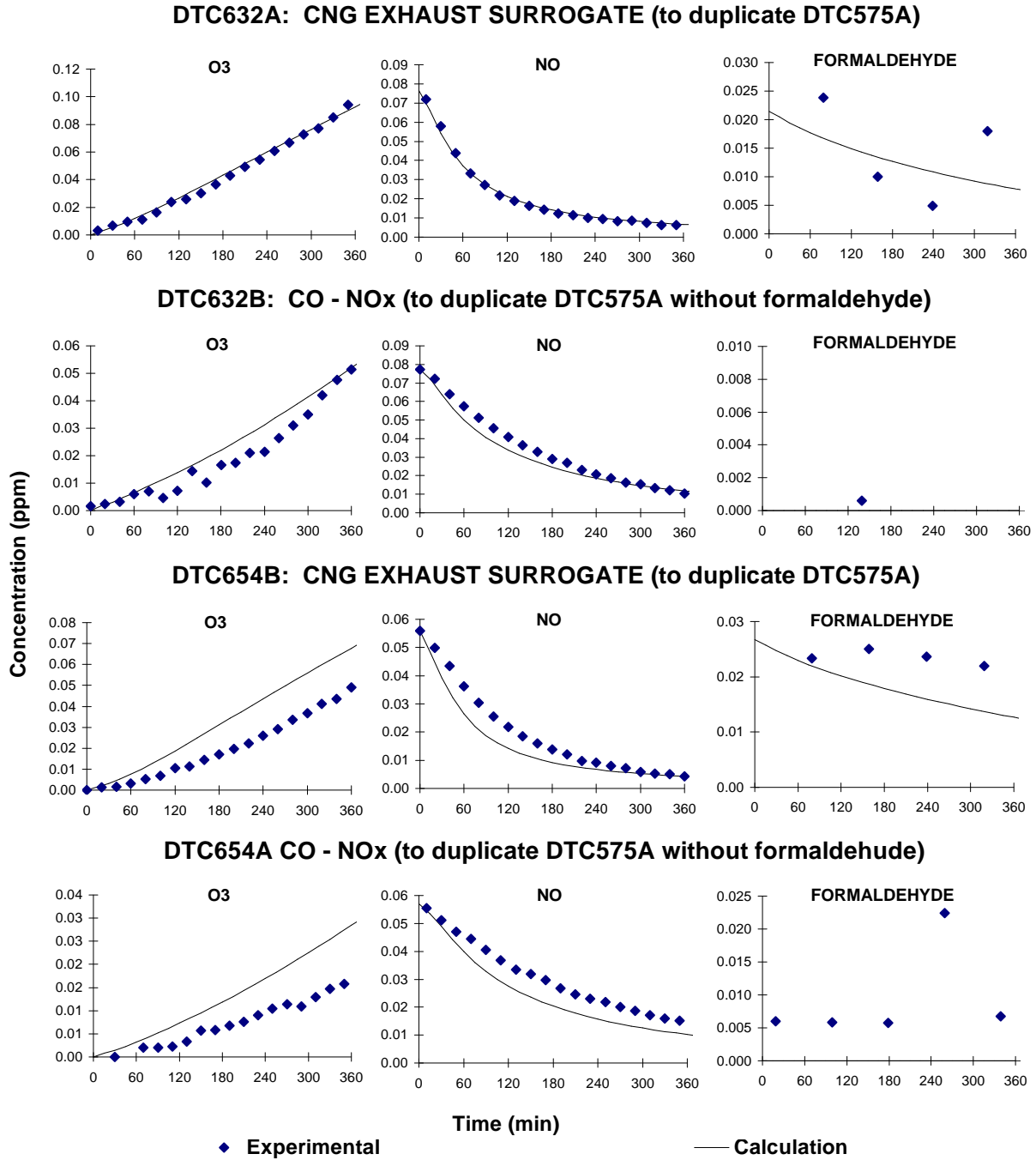
Figure 31.   Experimental and calculated concentration-time plots for ozone, NO, and formaldehyde in the CNG exhaust surrogate and CO - NOx experiments DTC632 and DTC654.

86

DTC568A: Mini-Surrogate + CNG Exhaust
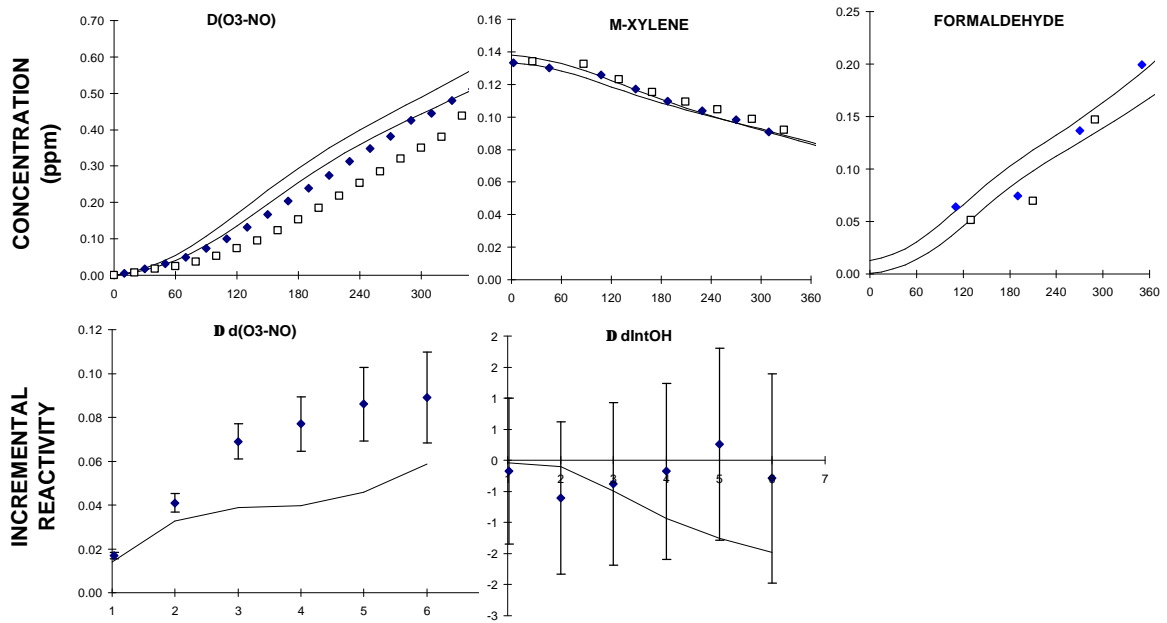
DTC569A: Mini-Surrogate + CNG Exhaust
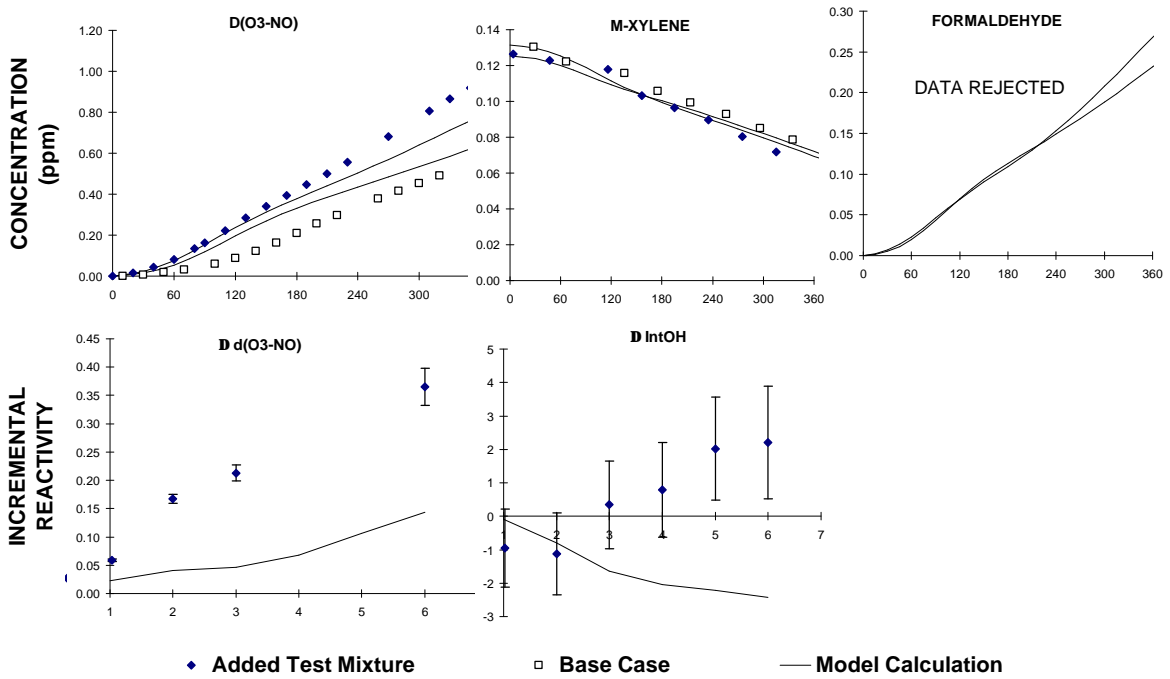
♦ **Added Test Mixture**   □ **Base Case**   —— **Model Calculation**

Figure 32   Experimental and calculated results of the mini-surrogate + CNG exhaust experiments DTC568 and DTC569.

87
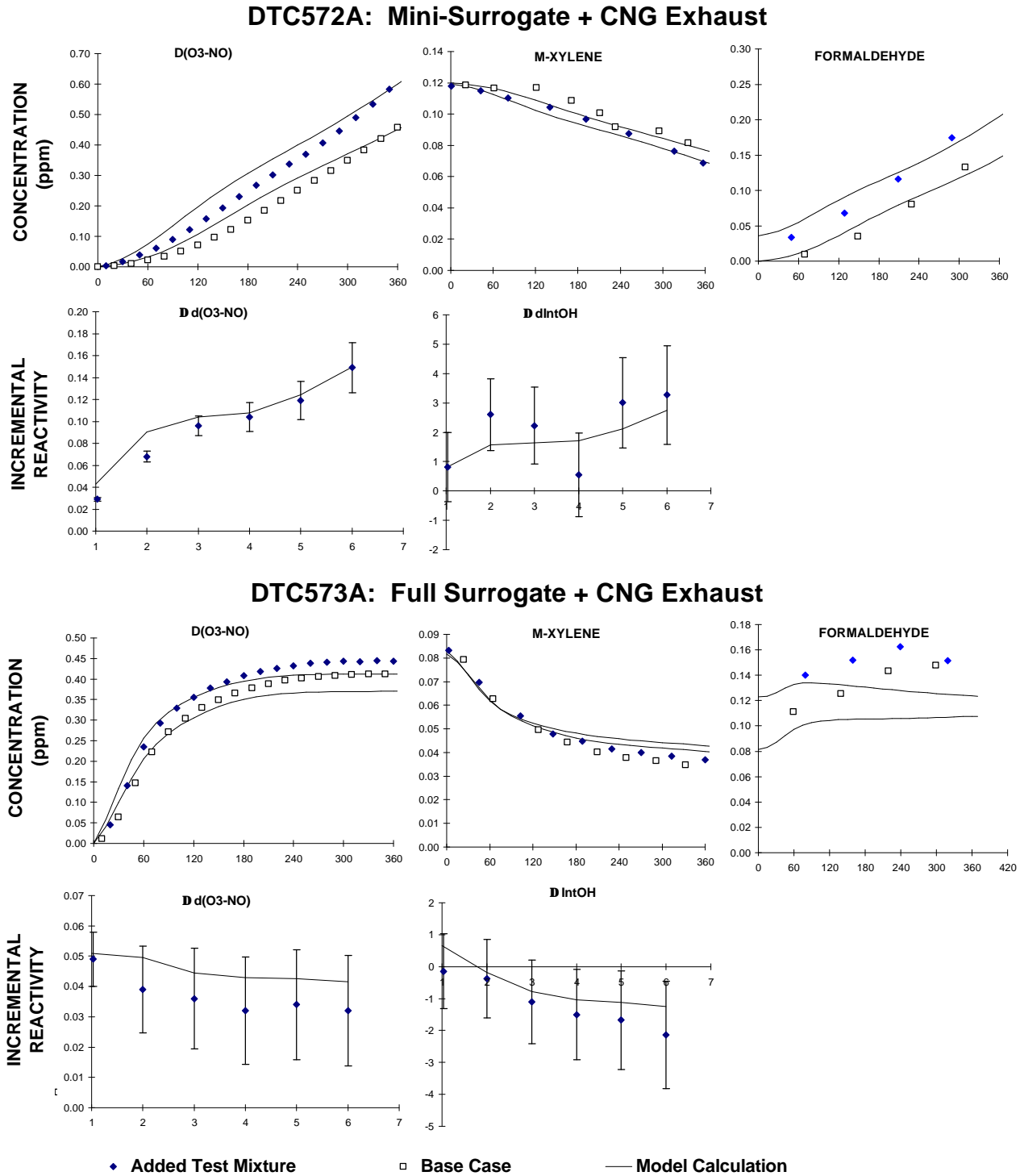
Figure 33. Experimental and calculated results of the mini-surrogate + CNG exhaust experiment DTC572 and the full surrogate + CNG exhaust experiment DTC573.

Figure 34 shows the results of the two mini-surrogate experiments with added synthetic CNG exhaust. The reactant levels in both experiments were designed to duplicate run DTC572, though more ozone formation occurred in run DTC633 because of the higher light intensity. As indicated above, the synthetic exhaust used in these experiments consisted only of CO and formaldehyde; the contributions of the other organics were ignored. A comparison of the data on Figures 33 and 34 shows that the relative effects of the added synthetic exhaust mixture was essentially the same as observed in the experiment these synthetic exhaust runs were designed to duplicate.

Model Simulation Results

Figures 30-34 also show the results of the model simulations of the actual or synthetic CNG exhaust experiments. As shown on Figures 30 and 31, the model tended to overpredict the rates if NO oxidation and O_3 formation in the CNG exhaust runs and the CO - NO_x and CO - formaldehyde - NO_x experiments designed to duplicate them. However, all these experiments have relatively slow NO oxidation and O_3 formation rates, which makes them sensitive to chamber effects such as the chamber radical source. Only Run DTC567 in particular has such low NO oxidation rates (with no O_3 formation) that it probably cannot be considered useful for mechanism evaluation. For the other experiments, the amount of underprediction of reactivity is comparable for the runs with actual as with synthetic exhaust, indicating that the discrepancy is not likely due to a problem with the exhaust itself.

The model simulations of the incremental reactivity experiments with CNG exhaust are shown on Figures 32 and 33. The model did not perform well in simulating the results of the first two mini-surrogate incremental reactivity runs (runs DTC568 and DTC569 shown on Figure 32), but good simulations of the results of the third mini-surrogate run and of the full surrogate run (runs DTC572 and DTC573 shown on Figure 33). The underprediction of the effect of CNG exhaust in Run DTC569A is probably due to the lack of reliable formaldehyde data for that run; the model simulation assumes that no formaldehyde is present in the exhaust, and better results are obtained if the initial formaldehyde in that run is assumed to be similar to that observed in the other CNG runs. Formaldehyde measurement errors may be the problem with the model simulation of run DTC568A as well, since the measured initial formaldehyde in that run (which was used in the model simulation) was lower than observed in the other runs. The formaldehyde data are probably more reliable in the subsequent runs, for which the model gave better predictions of the added CNG exhaust.

The model simulations of the incremental reactivity experiments with the synthetic CNG exhaust are shown on Figure 34. The ozone formation in the base case experiment was slightly underpredicted in

DTC655A: Mini-Surrogate + Synthetic CNG Exhaust (to duplicate DTC572)
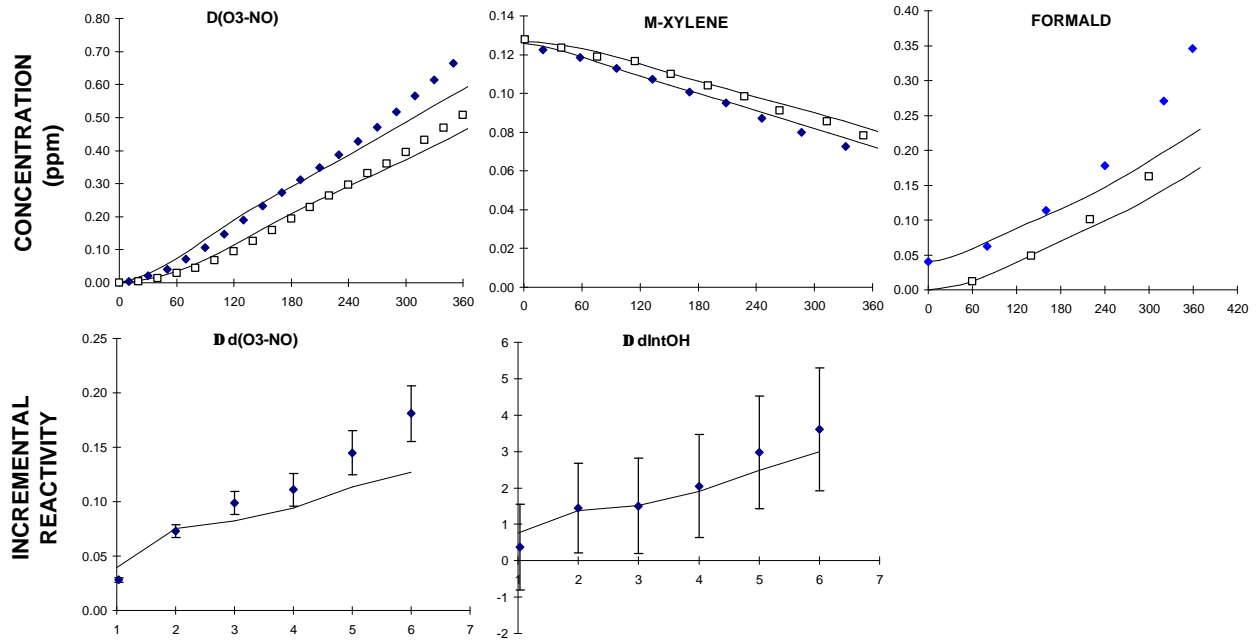
DTC633B: Mini-Surrogate + Synthetic CNG Exhaust (to duplicate DTC572)

◆ Added Test Mixture   □ Base Case   —— Model Calculation
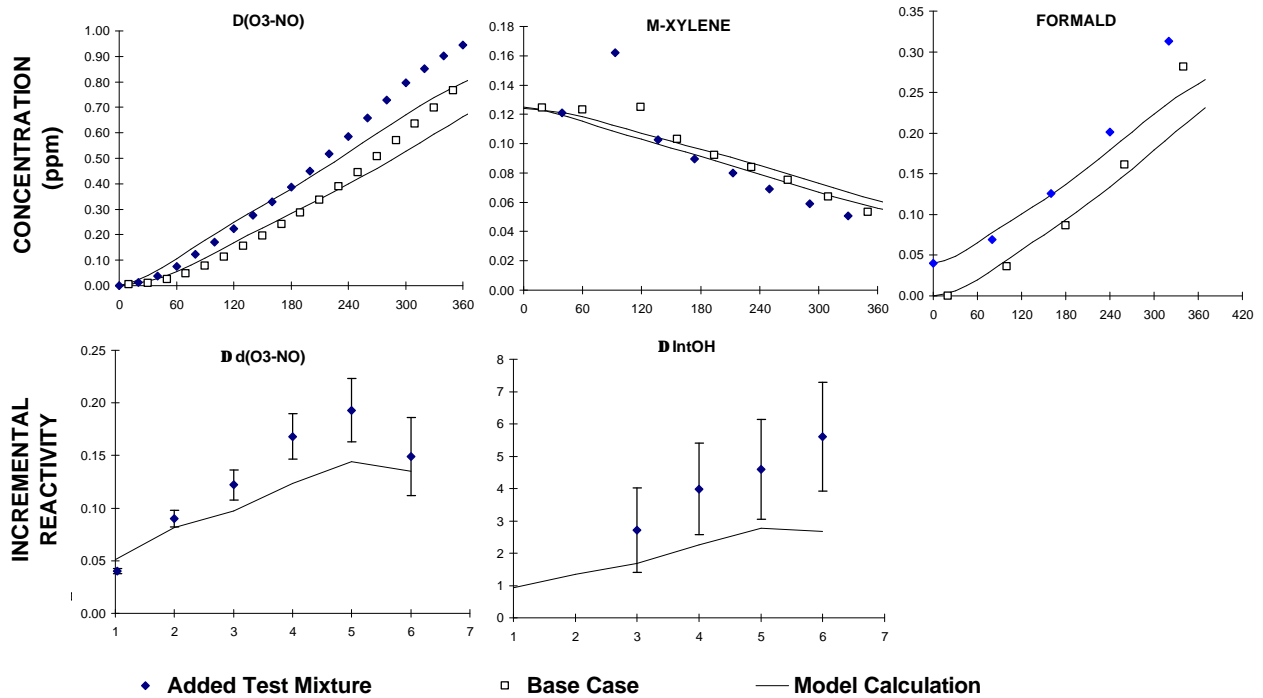
Figure 34.   Experimental and calculated results of the mini-surrogate + surrogate CNG exhaust experiments DTC655 and DTC633.

90

both cases, but the model gave a fair simulation of the relative effect of the synthetic exhausts, which, as indicated above, was about the same as the relative effect of the added exhaust in the run they were intended to duplicate.

Evaluation of RFG Exhausts
Exhaust Injection and Analyses

As shown on Table 1, above, experiments were carried out using exhausts from five different RFG-fueled vehicles, of various ages, mileages, and types. All of the experiments employing RFG exhausts were carried out during the second phase of the program, using the same procedure as discussed above for the Phase 2 M100, M85, and CNG exhausts. As before, the exhaust was transferred from the vehicle to the chamber using the Teflon transfer bag, and all these experiments employed cold start emissions, with the vehicle gradually accelerating to 40 mph in about 30 seconds, followed by steady state operation. The diluted exhaust in the transfer bag was analyzed using instrumentation in the VERL analytical laboratory prior to being injected into the environmental chamber, where the further diluted exhaust was analyzed using the analytical instrumentation in the chamber laboratory.

Summaries of the exhaust injections and analyses results for the RFG vehicles are shown on Tables 13 and 14, where Table 13 shows the data for the runs using exhausts from the 1991 Dodge Spirit (the "Rep Car") and the 1994 Chevrolet Suburban, and Table 14 shows the data for the runs using the 1997 Ford Taurus, the 1984 Toyota Pickup and the 1988 Honda Accord. The average total hydrocarbon (THC), NO_x, and CO measured in the raw exhausts during the injection into the transfer bag are summarized in Table 15, which also gives the standard deviations of the averages (as percentages, in parentheses) and the ranks of the various vehicles, sorted by total THC and CO levels. Reasonably consistent overall pollutant levels were observed in the various runs with a given vehicle, particularly for the THC levels.

As discussed above in conjunction with the FTP data, Tables 13 and 14 show that the cold start exhausts from these five vehicles vary widely in their levels of THC, NO_x, and CO. The highest pollutant levels were from the three relatively high-mileage in-use vehicles that were studied, with the lowest being the late model Ford Taurus. TheTHC/NO_x ratios also varied among the different vehicles, with the highest being the Toyota (4.5) and the Rep Car (2.8), and the lowest being the Accord and the Taurus (both <1). Thus, chamber data from a reasonably varied set of types of RFG exhausts is being obtained in this program.

Table 13. Summary of exhaust injections and analyses for the chamber runs using RFG exhaust from the 1991 Dodge Spirit ("Rep Car") and the 1994 Chevrolet Suburban.

	Dodge Spirit ("Rep Car")						
	DTC574	DTC576	DTC577	DTC581	DTC594	DTC585	DTC586
Exhaust							
Fill Duration (sec)	32	~30	33	34	31	36	32
NOx (ppm)	93.5	70.0	101.4	76.1	500.2	356.2	379.7
CO (ppm)	842	955	1061	837	9506	9708	8806
CO2 (%)	15.1	15.0	15.0	15.1	14.0	14.1	14.1
O2 (%)	0.087	0.019	0.042	0.117	0.582	0.562	0.620
THC (ppmC)	212.4	182.9	191.3	183.0	658.4	533.8	609.0
Methane (bench) (ppm)	60.2	55.5	55.4	52.8	98.0	89.8	87.1
Transfer Bag							
NOx (ppm)	3.95	4.09	4.53	3.91	23.47	15.03	15.90
CO (ppm)	26.78	59.44	30.51	26.72	633.93	331.28	539.49
CO2 (%)	0.59	0.69	0.54	0.60	0.56	0.49	0.51
THC (ppmC)	5.9	7.1	5.1	6.0	30.6	16.6	23.6
Methane (bench) (ppm)	2.4	2.7	1.9	2.1	5.9	2.9	3.92
Methane (GC) (ppm)	2.81	3.36	3.10	3.36		4.58	5.79
Formaldehyde (ppm)	0.44	0.49	0.38	0.42	0.93	0.65	0.85
Ethene	0.38			0.52	5.04	2.87	4.10
Propene					1.62		
Toluene	0.20			0.20	0.99	0.54	0.75
Xylenes	0.14		0.13		0.67	0.36	0.52
Exhaust/Transfer bag dilution							
Average	<u>28.3</u>	<u>20.3</u>	<u>30.3</u>	<u>26.4</u>	<u>19.9</u>	<u>29.0</u>	<u>23.2</u>
NOx (ppm)	23.7	17.1	22.4	19.5	21.3	23.7	23.9
CO (ppm)	31.4	16.1	34.8	31.3	15.0	29.3	16.3
CO2 (%)	25.5	21.7	27.9	25.1	25.1	28.7	27.6
THC (ppmC)	36.0	25.9	37.7	30.5	21.5	32.2	25.8
Methane (bench)	25.1	20.6	28.8	25.6	16.6	30.9	22.2
Chamber							
Side(s) injected	A+B	A	A	A	A+B	A	A
NOx	0.126	0.197	0.303	0.236	0.592	0.565	0.321
CO	0.62	2.61	1.90	1.45	15.52	12.19	10.12
Formaldehyde	0.017	0.029	0.045	0.035	0.028	0.035	0.017
Ethene	0.013		0.019		0.115	0.127	0.074
Propene					0.042		
Toluene	0.005			0.011	0.025	0.021	0.012
Xylenes	0.004		0.006		0.017	0.020	0.012
Transfer bag / Chamber dilution							
Average	<u>32.5</u>	<u>21.8</u>	<u>15.5</u>	<u>17.9</u>	<u>40.3</u>	<u>25.5</u>	<u>52.8</u>
NOx	31.2	20.8	15.0	16.6	39.6	26.6	49.5
CO	(43.5)	22.7	16.1	18.4	40.8	27.2	53.3
Formaldehyde	(26.8)	(16.8)	(8.4)	(12.2)	(32.8)	(18.7)	(50.8)
Ethene	28.3		27.9		43.8	22.6	55.6
Propene					38.1		
Toluene	36.2			18.8	39.8	25.8	(62.8)
Xylenes	34.2		20.9		39.5	(18.1)	(43.0)

Table 14. Summary of exhaust injections and analyses for the chamber runs using RFG exhaust from the 1997 Ford Taurus, the 1984 Toyota Pickup and the 1988 Honda Accord.

	Ford Taurus		Toyota Pickup			Honda Accord		
	DTC582	DTC583	DTC661	DTC662	DTC663	DTC665	DTC666	DTC667
Exhaust								
Fill Duration (sec)	32	46	45	60	45	35	45	48
NOx (ppm)	117.9	100.4	225	442	235	449	504	471
CO (ppm)	209	173	13909	9677	18843	4006	3864	3466
CO2 (%)	15.1	15.0	12.3	12.3	12.0	13.9	13.9	13.9
O2 (%)	0.126	0.107	2.61	2.95	2.65	0.78	0.78	0.85
THC (ppmC)	62.0	59.7	1323	1202	1502	389	416	405
Methane (bench) (ppm)	33.1	29.4	175	123	177	52.3	51.6	51.4
Transfer Bag								
NOx (ppm)	3.10	4.90	5.65	15.85	7.32	4.80	8.42	8.89
CO (ppm)	2.61	17.09	383	425	551	32.3	50.0	52.7
CO2 (%)	0.39	0.73	0.27	0.39	0.30	0.19	0.20	0.22
THC (ppmC)	0.60	2.25	35.33	44.44	40.41	12.67	5.86	6.47
Methane (bench) (ppm)	0.66	1.61	4.50	4.66	4.87	4.58	0.61	0.96
Methane (GC) (ppm)	1.14	2.52	7.69	7.84	7.76	3.24	3.31	3.23
Formaldehyde (ppm)			1.38	1.63	1.60	0.12	0.31	0.31
Ethene		0.12	3.48		3.95	0.76	1.16	1.25
Propene			1.43		1.59	0.25	0.37	0.40
Toluene			1.16	1.35	1.29		0.19	
Xylenes			0.72		0.80			
Exhaust/Transfer bag dilution								
Average	<u>42.3</u>	<u>21.5</u>	<u>39.6</u>	<u>27.1</u>	<u>35.9</u>	<u>83.4</u>	<u>69.4</u>	<u>59.6</u>
NOx (ppm)	38.0	20.5	39.8	27.9	32.0	93.6	59.9	53.0
CO (ppm)	80.0	(10.1)	36.3	22.8	34.2	(124.2)	77.4	65.8
CO2 (%)	38.6	20.6	45.7	31.5	40.0	73.3	69.4	63.0
THC (ppmC)	(103.3)	26.5	37.5	27.0	37.2	(30.7)	70.9	62.6
Methane (bench)	50.1	18.3	38.9	26.5	36.3	(11.4)	(84.6)	53.5
Chamber								
Side(s) injected	A+B	A	A+B	A	B	A+B	A	A+B
NOx	0.112	0.260	0.181	0.224	0.114	0.150	0.403	0.252
CO	0.12	0.78	12.26	5.83	7.40	1.05	2.70	1.83
Formaldehyde			0.063	0.032	0.046			
Ethene		0.010	0.100		0.060	0.026	0.034	0.043
Propene			0.046		0.022	0.008	0.021	0.012
Toluene			0.039	0.020	0.021		0.012	
Xylenes			0.024		0.013			
Transfer bag / Chamber dilution								
Average	<u>27.7</u>	<u>20.4</u>	<u>31.4</u>	<u>69.9</u>	<u>67.5</u>	<u>30.8</u>	<u>19.7</u>	<u>32.1</u>
NOx	27.7	18.8	31.2	70.8	64.2	32.1	20.9	35.3
CO	(22.0)	22.0	31.2	72.9	74.4	30.8	18.5	28.8
Formaldehyde			(21.8)	(51.5)	(34.7)			
Ethene		(12.4)	34.8	66.2	65.5	29.5	(34.3)	(29.3)
Propene			31.4		71.7	(30.3)	(17.4)	(33.5)
Toluene			30.1		61.5		(15.9)	
Xylenes			29.5		(62.3)			

Tables 13 and 14 shows that the exhaust, transfer bag, and chamber measurements were in most cases reasonably consistent in their measures of dilution from exhaust to transfer bag to chamber. Very good consistency in exhaust and transfer bag measurements were observed in the runs with the Rep Car, Suburban, and Toyota, though some apparently anomalous CO, THC, and methane measurements were seen in some of the Ford Taurus and Honda Accord runs. However, the dilution ratio in going from the transfer bag to the chamber is the most important factor in terms of data analysis, because this is needed when determining the detailed speciated NMHC compositions in the chamber (see below). For most runs the NO_x and CO data generally gave the most consistent and reliable measure of this dilution factor, though individual hydrocarbon measurements were also useful in most cases, except when the concentrations in the chamber were too low to measure with adequate precision. Because of the greater analytical uncertainty, dilution ratios derived from formaldehyde measurements were not used in deriving the average dilution ratio, though for many runs the dilution ratios from the formaldehyde data were reasonably consistent with those derived from the other measurements. When there were discrepancies the ratio derived from the formaldehyde data tended to be low, suggesting that the transfer bag measurements made by the VERL analytical laboratory may tend to be low or the chamber measurements made in the APL laboratory may tend to be high.

Detailed speciated hydrocarbon and aldehyde analyses were carried out on the diluted exhausts in the transfer bags in all the RFG experiments whose results are reported here. The results of these analyses are given in Table B-2 in Appendix B. Although the analytical instrumentation in the chamber lab could obtain measurements of certain individual species when the exhausts were injected into the chamber, the GC instrumentation in the chamber lab had neither the resolution nor the sensitivity to give complete information about the speciation of the these complex exhaust mixtures. Therefore, for modeling the chamber runs, the compositions of the exhaust components in the chamber were derived using the detailed speciated measurements of the transfer bag (as tabulated in Table B-2) and the transfer bag / chamber dilution ratios derived for the various runs as shown on Tables 13 and 14. However, the measurements using the chamber instrumentation were used for those species where such data were available. This would include the components of the surrogate mixtures that were added to the chamber prior to the exhaust injections in the incremental reactivity experiments.

Derivation of synthetic RFG exhausts

As with the other exhausts, experiments were carried out using synthetic CO and VOC mixtures designed to represent those in selected runs with actual exhaust. Such experiments were also conducted for the RFG exhausts, but because of the complexity of the VOC mixtures in these exhausts, it

Table 15. Average total hydrocarbon, CO, and NO_x levels in the RFG exhausts used in the chamber experiments.

Vehicle	Miles (K)	Level (Average ppm in exhaust)			Rank			THC / NO_x
		THC	CO	NOx	THC	CO	NO_x	NO_x
1984 Toyota	227	1342 (11%)	14143 (32%)	300 (41%)	1	1	3	4.5
1994 Suburban	58	600 (10%)	9340 (5%)	412 (19%)	2	2	2	1.5
1988 Accord	150	403 (3%)	3779 (7%)	475 (6%)	3	3	1	0.8
1991 Rep Car	14	192 (7%)	924 (12%)	85 (17%)	4	4	5	2.3
1997 Taurus	14	61 (3%)	191 (13%)	109 (11%)	5	5	4	0.6

as not practical to prepare synthetic mixtures duplicating the full range of compounds observed in these exhausts. Instead, simplified synthetic exhaust mixtures were employed, where a single compound was used to represent a group of compounds with similar chemical characteristics and reactivity. If the appropriate set of representative compounds is used, the reactivity of the simplified synthetic exhaust mixture should be about the same as that of a fully complex mixture where each measured compound is represented explicitly. If this is the case, an experiment using the simplified synthetic exhausts should give about the same result as one using a fully detailed synthetic exhaust mixture, which, in turn, should give the same result as the experiment with the actual exhaust mixture, assuming that the exhaust analysis was complete and accurate. These experiments can thus be used to test these assumptions.

The compounds detected in the various RFG exhausts, and the methods used to represent them, are listed in Table 16. As shown on the table, reactivity weighting factors were used to adjust for differences in reactivities of the individual compounds and the compound representing it. These were derived by ratios of the Maximum Incremental Reactivities (MIR's) of the compounds, relative to the MIR for the synthetic exhaust compound representing it. MIR's were used to derive the reactivity adjustments because this is a common measure used to compare reactivities of vehicle exhausts, and as indicated above is used as a basis for the "reactivity adjustment factors" in the California Clean Fuels/Low Emissions Vehicle regulations (CARB, 1993). To be consistent with the model simulations of the chamber experiments in this work, the MIRs used to derive these adjustments were calculated using the mechanism given in Appendix A, i.e., using the "SAPRC-97" mechanism documented by Carter et al (1997). Since the substitutions are being made on a molar basis, the MIR's used to derive the adjustments are given in units of moles O_3 per mole VOC emitted.

Table 16. Lumping used when deriving surrogate exhaust mixtures to represent VOC reactants in added RFG exhaust experiments. Weighting factors are derived by ratios of Maximum Incremental Reactivitities (MIR's) calculated using the mechanism listed in Appendix A, in units of moles O_3 per mole VOC emitted.

Compound	Weight	MIR	Compound	Weight	MIR	Compound	Weight	MIR
Negligible reactivity assumed			Represented by Ethene			Represented by 1,2,3-Trimethylbenzene		
Methane	0.00	0.01	Ethene	1.00	4.86	1,3,5-Trimethyl Benzene	1.11	34.20
Ethane	0.00	0.20				1,2,3-Trimethyl Benzene	1.00	30.78
			Represented by Propene			1,2,4-Trimethyl Benzene	0.43	13.32
Represented by n-Butane			Propene	1.00	9.66	C10 Trisub. Benzenes	0.85	26.10
Propane	0.37	0.52	1-Butene	1.28	12.36	C12 Trisub. Benzenes	0.85	26.10
n-Butane	1.00	1.40	3-Methyl-1-Butene	1.09	10.55	C10 Tetrasub. Benzenes	0.85	26.10
n-Pentane	1.54	2.17	1-Pentene	1.09	10.55			
Isobutane	1.13	1.59	1-Hexene	1.03	9.96	Represented by Formaldehyde		
Iso-Pentane	1.80	2.53	1-Heptene	0.96	9.31	Formaldehyde	1.00	4.11
Neopentane	0.70	0.99	1-Octene	0.88	8.48			
2-Methyl Pentane	2.38	3.35	1-Nonene	0.82	7.88	Represented by Acetaldehyde		
3-Methylpentane	2.52	3.54	C6 Terminal Alkanes	1.03	9.96	Acetaldehyde	1.00	5.74
2,2-Dimethyl Butane	1.59	2.24	C7 Terminal Alkanes	0.96	9.31			
2,3-Dimethyl Butane	1.53	2.15	C8 Terminal Alkanes	0.88	8.48	Represented by Lumped HIgher Aldehydes		
3,3-Dimethyl Pentane	1.82	2.56	Styrene	0.51	4.94	C3 Aldehydes	1.00	9.06
2,2,3-Trimethyl Butane	2.05	2.88	Ethyl Acetylene	1.28	12.36	C4 Aldehydes	1.00	9.06
2,2,4-Trimethyl Pentane	2.26	3.17				C5 Aldehydes	1.00	9.06
Cyclopentane	2.74	3.85	Represented by trans-2-Butene			C6 Aldehydes	1.00	9.06
Acetylene	0.14	0.19	Isobutene	0.44	6.72	C7 Aldehydes	1.00	9.06
Methyl Acetylene	2.97	4.17	2-Methyl-1-Butene	0.51	7.80	Acrolein	0.47	4.23
Methyl t-Butyl Ether	0.94	1.32	2-Methyl-1-Pentene	0.51	7.80	Methacrolein	0.86	7.76
			trans-2-Butene	1.00	15.36			
Represented by n-Octane			cis-2-Butene	0.96	14.76	Represented by Acetone		
n-Hexane	[a]	2.10	trans-2-Pentene	1.09	16.80	Acetone	1.00	0.59
n-Heptane	1.12	1.86	cis-2-Pentene	1.09	16.80			
n-Octane	1.00	1.66	2-Methyl-2-Butene	1.06	16.25	Represented by Lumped Higher Ketions		
n-Nonane	0.93	1.55	2-Methyl-2-Pentene	1.06	16.25	C4 Ketones	1.00	2.14
n-Decane	0.92	1.53	2-Hexenes	1.05	16.14			
n-Undecane	0.92	1.53	2-Heptenes	1.02	15.68	Represented by Benzaldehyde		
n-Dodecane	0.84	1.39	1,3-Butadiene	0.92	14.08	Benzaldehyde	1.00	< 0
2,4-Dimethyl Pentane	2.14	3.55	Cyclopentadiene	1.09	16.80	Toluadehyde	1.00	< 0
3-Methyl Hexane	2.19	3.63	Isoprene	0.86	13.25			
2-Methyl Hexane	2.19	3.63	Cyclopentene	0.83	12.70	Represented by Methanol		
2,3-Dimethyl Pentane	1.83	3.04	Cyclohexene	0.63	9.72	Methanol	1.00	0.43
2-Methyl Heptane	1.77	2.94	C6 Internal Alkenes	1.05	16.14			
3-Methyl Heptane	1.90	3.14	C7 Internal Alkenes	1.02	15.68			
4-Methyl Heptane	2.03	3.37	C8 Internal Alkenes	1.11	17.12			
2,3-Dimethyl Hexane	2.03	3.37	C6 Cyclic or di-olefins	1.05	16.14			
2,4-Dimethyl Hexane	2.97	4.92						
2,5-Dimethyl Hexane	2.93	4.85	Represented by Toluene					
2,3,4-Trimethyl Pentane	2.03	3.37	Benzene	0.13	1.30			
2,4-Dimethyl Heptane	2.90	4.81	Toluene	1.00	9.80			
3,5-Dimethyl Heptane	2.90	4.81	Ethyl Benzene	0.51	4.96			
2,2,5-Trimethyl Hexane	2.16	3.58	n-Propyl Benzene	0.46	4.46			
2,4-Dimethyl Octane	2.15	3.56	Isopropyl Benzene	0.48	4.72			
Methylcyclopentane	3.43	5.68	C10 Monosub. Benzenes	0.51	4.96			
Cyclohexane	1.77	2.93	Indan	0.30	2.90			
Methylcyclohexane	2.40	3.97	Naphthalene	0.34	3.37			
1,3-Dimeth. Cyclopentane	3.67	6.08						
Ethylcyclohexane	2.40	3.98	Represented by m-Xylene					
1,3-Dimethyl Cyclohexane	2.70	4.46	o-Xylene	0.60	18.64			
Branched C7 Alkanes	2.19	3.63	m-Xylene	1.00	31.28			
Branched C8 Alkanes	2.03	3.37	C8 Disub. Benzenes	0.60	18.77			
Branched C9 Alkanes	2.22	3.68	C9 Disub. Benzenes	0.60	18.77			
Branched C10 Alkanes	2.15	3.56	C10 Disub. Benzenes	0.60	18.77			
C7 Cycloalkanes	2.40	3.97	C11 Disub. Benzenes	0.60	18.77			
C8 Cycloalkanes	2.40	3.98						
Ethyl t-Butyl Ether	2.76	4.57						

[a] Due to an assignment error, the n-hexane in the mixture was not represented. However, the amounts of n-hexane present in these exhausts wa negligible.

For each of the exhaust experiments which were duplicated by synthetic exhaust runs whose data are presented in this report, Table 17 shows the concentrations of the various lumped groups derived from the detailed speciation of the runs, given in terms of the individual species used to represent the lumped groups. These were derived from the detailed exhaust speciation data for the runs given in Table B-2 in Appendix B (after applying the factors given in Tables 13 or 14 to account for the dilution in going from the transfer bag to the chamber), using the lumping and weighting factors shown on Table 16. The target initial VOC reactant concentrations in the synthetic exhaust runs designed to represent these exhaust experiments were based on these data, although for some runs the low amounts of 1,2,3-trimethylbenzene in the mixture were lumped with m-xylene, the low amounts of aldehydes were lumped with formaldehyde, and the low amounts of ketones and methanol were ignored. The actual measured concentrations of these species in the synthetic exhaust species are also shown on Table 17, indicating the degree to which the target injected concentrations were achieved. In most cases the targets were met reasonably well, though the initial formaldehyde measurements were variable in a few cases (being low in DTC664B and high in DTC681A).

Results for the 1991 Dodge Spirit (Rep Car)

A summary of the experimental runs carried out using or simulating exhaust from the 1991 Dodge Spirit (referred to as the "Rep Car" because it is used for reproducibility determination by the VERL), is given in Table 18. As indicated there, one experiment was carried out with exhaust alone and two experiments were carried out to duplicate, two experiments were carried out with exhaust added to the mini-surrogate mixture, one was carried out with the exhaust added to the full surrogate, and two each experiments were carried out with synthetic Rep Car exhaust added to the mini-surrogate or the full surrogate mixture. The synthetic exhaust-only experiments were carried out with the experiment duplicating the exhaust run on one side of the DTC, and an experiment with the same synthetic exhaust VOC mixture but with reduced NO_x on the other side. This was conducted to obtain information on the ability of the model to simulate the dependence of the reactivity of the synthetic exhausts when NO_x levels are more favorable for ozone formation. The table also indicates the figures where the experimental and calculated results are plotted.

Figure 35 shows concentration-time plots for ozone, NO, formaldehyde, ethene and m-xylene for the actual and synthetic exhaust only, and in the synthetic exhaust, reduced NO_x experiments, based on the Rep Car exhaust. Data were obtained for other major hydrocarbon species such as propene, toluene, n-butane, etc., but the ethene and m-xylene plots shown are representative of the data obtained. Results of model calculations are also shown.

97

Table 17. Summary of lumped group concentrations in the RFG exhaust runs which were duplicated in the synthetic exhausts, and the measured concentrations of those species in the synthetic exhaust experiments.

Compounds Representing Lumped Groups	Duplicating DTC574A			Duplicating DTC576A			Duplicating DTC577A		
	Exhaust Run	Surrogate Runs		Exhaust Run	Surrogate Runs		Exhaust Run	Surrogate Runs	
		639B	671B		672B	642B		643A	669A
n-Butane	0.033	0.035	0.036	0.051	0.057	0.059	0.045	0.040	0.030
n-Octane	0.029	0.029	0.030	0.044	0.048	0.049	0.043	0.043	0.041
Ethene	0.013	0.014	0.013	0.008	0.004	-0.012	0.019	0.022	0.019
Propene	0.009	0.010	0.009	0.017	0.024	0.015	0.012	0.013	0.011
t-2-Butene	0.005	0.006	0.005	0.012	0.016	0.013	0.010	0.000	0.010
Toluene	0.007	0.008	0.009	0.015	0.021	0.018	0.012	0.018	0.012
m-Xylene	0.007	0.012	0.013	0.011	0.010	0.013	0.011	0.009	0.009
1,2,3-Trimethyl-benzene [a]	0.002			0.004	0.010	0.011	0.004	0.009	0.009
Formaldehyde	0.016	0.019	0.019	0.031	0.045	0.033	0.045	0.037	0.046
Acetaldehyde [b]	0.001			0.002			0.001		
Higher Aldehydes [b]	0.001			0.001			0.003		
Benzaldehyde [c]	0.002			0.003					
Acetone [c]							0.000		
Higher Ketones [c]									
Methanol [c]	0.016			0.032			0.042		

Table 17 (concluded)

Compounds Representing Lumped Groups	Duplicating DTC584A			Duplicating DTC585A			Duplicating DTC666	
	Exhaust Run	Surrogate Runs		Exhaust Run	Surrogate Runs		Exhaust Run	Surrogate Run
		640B	660B		641A	664B		681A
n-Butane	0.098	0.098	0.102	0.079	0.085	0.085	0.023	0.031
n-Octane	0.105	0.111	0.102	0.081	0.076	0.085	0.017	0.022
Ethene	0.117	0.114	0.106	0.127	0.099	0.098	0.057	0.062
Propene	0.047	0.045	0.046	0.044	0.049	0.048	0.020	0.023
t-2-Butene	0.044	0.048	0.046	0.040	0.045	0.043	0.010	0.011
Toluene	0.030	0.031	0.028	0.025	0.033	0.029	0.011	0.021
m-Xylene	0.026	0.036	0.032	0.027	0.038	0.023	0.006	0.012
1,2,3-Trimethyl-benzene [a]	0.008			0.006	0.006	0.006	0.002	
Formaldehyde	0.031	0.044	0.049	0.035	0.039	0.011	0.015	0.029
Acetaldehyde [b]	0.008			0.007			0.003	
Higher Aldehydes [b]	0.003			0.002			0.001	
Benzaldehyde [c]	0.003			0.003				
Acetone [c]	0.001			0.000				
Higher Ketones [c]	0.001			0.000				
Methanol [c]	0.026			0.026				

[a] Lumped with and represented by m-xylene in runs duplicating DTC574A, DTC584A, and DTC666A.

[b] Lumped with and represented by formaldehyde

[c] Not represented. Assumed not to contribute significantly to the reactivity of this exhaust

Table 18.   Summary of experimental runs using actual or synthetic "Rep Car" or Suburban RFG Exhausts.

Type / Run	$k(NO_2+ h\upsilon)$ (min^{-1})	Initial Reactants (ppm)			Exhaust NMHC (ppmC)	Base ROG (ppmC)	Data Plots
		NO	NO2	CO			
Rep Car Exhaust Only							Fig.
DTC574A	0.20	0.12	0.01	3.4	0.50		35
Synthetic Rep Car Exhaust							
DTC639A	0.27	0.13	0.04	14.8	0.62		35
DTC671A	0.17	0.11	0.02	3.7	0.64		35
Synthetic Rep Car Exhaust with Reduced NOx							
DTC639B	0.27	0.08	0.04	15.0	0.62		35
DTC671B	0.17	0.07	0.01	3.6	0.64		35
Mini-Surrogate + Rep Car Exhaust							
DTC576A	0.20	0.32	0.11	4.9	1.01	5.41	36
DTC581A	0.19	0.30	0.11	4.0	0.98	5.56	36
Mini-Surrogate + Synthetic Rep Car Exhaust							
DTC672B	0.17	0.28	0.11	4.9	1.11	5.82	37
DTC642B	0.26	0.31	0.11	4.0	1.06	5.51	37
Full Surrogate + Rep Car Exhaust							
DTC577A	0.20	0.28	0.06	4.5	1.10	3.84	38
Full Surrogate + Synthetic Rep Car Exhaust							
DTC643A	0.26	0.29	0.07	4.0	0.90	4.13	39
DTC669A	0.17	0.21	0.06	3.5	0.85	4.26	39
Suburban Exhaust Only							
DTC584A	0.19	0.44	0.15	17.3	2.20		40
Synthetic Suburban Exhaust							
DTC640B	0.27	0.52	0.17	9.5	2.38		40
DTC660B	0.17	0.46	0.18	18.1	2.26		40
Synthetic Suburban Exhaust with Reduced NOx							
DTC640A	0.27	0.14	0.04	9.4	2.38		40
DTC660A	0.17	0.15	0.05	18.1	2.26		40
Mini-Surrogate + Suburban Exhaust							
DTC585A	0.19	0.45	0.11	14.5	1.78	5.82	41
Mini-Surrogate + Synthetic Suburban Exhaust							
DTC641A	0.27	0.43	0.13	12.7	2.10	5.49	42
DTC664B	0.17	0.41	0.13	11.4	1.98	5.54	42
Full Surrogate + Suburban Exhaust							
DTC586A	0.19	0.26	0.06	12.4	1.20	4.25	41
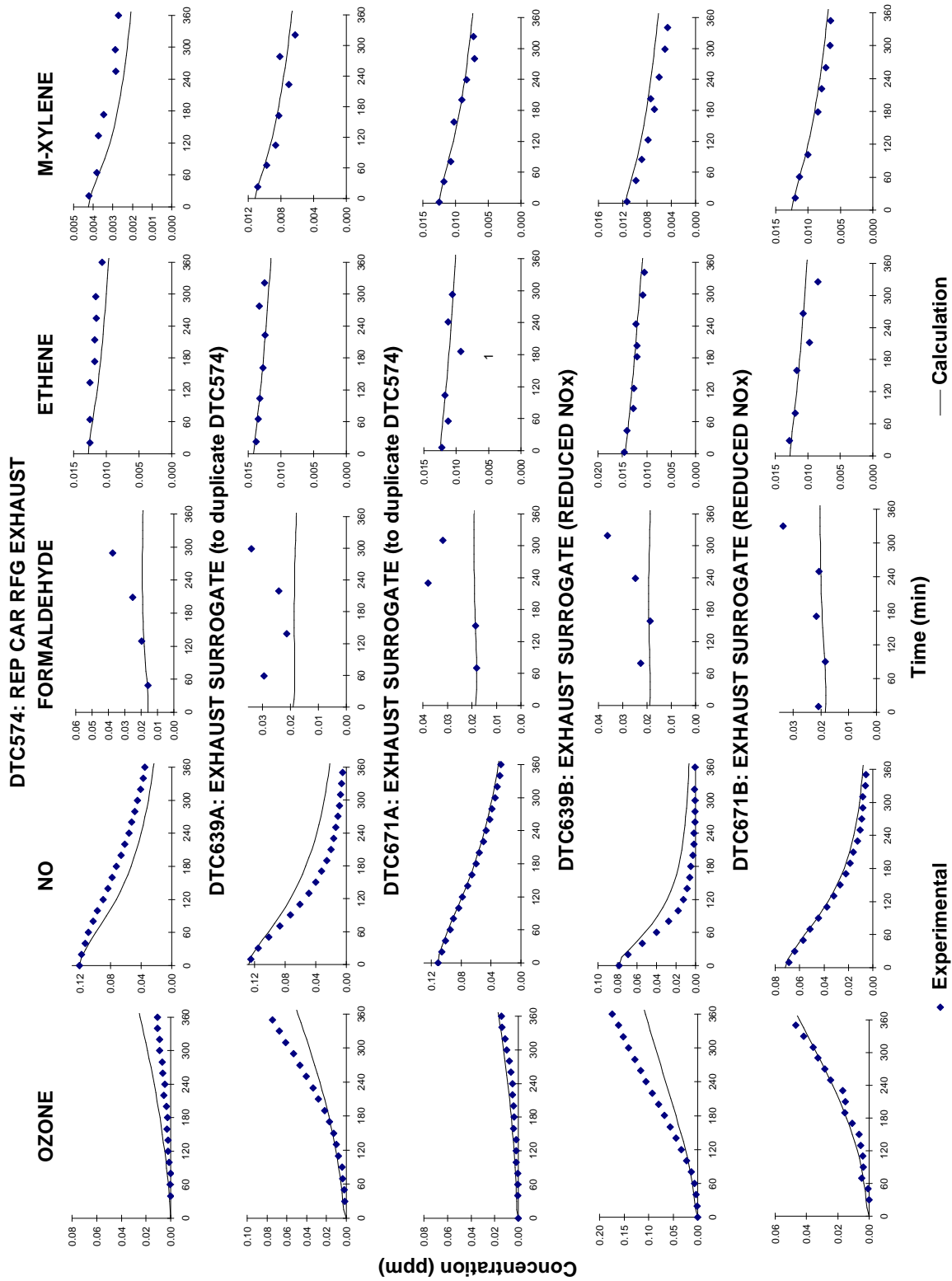
Figure 35. Experimental and calculated concentration-time plots for selected species for the Rep Car RFG exhaust and surrogate exhaust experiments.

100

Although the Rep Car had the lowest NO_x levels of the RFG vehicles studied and the second-highest ROG/NO_x ratios, the ROG/NO_x was still too low for significant O_3 to form in the exhaust only experiment (see plots for DTC574). The first synthetic exhaust run intended to duplicate DTC574 (DTC639A) gave considerably more ozone formation because of the higher light intensity, but the second synthetic exhaust run (DTC671A) gave essentially the same NO oxidation rate and low O_3 formation as the actual exhaust run. As expected, reducing the NO_x in the synthetic exhaust runs caused more rapid NO oxidation rates and greater O_3 formation.

The model tended to overpredict the NO oxidation rates and O_3 formation in the Rep Car exhaust-only run, but gave good simulations to the O_3 and NO data in all the synthetic Rep Car exhaust-only runs. However, runs with such low NO oxidation rates as DTC574 are highly sensitive to the assumed chamber radical source, and a relatively high radical source was assumed when modeling this run based on results of n-butane - NO_x experiments carried out around the same time. Somewhat better fits to the data are obtained if run DTC574 is simulated using the chamber conditions model which was assumed when simulating DTC671, though the NO oxidation rate is still slightly overpredicted. On the other hand, the model gives reasonably good simulations of the hydrocarbon consumption rates in that experiment, as it does in the synthetic exhaust runs as well.

Figures 36-39 show the results of the incremental reactivity experiments using the actual or synthetic Rep Car exhausts. The added exhausts were found to significantly enhance NO oxidation and O_3 formation rates, and also measurably increase integrated OH radical levels, in both of the mini-surrogate runs (see Figure 36) and in the full surrogate run (see Figure 38). The results of the two mini-surrogate with exhaust experiments were very similar.

The mini-surrogate with synthetic Rep Car exhaust runs (Figure 37) gave similar results to the runs with the actual results in terms of the relative effects of added exhaust, though run DTC642 had more rapid NO oxidation and O_3 formation on both the base case and added exhaust sides because of the higher light intensity. Likewise, the full surrogate with synthetic exhaust run with the higher light intensity (DTC643A) gave essentially the same relative effect of the added exhaust as observed in the run it was intended to duplicate, but had more rapid NO oxidation and O_3 formation on both the base case and the added exhaust sides. On the other hand, the second full surrogate with added synthetic exhaust run did not duplicate the actual exhaust run very well, giving more NO oxidation and O_3 formation on both sides, and a slightly smaller effect of added exhaust.
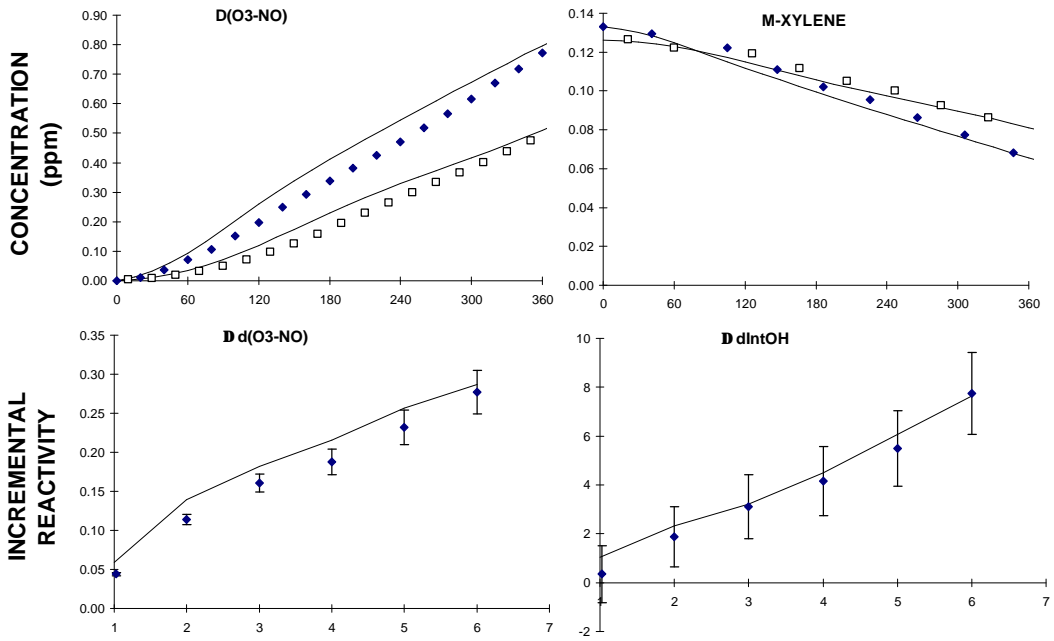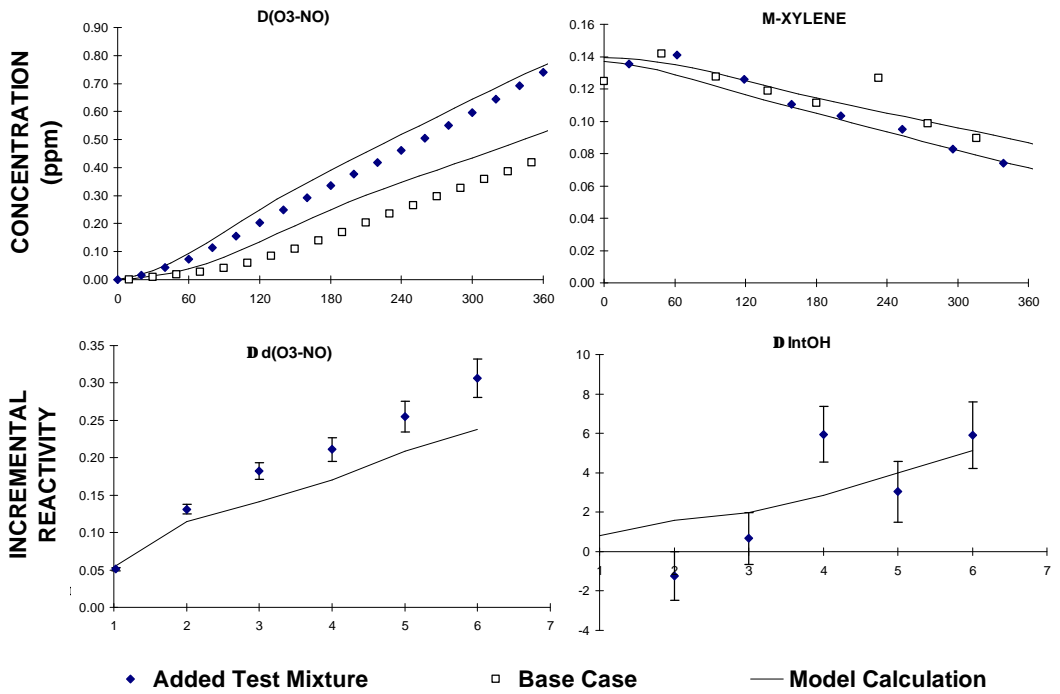
Figure 36.   Experimental and calculated results of the mini-surrogate + Rep Car exhaust experiments.

DTC642B: Mini-Surrogate + Synthetic Rep Car RFG Exhaust (Duplicates DTC576A)
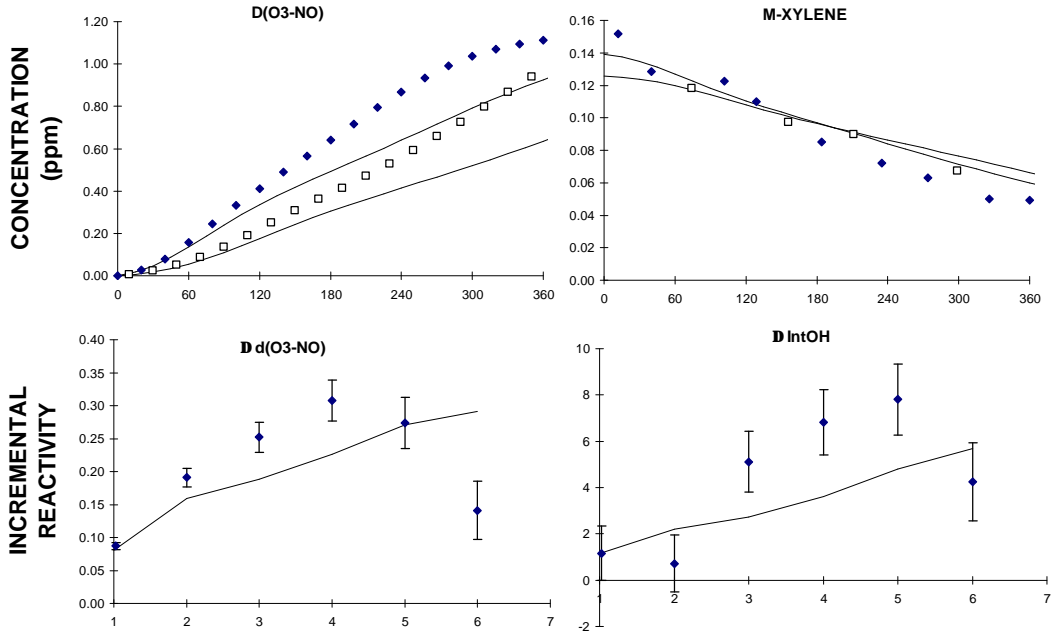
DTC672B: Mini-Surrogate + Synthetic Rep Car RFG Exhaust (Duplicates DTC576A)
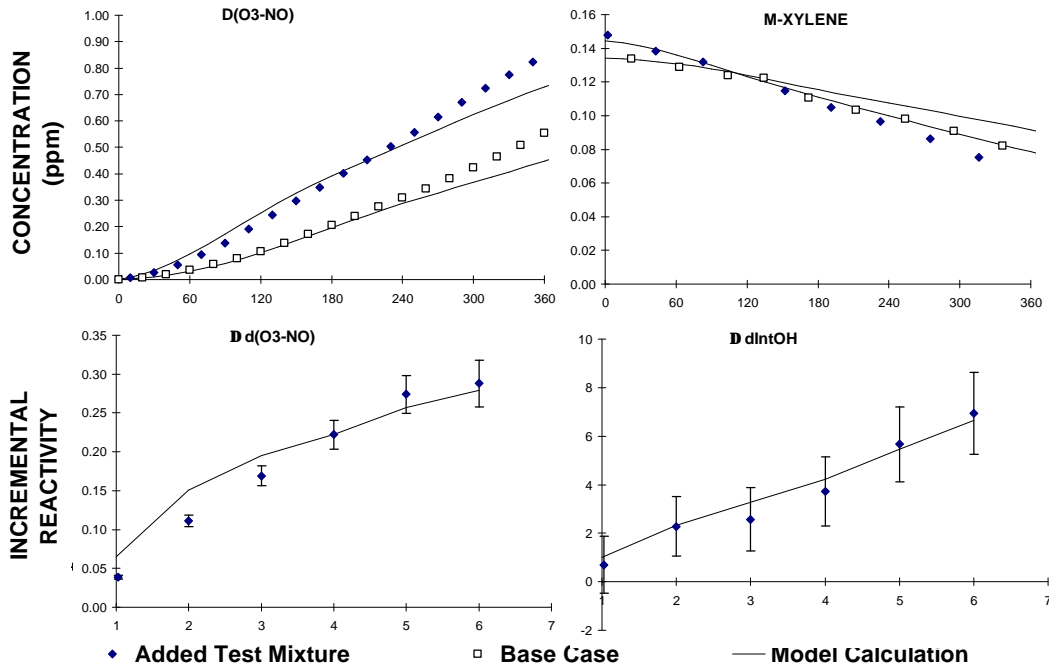
Figure 37.   Experimental and calculated results of the mini-surrogate + synthertic Rep Car exhaust experiments.
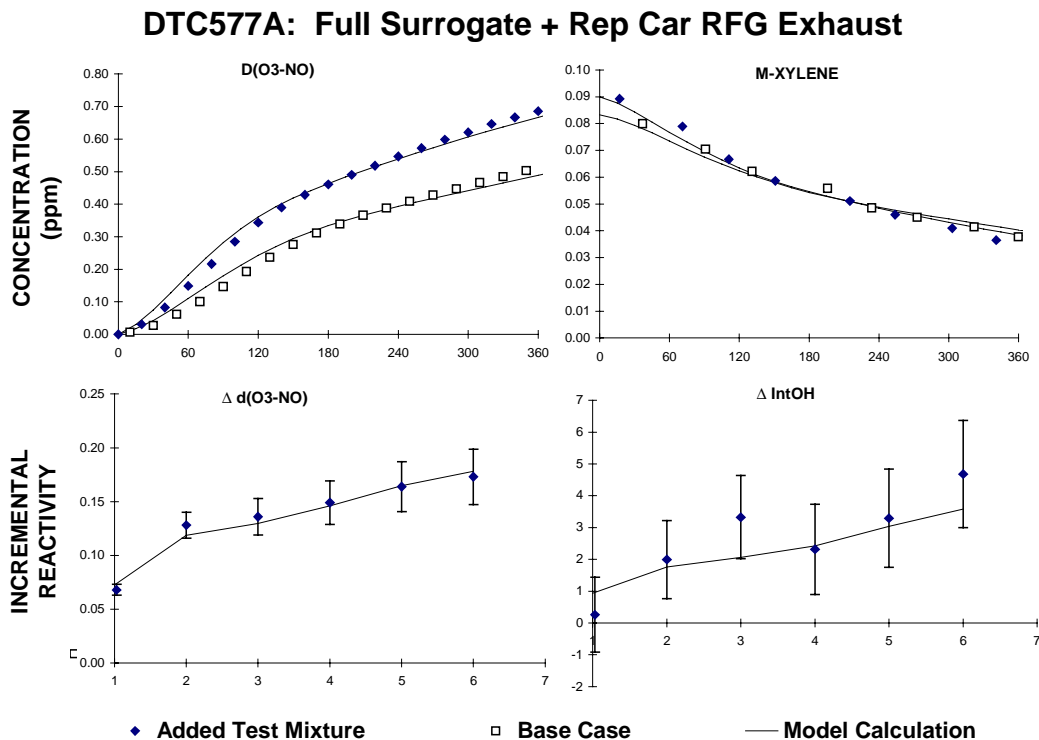
Figure 38.   Experimental and calculated results of the full surrogate with Rep Car exhaust experiment.

The model gave reasonably good simulations of the relative effects of the added exhausts in all of the experiments with the actual Rep Car exhausts, and in most of the runs with the added synthetic exhausts. The exception was the full surrogate with synthetic exhaust run DTC643 (Figure 39), where the relative effect of the added synthetic exhaust was somewhat underpredicted. However, the O_3 formation in the base case run was also underpredicted, though not to as great an extent as the other full surrogate with added synthetic exhaust run DTC669A. In the case of DTC669, where the model predicted the results on both sides should be much closer to the actual exhaust run it was supposed to duplicate than turned out to be the case. This suggests that there may be some contaminant or unusual background effects causing the unexpectedly high O_3 formation in run DTC669 that the model is not representing. Overall, the results of these incremental reactivity experiments indicate that there is no significant or consistent biases in the ability of the model to simulate the reactivities of the actual or synthetic Rep Car exhaust mixtures.

DTC643A: Full Surrogate + Synthetic Rep Car Exhaust
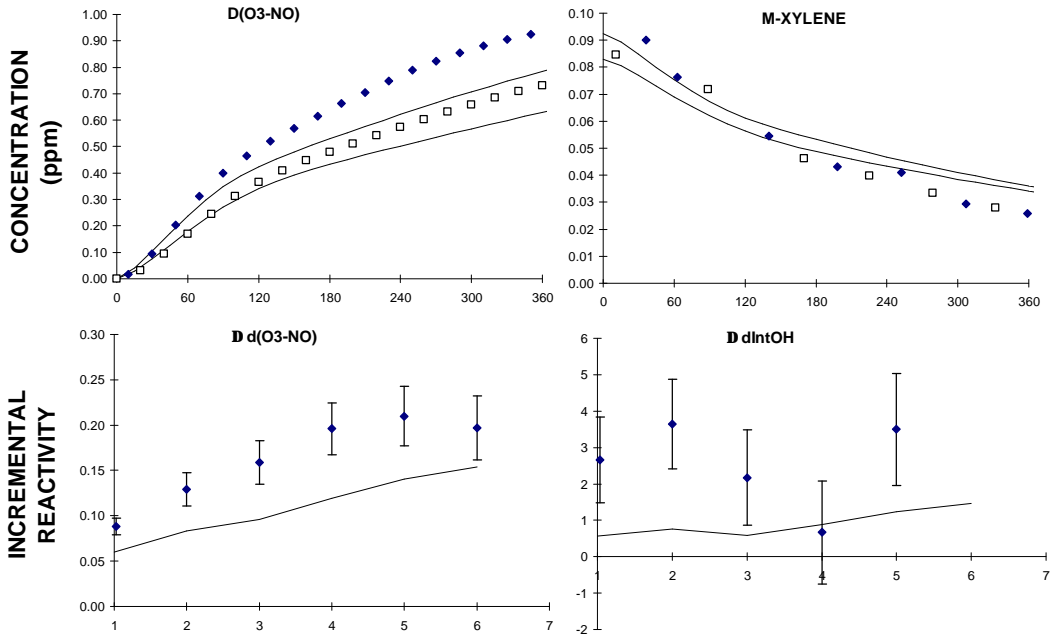
DTC669A: Full Surrogate + Synthetic Rep Car Exhaust
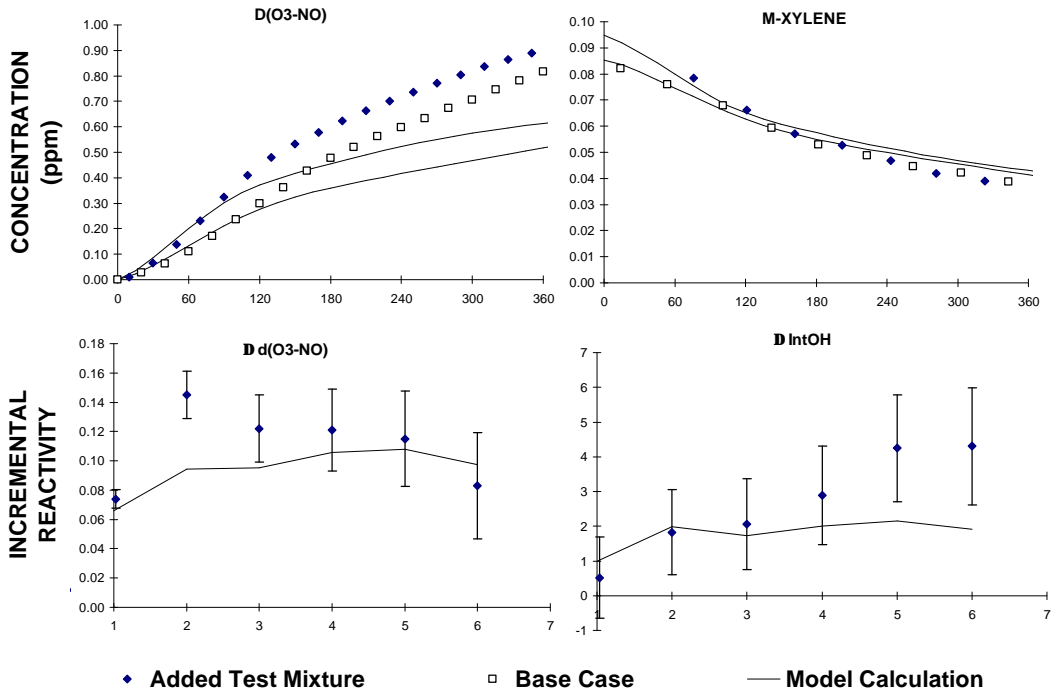
- ◆ **Added Test Mixture**
- □ **Base Case**
- —— **Model Calculation**

Figure 39.   Experimental and calculated results of the full surrogate + synthertic Rep Car exhaust experiments.

105

Results for the 1994 Chevrolet Suburban

The experiments carried out using actual or synthetic exhausts from the 1994 Chevrolet Suburban are also listed on Table 18, above. One experiment was carried out with exhaust alone, two with synthetic exhaust on one side and synthetic exhaust with reduced NO_x on the other, one each where the exhaust was added to the mini-surrogate or the full surrogate mixture, and two mini-surrogate experiments were carried out with synthetic exhaust. Table 18 indicates the figures where the data from these experiments are presented.

Figure 40 shows concentration-time plots of selected species measured in the Suburban exhaust and the synthetic Suburban exhaust experiments. Results of model simulations are also shown. Although the Suburban had three times higher exhaust levels than the Rep Car, the NO_x levels were over four times higher, giving a ROG/NO_x ratio which was too low for significant ozone formation to occur. The synthetic exhaust experiments gave very similar results as the run with the actual exhaust, though as expected somewhat faster NO oxidation was observed in the run with the higher light intensity. Reducing the NO_x levels resulted in a significant increase in the NO oxidation rates and O_3 formation in the synthetic exhaust runs. Except for the higher pollutant levels, the results are very similar to the Rep Car exhaust runs, discussed above.

The model gave a reasonably good simulation of the Suburban exhaust run, considering the relatively low ROG/NO_x levels and consequent sensitivity to chamber effects, and gave very good simulations of the synthetic exhaust runs, including the ozone formation in the low NO_x experiments. The hydrocarbon consumption and formaldehyde formation rates were well simulated in all these runs. Note that the model simulation of formaldehyde is much better in the Suburban experiments than in the Rep Car runs as shown on Figure 35. This is probably because of the relatively higher levels of formaldehyde present and formed in the Suburban exhausts, which can be measured more precisely than the lower levels formed from the Rep Car.

Figure 41 shows the results of the incremental reactivity experiments with the Suburban RFG exhaust. The added exhaust causes a significant increase in NO oxidation and O_3 formation and also increased integrated OH levels. The results were similar to those from the runs with the Rep Car exhausts, though the effect was larger because of the higher overall VOC levels. The model simulated the relative effects of the added exhaust reasonably well, though it tended to somewhat overpredict NO oxidation and O_3 formation rates in the base case experiments. The slight overprediction of exhaust reactivity in the mini-surrogate run is probably attributable to the overprediction of the base case experiment for this run.
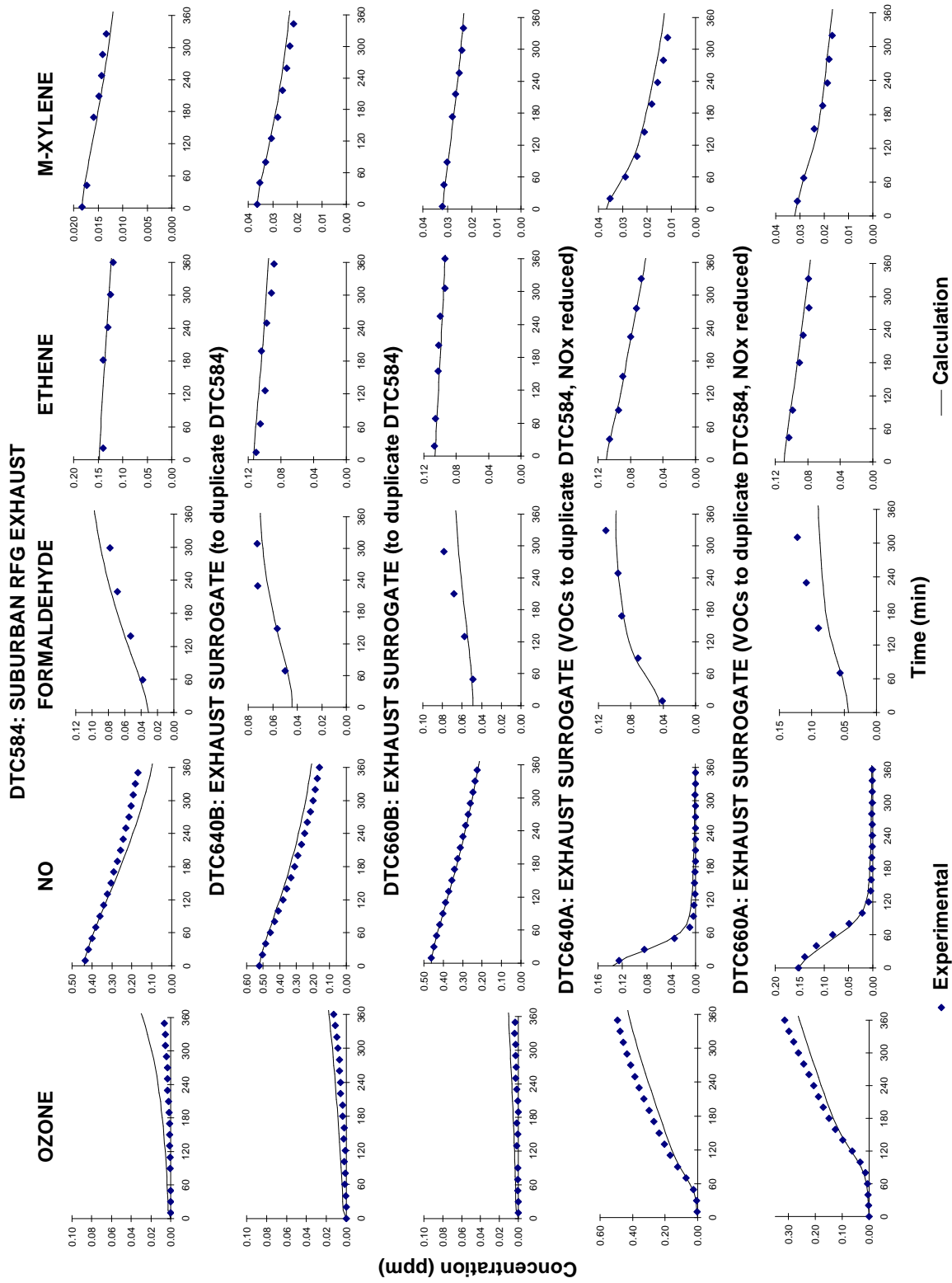
Figure 40.   Experimental and calculated concentration-time plots for selected species for the Suburban RFG exhaust and surrogate exhaust experiments.

107

DTC585A: Mini-Surrogate + Suburban RFG Exhaust
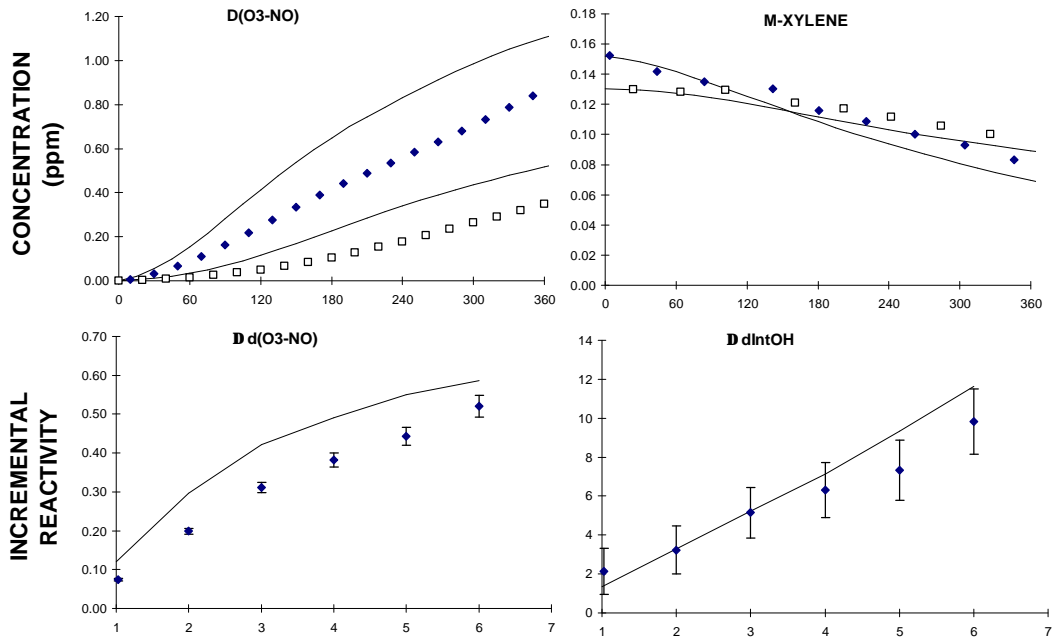
DTC586A: Full Surrogate + Suburban RFG Exhaust

◆ **Added Test Mixture**   □ **Base Case**   —— **Model Calculation**
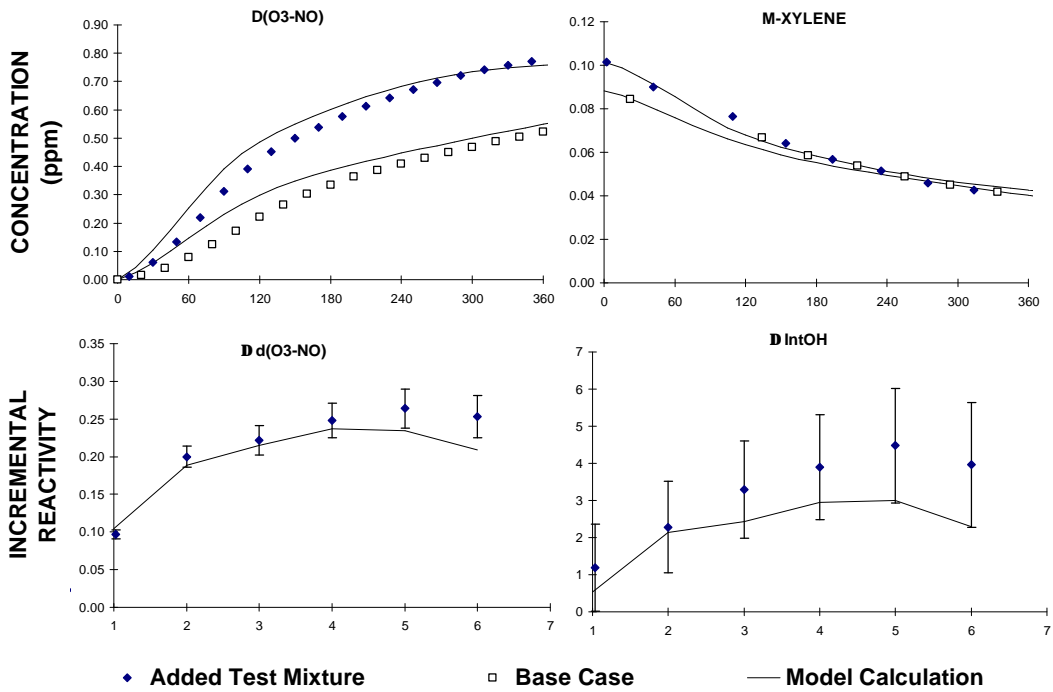
Figure 41.   Experimental and calculated results of the mini-surrogate and full-surrogate + Suburban RFG exhaust experiments.

Figure 42 shows the results of the mini-surrogate with added synthetic suburban exhausts designed to duplicate DTC585A. The relative effect of the added synthetic exhaust in the first experiment (DTC641) was slightly higher than observed in the exhaust run it was intended to duplicate, but the NO oxidation and O_3 formation rates in both sides were much higher because of the higher light intensity. The second mini-surrogate with synthetic exhaust run (DTC664) was a better duplicate of the conditions of the actual exhaust run, and the relative effect of the synthetic exhaust was very close to that of the actual exhaust. The model tended to slightly underpredict the effect of the added synthetic exhaust in both experiments, despite the fact that it gave somewhat better simulations of the base case run. However, the results do not indicate a large systematic difference between the ability of the model to simulate results of experiments with actual as compared with synthetic exhausts.

Results for the 1997 Ford Taurus

The experiments carried out using the exhaust from the 1997 Ford Taurus are summarized in Table 19, and selected data from those experiments are shown on Figure 43. Two experiments were carried out with exhaust from this vehicle, one with the exhaust itself, and one reactivity experiment with the exhaust added to the mini-surrogate. The results of the exhaust only experiment are shown on the top two sets of plots on Figure 43. The exhaust from this vehicle had the lowest VOC levels of all the RFG vehicles studied and also the lowest VOC/NO_x ratio, so essentially no ozone formation and very little NO oxidation occurred in the exhaust only experiment. Although VOC species were detected and quantified with the exhaust in the transfer bag (see Table B-2), once diluted into the chamber no VOC species were detectable. As with most of the other experiments with very low ROG/NO_x ratios, the model tended to overestimate the NO oxidation rate of the Taurus exhaust run.

The bottom plots show the results of the incremental reactivity experiment with the Taurus exhaust. Despite the very low VOC levels of the exhaust, the side with the added exhaust had somewhat greater rates of NO oxidation and O_3 formation and somewhat higher integrated OH radical levels than the base case side. But the increase in the $D(O_3$-NO) formation rate in the added exhaust side is only slightly greater than the higher $D(O_3$-NO) formation rates observed in Side A in the side equivalency tests, as indicated by the data for the side comparison test run DTC590, shown on Figure 7, above. However, the integrated OH levels in the side comparison tests were essentially the same, so the positive effect of the added exhaust on IntOH is probably real. The model correctly predicted the relative effects of the added Taurus exhaust in this reactivity experiment. Note that the model incorporates the somewhat higher radical source rate on Side A as indicated by the characterization runs, so the side differences in the chamber are to some extent taken into account.

DTC641A: Mini-Surrogate + Synthetic Suburban RFG Exhaust
(Duplicates DTC585)
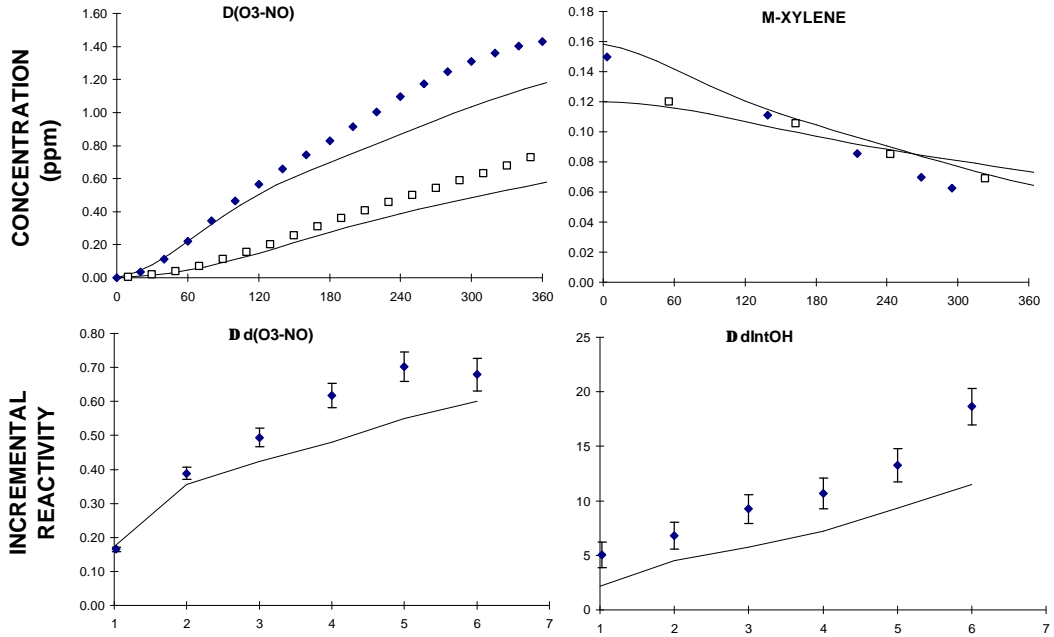
DTC664B: Mini-Surrogate + Synthetic Suburban RFG Exhaust
(Duplicates DTC585)

♦ **Added Test Mixture**   □ **Base Case**   —— **Model Calculation**
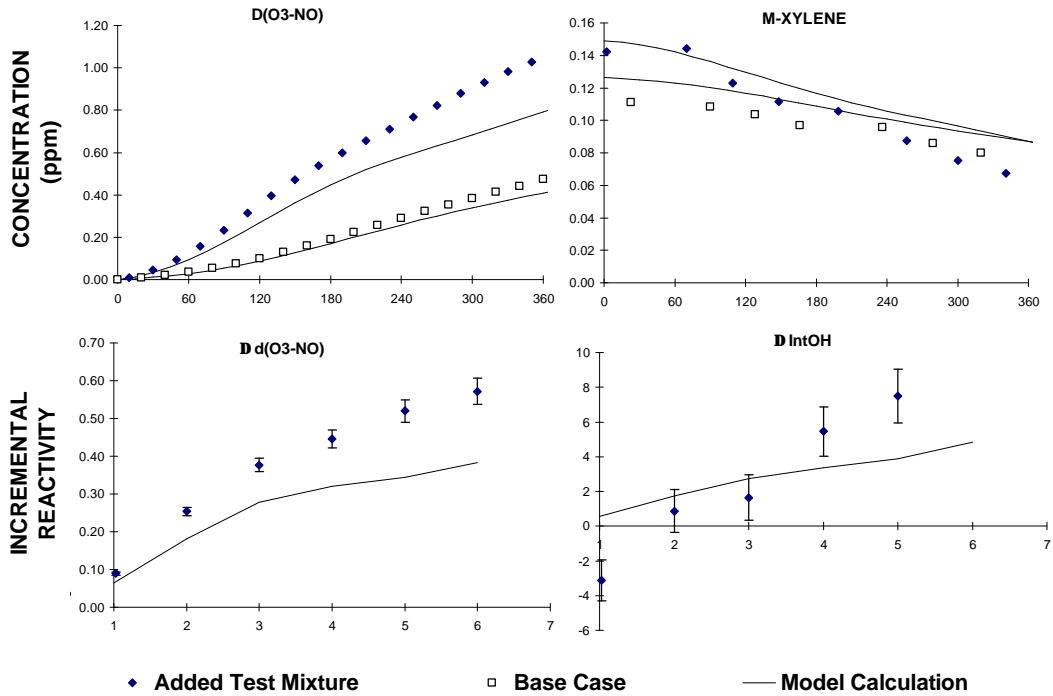
Figure 42.   Experimental and calculated results of the mini-surrogate + synthetic Suburban RFG exhaust experiments.

Table 19. Summary of experimental runs using actual or synthetic exhausts from the Taurus rental, Toyota truck, Honda Accord or Diesel Mercedes.

Type / Run	$k(NO_2+ h\upsilon)$ (min^{-1})	Initial Reactants (ppm)			Exhaust NMHC (ppmC)	Base ROG (ppmC)	Data Plots
		NO	NO2	CO			
Taurus Exhaust							
DTC582	0.19	0.11	0.01	2.1	0.05		8-1
Mini-Surrogate + Taurus Exhaust							
DTC583A	0.19	0.24	0.12	3.2	0.22	5.61	8-2
Toyota Exhaust							
DTC661A	0.17	0.16	0.02	14.1	2.96		8-1
Mini-Surrogate + Toyota Exhaust							
DTC662A	0.17	0.31	0.10	7.5	1.56	5.60	8-5
Full Surrogate + Toyota Exhaust							
DTC663B	0.17	0.21	0.05	8.8	1.54	4.09	8-5
Accord Exhaust							
DTC665A	0.17	0.13	0.01	3.0	0.27		8-1
Mini-Surrogate + Accord Exhaust							
DTC666A	0.17	0.35	0.06	4.5	0.68	5.64	8-3
Mini-Surrogate + Synthetic Accord Exhaust							
DTC681A	0.17	0.33	0.08	3.5	0.81	6.06	8-3
Full Surrogate + Accord Exhaust							
DTC667B	0.17	0.21	0.04	3.3	0.42	4.21	8-4
Full Surrogate + Diesel Exhaust							
DTC615B	0.18	0.38	0.34	2.4	0.07 [a]	4.16	8-6

[a] Based on analysis of fully diluted exhaust in the chamber. The only VOC detected was 37 ppb ethene. No transfer bag analyses were carried out.

DTC582A: TAURUS RFG EXHAUST

OZONE

NO

FORMALDEHYDE

Concentration (ppm)

DTC582A: TAURUS RFG EXHAUST

Time (min)

◆ **Experimental**　　　　　—— **Calculation**

DTC583A: Mini-Surrogate + Taurus RFG Exhaust

D(O3-NO)

M-XYLENE

CONCENTRATION (ppm)

D d(O3-NO)

D IntOH

INCREMENTAL REACTIVITY

◆ **Added Test Mixture**　　　□ **Base Case**　　　—— **Model Calculation**
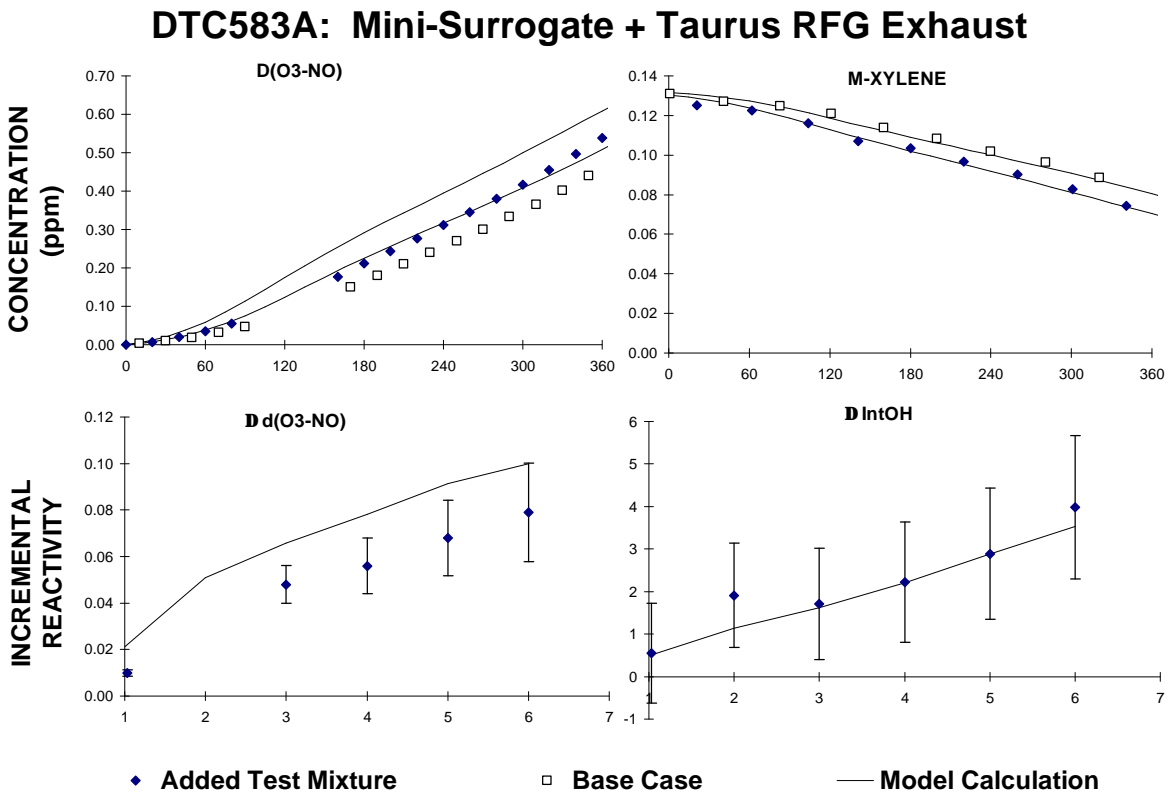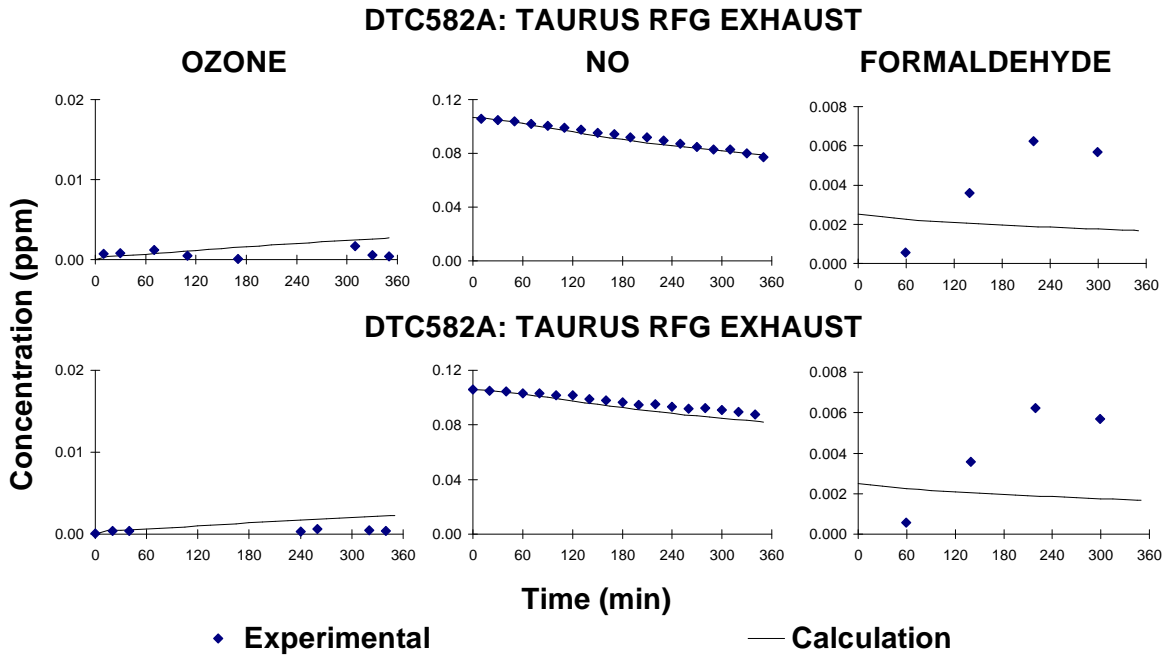
Figure 43.　　Experimental and calculated results of of the experiments with Ford Taurus RFG exhausts.

112

Because of the very low exhaust VOC levels in the 1997 Ford Taurus, the chamber experiments did not provide a very sensitive test of the model's ability to predict the reactivity of this exhaust. For that reason, synthetic exhaust experiments were not carried out to duplicate the results of these runs, nor were additional exhaust experiments carried out using this vehicle.

Results for the 1984 Toyota Pickup

The experiments carried out using exhausts from the 1984 Toyota pickup are summarized on Table 19. One experiment each with the exhaust alone, with the exhaust added to the mini-surrogate and with the exhaust added to the full surrogate were carried out. Although several synthetic Toyota exhaust experiments were also conducted, the results had to be rejected because of a problem discovered in the sample line (see Appendix C), so data from these runs are not reported.

The results of the exhaust only experiment for this vehicle are shown on Figure 44. The exhaust from this vehicle had the highest ROG levels and the highest ROG/NO$_x$ ratio of all RFG vehicles studied, and was the only case among the RFG vehicles where the exhaust only run yielded significant ozone formation. Formaldehyde was both initially present and formed during the irradiation, and non-negligible PAN formation occurred as well. The model simulation was reasonably consistent with the experimental results, though it slightly underpredicted the rate of NO oxidation and the amount of ozone formed. The model gave reasonably good simulations of the rates of hydrocarbon consumption in this run.

The results of the incremental reactivity experiments with the Toyota exhausts are shown on Figure 45. The added exhaust caused a significant increase in the rate of NO oxidation and rate and amount of ozone formed, and it caused a measurable increase in the integrated OH radical levels in the mini-surrogate run. Because of experimental variability, the effect of the exhaust on integrated OH in the full surrogate runs is somewhat uncertain, but it appears that the exhaust initially enhances it then depresses it later in the run when ozone formation has peaked. This depression of IntOH reactivity later in the run in experiments where the full ozone formation potential is achieved is frequently observed when reactive VOCs are added (Carter et al, 1995a). The model simulation gave a good fit to the relative effect of the added exhaust in the full surrogate run, but tended to underpredict the effect of the added exhaust on both D(O$_3$-NO) and IntOH reactivities in the mini-surrogate runs. This suggests that there may be a radical initiator present in this exhaust which is not detected and being represented by the model, since mini-surrogate experiments tend to be more sensitive to radical initiators (and inhibitors) than do runs using the full surrogate (Carter et al, 1995a). However, it could also be due to a problem with the model for exhaust constituents which were

DTC661: TOYOTA RFG EXHAUST

OZONE **NO** **FORMALDEHYDE**

ETHENE **M-XYLENE** **PAN**

DTC665: ACCORD RFG EXHAUST

OZONE **NO** **FORMALDEHYDE**

ETHENE **M-XYLENE**

Concentration (ppm)

Time (min)

◆ **Experimental** ── **Calculation**
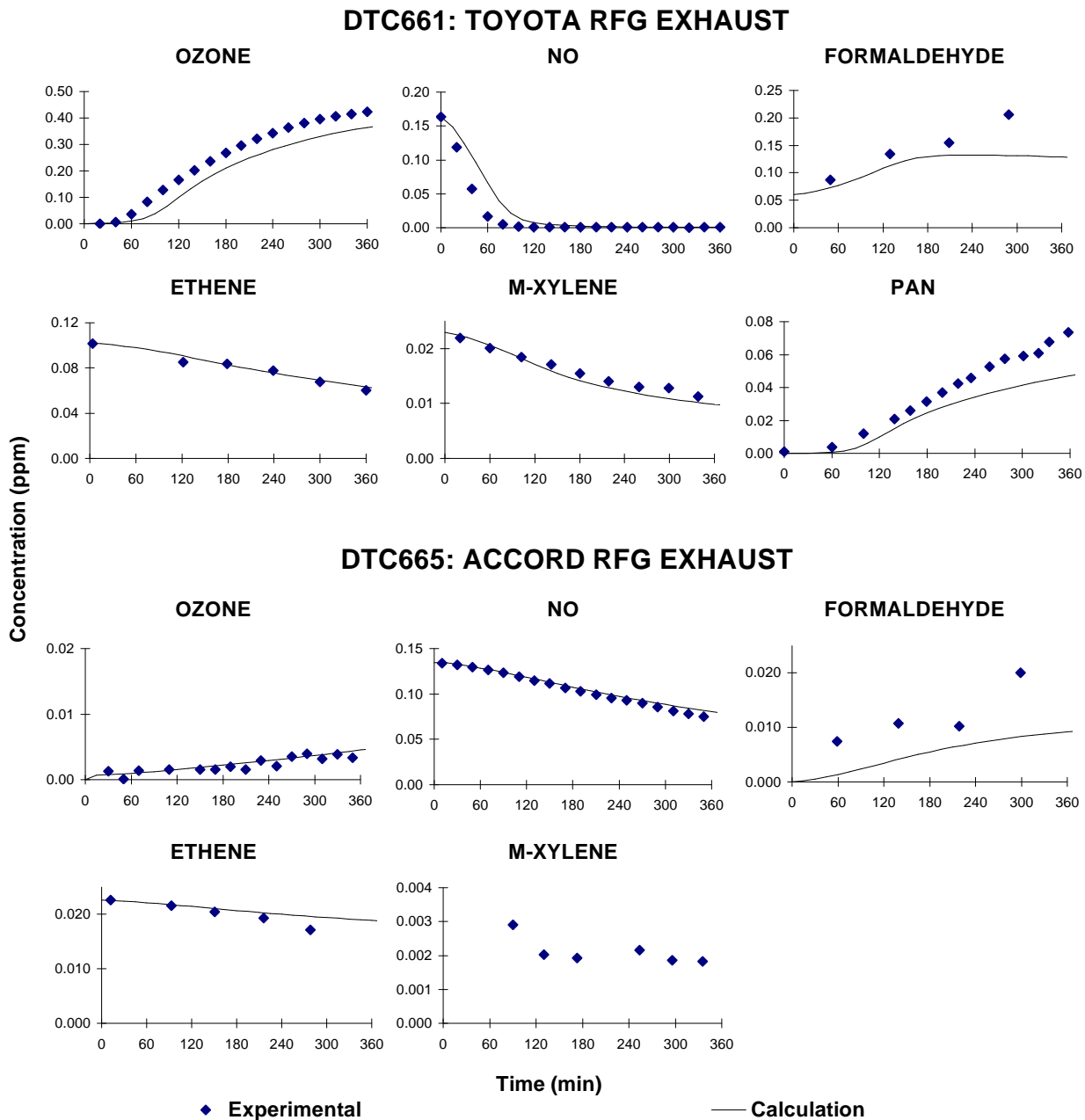
Figure 44. Experimental and calculated concentration-time plots for selected species for the Toyota and Accord RFG exhaust experiments.

114

DTC662A: Mini-Surrogate + Toyota RFG Exhaust

DTC663B: Full Surrogate + Toyota RFG Exhaust

♦ **Added Test Mixture**   □ **Base Case**   —— **Model Calculation**
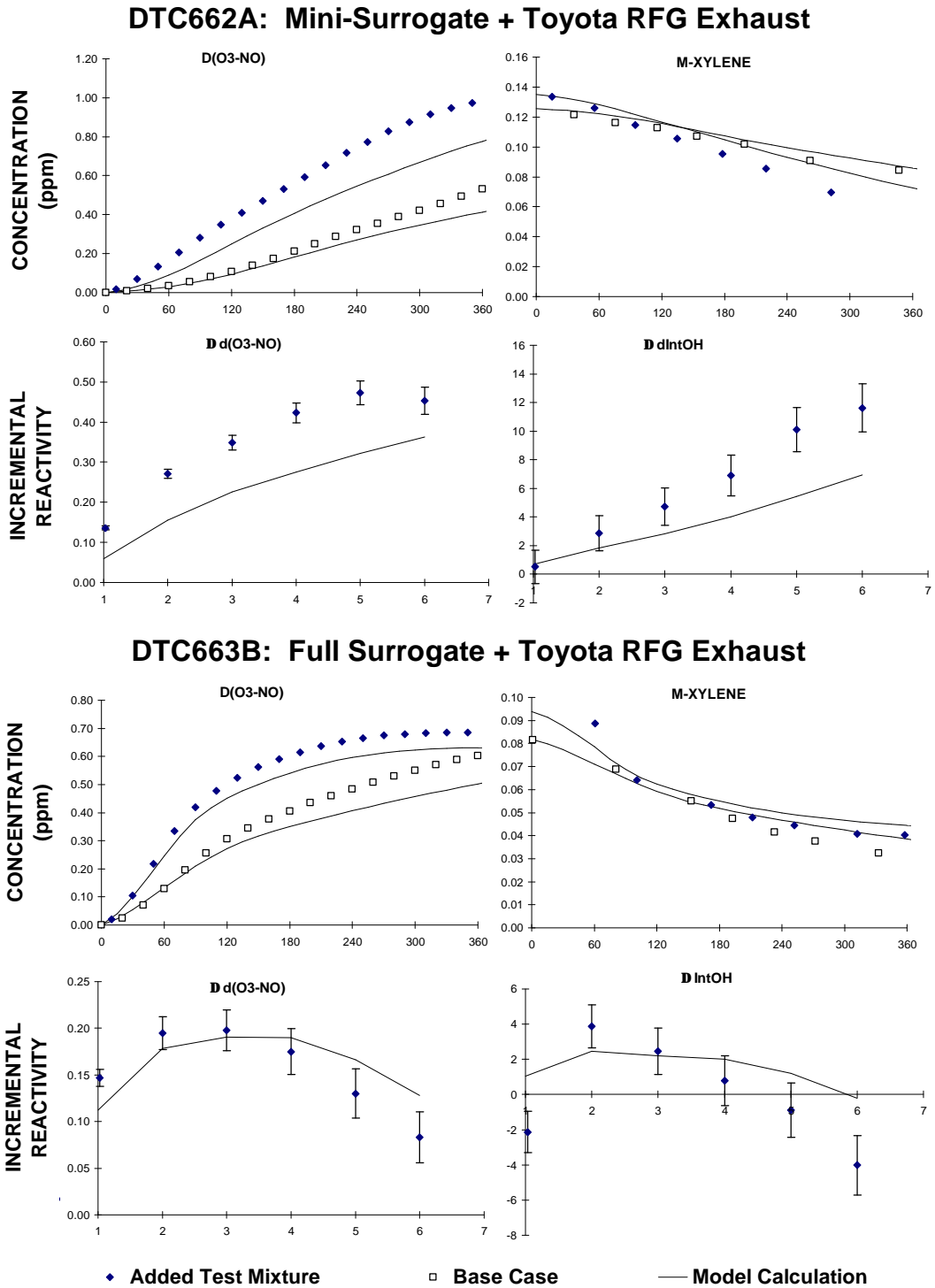
Figure 45.   Experimental and calculated results of the mini-surrogate and full-surrogate + Toyota RFG exhaust experiments.

115

present in higher levels in the Toyota exhausts than the exhausts from the other RFG vehicles discussed above.

Results for the 1988 Honda Accord

Table 19, above, summarizes the experiments carried out using actual or synthetic exhausts from the 1988 Honda Accord. One each experiment was carried out with the exhaust alone, with the exhaust added to the mini-surrogate and the exhaust added to the full surrogate. In addition, one experiment was carried out using synthetic Accord exhaust to duplicate the mini-surrogate with Accord exhaust run which provided data useful for evaluation.

The results of the exhaust only experiment for the Honda Accord are shown on Figure 44, above. Although this exhaust had moderately high ROG levels it also had the highest NO_x levels of the RFG vehicles studied, yielding a relatively low ROG/NO_x ratio. Because of this, essentially no ozone formation occurred in the Accord exhaust-only run, and only slow NO oxidation occurred. Although model simulations of such low ROG/NO_x experiments tend to be variable, the results of this particular run was reasonably well simulated by the model.

The results of the mini-surrogate with actual or synthetic Accord exhaust are shown on figure 46. The NO oxidation and ozone formation in the two experiments were almost exact duplicates of each other, indicating that the synthetic and actual exhausts had the same absolute and relative effects on these measures of reactivity. As with other RFG exhausts where measurable effects could be seen, the Accord RFG exhaust had a significant positive effect on NO oxidation and O_3 formation, and a measurable positive effect on integrated OH levels.

The results of the full surrogate with accord exhaust experiment are shown on Figure 47. Note that this experiment had only ~60% of the exhaust VOCs as did the mini-surrogate run, so a smaller effect of added exhaust would be expected on that basis. The effect of the added exhaust on $D(O_3-NO)$ was indeed relatively small, but it was still significantly larger than the side differences observed in the side comparison test experiment carried out immediately following this run (run DTC668, Figure 7). The effect of the exhaust on integrated OH levels was too small to measure.

As was the case with the Toyota exhaust, the model gave a reasonably good simulation of the relative effect of the exhaust in the full surrogate run but somewhat underpredicted its effect in the mini-surrogate run. On the other hand, the model gave a good simulation of the effect of the synthetic exhaust in

DTC666A: Mini-Surrogate + Accord RFG Exhaust

DTC681A: Mini-Surrogate + Synthetic Accord RFG Exhaust

♦ **Added Test Mixture**   □ **Base Case**   —— **Model Calculation**
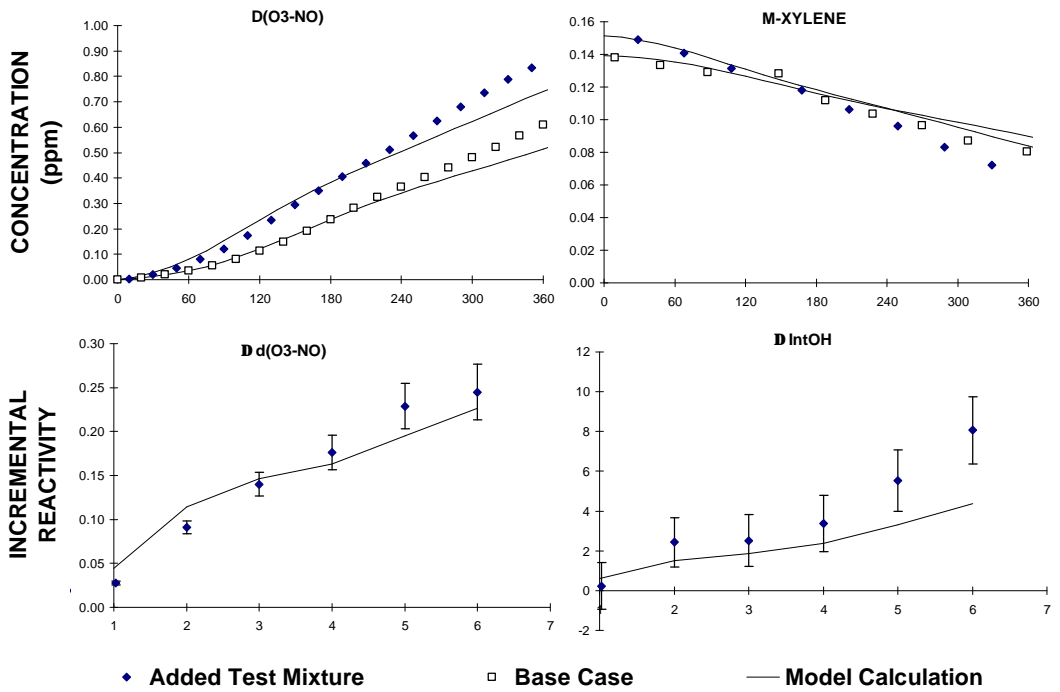
Figure 46.   Experimental and calculated results of the mini-surrogate + actual and synthetic Accord
RFG exhaust experiments.

117

DTC667B: Full Surrogate + Accord RFG Exhaust
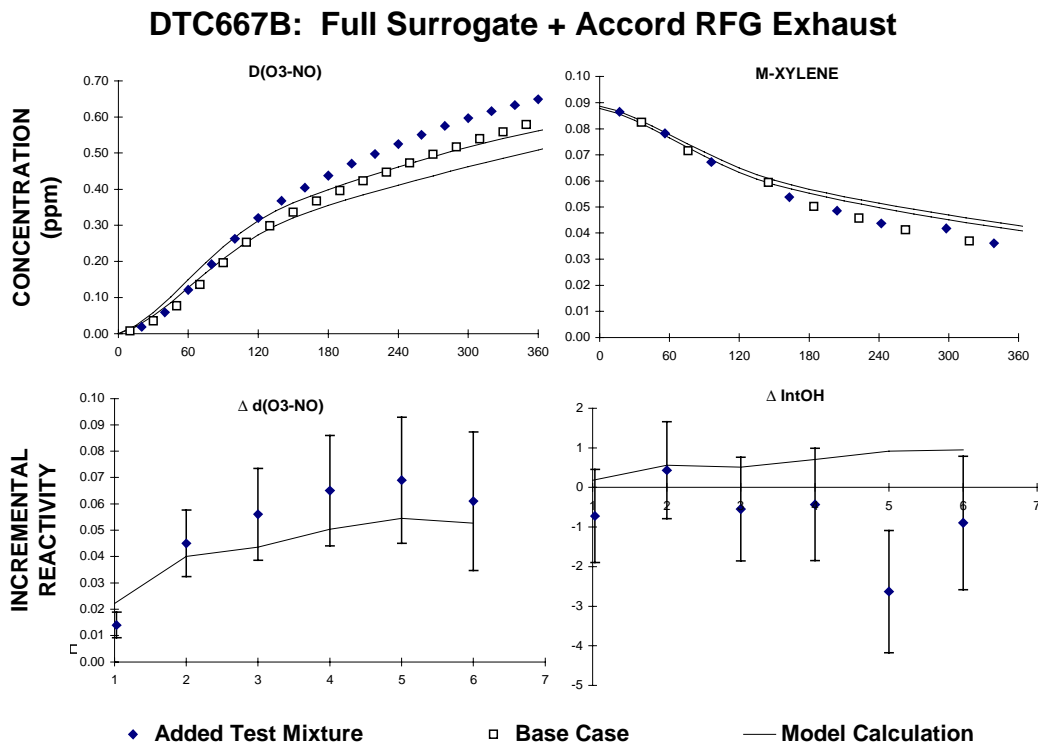
Figure 47.　　Experimental and calculated results of the full surrogate with Accord RFG exhaust experiment.

the run which duplicated the mini-surrogate with Accord exhaust run. This is despite the fact that the exhaust experiment itself reasonably closely duplicated the experiment with the actual exhaust. This suggests that the problem may be in the model for one of the exhaust components which is different than the species used in the synthetic exhaust runs. This may be the case for the Toyota as well, but usable synthetic exhaust runs for the Toyota, and replicate added exhaust runs for both vehicles, would be needed to assess this more unambiguously.

Exploratory Run with Diesel Exhaust

One exploratory experiment was carried out using exhaust from a 1984 diesel Mercedes sedan. As with the other exhausts studied for Phase 2 of this program, the vehicle was gradually accelerated to 40 mph in about 30 seconds, the exhaust was collected in the transfer bag for about 30 seconds, and the contents of the transfer bag were then injected into the chamber. However, to avoid contaminating the VERL sampling system with diesel exhaust, no VERL bench data were taken when the exhaust was collected, either from the raw exhaust or the exhaust in the transfer bag. In addition, because this was only an exploratory

118

experiment, and because dilution from the transfer bag to the chamber could not be estimate without VERL bench analyses of the transfer bag contents, no speciated analyses of the exhaust in the transfer bag were carried out. Therefore, the only data available on the composition of the exhaust were data obtained after the exhaust was injected into the chamber. The exhaust was injected into the chamber after the surrogate VOCs were injected into both sides, but before any NO_x injections were made. After the exhaust was injected, the NO_x was injected into the other side to yield the desired NO_x levels for the surrogate run, and a small supplemental NO injection was made to the exhaust side (increasing the NO in the added exhaust side by ~15%) to equalize the NO_x levels on both sides.

Table 19 lists the conditions and the reactant levels observed in the full surrogate with diesel exhaust experiment. As indicated on the table, the only VOC increase detected when the exhaust was injected into the chamber was ~37 ppb ethene. The results of this experiment are shown on Figure 48. It can be seen that the added diesel exhaust had a significant effect on the NO oxidation and O_3 formation rates throughout the experiment, and a measurable effect on the IntOH levels in the initial parts of the experiment, despite the fact that only very low levels of detected VOC in the exhaust, and despite the fact that the model predicted that this would have essentially no effect on the results. Furthermore, more formaldehyde formation was observed to occur during the irradiation in the added exhaust side than in the base case side. Clearly, there are components in the diesel exhaust which are significantly rates of NO oxidation and O_3 and formaldehyde formation which are not being detected in the chamber experiments. Experiments with more complete speciated analyses are clearly required to account for the observed reactivity of this exhaust. In particular, diesel is expected to significant amounts of higher molecular weight VOCs in the exhaust, which were not injected once the exhaust was diluted in the chamber. Although GC analyses using Tenax trapping, which should be suitable for detecting such high molecular weight species, was carried out, the sensitivity of the method employed may not be sufficient when the exhaust is diluted to the extent it was in the chamber.

DTC615B: Full Surrogate + Diesel Exhaust
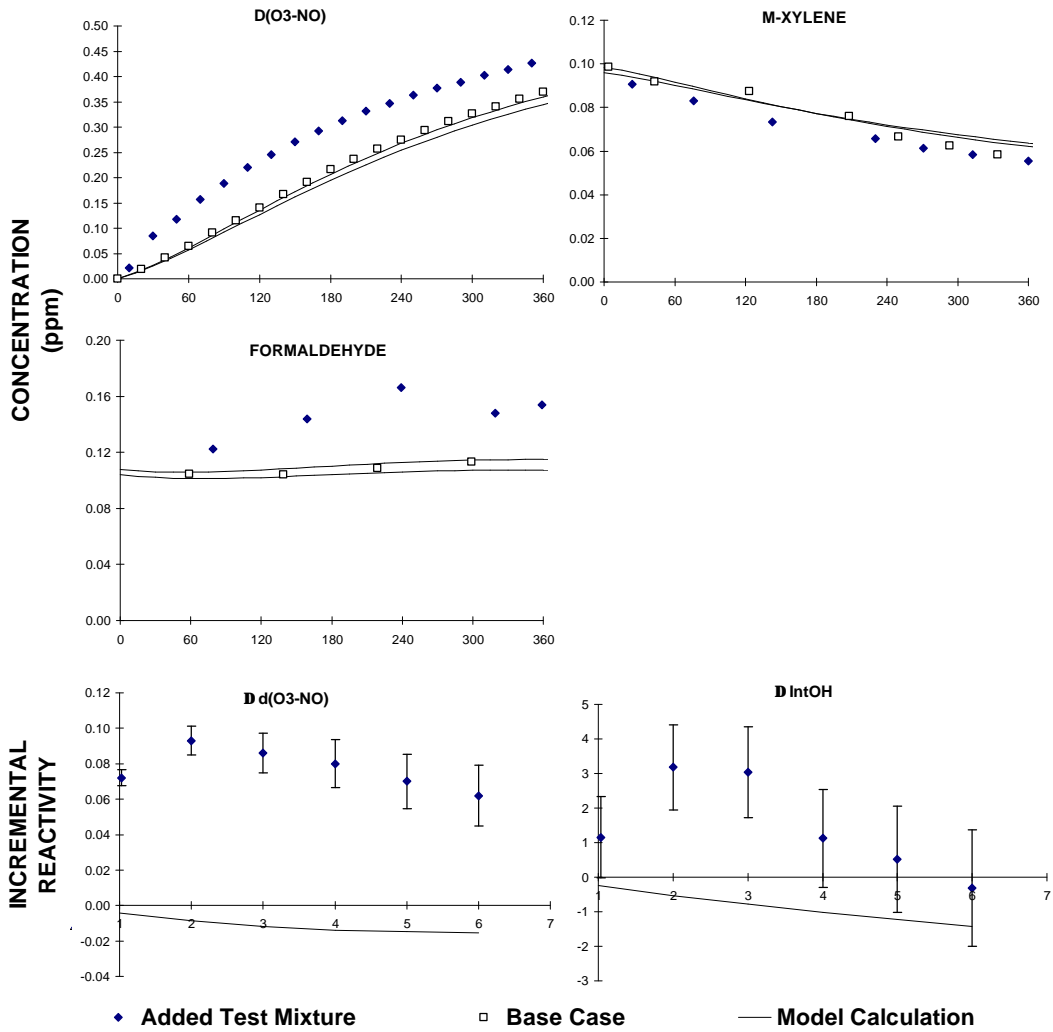
Figure 48.   Experimental and calculated results of full surrogate + Diesel exhaust experiment.

CONCLUSIONS

The objective of this project was to use an environmental chamber system interfaced to a state-of-the-art vehicle emissions facility to provide data to test whether current exhaust analysis methods can identify the important reactive species in exhausts using various vehicles and fuel types, and whether current chemical models can predict the impacts on ozone and other oxidants when the exhausts are irradiated. Although some experimental and model evaluation problems were encountered which are summarized below, we believe that overall this program has been successful in achieving these objective. Environmental chamber data which are sufficiently well characterized for model evaluation have been obtained using exhausts from vehicles fueled by LPG, M100, M85, CNG, and a variety of vehicles using Phase 2 reformulated gasoline (RFG), and an exploratory experiment was carried out using a diesel vehicle. Incremental reactivity experiments, in which the effect of adding the exhaust to VOC - NO_x mixture simulating photochemical smog precursors, were found to be particularly useful in providing reactivity evaluation data, especially for the lower reactivity exhausts or exhausts with low ROG/NO_x ratios. In most cases the results of the experiments with the exhausts were consistent with model predictions, and consistent with results of experiments using synthetic exhausts derived from mixtures of compounds measured in the actual exhausts. This indicates that in most cases the major exhaust constituents which contributes to the ozone impacts of these exhausts have probably been identified, and that current chemical mechanisms are reasonably successful in predicting the impacts of these species on ozone. The major exception noted in this study was diesel, where it was clear that the major reactive species have not been identified. There was also some evidence, albeit inconclusive, that the model is underpredicting the ozone impacts of some of the constituents of exhausts from the two high-mileage, in-use RFG-fueled vehicles which were studied. In addition, problems were encountered in the model's ability to simulate experiments containing formaldehyde or formaldehyde with methanol which affected the evaluation of the model for the methanol-containing fuels. However, the model successfully predicted the incremental effects of methanol-containing exhausts to surrogate mixtures simulating ambient environments. This was the case for most of the other exhaust studied as well.

Given below are summaries of conclusions which can be drawn from this work concerning general procedures for conducting environmental chamber studies for exhausts, followed by the summarized conclusions for the various types of exhausts for which information was obtained.

121

Procedures for Environmental Chamber Studies of Exhausts

One concern with the study of actual vehicle exhausts in environmental chamber studies is the introduction of artifacts due to surface reactions involving the high concentrations of vehicle exhaust and moisture prior to the dilution of the exhaust in the chamber. The formation of nitrous acid due to the heterogeneous hydrolysis of NO_2 or from the reaction of $NO + NO_2 + H_2O$ on surfaces, or the heterogeneous formation of methyl nitrite (CH3ONO) in possible surface reactions involving methanol, NO_x and water in exhausts involving methanol-containing fuels are specific concerns. An objective of the experimental design was to minimize these by immediately diluting the exhaust with dry air to reduce both the concentrations of pollutants and the humidity.

With the possible exception of the diesel experiment, for which no conclusions can be made because of the lack of complete VOC analysis, the results of this program indicated that this is not a significant problem for any of the vehicles or sampling methods employed. The results of the exhaust chamber experiments give no evidence of excess reactivity which could be attributed to nitrite contamination. Such contamination would show up as higher rates of initial NO oxidation than could be accounted for in the model simulations, or obscured in runs with synthetic exhaust mixtures. This was not observed. Further evidence for the lack of significant problems with our dilution and transfer technique for LPG, was based on obtaining very similar results (after using the model to account for differences in initial reactant concentrations) when the LPG exhaust was transferred to the chamber using Teflon transfer bag as when using the mini-diluter system. In addition, for all exhausts except for diesel (which was not studied) and possibly the high-mileage RFG vehicles very similar results were obtained using synthetic exhaust mixtures as using actual exhausts, indicating negligible contribution of nitrites or other unidentified high reactivity species in the exhausts which are not in the synthetic exhaust mixtures.

It was found that care must be taken to avoid loss of formaldehyde on surfaces when transferring exhausts to the chamber. During the first phase of the program long sample lines were used to transfer diluted exhausts from the vehicle to the chamber, and there was some evidence for formaldehyde loss on the sample lines. This is despite the fact that care was taken to prevent the humidity of the diluted exhaust in the sample lines from exceeding ~50%. This apparent loss was not observed during the second phase of the program when a large Teflon bag was used to transfer the exhaust from the vehicle to the chamber. On the other hand, there was no evidence for loss of any of the species present in LPG exhausts in the sample line, nor, as indicated above, of formation of nitrites or other artifacts. But since formaldehyde makes a non-

negligible contribution to other exhausts besides those from methanol vehicles, it is concluded that use of long sample lines should be avoided, even when the exhaust is highly diluted.

In the studies of complex exhausts such as formed from RFG-fueled vehicles, more accurate analyses of species in the exhaust can be obtained by sampling exhaust which is less completely diluted than is appropriate for environmental chamber experiments. But if this approach is used, it is important that the ratio of the dilution of the exhaust at the time it is analyzed to the dilution of the exhaust once it is added into the chamber be accurately determined. In this study all the exhausts except LPG were analyzed at higher concentrations in the transfer bag prior to their injection in the chamber, with the dilution ratios being obtained using primarily NO and CO measurements, but in some cases also measurements of individual VOCs. These measures were usually consistent but some inconsistencies occurred in several runs, and overall the dilution ratios were probably uncertain by ~15%. This uncertainty could be reduced in future studies by developing consistently accurate methods to measure this dilution ratio which can serve as the primary standard in this regard.

Effect of Vehicle Operation Mode

To obtain a useful measure of the effects of the VOCs present in the exhaust mixtures on ozone formation and other measures of air pollution, it is necessary to introduce a sufficient amount of exhaust VOCs in the chamber to yield a measurable effect. There are several factors limiting the concentrations of exhaust introduced. To avoid introduction of artifacts due to interactions of high concentrations of NO_x in the exhaust with liquid water or high levels of humidity, it is necessary to dilute the exhaust stream so that the humidity at room temperature in the sample line or transfer vessel is no greater than 50%. In addition, since NO_x is also present in the exhaust, the exhausts must be diluted to an extent so the NO_x introduced into the chamber is a reasonable representation of ambient conditions, and is not so high relative to the VOC levels that it prevents significant ozone formation from occurring. This means that environmental chamber studies are not useful for providing reactivity information from vehicles from sufficiently "clean" vehicles.

The LPG and the M100 vehicles employed in the first phase of this study were found to have only very low levels of reactive VOCs in the exhaust after the first ~5 minutes of operation. This was expected to be the case, to varying degrees, for the other vehicles as well. In the case of the LPG vehicle, the only reactive pollutants other than NO_x after the cold start period were CO and relatively low levels of propane. Although some measurable reactivity information was obtained from this mode, it was of low precision because of its very small effect on ozone formation. The M100 vehicle was found not to have any detectable methanol or formaldehyde when introduced into the chamber after the catalyst had warmed up, and thus no

123

experiments with M100 in this operating mode was carried out. Therefore, at least for these particular vehicles, reactivity data could only be obtained for cold-start emissions. For that reason, only cold start emissions were studied in both phases of this program.

LPG Reactivity

The species accounting for the reactivity of cold-start exhaust from the LPG vehicle were found to be CO, propane, isobutane, n-butane, ethylene, and propene. In terms of contribution to MIR, the major species are ethene (~35%), CO (~30%), propene (~20%), and propane (~15%). There are apparently no undetected compounds significantly affecting the reactivity of the cold-start LPG exhaust, because experiments with synthetic exhausts made up with these compounds in the appropriate proportions with NO_x gave essentially the same results. The model performed reasonably well in simulating the results of the LPG experiments. This is expected, because the main contributors to LPG reactivity are simple compounds whose mechanisms are believed to be reasonably well understood, and which have been individually evaluated previously using chamber data (e.g., Carter et al, 1993a, 1995a-c, 1997).

Based on these results, we can conclude that we understand the compounds and mechanisms accounting for the ozone impacts of the cold-start exhaust from this type of LPG-fueled vehicle. Although the mass emission rates of the LPG vehicle tested were higher than the appropriate emission standard would indicate, the hydrocarbon profiles found in this study are consistent with previous work and indicate the results should be representative of LPG vehicles in general.

M100 and M85 Reactivity

The species accounting for the reactivity of the cold-start M100 emissions were, as expected, methanol and formaldehyde. Methanol and formaldehyde were also found to be the only species measured in high enough levels to contribute significantly to the reactivity of the cold-start M85 exhausts as well. No significant differences were observed in incremental reactivity experiments between actual cold-start M100 and M85 exhaust and the methanol/formaldehyde/NO_x mixtures designed to simulate them. This indicates that there are probably no significant contributors to M100 and M85's reactivity which are not being detected, and that the hydrocarbons from at least the M85 vehicle used in this study do not contribute measurable to the cold-start exhaust reactivity. In no case was there any evidence for any contribution of methyl nitrite to M100's reactivity, which, if it were significant, would be apparent in the initial NO oxidation rate.

The results of the model simulations of the M100 reactivity experiments gave similar results with the synthetic M100 and M85 exhausts as the actual exhausts, providing further support to our conclusion that the observed methanol and formaldehyde are the main contributors to M100's reactivity, and that undetected compounds do not play a significant role. The simulations also did not indicate large significant biases in the model, though some inconsistencies were observed. These inconsistencies appeared to be due to problems with the models ability to simulate any experiments with formaldehyde or methanol, regardless of whether they are in synthetic mixtures or in actual exhausts. In particular, the model had a slight but consistent biases towards underprediction of reactivity of formaldehyde in this chamber, and overprediction of reactivity of methanol or methanol + formaldehyde when irradiated in the absence of other VOCs. (Note that this overprediction in the simulations of the methanol-containing systems cannot be attributed to formation of methyl nitrite, since the presence of methyl nitrite in the model simulation would make the overprediction even worse.) These biases were essentially the same when simulating actual M100 or M85 exhausts as when simulating synthetic methanol + formaldehyde - NO_x mixtures. On the other hand, the model simulated the incremental effects of adding the exhausts or methanol + formaldehyde mixtures to photochemical smog surrogate mixtures without any apparent consistent biases. The reasons for these biases in the simulations of experiments with methanol and/or formaldehyde in the absence of other pollutants is and may be due to problems with chamber characterization, since the atmospheric reactions of these compounds are believed to be reasonably well established. If this is the case, the experiments with the more realistic mixtures appear to be less sensitive to this characterization problem. In any case, the results of the reactivity experiments suggest that the model will probably perform reasonably well in simulating the reactivities of methanol exhausts in the atmosphere.

CNG Reactivity

The only species detected in the cold-start CNG exhausts studied in this program at levels sufficient to affect ozone formation were NO_x, CO, and formaldehyde. The levels of methane and other hydrocarbons detected in these exhausts were insufficient to significantly affect predicted reactivity. Although essentially no O_3 formation occurs when the exhaust is irradiated by itself, the CO and formaldehyde levels in the cold start CNG exhausts were sufficient to have a measurable (and positive) effect on NO oxidation and O_3 formation when added to smog surrogate VOC - NO_x mixtures. Essentially the same results were obtained in experiments using CO and formaldehyde mixtures at the same levels as measured in the CNG exhaust experiments, and the results were consistent with model predictions. This indicates that CO and formaldehyde are indeed the major species accounting for CNG reactivity. Significantly less reactivity was observed when formaldehyde was omitted from the synthetic CNG mixtures, indicating that the formaldehyde in CNG exhaust makes a non-negligible contribution to its reactivity, at least in the chamber experiments.

RFG Reactivity

The five RFG-fueled vehicles used in this program represented a variety of vehicle types, mileages, and NO_x and VOC pollutant levels, and thus provided a good survey of cold-start exhausts from gasoline-fueled vehicles. The VOC levels in the cold-start exhaust of the cleanest of the vehicles studied, a low-mileage 1997 Ford Taurus, were too low for the chamber experiments to provide a very precise measurement of the VOC reactivity, but the chamber data were useful in confirming that the overall reactivity was indeed as low as indicated by the exhaust analysis and the model predictions. In particular, the experiments with the 1997 Ford Taurus indicated there were no unmeasured species in the cold-start exhaust contributing significantly to its reactivity. The other four vehicles studied had sufficiently high VOC levels for to permit quantitative reactivity measurements to be obtained from the environmental chamber data.

The cold-start exhausts from these other four vehicles were found to significantly enhance rates of NO oxidation and O_3 formation when added to surrogate - NO_x mixtures, and to measurably increase integrated OH radical levels. Experiments using synthetic RFG exhaust mixtures, derived by lumping VOCs of similar types and reactivities together and using a single compound to represent each VOC type, gave very similar results as the experiments with the actual exhausts. This indicates that representing the complex exhaust mixtures by simpler synthetic mixtures, with reactivity weighting based on relative MIR values to account for differences among individual VOCs of the various types, give reasonably good approximations

of the overall effects of the exhausts on NO oxidation, ozone formation, and overall radical levels in the environmental chamber experiments. More significantly, this also indicates that, as with the LPG, methanol-containing and CNG exhausts discussed above, there is no significant contribution to reactivity caused by undetected compounds in the exhaust, and that the exhaust analyses methods currently employed for RFG exhausts are accounting for the major components causing their reactivities.

The model preformed reasonably well in simulating most of the actual and synthetic RFG exhaust experiments. The results of all the synthetic exhaust experiments were simulated without significant consistent bias, as were the results of the experiments using the actual exhausts from the moderately low VOC 1991 Dodge Spirit used for reproducibility studies in our laboratories, and from the relatively high VOC Chevrolet Suburban. Thus for these two vehicles (and also for the 1997 Taurus, where both the model and the experiment indicated low reactivity), the model is able to satisfactorily account for the reactivities of their cold-start exhausts. For the older, higher mileage 1988 Honda Accord and 1984 Toyota pickup, the model preformed reasonably well in simulating the experiments with the exhausts alone or when the exhaust was added to a mixture representative to VOCs measured in ambient air, but the model somewhat underpredicted the effect of the exhaust on NO oxidation and O_3 formation when added to a simpler mini-surrogate - NO_x mixture. This is despite the fact that, for the Accord at least, the synthetic exhaust had about the same effect on the mini-surrogate as the actual exhaust, and the model simulated the mini-surrogate with surrogate Accord exhaust run reasonably well. It may be that there is a constituent of these exhausts which is not well represented by the model and is better represented by the model for the compound used in the synthetic exhaust to represent it. However, more replicate experiments with these vehicles, and experiments with other relatively high mileage, in-use vehicles would be needed to determine if this is a consistent problem, or just a problem with the characterization of the two experiments involved, which were not replicated. However, even for these vehicles the model performs reasonably well in simulating the exhaust reactivity in the experiments with the more realistic surrogate, indicating that it probably will also do so in simulating the effects of these and the other RFG exhausts in the atmosphere.

Diesel Reactivity

The exploratory experiment carried out with a high-mileage 1984 diesel sedan indicate that the cold-start exhaust from this vehicle can significantly enhance NO oxidation and O_3 formation rates and also measurably increase integrated OH radical levels. However, the species accounting for this reactivity have not been accounted for. It is clearly not due to light hydrocarbons such as $C_{\leq}10$ alkenes, olefins, or aromatics, or $C_{\leq}3$ oxygenates such as formaldehyde and acetaldehyde, levels of these compounds in the chamber was either below the detection limits or too small to significantly affect the results. It is clear that

127

chamber experiments need to be carried out with more comprehensive analyses need to be carried out before we can assess whether we can understand the factors accounting for the reactivities of diesel exhausts.

REFERENCES

Atkinson, R. (1989): "Kinetics and Mechanisms of the Gas-Phase Reactions of the Hydroxyl Radical with Organic Compounds," J. Phys. Chem. Ref. Data, Monograph No. 1.

Black, F., and Kleindienst, T. (1995) "Characterization of Alternative Fuel Vehicle Emissions Composition and Ozone." EPA/600/R-96/135.

CARB (1992): "Notice of Public Hearing to Consider the Adoption of Amendments to the Certification and Compliance Test Procedures for Alternative Fuel Retrofit Systems for Motor Vehicles," California Air Resources Board, May 14, 1992.

CARB (1993): "Proposed Regulations for Low-Emission Vehicles and Clean Fuels ─ Staff Report and Technical Support Document," California Air Resources Board, Sacramento, CA, August 13, 1990. See also Appendix VIII of "California Exhaust Emission Standards and Test Procedures for 1988 and Subsequent Model Passenger Cars, Light Duty Trucks and Medium Duty Vehicles," as last amended September 22, 1993. Incorporated by reference in Section 1960.1 (k) of Title 13, California Code of Regulations.

CARB (1994). "Mobile Source Emission Standards Summary." From Title 13, Ch. 3 California Code of Regulations.

Carter, W. P. L. (1993): "Development and Application of an Up-To-Date Photochemical Mechanism for Airshed Modeling and Reactivity Assessment," Final report for California Air Resources Board Contract No. A934-094, April 26.

Carter, W. P. L. and R. Atkinson (1987): "An Experimental Study of Incremental Hydrocarbon Reactivity," Environ. Sci. Technol., 21, 670-679

Carter, W. P. L. (1990): "A Detailed Mechanism for the Gas-Phase Atmospheric Reactions of Organic Compounds," Atmos. Environ., 24A, 481-518.

Carter, W. P. L., and F. W. Lurmann (1990): "Evaluation of the RADM Gas-Phase Chemical Mechanism," Final Report, EPA-600/3-90-001.

Carter, W. P. L. and F. W. Lurmann (1991): "Evaluation of a Detailed Gas-Phase Atmospheric Reaction Mechanism using Environmental Chamber Data," Atmos. Environ. 25A, 2771-2806.

Carter, W. P. L., J. A. Pierce, I. L. Malkina, D. Luo and W. D. Long (1993a): "Environmental Chamber Studies of Maximum Incremental Reactivities of Volatile Organic Compounds," Report to Coordinating Research Council, Project No. ME-9, California Air Resources Board Contract No. A032-0692; South Coast Air Quality Management District Contract No. C91323, United States Environmental Protection Agency Cooperative Agreement No. CR-814396-01-0, University Corporation for Atmospheric Research Contract No. 59166, and Dow Corning Corporation. April 1.

Carter, W. P. L, D. Luo, I. L. Malkina, and J. A. Pierce (1993b): "An Experimental and Modeling Study of the Photochemical Ozone Reactivity of Acetone," Final Report to Chemical Manufacturers Association Contract No. KET-ACE-CRC-2.0. December 10.

Carter, W. P. L. (1994): "Development of Ozone Reactivity Scales for Volatile Organic Compounds," J. Air and Waste Manage. Assoc., 44, 881-899.

Carter, W. P. L., D. Luo, I. L. Malkina, and J. A. Pierce (1995a): "Environmental Chamber Studies of Atmospheric Reactivities of Volatile Organic Compounds. Effects of Varying Chamber and Light Source," Final report to National Renewable Energy Laboratory, Contract XZ-2-12075, Coordinating Research Council, Inc., Project M-9, California Air Resources Board, Contract A032-0692, and South Coast Air Quality Management District, Contract C91323, March 26.

Carter, W. P. L., D. Luo, I. L. Malkina, and J. A. Pierce (1995b): "Environmental Chamber Studies of Atmospheric Reactivities of Volatile Organic Compounds. Effects of Varying Chamber and Light Source," Final report to National Renewable Energy Laboratory, Contract XZ-2-12075, Coordinating Research Council, Inc., Project M-9, California Air Resources Board, Contract A032-0692, and South Coast Air Quality Management District, Contract C91323, March 26.

Carter, W. P. L., D. Luo, I. L. Malkina, and D. Fitz (1995c): "The University of California, Riverside Environmental Chamber Data Base for Evaluating Oxidant Mechanism. Indoor Chamber Experiments through 1993," Report submitted to the U.S. Environmental Protection Agency, EPA/AACTUAL, Research Triangle Park, NC., March 20..

Carter, W. P. L. (1995): "Computer Modeling of Environmental Chamber Measurements of Maximum Incremental Reactivities of Volatile Organic Compounds," Atmos. Environ., 29, 2513-2517.

Carter, W. P. L., D. Luo, and I. L. Malkina (1997): "Environmental Chamber Studies for Development of an Updated Photochemical Mechanism for VOC Reactivity Assessment," Final report to California Air Resources Board Contract 92-345, Coordinating Research Council Project M-9, and National Renewable Energy Laboratory Contract ZF-2-12252-07. November 26.

Clean Fleet (1995). Final report: Volume 7,. National Renewable Energy Lab., Golden, CO (United States) . Dec 1995 . DOE Contract AC3683CH10093 . Sup.Doc.Num. E 1.99:DE96007965. NTIS DE96007965 . DOE/CH/10093--T25-Vol.7

CFR (1977): Code of Federal Regulations (1997), Title 40 Chapter 1, U.S. Government Printing Office.

Gabele, P. A. (1990): "Characterization of Emissions from a Variable Gasoline/Methanol Fueled Car," J. Air Waste Mange. Assoc., 40, pp. 296-304.

Jeffries, H.E.; K. G. Sexton; T.P. Morris, H. Jackson, R.G. Goodman, R.M. Kamens; and M.S. Holleman (1985a). Outdoor smog chamber experiments using automobile exhaust. Final Report, EPA-600/3-85-032.

Jeffries, H. E., K. G. Sexton, and M. S. Holleman (1985b): "Outdoor Smog Chamber experiments: Reactivity of Methanol Exhaust", Final Report, EPA-600/3-85-009a, September

Johnson, G. M. (1983): "Factors Affecting Oxidant Formation in Sydney Air," in "The Urban Atmosphere -- Sydney, a Case Study." Eds. J. N. Carras and G. M. Johnson (CSIRO, Melbourne), pp. 393-408.

Kelly, N.A.; P. Wang; S.M. Japar; M.D. Huley; and T.J. Wallington (1994). Measurement of the atmospheric reactivity of emissions from gasoline and alternative-fueled vehicles, assessment of available methodologies. First-Year Final Report, CRC Contract No. AQ-6-1-92, Environmental Research Consortium.

Kelly, K.J.; Bailey, B.K.; Coburn, T.C.; Clark, W.; Eudy, L.; and Lissiuk, P. (1996): "Light-Duty Vehicle Program Emissions Results", National Renewable Energy Laboratory NREL/TP-425-21294. October.

Kleindienst, T.E. (1994). Photochemical reactivity studies of emissions from alternative fuels. Draft final report to the National Renewable Energy Laboratory, submitted by ManTech Environmental Technology, Inc., Contract No. TS-2-11116-1, November.

Norbeck, J. M., T. J. Truex, M. R. Smith, and T. Durbin (1998): "Inventory of AFVs and AFV Comparison: OEM vs Retrofits," Final Report for South Coast Air Quality Management District Contract 97029, September 25.

Siegel, W. O., J. F. O. Richert, T. E. Jensen, D. Schuetzle, S. J. Swarin, J. F. Loo, A. Prostak, D. Nagy, A. M. Schlenker (1993): "Improved Emissions Speciation Methodology for Phase II of the Auto/Oil Air Quality Improvement Research Program-Hydrocarbons and Oxygenates", SAE Paper 930142.

Zafonte, L.; P.L. Rieger; and J.R. Holmes (1977). Nitrogen dioxide photolysis in the Los Angeles atmosphere. *Environ. Sci. Technol.,* 11:483-487.

APPENDIX A
LISTING OF THE CHEMICAL MECHANISM

The chemical mechanism used in the environmental chamber and atmospheric model simulations discussed in this report is given in Tables A-1 through A-4. Table A-1 lists the species used in the mechanism, Table A-2 gives the reactions and rate constants, Table A-3 gives the parameters used to calculate the rates of the photolysis reactions, and Table A-4 gives the values and derivations of the chamber-dependent parameters used when modeling the environmental chamber experiments. Footnotes to Table A-2 indicate the format used for the reaction listing.

Table A-1.   List of species in the chemical mechanism used in the model simulations for this study.

Name	Description
Constant Species.	
O2	Oxygen
M	Air
H2O	Water
Active Inorganic Species.	
O3	Ozone
NO	Nitric Oxide
NO2	Nitrogen Dioxide
NO3	Nitrate Radical
N2O5	Nitrogen Pentoxide
HONO	Nitrous Acid
HNO3	Nitric Acid
HNO4	Peroxynitric Acid
HO2H	Hydrogen Peroxide
Active Radical Species and Operators.	
HO2.	Hydroperoxide Radicals
RO2.	Operator to Calculate Total Organic Peroxy Radicals
RCO3.	Operator to Calculate Total Acetyl Peroxy Radicals
Active Reactive Organic Product Species.	
CO	Carbon Monoxide
HCHO	Formaldehyde
CCHO	Acetaldehyde
RCHO	Lumped C3+ Aldehydes
ACET	Acetone
MEK	Lumped Ketones
PHEN	Phenol
CRES	Cresols
BALD	Aromatic aldehydes (e.g., benzaldehyde)
GLY	Glyoxal
MGLY	Methyl Glyoxal
BACL	Biacetyl or other lumped α-dicarbonyls, including α-keto esters

Name	Description
AFG1	Reactive Aromatic Fragmentation Products from benzene and naphthalene
AFG2	Other Reactive Aromatic Fragmentation Products
AFG3	Aromatic Fragmentation Products used in adjusted m-xylene mechanism
RNO3	Organic Nitrates
NPHE	Nitrophenols
ISOPROD	Lumped isoprene product species
PAN	Peroxy Acetyl Nitrate
PPN	Peroxy Propionyl Nitrate
GPAN	PAN Analogue formed from Glyoxal
PBZN	PAN Analogues formed from Aromatic Aldehydes
-OOH	Operator Representing Hydroperoxy Groups

Non-Reacting Species

CO2	Carbon Dioxide
-C	"Lost Carbon"
-N	"Lost Nitrogen"
H2	Hydrogen

Steady State Species and Operators.

HO.	Hydroxyl Radicals
O	Ground State Oxygen Atoms
O*1D2	Excited Oxygen Atoms
RO2-R.	Peroxy Radical Operator representing NO to NO_2 conversion with HO_2 formation.
RO2-N.	Peroxy Radical Operator representing NO consumption with organic nitrate formation.
RO2-NP.	Peroxy Radical Operator representing NO consumption with nitrophenol formation
R2O2.	Peroxy Radical Operator representing NO to NO_2 conversion.
CCO-O2.	Peroxy Acetyl Radicals
C2CO-O2.	Peroxy Propionyl Radicals
HCOCO-O2.	Peroxyacyl Radical formed from Glyoxal
BZ-CO-O2.	Peroxyacyl Radical formed from Aromatic Aldehydes
HOCOO.	Intermediate formed in Formaldehyde + HO_2 reaction
BZ-O.	Phenoxy Radicals
BZ(NO2)-O.	Nitratophenoxy Radicals
HOCOO.	Radical Intermediate formed in the HO_2 + Formaldehyde system.
(HCHO2)	Excited Criegee biradicals formed from $=CH_2$ groups
(CCHO2)	Excited Criegee biradicals formed from $=CHCH_3$ groups
(RCHO2)	Excited Criegee biradicals formed from =CHR groups, where R not CH_3
(C(C)CO2)	Excited Criegee biradicals formed from $=C(CH_3)_2$ groups
(C(R)CO2)	Excited Criegee biradicals formed from $=C(CH_3)R$ or CR_2 groups
(BZCHO2)	Excited Criegee biradicals formed from styrenes
(C:CC(C)O2)	Excited Criegee biradicals formed from isoprene
(C:C(C)CHO2)	Excited Criegee biradicals formed from isoprene
(C2(O2)CHO)	Excited Criegee biradicals formed from isoprene products
(HOCCHO2)	Excited Criegee biradicals formed from isoprene products
(HCOCHO2)	Excited Criegee biradicals formed from isoprene products
(C2(O2)COH)	Excited Criegee biradicals formed from isoprene products

Table A-1, (continued)

Name	Description

Primary Organic Reactants

Name	Description
CH4	Methane
ETHANE	Ethane
PROPANE	Propane
N-C4	n-Butane
N-C6	n-Hexane
N-C8	n-Octane
N-C9	n-Nonane
N-C10	n-Decane
N-C11	n-Undecane
N-C12	n-Dodecane
2-ME-C3	Isobutane
2-ME-C4	Isopentane
22-DM-C3	Neopentane
2-ME-C5	2-Methyl Pentane
3-ME-C5	3-Methylpentane
22-DM-C4	2,2-Dimethyl Butane
23-DM-C4	2,3-Dimethyl Butane
2-ME-C6	2-Methyl Hexane
3-ME-C6	3-Methyl Hexane
24-DM-C5	2,4-Dimethyl Pentane
23-DM-C5	2,3-Dimethyl Pentane
33-DM-C5	3,3-Dimethyl Pentane
223TM-C4	2,2,3-Trimethyl Butane
BR-C7	Branched C7 Alkanes (Represented by 3-Methyl Hexane)
2-ME-C7	2-Methyl Heptane
3-ME-C7	3-Methyl Heptane
4-ME-C7	4-Methyl Heptane
23-DM-C6	2,3-Dimethyl Hexane
24-DM-C6	2,4-Dimethyl Hexane
25-DM-C6	2,5-Dimethyl Hexane
224TM-C5	2,2,4-Trimethyl Pentane
234TM-C5	2,3,4-Trimethyl Pentane
BR-C8	Branched C8 Alkanes (Represented by 4-Methyl Heptane)
4-ET-C7	4-Ethyl Heptane
24-DM-C7	2,4-Dimethyl Heptane
225TM-C6	2,2,5-Trimethyl Hexane
35-DM-C7	3,5-Dimethyl Heptane (Represented by 3,4-Propyl Heptane)
BR-C9	Branched C9 Alkanes (Represented by 4-Ethyl Heptane)
BR-C10	Branched C10 Alkanes (Represented by 3,4-Propyl Heptane)
4-PR-C7	3,4-Propyl Heptane
24-DM-C8	2,4-Dimethyl Octane (Represented by Branched C10 Alkanes)
CYCC5	Cyclopentane
CYCC6	Cyclohexane
ME-CYCC5	Methylcyclopentane
ME-CYCC6	Methylcyclohexane
13DMCYC5	1,3-Dimeth. Cyclopentane

Name	Description
ET-CYCC5	Ethyl Cyclopentane
CYC-C7	C7 Cycloalkanes (Represented by Methylcyclohexane)
ET-CYCC6	Ethylcyclohexane
13DMCYC6	1,3-Dimethyl Cyclohexane
CYC-C8	C8 Cycloalkanes (Represented by Ethylcyclohexane)
ETHENE	Ethene
PROPENE	Propene
1-BUTENE	1-Butene
T-2-BUTE	trans-2-Butene
C-2-BUTE	cis-2-Butene
ISOBUTEN	Isobutene
13-BUTDE	1,3-Butadiene
3M-1-BUT	3-Methyl-1-Butene
1-PENTEN	1-Pentene
2M-1-BUT	2-Methyl-1-Butene
2M-2-BUT	2-Methyl-2-Butene
2-C5-OLE	2-Pentenes
CYC-PNTE	Cyclopentene
T-2-PENT	trans-2-Pentene (Represented by 2-Pentenes)
C-2-PENT	cis-2-Pentene (Represented by 2-Pentenes)
CYC-PNDE	Cyclopentadiene (Represented by 2-Pentenes)
1-HEXENE	1-Hexene
2-C6-OLE	2-Hexenes
CYC-HEXE	Cyclohexene
2M-1-PEN	2-Methyl-1-Pentene (Represented by 2-Methyl-1-Butene)
2M-2-PEN	2-Methyl-2-Pentene (Represented by 2-Methyl-2-Butene)
C6-OLE1	C6 Terminal Alkanes (Represented by 1-Hexene)
C6-OLE2	C6 Internal Alkenes (Represented by 2-Hexenes)
C6-OL2D	C6 Cyclic or di-olefins (Represented by 2-Hexenes)
1-C7-OLE	1-Heptene
2-C7-OLE	2-Heptenes
C7-OLE1	C7 Terminal Alkanes (Represented by 1-Heptene)
C7-OLE2	C7 Internal Alkenes (Represented by 2-Heptenes)
1-C8-OLE	1-Octene
3-C8-OLE	3-Octenes
C8-OLE1	C8 Terminal Alkanes (Represented by 1-Octene)
C8-OLE2	C8 Internal Alkenes (Represented by 3-Octenes)
1-C9-OLE	1-Nonene
ISOP	Isoprene
BENZENE	Benzene
TOLUENE	Toluene
C2-BENZ	Ethyl Benzene
I-C3-BEN	Isopropyl Benzene
N-C3-BEN	n-Propyl Benzene
M-XYLENE	m-Xylene

Table A-1, (continued)

Name	Description
O-XYLENE	o-Xylene
P-XYLENE	p-Xylene
C8-BEN2	C8 Disub. Benzenes (Represented by m-Xylene)
135-TMB	1,3,5-Trimethyl Benzene
123-TMB	1,2,3-Trimethyl Benzene
124-TMB	1,2,4-Trimethyl Benzene
C9-BEN2	C9 Disub. Benzenes (Represented by m-Xylene)
NAPHTHAL	Naphthalene
C10-BEN1	C10 Monosub. Benzenes (Represented by Ethyl Benzene)
C10-BEN2	C10 Disub. Benzenes (Represented by m-Xylene)
C10-BEN3	C10 Trisub. Benzenes (Represented by 1,3,5-Trimethyl Benzene)
C10-BEN4	C10 Tetrasub. Benzenes (Represented by 1,3,5-Trimethyl Benzene)
C12-BEN3	C12 Trisub. Benzenes (Represented by 1,3,5-Trimethyl Benzene)
C11-BEN2	C11 Disub. Benzenes (Represented by m-Xylene)
23-DMN	2,3-Dimethyl Naphth.
ME-NAPH	Methyl Naphthalenes
TETRALIN	Tetralin
INDAN	Indan (Represented by Tetralin)
STYRENE	Styrene
ACETYLEN	Acetylene
ME-ACTYL	Methyl Acetylene
ET-ACTYL	Ethyl Acetylene (Represented by 1-Butene)
MEOH	Methanol
MTBE	Methyl t-Butyl Ether
ETBE	Ethyl t-Butyl Ether

Table A-2.   List of reactions in the chemical mechanism used in the model simulations for this study.

```
─────────────────────────────────────────────────────────────────────────────────
Rxn.        Kinetic Parameters [a]
          ─────────────────────────────    Reactions [b]
Label  k(300)     A        Ea     B
─────────────────────────────────────────────────────────────────────────────────

Inorganic Reactions

1           (Phot. Set = NO2      )    NO2 + HV = NO + O
2      6.00E-34  6.00E-34  0.00 -2.30   O + O2 + M = O3 + M
3A     9.69E-12  6.50E-12 -0.24  0.00   O + NO2 = NO + O2
3B     1.55E-12   (Falloff Kinetics)   O + NO2 = NO3 + M
       k0    =   9.00E-32  0.00 -2.00
       kINF =    2.20E-11  0.00  0.00
                 F= 0.60   n= 1.00
4      1.88E-14  2.00E-12  2.78  0.00   O3 + NO = NO2 + O2
5      3.36E-17  1.40E-13  4.97  0.00   O3 + NO2 = O2 + NO3
6      2.80E-11  1.70E-11 -0.30  0.00   NO + NO3 = 2 NO2
7      1.92E-38  3.30E-39 -1.05  0.00   NO + NO + O2 = 2 NO2
8      1.26E-12   (Falloff Kinetics)   NO2 + NO3 = N2O5
       k0    =   2.20E-30  0.00 -4.30
       kINF =    1.50E-12  0.00 -0.50
                 F= 0.60   n= 1.00
9      5.53E+10  9.09E+26 22.26  0.00   N2O5 + #RCON8 = NO2 + NO3
10     1.00E-21   (No T Dependence)    N2O5 + H2O = 2 HNO3
11     4.17E-16  2.50E-14  2.44  0.00   NO2 + NO3 = NO + NO2 + O2
12A         (Phot. Set = NO3NO    )    NO3 + HV = NO + O2
12B         (Phot. Set = NO3NO2   )    NO3 + HV = NO2 + O
13A         (Phot. Set = O3O3P    )    O3 + HV = O + O2
13B         (Phot. Set = O3O1D    )    O3 + HV = O*1D2 + O2
14     2.20E-10   (No T Dependence)    O*1D2 + H2O = 2 HO.
15     2.92E-11  1.92E-11 -0.25  0.00   O*1D2 + M = O + M
16     4.81E-12   (Falloff Kinetics)   HO. + NO = HONO
       k0    =   7.00E-31  0.00 -2.60
       kINF =    1.50E-11  0.00 -0.50
                 F= 0.60   n= 1.00
17          (Phot. Set = HONO     )    HONO + HV = HO. + NO
18     1.13E-11   (Falloff Kinetics)   HO. + NO2 = HNO3
       k0    =   2.60E-30  0.00 -3.20
       kINF =    2.40E-11  0.00 -1.30
                 F= 0.60   n= 1.00
19     1.03E-13  6.45E-15 -1.65  0.00   HO. + HNO3 = H2O + NO3
21     2.40E-13   (No T Dependence)    HO. + CO = HO2. + CO2
22     6.95E-14  1.60E-12  1.87  0.00   HO. + O3 = HO2. + O2
23     8.28E-12  3.70E-12 -0.48  0.00   HO2. + NO = HO. + NO2
24     1.37E-12   (Falloff Kinetics)   HO2. + NO2 = HNO4
       k0    =   1.80E-31  0.00 -3.20
       kINF =    4.70E-12  0.00 -1.40
                 F= 0.60   n= 1.00
25     7.92E+10  4.76E+26 21.66  0.00   HNO4 + #RCON24 = HO2. + NO2
27     4.61E-12  1.30E-12 -0.75  0.00   HNO4 + HO. = H2O + NO2 + O2
28     2.08E-15  1.10E-14  0.99  0.00   HO2. + O3 = HO. + 2 O2
29A    1.73E-12  2.20E-13 -1.23  0.00   HO2. + HO2. = HO2H + O2
29B    5.00E-32  1.90E-33 -1.95  0.00   HO2. + M = HO2H + O2
29C    3.72E-30  3.10E-34 -5.60  0.00   HO2. + HO2. + H2O = HO2H + O2 + H2O
29D    2.65E-30  6.60E-35 -6.32  0.00   HO2. + HO2. + H2O = HO2H + O2 + H2O
30A    1.73E-12  2.20E-13 -1.23  0.00   NO3 + HO2. = HNO3 + O2
30B    5.00E-32  1.90E-33 -1.95  0.00   NO3 + HO2. + M = HNO3 + O2
30C    3.72E-30  3.10E-34 -5.60  0.00   NO3 + HO2. + H2O = HNO3 + O2 + H2O
30D    2.65E-30  6.60E-35 -6.32  0.00   NO3 + HO2. + H2O = HNO3 + O2 + H2O
31          (Phot. Set = H2O2     )    HO2H + HV = 2 HO.
32     1.70E-12  3.30E-12  0.40  0.00   HO2H + HO. = HO2. + H2O
33     9.90E-11  4.60E-11 -0.46  0.00   HO. + HO2. = H2O + O2

Peroxy Radical Operators

B1     7.68E-12  4.20E-12 -0.36  0.00   RO2. + NO = NO
B2     2.25E-11   (Falloff Kinetics)   RCO3. + NO = NO
       k0    =   5.65E-28  0.00 -7.10
       kINF =    2.64E-11  0.00 -0.90
                 F= 0.27   n= 1.00
B4     1.04E-11   (Falloff Kinetics)   RCO3. + NO2 = NO2
       k0    =   2.57E-28  0.00 -7.10
       kINF =    1.20E-11  0.00 -0.90
                 F= 0.30   n= 1.00
B5     4.90E-12  3.40E-13 -1.59  0.00   RO2. + HO2. = HO2. + RO2-HO2-PROD
B6     4.90E-12  3.40E-13 -1.59  0.00   RCO3. + HO2. = HO2. + RO2-HO2-PROD
B8     1.00E-15   (No T Dependence)    RO2. + RO2. = RO2-RO2-PROD
```

Table A-2 (continued)

Rxn. Label	Kinetic Parameters [a]				Reactions [b]
	k(300)	A	Ea	B	

```
B9    1.09E-11  1.86E-12  -1.05  0.00   RO2. + RCO3. = RO2-RO2-PROD
B10   1.64E-11  2.80E-12  -1.05  0.00   RCO3. + RCO3. = RO2-RO2-PROD

B11        (Same k as for RO2.     )    RO2-R. + NO = NO2 + HO2.
B12        (Same k as for RO2.     )    RO2-R. + HO2. = -OOH
B13        (Same k as for RO2.     )    RO2-R. + RO2. = RO2. + 0.5 HO2.
B14        (Same k as for RO2.     )    RO2-R. + RCO3. = RCO3. + 0.5 HO2.

B19        (Same k as for RO2.     )    RO2-N. + NO = RNO3
B20        (Same k as for RO2.     )    RO2-N. + HO2. = -OOH + MEK + 1.5 -C
B21        (Same k as for RO2.     )    RO2-N. + RO2. = RO2. + 0.5 HO2. + MEK + 1.5 -C
B22        (Same k as for RO2.     )    RO2-N. + RCO3. = RCO3. + 0.5 HO2. + MEK + 1.5 -C

B15        (Same k as for RO2.     )    R2O2. + NO = NO2
B16        (Same k as for RO2.     )    R2O2. + HO2. =
B17        (Same k as for RO2.     )    R2O2. + RO2. = RO2.
B18        (Same k as for RO2.     )    R2O2. + RCO3. = RCO3.

B23        (Same k as for RO2.     )    RO2-XN. + NO = -N
B24        (Same k as for RO2.     )    RO2-XN. + HO2. = -OOH
B25        (Same k as for RO2.     )    RO2-XN. + RO2. = RO2. + 0.5 HO2.
B26        (Same k as for RO2.     )    RO2-XN. + RCO3. = RCO3. + HO2.

G2         (Same k as for RO2.     )    RO2-NP. + NO = NPHE
G3         (Same k as for RO2.     )    RO2-NP. + HO2. = -OOH + 6 -C
G4         (Same k as for RO2.     )    RO2-NP. + RO2. = RO2. + 0.5 HO2. + 6 -C
G5         (Same k as for RO2.     )    RO2-NP. + RCO3. = RCO3. + HO2. + 6 -C
```

Operator Added to Represent Possible NO₂ to NO Conversions

```
           (Same k as for BZ-O.  )    xNO2 + NO2 = NO
           (Same k as for BZ-O.  )    xNO2 + HO2. =
           (Same k as for BZ-O.  )    xNO2 =
```

Excited Criegee Biradicals

```
RZ1            (fast)              (HCHO2) = 0.7 HCOOH + 0.12 "HO. + HO2. + CO" + 0.18 "H2 +
                                      CO2"
RZ2            (fast)              (CCHO2) = 0.25 CCOOH + 0.15 "CH4 + CO2" + 0.6 HO. +
                                      0.3 "CCO-O2. + RCO3." + 0.3 "RO2-R. + HCHO + CO + RO2."
RZ3            (fast)              (RCHO2) = 0.25 CCOOH + 0.15 CO2 + 0.6 HO. + 0.3 "C2CO-O2. +
                                      RCO3." + 0.3 "RO2-R. + CCHO + CO + RO2." + 0.55 -C
RZ4            (fast)              (C(C)CO2) = HO. + R2O2. + HCHO + CCO-O2. + RCO3. + RO2.
RZ5            (fast)              (C(R)CO2) = HO. + CCO-O2. + CCHO + R2O2. + RCO3. + RO2.
RZ6            (fast)              (CYCCO2) = 0.3 "HO. + C2CO-O2. + R2O2. + RCO3. + RO2." +
                                      0.3 RCHO + 4.2 -C
RZ8            (fast)              (BZCHO2) = 0.5 "BZ-O. + R2O2. + CO + HO."
ISZ1           (fast)              (C:CC(C)O2) = HO. + R2O2. + HCHO + C2CO-O2. + RO2. + RCO3.
ISZ2           (fast)              (C:C(C)CHO2) = 0.75 RCHO + 0.25 ISOPROD + 0.5 -C
MAZ1           (fast)              (C2(O2)CHO) = HO. + R2O2. + HCHO + HCOCO-O2. + RO2. + RCO3.
M1Z1           (fast)              (HOCCHO2) = 0.6 HO. + 0.3 "CCO-O2. + RCO3." + 0.3 "RO2-R. +
                                      HCHO + CO + RO2." + 0.8 -C
M2Z1           (fast)              (HCOCHO2) = 0.12 "HO2. + 2 CO + HO." + 0.74 -C +
                                      0.51 "CO2 + HCHO"
M2Z2           (fast)              (C2(O2)COH) = HO. + MGLY + HO2. + R2O2. + RO2.
```

Organic Product Species

```
B7         (Phot. Set = CO2H    )    -OOH + HV = HO2. + HO.
B7A   1.81E-12  1.18E-12  -0.25  0.00   HO. + -OOH = HO.
B7B   3.71E-12  1.79E-12  -0.44  0.00   HO. + -OOH = RO2-R. + RO2.

C1         (Phot. Set = HCHONEWR)    HCHO + HV = 2 HO2. + CO
C2         (Phot. Set = HCHONEWM)    HCHO + HV = H2 + CO
C3    9.76E-12  1.13E-12  -1.29  2.00   HCHO + HO. = HO2. + CO + H2O
C4    7.79E-14  9.70E-15  -1.24  0.00   HCHO + HO2. = HOCOO.
C4A   1.77E+02  2.40E+12  13.91  0.00   HOCOO. = HO2. + HCHO
C4B        (Same k as for RO2.     )    HOCOO. + NO = -C + NO2 + HO2.
C9    6.38E-16  2.80E-12   5.00  0.00   HCHO + NO3 = HNO3 + HO2. + CO

C10   1.57E-11  5.55E-12  -0.62  0.00   CCHO + HO. = CCO-O2. + H2O + RCO3.
C11A       (Phot. Set = CCHOR   )    CCHO + HV = CO + HO2. + HCHO + RO2-R. + RO2.
```

A-7

```
─────────────────────────────────────────────────────────────────────────────
Rxn.       Kinetic Parameters [a]
        ─────────────────────────────── Reactions [b]
Label  k(300)    A       Ea    B
─────────────────────────────────────────────────────────────────────────────


C12    2.84E-15  1.40E-12  3.70  0.00   CCHO + NO3 = HNO3 + CCO-O2. + RCO3.

C25    1.97E-11  8.50E-12 -0.50  0.00   RCHO + HO. = C2CO-O2. + RCO3.
C26       (Phot. Set = RCHO     )       RCHO + HV = CCHO + RO2-R. + RO2. + CO + HO2.
C27    2.84E-15  1.40E-12  3.70  0.00   NO3 + RCHO = HNO3 + C2CO-O2. + RCO3.

C38    2.23E-13  4.81E-13  0.46  2.00   ACET + HO. = R2O2. + HCHO + CCO-O2. + RCO3. + RO2.
C39       (Phot. Set = ACET-93C)        ACET + HV = CCO-O2. + HCHO + RO2-R. + RCO3. + RO2.

C44    1.16E-12  2.92E-13 -0.82  2.00   MEK + HO. = H2O + 0.5 "CCHO + HCHO + CCO-O2. + C2CO-O2." +
                                            RCO3. + 1.5 "R2O2. + RO2."
C57       (Phot. Set = KETONE  )        MEK + HV + #0.1 = CCO-O2. + CCHO + RO2-R. + RCO3. + RO2.

C95    2.07E-12  2.19E-11  1.41  0.00   RNO3 + HO. = NO2 + 0.155 MEK + 1.05 RCHO + 0.48 CCHO +
                                            0.16 HCHO + 0.11 -C + 1.39 "R2O2. + RO2."

C58A      (Phot. Set = GLYOXAL1)        GLY + HV  = 0.8 HO2. + 0.45 HCHO + 1.55 CO
C58B      (Phot. Set = GLYOXAL2)        GLY + HV + #0.029 = 0.13 HCHO + 1.87 CO
C59    1.14E-11   (No T Dependence)     GLY + HO. = 0.6 HO2. + 1.2 CO + 0.4 "HCOCO-O2. + RCO3."
C60       (Same k as for CCHO    )      GLY + NO3 = HNO3 + 0.6 HO2. + 1.2 CO + 0.4 "HCOCO-O2. +
                                            RCO3."

C68A      (Phot. Set = MEGLYOX1)        MGLY + HV = HO2. + CO + CCO-O2. + RCO3.
C68B      (Phot. Set = MEGLYOX2)        MGLY + HV + 0.107 = HO2. + CO + CCO-O2. + RCO3.
C69    1.72E-11   (No T Dependence)     MGLY + HO. = CO + CCO-O2. + RCO3.
C70       (Same k as for CCHO    )      MGLY + NO3 = HNO3 + CO + CCO-O2. + RCO3.

G7     1.14E-11   (No T Dependence)     HO. + AFG1 = HCOCO-O2. + RCO3.
G8        (Phot. Set = ACROLEIN)        AFG1 + HV + #0.029 = HO2. + HCOCO-O2. + RCO3.

U2OH   1.72E-11   (No T Dependence)     HO. + AFG2 = C2CO-O2. + RCO3.
U2HV      (Phot. Set = ACROLEIN)        AFG2 + HV = HO2. + CO + CCO-O2. + RCO3.

G46    2.63E-11   (No T Dependence)     HO. + PHEN = 0.15 RO2-NP. + 0.85 RO2-R. + 0.2 GLY +
                                            4.7 -C + RO2.
G51    3.60E-12   (No T Dependence)     NO3 + PHEN = HNO3 + BZ-O.
G52    4.20E-11   (No T Dependence)     HO. + CRES = 0.15 RO2-NP. + 0.85 RO2-R. + 0.2 MGLY +
                                            5.5 -C + RO2.
G57    2.10E-11   (No T Dependence)     NO3 + CRES = HNO3 + BZ-O. + -C
G30    1.29E-11   (No T Dependence)     BALD + HO. = BZ-CO-O2. + RCO3.
G31       (Phot. Set = BZCHO   )        BALD + HV + #0.05 = 7 -C
G32    2.61E-15  1.40E-12  3.75  0.00   BALD + NO3 = HNO3 + BZ-CO-O2.

G58    3.60E-12   (No T Dependence)     NPHE + NO3 = HNO3 + BZ(NO2)-O.
G59       (Same k as for BZ-O.   )      BZ(NO2)-O. + NO2 = 2 -N + 6 -C
G60       (Same k as for RO2.    )      BZ(NO2)-O. + HO2. = NPHE
G61       (Same k as for BZ-O.   )      BZ(NO2)-O. = NPHE

C13       (Same k as for RCO3.   )      CCO-O2. + NO = CO2 + NO2 + HCHO + RO2-R. + RO2.
C14       (Same k as for RCO3.   )      CCO-O2. + NO2 = PAN
C15       (Same k as for RCO3.   )      CCO-O2. + HO2. = -OOH + CO2 + HCHO
C16       (Same k as for RCO3.   )      CCO-O2. + RO2. = RO2. + 0.5 HO2. + CO2 + HCHO
C17       (Same k as for RCO3.   )      CCO-O2. + RCO3. = RCO3. + HO2. + CO2 + HCHO
C18    6.50E-04   (Falloff Kinetics)    PAN = CCO-O2. + NO2 + RCO3.
        k0   =   4.90E-03 23.97  0.00
        kINF =   4.00E+16 27.08  0.00
                 F= 0.30  n= 1.00

C28       (Same k as for RCO3.   )      C2CO-O2. + NO = CCHO + RO2-R. + CO2 + NO2 + RO2.
C29    8.40E-12   (No T Dependence)     C2CO-O2. + NO2 = PPN
C30       (Same k as for RCO3.   )      C2CO-O2. + HO2. = -OOH + CCHO + CO2
C31       (Same k as for RCO3.   )      C2CO-O2. + RO2. = RO2. + 0.5 HO2. + CCHO + CO2
C32       (Same k as for RCO3.   )      C2CO-O2. + RCO3. = RCO3. + HO2. + CCHO + CO2
C33    6.78E-04  1.60E+17 27.97  0.00   PPN = C2CO-O2. + NO2 + RCO3.

C62       (Same k as for RCO3.   )      HCOCO-O2. + NO = NO2 + CO2 + CO + HO2.
C63       (Same k as for RCO3.   )      HCOCO-O2. + NO2 = GPAN
C65       (Same k as for RCO3.   )      HCOCO-O2. + HO2. = -OOH + CO2 + CO
C66       (Same k as for RCO3.   )      HCOCO-O2. + RO2. = RO2. + 0.5 HO2. + CO2 + CO
C67       (Same k as for RCO3.   )      HCOCO-O2. + RCO3. = RCO3. + HO2. + CO2 + CO
C64       (Same k as for PAN     )      GPAN = HCOCO-O2. + NO2 + RCO3.
```

Table A-2 (continued)

───

Rxn.	Kinetic Parameters [a]				Reactions [b]
Label	k(300)	A	Ea	B	

───

```
G33      (Same k as for RCO3.    )   BZ-CO-O2. + NO = BZ-O. + CO2 + NO2 + R2O2. + RO2.
G43  3.53E-11  1.30E-11  -0.60  0.00  BZ-O. + NO2 = NPHE
G44      (Same k as for RO2.     )   BZ-O. + HO2. = PHEN
G45  1.00E-03   (No T Dependence)    BZ-O. = PHEN
G34  8.40E-12   (No T Dependence)    BZ-CO-O2. + NO2 = PBZN
G36      (Same k as for RCO3.    )   BZ-CO-O2. + HO2. = -OOH + CO2 + PHEN
G37      (Same k as for RCO3.    )   BZ-CO-O2. + RO2. = RO2. + 0.5 HO2. + CO2 + PHEN
G38      (Same k as for RCO3.    )   BZ-CO-O2. + RCO3. = RCO3. + HO2. + CO2 + PHEN
G35  2.17E-04  1.60E+15  25.90  0.00  PBZN = BZ-CO-O2. + NO2 + RCO3.

IPOH  3.36E-11   (No T Dependence)   ISOPROD + HO. = 0.293 CO + 0.252 CCHO + 0.126 HCHO +
                                       0.041 GLY + 0.021 RCHO + 0.168 MGLY + 0.314 MEK +
                                       0.503 RO2-R. + 0.21 CCO-O2. + 0.288 C2CO-O2. +
                                       0.21 R2O2. + 0.713 RO2. + 0.498 RCO3. + -0.112 -C
IPO3  7.11E-18   (No T Dependence)   ISOPROD + O3 = 0.02 CCHO + 0.04 HCHO + 0.01 GLY +
                                       0.84 MGLY + 0.09 MEK + 0.66 (HCHO2) + 0.09 (HCOCHO2) +
                                       0.18 (HOCCHO2) + 0.06 (C2(O2)CHO) + 0.01 (C2(O2)COH) +
                                       -0.39 -C
IPHV       (Phot. Set = ACROLEIN)    ISOPROD + HV + 0.0036 = 0.333 CO + 0.067 CCHO + 0.9 HCHO +
                                       0.033 MEK + 0.333 HO2. + 0.7 RO2-R. + 0.267 CCO-O2. +
                                       0.7 C2CO-O2. + 0.7 RO2. + 0.967 RCO3. + -0.133 -C
IPN3  1.00E-15   (No T Dependence)   ISOPROD + NO3 = 0.643 CO + 0.282 HCHO + 0.85 RNO3 +
                                       0.357 RCHO + 0.925 HO2. + 0.075 C2CO-O2. + 0.075 R2O2. +
                                       0.925 RO2. + 0.075 RCO3. + 0.075 HNO3 + -2.471 -C
```

Hydrocarbon Species Represented Explicitly

```
8.71E-15  6.25E-13   2.55  2.00  METHANE + HO. = RO2-R. + HCHO + RO2.
2.74E-13  1.28E-12   0.92  2.00  ETHANE + HO. = RO2-R. + CCHO + RO2.
1.17E-12  1.35E-12   0.09  2.00  PROPANE + HO. = #.039 RO2-XN. + #.961 RO2-R. + .658 ACET +
                                   #.303 RCHO + #.116 -C + RO2.
2.56E-12  1.36E-12  -0.38  2.00  N-C4 + HO. = 0.076 RO2-N. + 0.924 RO2-R. + 0.397 R2O2. +
                                   0.001 HCHO + 0.571 CCHO + 0.14 RCHO + 0.533 MEK +
                                   -0.076 -C + 1.397 RO2.
4.11E-12  1.89E-12  -0.46  2.00  N-C5 + HO. = #.12 RO2-N. + #.88 RO2-R. + #.544 R2O2. +
                                   #.007 HCHO + #.08 CCHO + #.172 RCHO + #.929 MEK +
                                   #.001 -C + #1.544 RO2.
5.63E-12  1.35E-11   0.52  0.00  N-C6 + HO. = 0.185 RO2-N. + 0.815 RO2-R. + 0.738 R2O2. +
                                   0.02 CCHO + 0.105 RCHO + 1.134 MEK + 0.186 -C +
                                   1.738 RO2.
8.76E-12  3.15E-11   0.76  0.00  N-C8 + HO. = 0.333 RO2-N. + 0.667 RO2-R. + 0.706 R2O2. +
                                   0.002 RCHO + 1.333 MEK + 0.998 -C + 1.706 RO2.
1.02E-11  2.17E-11   0.45  0.00  N-C9 + HO. = #.373 RO2-N. + #.627 RO2-R. + #.673 R2O2. +
                                   #.001 RCHO + #1.299 MEK + #1.934 -C + #1.673 RO2.
1.17E-11  2.47E-11   0.45  0.00  N-C10 + HO. = #.397 RO2-N. + #.603 RO2-R. + #.659 R2O2. +
                                   #.001 RCHO + #1.261 MEK + #2.969 -C + #1.659 RO2.
1.33E-11  2.81E-11   0.45  0.00  N-C11 + HO. = #.411 RO2-N. + #.589 RO2-R. + #.654 R2O2. +
                                   #.001 RCHO + #1.241 MEK + #3.975 -C + #1.654 RO2.
1.43E-11  3.02E-11   0.45  0.00  N-C12 + HO. = #.42 RO2-N. + #.58 RO2-R. + #.644 R2O2. +
                                   #.001 RCHO + #1.223 MEK + #5.004 -C + #1.644 RO2.

2.36E-12  9.36E-13  -0.55  2.00  2-ME-C3 + HO. = #.027 RO2-N. + #.229 RO2-R. + #.744 R2O2. +
                                   #.229 HCHO + #.66 -C + RO2. + #.744 C2(C)-O.
3.95E-12  5.11E-12   0.15  0.00  2-ME-C4 + HO. = #.064 RO2-N. + #.002 RO2-XN. +
                                   #.933 RO2-R. + #.734 R2O2. + #.614 CCHO + #.611 ACET +
                                   #.133 RCHO + #.303 MEK + #.007 -C + #1.734 RO2.
8.63E-13  1.61E-12   0.37  2.00  22-DM-C3 + HO. = #.051 RO2-N. + #.949 RO2-R. + #.019 R2O2. +
                                   #.019 HCHO + #.01 ACET + #.939 RCHO + #1.878 -C +
                                   #1.019 RO2.
5.66E-12  8.21E-12   0.22  0.00  2-ME-C5 + HO. = #.122 RO2-N. + #.005 RO2-XN. +
                                   #.873 RO2-R. + #.749 R2O2. + #.006 HCHO + #.023 CCHO +
                                   #.223 ACET + #.545 RCHO + #.724 MEK + #.137 -C +
                                   #1.749 RO2.
5.76E-12  6.68E-12   0.09  0.00  3-ME-C5 + HO. = #.112 RO2-N. + #.888 RO2-R. + #.86 R2O2. +
                                   #.005 HCHO + #.523 CCHO + #.089 RCHO + #1.003 MEK +
                                   #.11 -C + #1.86 RO2.
2.36E-12  2.84E-11   1.48  0.00  22-DM-C4 + HO. = #.153 RO2-N. + #.847 RO2-R. + #.96 R2O2. +
                                   #.295 HCHO + #.303 CCHO + #.295 ACET + #.372 RCHO +
                                   #.542 MEK + #.164 -C + #1.96 RO2.
5.50E-12  4.59E-12  -0.11  0.00  23-DM-C4 + HO. = #.061 RO2-N. + #.039 RO2-XN. +
                                   #.901 RO2-R. + #.944 R2O2. + #1.584 ACET + #.128 RCHO +
                                   #.096 MEK + #.177 -C + #1.944 RO2.
```

Table A-2 (continued)

───

Rxn.	Kinetic Parameters [a]			
Label	k(300)	A	Ea	B

───

```
           Reactions [b]
```

───

```
6.87E-12  1.07E-11  0.26  0.00   2-ME-C6 + HO. = #.196 RO2-N. + #.803 RO2-R. + #.858 R2O2. +
                                   #.03 HCHO + #.037 CCHO + #.036 ACET + #.118 RCHO +
                                   #1.265 MEK + #.393 -C + #1.858 RO2.
7.24E-12  9.34E-12  0.15  0.00   3-ME-C6 + HO. = #.182 RO2-N. + #.002 RO2-XN. +
                                   #.815 RO2-R. + #.842 R2O2. + #.127 CCHO + #.329 RCHO +
                                   #1.119 MEK + #.369 -C + #1.842 RO2.
6.92E-12    (No T Dependence)    24-DM-C5 + HO. = #.131 RO2-N. + #.002 RO2-XN. +
                                   #.867 RO2-R. + #.844 R2O2. + #.257 ACET + #.772 RCHO +
                                   #.682 MEK + #.531 -C + #1.844 RO2.
7.29E-12  6.19E-12 -0.10  0.00   23-DM-C5 + HO. = #.128 RO2-N. + #.011 RO2-XN. +
                                   #.86 RO2-R. + #1.101 R2O2. + #.036 HCHO + #.253 CCHO +
                                   #.39 ACET + #.185 RCHO + #.96 MEK + #.252 -C + #2.101 RO2.
3.15E-12  1.39E-11  0.89  0.00   33-DM-C5 + HO. = #.231 RO2-N. + #.769 RO2-R. + #.94 R2O2. +
                                   #.04 HCHO + #.289 CCHO + #.145 ACET + #.237 RCHO +
                                   #.907 MEK + #.453 -C + #1.94 RO2.
4.24E-12  8.14E-13 -0.98  2.00   223TM-C4 + HO. = #.107 RO2-N. + #.893 RO2-R. +
                                   #1.581 R2O2. + #.637 HCHO + #1.291 ACET + #.255 RCHO +
                                   #.255 MEK + #.165 -C + #2.581 RO2.
8.29E-12  1.34E-11  0.29  0.00   2-ME-C7 + HO. = #.26 RO2-N. + #.74 RO2-R. + #.839 R2O2. +
                                   #.022 HCHO + #.025 CCHO + #.018 ACET + #.118 RCHO +
                                   #1.36 MEK + #.779 -C + #1.839 RO2.
8.65E-12  1.20E-11  0.19  0.00   3-ME-C7 + HO. = #.245 RO2-N. + #.755 RO2-R. + #.867 R2O2. +
                                   #.072 CCHO + #.066 RCHO + #1.425 MEK + #.733 -C +
                                   #1.867 RO2.
8.65E-12  1.20E-11  0.19  0.00   4-ME-C7 + HO. = #.244 RO2-N. + #.002 RO2-XN. +
                                   #.753 RO2-R. + #.803 R2O2. + #.352 RCHO + #1.204 MEK +
                                   #.906 -C + #1.803 RO2.
8.70E-12  8.50E-12 -0.01  0.00   23-DM-C6 + HO. = #.175 RO2-N. + #.008 RO2-XN. +
                                   #.817 RO2-R. + #1.051 R2O2. + #.006 HCHO + #.01 CCHO +
                                   #.125 ACET + #.241 RCHO + #1.363 MEK + #.548 -C +
                                   #2.051 RO2.
8.70E-12  8.50E-12 -0.01  0.00   24-DM-C6 + HO. = #.178 RO2-N. + #.822 RO2-R. + #.968 R2O2. +
                                   #.045 HCHO + #.122 CCHO + #.027 ACET + #.339 RCHO +
                                   #1.257 MEK + #.698 -C + #1.968 RO2.
8.33E-12  9.35E-12  0.07  0.00   25-DM-C6 + HO. = #.188 RO2-N. + #.812 RO2-R. +
                                   #1.731 R2O2. + #.422 HCHO + #.518 ACET + #.165 RCHO +
                                   #1.008 MEK + #.563 -C + #2.731 RO2.
3.72E-12  1.61E-11  0.87  0.00   224TM-C5 + HO. = #.11 RO2-N. + #.89 RO2-R. + #.89 RCHO +
                                   #1.11 MEK + #.34 -C + RO2.
8.74E-12  6.05E-12 -0.22  0.00   234TM-C5 + HO. = #.128 RO2-N. + #.016 RO2-XN. +
                                   #.855 RO2-R. + #1.312 R2O2. + #.066 HCHO + #.037 CCHO +
                                   #.518 ACET + #.332 RCHO + #1.075 MEK + #.368 -C +
                                   #2.312 RO2.
1.06E-11  1.29E-11  0.12  0.00   4-ET-C7 + HO. = #.271 RO2-N. + #.002 RO2-XN. +
                                   #.727 RO2-R. + #.804 R2O2. + #.002 HCHO + #.059 CCHO +
                                   #.303 RCHO + #1.167 MEK + #1.949 -C + #1.804 RO2.
1.01E-11  1.09E-11  0.05  0.00   24-DM-C7 + HO. = #.223 RO2-N. + #.001 RO2-XN. +
                                   #.776 RO2-R. + #.933 R2O2. + #.033 HCHO + #.02 CCHO +
                                   #.015 ACET + #.385 RCHO + #1.257 MEK + #1.586 -C +
                                   #1.933 RO2.
6.16E-12  1.00E-11  0.29  0.00   225TM-C6 + HO. = #.27 RO2-N. + #.73 RO2-R. + #1.081 R2O2. +
                                   #.039 HCHO + #.36 ACET + #.434 RCHO + #.977 MEK +
                                   #1.32 -C + #2.081 RO2.
1.20E-11  1.55E-11  0.15  0.00   4-PR-C7 + HO. = #.301 RO2-N. + #.002 RO2-XN. +
                                   #.696 RO2-R. + #.775 R2O2. + #.004 CCHO + #.328 RCHO +
                                   #1.139 MEK + #2.945 -C + #1.775 RO2.

5.19E-12  1.92E-12 -0.59  2.00   CYCC5 + HO. = #.127 RO2-N. + #.873 RO2-R. + #1.745 R2O2. +
                                   #.873 RCHO + #.218 MEK + #.873 CO + #2.745 RO2.
7.54E-12  2.39E-12 -0.68  2.00   CYCC6 + HO. = #.193 RO2-N. + #.807 RO2-R. + #.352 R2O2. +
                                   #.003 HCHO + #.333 RCHO + #.816 MEK + #.003 CO2 +
                                   #.765 -C + #1.352 RO2.
8.10E-12  1.25E-11  0.26  0.00   ME-CYCC5 + HO. = #.153 RO2-N. + #.847 RO2-R. +
                                   #1.978 R2O2. + #.283 HCHO + #.697 RCHO + #.49 MEK +
                                   #.564 CO + #.189 CO2 + #.153 -C + #2.978 RO2.
1.03E-11  1.34E-11  0.16  0.00   ME-CYCC6 + HO. = #.216 RO2-N. + #.784 RO2-R. + #.928 R2O2. +
                                   #.092 HCHO + #.001 CCHO + #.466 RCHO + #.987 MEK +
                                   #.003 CO + #.046 CO2 + #.432 -C + #1.928 RO2.
8.66E-12  9.53E-12  0.06  0.00   13DMCYC5 + HO. = #.16 RO2-N. + #.84 RO2-R. + #2.118 R2O2. +
                                   #.517 HCHO + #.478 RCHO + #.825 MEK + #.284 CO +
                                   #.344 CO2 + #.32 -C + #3.118 RO2.
```

Table A-2 (continued)

```
───────────────────────────────────────────────────────────────────────────────
Rxn.        Kinetic Parameters [a]
          ─────────────────────────────   Reactions [b]
Label  k(300)    A       Ea     B
───────────────────────────────────────────────────────────────────────────────

       8.97E-12  1.22E-11  0.18  0.00   ET-CYCC5 + HO. = #.207 RO2-N. + #.793 RO2-R. +
                                          #1.849 R2O2. + #.009 HCHO + #.34 CCHO + #.523 RCHO +
                                          #.674 MEK + #.336 CO + #.261 CO2 + #.41 -C + #2.849 RO2.
       1.23E-11  1.44E-11  0.09  0.00   ET-CYCC6 + HO. = #.265 RO2-N. + #.735 RO2-R. +
                                          #1.282 R2O2. + #.186 HCHO + #.293 CCHO + #.347 RCHO +
                                          #.811 MEK + #.01 CO + #.185 CO2 + #1.424 -C + #2.282 RO2.
       1.21E-11  1.16E-11 -0.03  0.00   13DMCYC6 + HO. = #.215 RO2-N. + #.785 RO2-R. +
                                          #1.386 R2O2. + #.17 HCHO + #.001 CCHO + #.499 RCHO +
                                          #1.131 MEK + #.002 CO + #.084 CO2 + #.646 -C + #2.386 RO2.

       8.43E-12  1.96E-12 -0.87  0.00   ETHENE + HO. = RO2-R. + RO2. + #1.56 HCHO + #.22 CCHO
       1.68E-18  9.14E-15  5.13  0.00   ETHENE + O3 = HCHO + (HCHO2)
       2.18E-16  4.39E-13  4.53  2.00   ETHENE + NO3 = R2O2. + RO2. + #2 HCHO + NO2
       7.42E-13  1.04E-11  1.57  0.00   ETHENE + O = RO2-R. + HO2. + RO2. + HCHO + CO
       2.60E-11  4.85E-12 -1.00  0.00   PROPENE + HO. = RO2-R. + RO2. + HCHO + CCHO
       1.05E-17  5.51E-15  3.73  0.00   PROPENE + O3 = #.6 HCHO + #.4 CCHO + #.4 (HCHO2) +
                                          #.6 (CCHO2)
       9.74E-15  4.59E-13  2.30  0.00   PROPENE + NO3 = R2O2. + RO2. + HCHO + CCHO + NO2
       4.01E-12  1.18E-11  0.64  0.00   PROPENE + O = #.4 HO2. + #.5 RCHO + #.5 MEK + #-0.5 -C
       3.11E-11  6.55E-12 -0.93  0.00   1-BUTENE + HO. = RO2-R. + RO2. + HCHO + RCHO
       1.00E-17  3.36E-15  3.47  0.00   1-BUTENE + O3 = #.6 HCHO + #.4 RCHO + #.4 (HCHO2) +
                                          #.6 (RCHO2)
       1.23E-14  2.04E-13  1.67  0.00   1-BUTENE + NO3 = R2O2. + RO2. + HCHO + RCHO + NO2
       4.22E-12  1.25E-11  0.65  0.00   1-BUTENE + O = #.4 HO2. + #.5 RCHO + #.5 MEK + #.5 -C
       6.30E-11  1.01E-11 -1.09  0.00   T-2-BUTE + HO. = RO2-R. + RO2. + #2 CCHO
       1.95E-16  6.64E-15  2.10  0.00   T-2-BUTE + O3 = CCHO + (CCHO2)
       3.92E-13  1.10E-13 -0.76  2.00   T-2-BUTE + NO3 = R2O2. + RO2. + #2 CCHO + NO2
       2.34E-11  2.26E-11 -0.02  0.00   T-2-BUTE + O = #.4 HO2. + #.5 RCHO + #.5 MEK + #.5 -C
       5.58E-11  1.10E-11 -0.97  0.00   C-2-BUTE + HO. = RO2-R. + RO2. + #2 CCHO
       1.28E-16  3.22E-15  1.92  0.00   C-2-BUTE + O3 = CCHO + (CCHO2)
       3.47E-13  9.71E-14 -0.76  2.00   C-2-BUTE + NO3 = R2O2. + RO2. + #2 CCHO + NO2
       1.80E-11  1.21E-11 -0.23  0.00   C-2-BUTE + O = #.4 HO2. + #.5 RCHO + #.5 MEK + #.5 -C
       3.14E-11  5.32E-12 -1.06  0.00   3M-1-BUT + HO. = #.84 RO2-R. + #.16 RO2-N. + RO2. +
                                          #.84 HCHO + #.84 RCHO + #.84 -C
       1.00E-17  3.36E-15  3.47  0.00   3M-1-BUT + O3 = #.6 HCHO + RCHO + #-0.2 -C + #.4 (HCHO2) +
                                          #.6 (CCHO2)
       1.23E-14  2.04E-13  1.67  0.00   3M-1-BUT + NO3 = R2O2. + RO2. + HCHO + RCHO + -C + NO2
       4.22E-12  1.25E-11  0.65  0.00   3M-1-BUT + O = #.4 HO2. + #.5 RCHO + #.5 MEK + #1.5 -C
       3.10E-11  5.80E-12 -1.00  0.00   1-PENTEN + HO. = #.84 RO2-R. + #.16 RO2-N. + RO2. +
                                          #.84 HCHO + #.84 RCHO + #.84 -C
       1.04E-17  3.36E-15  3.44  0.00   1-PENTEN + O3 = #.6 HCHO + RCHO + #-0.2 -C + #.4 (HCHO2) +
                                          #.6 (CCHO2)
       1.23E-14  2.04E-13  1.67  0.00   1-PENTEN + NO3 = R2O2. + RO2. + HCHO + RCHO + -C + NO2
       4.22E-12  1.25E-11  0.65  0.00   1-PENTEN + O = #.4 HO2. + #.5 RCHO + #.5 MEK + #1.5 -C
       3.66E-11  6.84E-12 -1.00  0.00   1-HEXENE + HO. = #.775 RO2-R. + #.225 RO2-N. + RO2. +
                                          #.775 HCHO + #.775 RCHO + #1.775 -C
       1.14E-17  3.36E-15  3.39  0.00   1-HEXENE + O3 = #.6 HCHO + RCHO + #.8 -C + #.4 (HCHO2) +
                                          #.6 (CCHO2)
       1.23E-14  2.04E-13  1.67  0.00   1-HEXENE + NO3 = R2O2. + RO2. + HCHO + RCHO + #2 -C + NO2
       4.22E-12  1.25E-11  0.65  0.00   1-HEXENE + O = #.4 HO2. + #.5 RCHO + #.5 MEK + #2.5 -C
       3.66E-11  6.84E-12 -1.00  0.00   1-C7-OLE + HO. = #.73 RO2-R. + #.27 RO2-N. + RO2. +
                                          #.73 HCHO + #.73 RCHO + #2.73 -C
       1.14E-17  3.36E-15  3.39  0.00   1-C7-OLE + O3 = #.6 HCHO + RCHO + #1.8 -C + #.4 (HCHO2) +
                                          #.6 (CCHO2)
       1.30E-14  6.55E-12  3.71  0.00   1-C7-OLE + NO3 = R2O2. + RO2. + HCHO + RCHO + #3 -C + NO2
       4.22E-12  1.25E-11  0.65  0.00   1-C7-OLE + O = #.4 HO2. + #.5 RCHO + #.5 MEK + #3.5 -C
       3.66E-11  6.84E-12 -1.00  0.00   1-C8-OLE + HO. = #.67 RO2-R. + #.33 RO2-N. + RO2. +
                                          #.67 HCHO + #.67 RCHO + #3.67 -C
       1.14E-17  3.36E-15  3.39  0.00   1-C8-OLE + O3 = #.6 HCHO + RCHO + #2.8 -C + #.4 (HCHO2) +
                                          #.6 (CCHO2)
       1.30E-14  6.55E-12  3.71  0.00   1-C8-OLE + NO3 = R2O2. + RO2. + HCHO + RCHO + #4 -C + NO2
       4.22E-12  1.25E-11  0.65  0.00   1-C8-OLE + O = #.4 HO2. + #.5 RCHO + #.5 MEK + #4.5 -C
       3.66E-11  6.84E-12 -1.00  0.00   1-C9-OLE + HO. = #.63 RO2-R. + #.37 RO2-N. + RO2. +
                                          #.63 HCHO + #.63 RCHO + #4.63 -C
       1.14E-17  3.36E-15  3.39  0.00   1-C9-OLE + O3 = #.6 HCHO + RCHO + #3.8 -C + #.4 (HCHO2) +
                                          #.6 (CCHO2)
       1.30E-14  6.55E-12  3.71  0.00   1-C9-OLE + NO3 = R2O2. + RO2. + HCHO + RCHO + #5 -C + NO2
       4.22E-12  1.25E-11  0.65  0.00   1-C9-OLE + O = #.4 HO2. + #.5 RCHO + #.5 MEK + #5.5 -C
       5.09E-11  9.47E-12 -1.00  0.00   ISOBUTEN + HO. = #.9 RO2-R. + #.1 RO2-N. + RO2. + #.9 HCHO +
                                          #.9 ACET + #-0.1 -C
       1.17E-17  2.70E-15  3.24  0.00   ISOBUTEN + O3 = #.82 HCHO + #.18 ACET + #.18 (HCHO2) +
                                          #.82 (C(C)CO2)
```

Table A-2 (continued)

```
──────────────────────────────────────────────────────────────────────────────
Rxn.        Kinetic Parameters [a]
            ───────────────────────────    Reactions [b]
Label  k(300)     A       Ea     B
──────────────────────────────────────────────────────────────────────────────

       3.32E-13   (No T Dependence)    ISOBUTEN + NO3 = R2O2. + RO2. + HCHO + ACET + NO2
       1.53E-11  1.76E-11   0.09  0.00  ISOBUTEN + O = #.4 HO2. + #.5 RCHO + #.5 MEK + .5 -C
       5.99E-11  1.12E-11  -1.00  0.00  2M-1-BUT + HO. = #.9 RO2-R. + #.1 RO2-N. + RO2. + #.9 HCHO +
                                          #.9 MEK
       1.17E-17  2.70E-15   3.24  0.00  2M-1-BUT + O3 = #.82 HCHO + MEK + #-2.46 -C + #.18 (HCHO2) +
                                          #.82 (C(C)CO2)
       3.32E-13   (No T Dependence)    2M-1-BUT + NO3 = R2O2. + RO2. + HCHO + MEK + NO2
       1.53E-11  1.76E-11   0.09  0.00  2M-1-BUT + O = #.4 HO2. + #.5 RCHO + #.5 MEK + #1.5 -C
       8.60E-11  1.92E-11  -0.89  0.00  2M-2-BUT + HO. = #.84 RO2-R. + #.16 RO2-N. + RO2. +
                                          #.84 CCHO + #.84 ACET
       4.11E-16  6.51E-15   1.65  0.00  2M-2-BUT + O3 = #.6 CCHO + #.4 ACET + #.4 (CCHO2) +
                                          #.6 (C(C)CO2)
       9.37E-12   (No T Dependence)    2M-2-BUT + NO3 = R2O2. + RO2. + CCHO + ACET + NO2
       4.73E-11  2.50E-11  -0.38  0.00  2M-2-BUT + O = #.4 HO2. + #.5 RCHO + #.5 MEK + #1.5 -C
       6.56E-11  1.22E-11  -1.00  0.00  2-C5-OLE + HO. = #.84 RO2-R. + #.16 RO2-N. + RO2. +
                                          #.84 CCHO + #.84 RCHO
       2.68E-16  7.68E-15   2.00  0.00  2-C5-OLE + O3 = #.5 CCHO + #.5 RCHO + #.5 (CCHO2) +
                                          #.5 (RCHO2)
       3.92E-13  1.10E-13  -0.76  2.00  2-C5-OLE + NO3 = R2O2. + RO2. + CCHO + RCHO + NO2
       3.00E-11   (No T Dependence)    2-C5-OLE + O = #.4 HO2. + #.5 RCHO + #.5 MEK + #1.5 -C
       6.56E-11  1.22E-11  -1.00  0.00  2-C6-OLE + HO. = #.775 RO2-R. + #.225 RO2-N. + RO2. +
                                          #.775 CCHO + #.775 RCHO + -C
       2.68E-16  7.68E-15   2.00  0.00  2-C6-OLE + O3 = #.5 CCHO + #.5 RCHO + -C + #.5 (CCHO2) +
                                          #.5 (RCHO2)
       3.92E-13  1.10E-13  -0.76  2.00  2-C6-OLE + NO3 = R2O2. + RO2. + CCHO + RCHO + -C + NO2
       3.00E-11   (No T Dependence)    2-C6-OLE + O = #.4 HO2. + #.5 RCHO + #.5 MEK + #2.5 -C
       6.56E-11  1.22E-11  -1.00  0.00  2-C7-OLE + HO. = #.73 RO2-R. + #.27 RO2-N. + RO2. +
                                          #.73 CCHO + #.73 RCHO + #2 -C
       2.68E-16  7.68E-15   2.00  0.00  2-C7-OLE + O3 = #.5 CCHO + #.5 RCHO + #2 -C + #.5 (CCHO2) +
                                          #.5 (RCHO2)
       3.92E-13  1.10E-13  -0.76  2.00  2-C7-OLE + NO3 = R2O2. + RO2. + CCHO + RCHO + #2 -C + NO2
       3.00E-11   (No T Dependence)    2-C7-OLE + O = #.4 HO2. + #.5 RCHO + #.5 MEK + #3.5 -C
       6.56E-11  1.22E-11  -1.00  0.00  3-C8-OLE + HO. = #.67 RO2-R. + #.33 RO2-N. + RO2. +
                                          #1.34 RCHO + #2.33 -C
       2.68E-16  7.68E-15   2.00  0.00  3-C8-OLE + O3 = RCHO + #2 -C + (RCHO2)
       3.92E-13  1.10E-13  -0.76  2.00  3-C8-OLE + NO3 = R2O2. + RO2. + #2 RCHO + #2 -C + NO2
       3.00E-11   (No T Dependence)    3-C8-OLE + O = #.4 HO2. + #.5 RCHO + #.5 MEK + #4.5 -C
       6.59E-11  1.48E-11  -0.89  0.00  13-BUTDE + HO. = RO2-R. + RO2. + HCHO + RCHO
       6.64E-18  1.34E-14   4.54  0.00  13-BUTDE + O3 = #.6 HCHO + RCHO + #-1.2 -C + #.4 (HCHO2) +
                                          #.6 (CCHO2)
       1.00E-13   (No T Dependence)    13-BUTDE + NO3 = R2O2. + RO2. + HCHO + RCHO + NO2
       2.10E-11   (No T Dependence)    13-BUTDE + O = #.4 HO2. + #.5 RCHO + #.5 MEK + #.5 -C
       6.64E-11  1.24E-11  -1.00  0.00  CYC-PNTE + HO. = #.85 RO2-R. + #.15 RO2-N. + RO2. +
                                          #.85 RCHO + #1.7 -C
       6.43E-16  1.62E-14   1.92  0.00  CYC-PNTE + O3 = #2 -C + (RCHO2)
       3.58E-13  1.10E-11   2.04  0.00  CYC-PNTE + NO3 = R2O2. + RO2. + RCHO + #2 -C + NO2
       2.40E-11   (No T Dependence)    CYC-PNTE + O = #.4 HO2. + #.5 RCHO + #.5 MEK + #1.5 -C
       6.69E-11  1.25E-11  -1.00  0.00  CYC-HEXE + HO. = #.85 RO2-R. + #.15 RO2-N. + RO2. +
                                          #.85 RCHO + #2.7 -C
       7.38E-17  1.86E-15   1.92  0.00  CYC-HEXE + O3 = #3 -C + (RCHO2)
       3.47E-13  9.71E-14  -0.76  2.00  CYC-HEXE + NO3 = R2O2. + RO2. + RCHO + #3 -C + NO2
       2.20E-11   (No T Dependence)    CYC-HEXE + O = #.4 HO2. + #.5 RCHO + #.5 MEK + #2.5 -C

       9.88E-11  2.54E-11  -0.81  0.00  ISOP + HO. = 0.088 RO2-N. + 0.912 RO2-R. + 0.629 HCHO +
                                          0.912 ISOPROD + 0.079 R2O2. + 1.079 RO2. + 0.283 -C
       1.34E-17  7.86E-15   3.80  0.00  ISOP + O3 = 0.4 HCHO + 0.6 ISOPROD + 0.55 (HCHO2) +
                                          0.2 (C:CC(C)O2) + 0.2 (C:C(C)CHO2) + 0.05 -C
       3.60E-11   (No T Dependence)    ISOP + O = 0.75 "ISOPROD + -C "+ 0.25 "C2CO-O2. + RCO3. +
                                          2 HCHO + RO2-R. + RO2."
       6.81E-13  3.03E-12   0.89  0.00  ISOP + NO3 = 0.8 "RCHO + RNO3 + RO2-R." + 0.2 "ISOPROD +
                                          R2O2. + NO2" + RO2. + -2.2 -C
       1.50E-19   (No T Dependence)    ISOP + NO2 = 0.8 "RCHO + RNO3 + RO2-R." + 0.2 "ISOPROD +
                                          R2O2. + NO" + RO2. + -2.2 -C

       1.28E-12  2.50E-12   0.40  0.00  BENZENE + HO. = #.236 PHEN + #.207 GLY + #1.75 AFG1 +
                                          #.764 RO2-R. + #.236 HO2. + #.67 -C + #.764 RO2.
       5.91E-12  1.81E-12  -0.70  0.00  TOLUENE + HO. = #.085 BALD + #.26 CRES + #.118 GLY +
                                          #.131 MGLY + #.49 AFG2 + #.74 RO2-R. + #.26 HO2. +
                                          #2.486 -C + #.74 RO2.
       7.10E-12   (No T Dependence)    C2-BENZ + HO. = #.085 BALD + #.26 CRES + #.118 GLY +
                                          #.131 MGLY + #.49 AFG2 + #.74 RO2-R. + #.26 HO2. +
                                          #3.486 -C + #.74 RO2.
```

A-12

Table A-2 (continued)

_____

Rxn.   Kinetic Parameters [a]
        _____   Reactions [b]
Label   k(300)   A   Ea   B
_____

```
        6.50E-12   (No T Dependence)     I-C3-BEN + HO. = #.085 BALD + #.26 CRES + #.118 GLY +
                                             #.131 MGLY + #.49 AFG2 + #.74 RO2-R. + #.26 HO2. +
                                             #4.486 -C + #.74 RO2.
        6.00E-12   (No T Dependence)     N-C3-BEN + HO. = #.085 BALD + #.26 CRES + #.118 GLY +
                                             #.131 MGLY + #.49 AFG2 + #.74 RO2-R. + #.26 HO2. +
                                             #4.486 -C + #.74 RO2.
        2.36E-11   (No T Dependence)     M-XYLENE + HO. = #.04 BALD + #.18 CRES + #.108 GLY +
                                             #.37 MGLY + #.75 AFG2 + #.82 RO2-R. + #.18 HO2. +
                                             #2.884 -C + #.82 RO2.
        1.37E-11   (No T Dependence)     O-XYLENE + HO. = #.04 BALD + #.18 CRES + #.108 GLY +
                                             #.37 MGLY + #.75 AFG2 + #.82 RO2-R. + #.18 HO2. +
                                             #2.884 -C + #.82 RO2.
        1.43E-11   (No T Dependence)     P-XYLENE + HO. = #.04 BALD + #.18 CRES + #.108 GLY +
                                             #.37 MGLY + #.75 AFG2 + #.82 RO2-R. + #.18 HO2. +
                                             #2.884 -C + #.82 RO2.
        5.75E-11   (No T Dependence)     135-TMB + HO. = #.03 BALD + #.18 CRES + #.62 MGLY +
                                             #.75 AFG2 + #.82 RO2-R. + #.18 HO2. + #3.42 -C + #.82 RO2.
        3.27E-11   (No T Dependence)     123-TMB + HO. = #.03 BALD + #.18 CRES + #.62 MGLY +
                                             #.75 AFG2 + #.82 RO2-R. + #.18 HO2. + #3.42 -C + #.82 RO2.
        3.25E-11   (No T Dependence)     124-TMB + HO. = #.03 BALD + #.18 CRES + #.62 MGLY +
                                             #.75 AFG2 + #.82 RO2-R. + #.18 HO2. + #3.42 -C + #.82 RO2.
        2.16E-11   (No T Dependence)     NAPHTHAL + HO. = #.17 PHEN + #.14 RO2-NP. + #.32 AFG1 +
                                             #.69 RO2-R. + #.17 HO2. + #7.5 -C + #.83 RO2.
        7.70E-11   (No T Dependence)     23-DMN + HO. = #.04 CRES + #.49 MGLY + #.16 RO2-NP. +
                                             #.85 AFG1 + #.8 RO2-R. + #.04 HO2. + #7.59 -C + #.96 RO2.
        5.20E-11   (No T Dependence)     ME-NAPH + HO. = #.085 PHEN + #.02 CRES + #.245 MGLY +
                                             #.15 RO2-NP. + #.585 AFG1 + #.745 RO2-R. + #.105 HO2. +
                                             #7.545 -C + #.895 RO2.
        3.43E-11   (No T Dependence)     TETRALIN + HO. = #.09 PHEN + #.12 RO2-NP. + #.164 AFG1 +
                                             #.79 RO2-R. + #.09 HO2. + #8.412 -C + #.91 RO2.
        5.73E-11  1.07E-11 -1.00  0.00   STYRENE + HO. = #.9 RO2-R. + #.1 RO2-N. + RO2. + #.9 HCHO +
                                             #.9 BALD + #.3 -C
        1.77E-17  3.36E-15  3.13  0.00   STYRENE + O3 = #.6 HCHO + #.4 BALD + #2.8 -C + #.4 (HCHO2) +
                                             #.6 (BZCHO2)
        1.50E-13   (No T Dependence)     STYRENE + NO3 = R2O2. + RO2. + HCHO + BALD + NO2
        1.80E-11  1.21E-11 -0.23  0.00   STYRENE + O = #.4 HO2. + #.5 RCHO + #.5 MEK + #4.5 -C

        8.18E-13  5.03E-12  1.08  0.00   ACETYLEN + HO. = #.15 RO2-R. + #.3 HO2. + #.3 CO + #1.7 -C +
                                             #.55 HO. + #.7 GLY2 + #.15 RO2.
        6.06E-12   (No T Dependence)     ME-ACTYL + HO. = RO2-R. + RCHO + RO2.

        9.42E-13  5.75E-13 -0.29  2.00   MEOH + HO. = HO2. + HCHO

        2.84E-12  6.13E-13 -0.91  2.00   MTBE + HO. = #.02 RO2-N. + #.98 RO2-R. + #.37 R2O2. +
                                             #.39 HCHO + #.41 MEK + #2.87 -C + #1.37 RO2.
        7.50E-12   (No T Dependence)     ETBE + HO. = #.03 RO2-N. + #.97 RO2-R. + #1.16 R2O2. +
                                             #1.16 HCHO + #.57 MEK + #2.41 -C + #2.16 RO2.
```

Reactions used to Represent Chamber-Dependent Processes [c]

```
O3W    (varied)  (No T Dependence)     O3 =
N25I   (varied)  (No T Dependence)     N2O5 = 2 NOX-WALL
N25S   (varied)  (No T Dependence)     N2O5 + H2O = 2 NOX-WALL
NO2W   (varied)  (No T Dependence)     NO2 = (yHONO) HONO + (1-yHONO) NOX-WALL
XSHC   (varied)  (No T Dependence)     HO. = HO2.
RSI      (Phot. Set = NO2    )         HV + #RS/K1 = HO.
ONO2     (Phot. Set = NO2    )         HV + #E-NO2/K1 = NO2 + #-1 NOX-WALL
```

_____

[a] Except as noted, the expression for the rate constant is $k = A \, e^{Ea/RT} (T/300)^B$. Rate constants and
     A factor are in cm, molecule, sec. units. Units of Ea is kcal mole^{-1}. "Phot Set" means this is
     a photolysis reaction, with the absorption coefficients and quantum yields given in Table A-3. In
     addition, if "#(number)" or "#(parameter)" is given as a reactant, then the value of that number
     or parameter is multiplied by the result in the "rate constant expression" columns to obtain the
     rate constant used. Furthermore, "#RCONnn" as a reactant means that the rate constant for the
     reaction is obtained by multiplying the rate constant given by that for reaction "nn". Thus, the
     rate constant given is actually an equilibrium constant.
[b] The format of the reaction listing is the same as that used in the documentation of the detailed
     mechanism (Carter 1990).
[c] See Table A-4 for the values of the parameters used for the specific chambers modeled in this study.

Table A-3.   Absorption cross sections and quantum yields for photolysis reactions.

WL (nm)	Abs (cm²)	QY	WL (nm)	Abs (cm²)	QY	WL (nm)	Abs (cm²)	QY	WL (nm)	Abs (cm²)	QY	WL (nm)	Abs (cm²)	QY

Photolysis File = NO2

WL (nm)	Abs (cm²)	QY	WL (nm)	Abs (cm²)	QY	WL (nm)	Abs (cm²)	QY	WL (nm)	Abs (cm²)	QY	WL (nm)	Abs (cm²)	QY
250.0	2.83E-20	1.000	255.0	1.45E-20	1.000	260.0	1.90E-20	1.000	265.0	2.05E-20	1.000	270.0	3.13E-20	1.000
275.0	4.02E-20	1.000	280.0	5.54E-20	1.000	285.0	6.99E-20	1.000	290.0	8.18E-20	0.999	295.0	9.67E-20	0.998
300.0	1.17E-19	0.997	305.0	1.66E-19	0.996	310.0	1.76E-19	0.995	315.0	2.25E-19	0.994	320.0	2.54E-19	0.993
325.0	2.79E-19	0.992	330.0	2.99E-19	0.991	335.0	3.45E-19	0.990	340.0	3.88E-19	0.989	345.0	4.07E-19	0.988
350.0	4.10E-19	0.987	355.0	5.13E-19	0.986	360.0	4.51E-19	0.984	365.0	5.78E-19	0.983	370.0	5.42E-19	0.981
375.0	5.35E-19	0.979	380.0	5.99E-19	0.975	381.0	5.98E-19	0.974	382.0	5.97E-19	0.973	383.0	5.96E-19	0.972
384.0	5.95E-19	0.971	385.0	5.94E-19	0.969	386.0	5.95E-19	0.967	387.0	5.96E-19	0.966	388.0	5.98E-19	0.964
389.0	5.99E-19	0.962	390.0	6.00E-19	0.960	391.0	5.98E-19	0.959	392.0	5.96E-19	0.957	393.0	5.93E-19	0.953
394.0	5.91E-19	0.950	395.0	5.89E-19	0.942	396.0	6.06E-19	0.922	397.0	6.24E-19	0.870	398.0	6.41E-19	0.820
399.0	6.59E-19	0.760	400.0	6.76E-19	0.695	401.0	6.67E-19	0.635	402.0	6.58E-19	0.560	403.0	6.50E-19	0.485
404.0	6.41E-19	0.425	405.0	6.32E-19	0.350	406.0	6.21E-19	0.290	407.0	6.10E-19	0.225	408.0	5.99E-19	0.185
409.0	5.88E-19	0.153	410.0	5.77E-19	0.130	411.0	5.88E-19	0.110	412.0	5.98E-19	0.094	413.0	6.09E-19	0.083
414.0	6.19E-19	0.070	415.0	6.30E-19	0.059	416.0	6.29E-19	0.048	417.0	6.27E-19	0.039	418.0	6.26E-19	0.030
419.0	6.24E-19	0.023	420.0	6.23E-19	0.018	421.0	6.18E-19	0.012	422.0	6.14E-19	0.008	423.0	6.09E-19	0.004
424.0	6.05E-19	0.000	425.0	6.00E-19	0.000									

Photolysis File = NO3NO

WL (nm)	Abs (cm²)	QY	WL (nm)	Abs (cm²)	QY	WL (nm)	Abs (cm²)	QY	WL (nm)	Abs (cm²)	QY	WL (nm)	Abs (cm²)	QY
585.0	2.77E-18	0.000	590.0	5.14E-18	0.250	595.0	4.08E-18	0.400	600.0	2.83E-18	0.250	605.0	3.45E-18	0.200
610.0	1.48E-18	0.200	615.0	1.96E-18	0.100	620.0	3.58E-18	0.100	625.0	9.25E-18	0.050	630.0	5.66E-18	0.050
635.0	1.45E-18	0.030	640.0	1.11E-18	0.000									

Photolysis File = NO3NO2

WL (nm)	Abs (cm²)	QY	WL (nm)	Abs (cm²)	QY	WL (nm)	Abs (cm²)	QY	WL (nm)	Abs (cm²)	QY	WL (nm)	Abs (cm²)	QY
400.0	0.00E+00	1.000	405.0	3.00E-20	1.000	410.0	4.00E-20	1.000	415.0	5.00E-20	1.000	420.0	8.00E-20	1.000
425.0	1.00E-19	1.000	430.0	1.30E-19	1.000	435.0	1.80E-19	1.000	440.0	1.90E-19	1.000	445.0	2.20E-19	1.000
450.0	2.80E-19	1.000	455.0	3.30E-19	1.000	460.0	3.70E-19	1.000	465.0	4.30E-19	1.000	470.0	5.10E-19	1.000
475.0	6.00E-19	1.000	480.0	6.40E-19	1.000	485.0	6.90E-19	1.000	490.0	8.80E-19	1.000	495.0	9.50E-19	1.000
500.0	1.01E-18	1.000	505.0	1.10E-18	1.000	510.0	1.32E-18	1.000	515.0	1.40E-18	1.000	520.0	1.45E-18	1.000
525.0	1.48E-18	1.000	530.0	1.94E-18	1.000	535.0	2.04E-18	1.000	540.0	1.81E-18	1.000	545.0	1.81E-18	1.000
550.0	2.36E-18	1.000	555.0	2.68E-18	1.000	560.0	3.07E-18	1.000	565.0	2.53E-18	1.000	570.0	2.54E-18	1.000
575.0	2.74E-18	1.000	580.0	3.05E-18	1.000	585.0	2.77E-18	1.000	590.0	5.14E-18	0.750	595.0	4.08E-18	0.600
600.0	2.83E-18	0.550	605.0	3.45E-18	0.400	610.0	1.45E-18	0.300	615.0	1.96E-18	0.250	620.0	3.58E-18	0.200
625.0	9.25E-18	0.150	630.0	5.66E-18	0.050	635.0	1.45E-18	0.000						

Photolysis File = O3O3P

WL (nm)	Abs (cm²)	QY	WL (nm)	Abs (cm²)	QY	WL (nm)	Abs (cm²)	QY	WL (nm)	Abs (cm²)	QY	WL (nm)	Abs (cm²)	QY
280.0	3.97E-18	0.100	281.0	3.60E-18	0.100	282.0	3.24E-18	0.100	283.0	3.01E-18	0.100	284.0	2.73E-18	0.100
285.0	2.44E-18	0.100	286.0	2.21E-18	0.100	287.0	2.01E-18	0.100	288.0	1.76E-18	0.100	289.0	1.58E-18	0.100
290.0	1.41E-18	0.100	291.0	1.26E-18	0.100	292.0	1.10E-18	0.100	293.0	9.89E-19	0.100	294.0	8.59E-19	0.100
295.0	7.70E-19	0.100	296.0	6.67E-19	0.100	297.0	5.84E-19	0.100	298.0	5.07E-19	0.100	299.0	4.52E-19	0.100
300.0	3.92E-19	0.100	301.0	3.42E-19	0.100	302.0	3.06E-19	0.100	303.0	2.60E-19	0.100	304.0	2.37E-19	0.100
305.0	2.01E-19	0.112	306.0	1.79E-19	0.149	307.0	1.56E-19	0.197	308.0	1.38E-19	0.259	309.0	1.25E-19	0.339
310.0	1.02E-19	0.437	311.0	9.17E-20	0.546	312.0	7.88E-20	0.652	313.0	6.77E-20	0.743	314.0	6.35E-20	0.816
315.0	5.10E-20	0.872	316.0	4.61E-20	0.916	317.0	4.17E-20	0.949	318.0	3.72E-20	0.976	319.0	2.69E-20	0.997
320.0	3.23E-20	1.000	330.0	6.70E-21	1.000	340.0	1.70E-21	1.000	350.0	4.00E-22	1.000	355.0	0.00E+00	1.000
400.0	0.00E+00	1.000	450.0	1.60E-22	1.000	500.0	1.34E-21	1.000	550.0	3.32E-21	1.000	600.0	5.06E-21	1.000
650.0	2.45E-21	1.000	700.0	8.70E-22	1.000	750.0	3.20E-22	1.000	800.0	1.60E-22	1.000	900.0	0.00E+00	1.000

Photolysis File = O3O1D

WL (nm)	Abs (cm²)	QY	WL (nm)	Abs (cm²)	QY	WL (nm)	Abs (cm²)	QY	WL (nm)	Abs (cm²)	QY	WL (nm)	Abs (cm²)	QY
280.0	3.97E-18	0.900	281.0	3.60E-18	0.900	282.0	3.24E-18	0.900	283.0	3.01E-18	0.900	284.0	2.73E-18	0.900
285.0	2.44E-18	0.900	286.0	2.21E-18	0.900	287.0	2.01E-18	0.900	288.0	1.76E-18	0.900	289.0	1.58E-18	0.900
290.0	1.41E-18	0.900	291.0	1.26E-18	0.900	292.0	1.10E-18	0.900	293.0	9.89E-19	0.900	294.0	8.59E-19	0.900
295.0	7.70E-19	0.900	296.0	6.67E-19	0.900	297.0	5.84E-19	0.900	298.0	5.07E-19	0.900	299.0	4.52E-19	0.900
300.0	3.92E-19	0.900	301.0	3.42E-19	0.900	302.0	3.06E-19	0.900	303.0	2.60E-19	0.900	304.0	2.37E-19	0.900
305.0	2.01E-19	0.888	306.0	1.79E-19	0.851	307.0	1.56E-19	0.803	308.0	1.38E-19	0.741	309.0	1.25E-19	0.661
310.0	1.02E-19	0.563	311.0	9.17E-20	0.454	312.0	7.88E-20	0.348	313.0	6.77E-20	0.257	314.0	6.35E-20	0.184
315.0	5.10E-20	0.128	316.0	4.61E-20	0.084	317.0	4.17E-20	0.051	318.0	3.72E-20	0.024	319.0	2.69E-20	0.003
320.0	3.23E-20	0.000												

Photolysis File = HONO

WL (nm)	Abs (cm²)	QY	WL (nm)	Abs (cm²)	QY	WL (nm)	Abs (cm²)	QY	WL (nm)	Abs (cm²)	QY	WL (nm)	Abs (cm²)	QY
311.0	0.00E+00	1.000	312.0	2.00E-21	1.000	313.0	4.20E-21	1.000	314.0	4.60E-21	1.000	315.0	4.20E-21	1.000
316.0	3.00E-21	1.000	317.0	4.60E-21	1.000	318.0	3.60E-20	1.000	319.0	6.10E-20	1.000	320.0	2.10E-20	1.000
321.0	4.27E-20	1.000	322.0	4.01E-20	1.000	323.0	3.93E-20	1.000	324.0	4.01E-20	1.000	325.0	4.04E-20	1.000
326.0	3.13E-20	1.000	327.0	4.12E-20	1.000	328.0	7.55E-20	1.000	329.0	6.64E-20	1.000	330.0	7.29E-20	1.000
331.0	8.70E-20	1.000	332.0	1.38E-19	1.000	333.0	5.91E-20	1.000	334.0	5.91E-20	1.000	335.0	6.45E-20	1.000
336.0	5.91E-20	1.000	337.0	4.58E-20	1.000	338.0	1.91E-19	1.000	339.0	1.63E-19	1.000	340.0	1.05E-19	1.000
341.0	8.70E-20	1.000	342.0	3.35E-19	1.000	343.0	2.01E-19	1.000	344.0	1.02E-19	1.000	345.0	8.54E-20	1.000
346.0	8.32E-20	1.000	347.0	8.20E-20	1.000	348.0	7.49E-20	1.000	349.0	7.13E-20	1.000	350.0	6.83E-20	1.000
351.0	1.74E-19	1.000	352.0	1.14E-19	1.000	353.0	3.71E-19	1.000	354.0	4.96E-19	1.000	355.0	2.46E-19	1.000
356.0	1.19E-19	1.000	357.0	9.35E-20	1.000	358.0	7.78E-20	1.000	359.0	7.29E-20	1.000	360.0	6.83E-20	1.000
361.0	6.90E-20	1.000	362.0	7.32E-20	1.000	363.0	9.00E-20	1.000	364.0	1.21E-19	1.000	365.0	1.33E-19	1.000
366.0	2.13E-19	1.000	367.0	3.52E-19	1.000	368.0	4.50E-19	1.000	369.0	2.93E-19	1.000	370.0	1.19E-19	1.000
371.0	9.46E-20	1.000	372.0	8.85E-20	1.000	373.0	7.44E-20	1.000	374.0	4.77E-20	1.000	375.0	2.70E-20	1.000
376.0	1.90E-20	1.000	377.0	1.50E-20	1.000	378.0	1.90E-20	1.000	379.0	5.80E-20	1.000	380.0	7.78E-20	1.000
381.0	1.14E-19	1.000	382.0	1.40E-19	1.000	383.0	1.72E-19	1.000	384.0	1.99E-19	1.000	385.0	1.90E-19	1.000
386.0	1.19E-19	1.000	387.0	5.65E-20	1.000	388.0	3.20E-20	1.000	389.0	1.90E-20	1.000	390.0	1.20E-20	1.000
391.0	5.00E-21	1.000	392.0	0.00E+00	1.000									

Photolysis File = H2O2

WL (nm)	Abs (cm²)	QY	WL (nm)	Abs (cm²)	QY	WL (nm)	Abs (cm²)	QY	WL (nm)	Abs (cm²)	QY	WL (nm)	Abs (cm²)	QY
250.0	8.30E-20	1.000	255.0	6.70E-20	1.000	260.0	5.20E-20	1.000	265.0	4.20E-20	1.000	270.0	3.20E-20	1.000
275.0	2.50E-20	1.000	280.0	2.00E-20	1.000	285.0	1.50E-20	1.000	290.0	1.13E-20	1.000	295.0	8.70E-21	1.000
300.0	6.60E-21	1.000	305.0	4.90E-21	1.000	310.0	3.70E-21	1.000	315.0	2.80E-21	1.000	320.0	2.00E-21	1.000
325.0	1.50E-21	1.000	330.0	1.20E-21	1.000	335.0	9.00E-22	1.000	340.0	7.00E-22	1.000	345.0	5.00E-22	1.000
350.0	3.00E-22	1.000	355.0	0.00E+00	1.000									

Table A-3. (continued)

WL (nm)	Abs (cm^2)	QY	WL (nm)	Abs (cm^2)	QY	WL (nm)	Abs (cm^2)	QY	WL (nm)	Abs (cm^2)	QY	WL (nm)	Abs (cm^2)	QY

Photolysis File = CO2H

WL (nm)	Abs (cm^2)	QY	WL (nm)	Abs (cm^2)	QY	WL (nm)	Abs (cm^2)	QY	WL (nm)	Abs (cm^2)	QY	WL (nm)	Abs (cm^2)	QY
210.0	3.75E-19	1.000	220.0	2.20E-19	1.000	230.0	1.38E-19	1.000	240.0	8.80E-20	1.000	250.0	5.80E-20	1.000
260.0	3.80E-20	1.000	270.0	2.50E-20	1.000	280.0	1.50E-20	1.000	290.0	9.00E-21	1.000	300.0	5.80E-21	1.000
310.0	3.40E-21	1.000	320.0	1.90E-21	1.000	330.0	1.10E-21	1.000	340.0	6.00E-22	1.000	350.0	4.00E-22	1.000
360.0	0.00E+00	1.000												

Photolysis File = HCHONEWR

WL (nm)	Abs (cm^2)	QY	WL (nm)	Abs (cm^2)	QY	WL (nm)	Abs (cm^2)	QY	WL (nm)	Abs (cm^2)	QY	WL (nm)	Abs (cm^2)	QY
280.0	2.49E-20	0.590	280.5	1.42E-20	0.596	281.0	1.51E-20	0.602	281.5	1.32E-20	0.608	282.0	9.73E-21	0.614
282.5	6.76E-21	0.620	283.0	5.82E-21	0.626	283.5	9.10E-21	0.632	284.0	3.71E-20	0.638	284.5	4.81E-20	0.644
285.0	3.95E-20	0.650	285.5	2.87E-20	0.656	286.0	2.24E-20	0.662	286.5	1.74E-20	0.668	287.0	1.13E-20	0.674
287.5	1.10E-20	0.680	288.0	2.62E-20	0.686	288.5	4.00E-20	0.692	289.0	3.55E-20	0.698	289.5	2.12E-20	0.704
290.0	1.07E-20	0.710	290.5	1.35E-20	0.713	291.0	1.99E-20	0.717	291.5	1.56E-20	0.721	292.0	8.65E-21	0.724
292.5	5.90E-21	0.727	293.0	1.11E-20	0.731	293.5	6.26E-20	0.735	294.0	7.40E-20	0.738	294.5	5.36E-20	0.741
295.0	4.17E-20	0.745	295.5	3.51E-20	0.749	296.0	2.70E-20	0.752	296.5	1.75E-20	0.755	297.0	1.16E-20	0.759
297.5	1.51E-20	0.763	298.0	3.69E-20	0.766	298.5	4.40E-20	0.769	299.0	3.44E-20	0.773	299.5	2.02E-20	0.776
300.0	1.06E-20	0.780	300.4	7.01E-21	0.780	300.6	8.63E-21	0.779	300.8	1.47E-20	0.779	301.0	2.01E-20	0.779
301.2	2.17E-20	0.779	301.4	1.96E-20	0.779	301.6	1.54E-20	0.778	301.8	1.26E-20	0.778	302.0	1.03E-20	0.778
302.2	8.53E-21	0.778	302.4	7.13E-21	0.778	302.6	6.61E-21	0.777	302.8	1.44E-20	0.777	303.0	3.18E-20	0.777
303.2	3.81E-20	0.777	303.4	5.57E-20	0.777	303.6	6.91E-20	0.776	303.8	6.58E-20	0.776	304.0	6.96E-20	0.776
304.2	5.79E-20	0.776	304.4	5.24E-20	0.776	304.6	4.30E-20	0.775	304.8	3.28E-20	0.775	305.0	3.60E-20	0.775
305.2	5.12E-20	0.775	305.4	4.77E-20	0.775	305.6	4.43E-20	0.774	305.8	4.60E-20	0.774	306.0	4.01E-20	0.774
306.2	3.28E-20	0.774	306.4	2.66E-20	0.774	306.6	2.42E-20	0.773	306.8	1.95E-20	0.773	307.0	1.58E-20	0.773
307.2	1.37E-20	0.773	307.4	1.19E-20	0.773	307.6	1.01E-20	0.772	307.8	9.01E-21	0.772	308.0	8.84E-21	0.772
308.2	2.08E-20	0.772	308.4	2.39E-20	0.772	308.6	3.08E-20	0.771	308.8	3.39E-20	0.771	309.0	3.18E-20	0.771
309.2	3.06E-20	0.771	309.4	2.84E-20	0.771	309.6	2.46E-20	0.770	309.8	1.95E-20	0.770	310.0	1.57E-20	0.770
310.2	1.26E-20	0.767	310.4	9.26E-21	0.764	310.6	7.71E-21	0.761	310.8	6.05E-21	0.758	311.0	5.13E-21	0.755
311.2	4.82E-21	0.752	311.4	4.54E-21	0.749	311.6	6.81E-21	0.746	311.8	1.04E-20	0.743	312.0	1.43E-20	0.740
312.2	1.47E-20	0.737	312.4	1.35E-20	0.734	312.6	1.13E-20	0.731	312.8	9.86E-21	0.728	313.0	7.82E-21	0.725
313.2	6.48E-21	0.722	313.4	1.07E-20	0.719	313.6	2.39E-20	0.716	313.8	3.80E-20	0.713	314.0	5.76E-20	0.710
314.2	6.14E-20	0.707	314.4	7.45E-20	0.704	314.6	5.78E-20	0.701	314.8	5.59E-20	0.698	315.0	4.91E-20	0.695
315.2	4.37E-20	0.692	315.4	3.92E-20	0.689	315.6	2.89E-20	0.686	315.8	2.82E-20	0.683	316.0	2.10E-20	0.680
316.2	1.66E-20	0.677	316.4	2.05E-20	0.674	316.6	4.38E-20	0.671	316.8	5.86E-20	0.668	317.0	6.28E-20	0.665
317.2	5.07E-20	0.662	317.4	4.33E-20	0.659	317.6	4.17E-20	0.656	317.8	3.11E-20	0.653	318.0	2.64E-20	0.650
318.2	2.24E-20	0.647	318.4	1.70E-20	0.644	318.6	1.24E-20	0.641	318.8	1.11E-20	0.638	319.0	7.70E-21	0.635
319.2	6.36E-21	0.632	319.4	5.36E-21	0.629	319.6	4.79E-21	0.626	319.8	6.48E-21	0.623	320.0	1.48E-20	0.620
320.2	1.47E-20	0.614	320.4	1.36E-20	0.608	320.6	1.69E-20	0.601	320.8	1.32E-20	0.595	321.0	1.49E-20	0.589
321.2	1.17E-20	0.583	321.4	1.15E-20	0.577	321.6	9.64E-21	0.570	321.8	7.26E-21	0.564	322.0	5.94E-21	0.558
322.2	4.13E-21	0.552	322.4	3.36E-21	0.546	322.6	2.39E-21	0.539	322.8	2.01E-21	0.533	323.0	1.76E-21	0.527
323.2	2.82E-21	0.521	323.4	4.65E-21	0.515	323.6	7.00E-21	0.508	323.8	7.80E-21	0.502	324.0	7.87E-21	0.496
324.2	6.59E-21	0.490	324.4	5.60E-21	0.484	324.6	4.66E-21	0.477	324.8	4.21E-21	0.471	325.0	7.77E-21	0.465
325.2	2.15E-20	0.459	325.4	3.75E-20	0.453	325.6	4.10E-20	0.446	325.8	6.47E-20	0.440	326.0	7.59E-20	0.434
326.2	6.51E-20	0.428	326.4	5.53E-20	0.422	326.6	5.76E-20	0.415	326.8	4.43E-20	0.409	327.0	3.44E-20	0.403
327.2	3.22E-20	0.397	327.4	2.13E-20	0.391	327.6	1.91E-20	0.384	327.8	1.42E-20	0.378	328.0	9.15E-21	0.372
328.2	6.79E-21	0.366	328.4	4.99E-21	0.360	328.6	4.77E-21	0.353	328.8	1.75E-20	0.347	329.0	3.27E-20	0.341
329.2	3.99E-20	0.335	329.4	5.13E-20	0.329	329.6	4.00E-20	0.322	329.8	3.61E-20	0.316	330.0	3.38E-20	0.310
330.2	3.08E-20	0.304	330.4	2.16E-20	0.298	330.6	2.09E-20	0.291	330.8	1.41E-20	0.285	331.0	9.95E-21	0.279
331.2	7.76E-21	0.273	331.4	6.16E-21	0.267	331.6	4.06E-21	0.260	331.8	3.03E-21	0.254	332.0	2.41E-21	0.248
332.2	1.74E-21	0.242	332.4	1.33E-21	0.236	332.6	2.70E-21	0.229	332.8	1.65E-21	0.223	333.0	1.17E-21	0.217
333.2	9.84E-22	0.211	333.4	8.52E-22	0.205	333.6	6.32E-22	0.198	333.8	5.21E-22	0.192	334.0	1.46E-21	0.186
334.2	1.80E-21	0.180	334.4	1.43E-21	0.174	334.6	1.03E-21	0.167	334.8	7.19E-22	0.161	335.0	4.84E-22	0.155
335.2	2.73E-22	0.149	335.4	1.34E-22	0.143	335.6	-1.62E-22	0.136	335.8	1.25E-22	0.130	336.0	4.47E-22	0.124
336.2	1.23E-21	0.118	336.4	2.02E-21	0.112	336.6	3.00E-21	0.105	336.8	2.40E-21	0.099	337.0	3.07E-21	0.093
337.2	2.29E-21	0.087	337.4	2.46E-21	0.081	337.6	2.92E-21	0.074	337.8	8.10E-21	0.068	338.0	1.82E-20	0.062
338.2	3.10E-20	0.056	338.4	3.24E-20	0.050	338.6	4.79E-20	0.043	338.8	5.25E-20	0.037	339.0	5.85E-20	0.031
339.2	4.33E-20	0.025	339.4	4.20E-20	0.019	339.6	3.99E-20	0.012	339.8	3.11E-20	0.006	340.0	2.72E-20	0.000

Photolysis File = HCHONEWM

WL (nm)	Abs (cm^2)	QY	WL (nm)	Abs (cm^2)	QY	WL (nm)	Abs (cm^2)	QY	WL (nm)	Abs (cm^2)	QY	WL (nm)	Abs (cm^2)	QY
280.0	2.49E-20	0.350	280.5	1.42E-20	0.346	281.0	1.51E-20	0.341	281.5	1.32E-20	0.336	282.0	9.73E-21	0.332
282.5	6.76E-21	0.327	283.0	5.82E-21	0.323	283.5	9.10E-21	0.319	284.0	3.71E-20	0.314	284.5	4.81E-20	0.309
285.0	3.95E-20	0.305	285.5	2.87E-20	0.301	286.0	2.24E-20	0.296	286.5	1.74E-20	0.291	287.0	1.13E-20	0.287
287.5	1.10E-20	0.282	288.0	2.62E-20	0.278	288.5	4.00E-20	0.273	289.0	3.55E-20	0.269	289.5	2.12E-20	0.264
290.0	1.07E-20	0.260	290.5	1.35E-20	0.258	291.0	1.99E-20	0.256	291.5	1.56E-20	0.254	292.0	8.65E-21	0.252
292.5	5.90E-21	0.250	293.0	1.11E-20	0.248	293.5	6.26E-20	0.246	294.0	7.40E-20	0.244	294.5	5.36E-20	0.242
295.0	4.17E-20	0.240	295.5	3.51E-20	0.238	296.0	2.70E-20	0.236	296.5	1.75E-20	0.234	297.0	1.16E-20	0.232
297.5	1.51E-20	0.230	298.0	3.69E-20	0.228	298.5	4.40E-20	0.226	299.0	3.44E-20	0.224	299.5	2.02E-20	0.222
300.0	1.06E-20	0.220	300.4	7.01E-21	0.220	300.6	8.63E-21	0.221	300.8	1.47E-20	0.221	301.0	2.01E-20	0.221
301.2	2.17E-20	0.221	301.4	1.96E-20	0.221	301.6	1.54E-20	0.222	301.8	1.26E-20	0.222	302.0	1.03E-20	0.222
302.2	8.53E-21	0.222	302.4	7.13E-21	0.222	302.6	6.61E-21	0.223	302.8	1.44E-20	0.223	303.0	3.18E-20	0.223
303.2	3.81E-20	0.223	303.4	5.57E-20	0.223	303.6	6.91E-20	0.224	303.8	6.58E-20	0.224	304.0	6.96E-20	0.224
304.2	5.79E-20	0.224	304.4	5.24E-20	0.224	304.6	4.30E-20	0.225	304.8	3.28E-20	0.225	305.0	3.60E-20	0.225
305.2	5.12E-20	0.225	305.4	4.77E-20	0.225	305.6	4.43E-20	0.226	305.8	4.60E-20	0.226	306.0	4.01E-20	0.226
306.2	3.28E-20	0.226	306.4	2.66E-20	0.226	306.6	2.42E-20	0.227	306.8	1.95E-20	0.227	307.0	1.58E-20	0.227
307.2	1.37E-20	0.227	307.4	1.19E-20	0.227	307.6	1.01E-20	0.228	307.8	9.01E-21	0.228	308.0	8.84E-21	0.228
308.2	2.08E-20	0.228	308.4	2.39E-20	0.228	308.6	3.08E-20	0.229	308.8	3.39E-20	0.229	309.0	3.18E-20	0.229
309.2	3.06E-20	0.229	309.4	2.84E-20	0.229	309.6	2.46E-20	0.230	309.8	1.95E-20	0.230	310.0	1.57E-20	0.230
310.2	1.26E-20	0.233	310.4	9.26E-21	0.236	310.6	7.71E-21	0.239	310.8	6.05E-21	0.242	311.0	5.13E-21	0.245
311.2	4.82E-21	0.248	311.4	4.54E-21	0.251	311.6	6.81E-21	0.254	311.8	1.04E-20	0.257	312.0	1.43E-20	0.260
312.2	1.47E-20	0.263	312.4	1.35E-20	0.266	312.6	1.13E-20	0.269	312.8	9.86E-21	0.272	313.0	7.82E-21	0.275
313.2	6.48E-21	0.278	313.4	1.07E-20	0.281	313.6	2.39E-20	0.284	313.8	3.80E-20	0.287	314.0	5.76E-20	0.290
314.2	6.14E-20	0.293	314.4	7.45E-20	0.296	314.6	5.78E-20	0.299	314.8	5.59E-20	0.302	315.0	4.91E-20	0.305
315.2	4.37E-20	0.308	315.4	3.92E-20	0.311	315.6	2.89E-20	0.314	315.8	2.82E-20	0.317	316.0	2.10E-20	0.320
316.2	1.66E-20	0.323	316.4	2.05E-20	0.326	316.6	4.38E-20	0.329	316.8	5.86E-20	0.332	317.0	6.28E-20	0.335
317.2	5.07E-20	0.338	317.4	4.33E-20	0.341	317.6	4.17E-20	0.344	317.8	3.11E-20	0.347	318.0	2.64E-20	0.350
318.2	2.24E-20	0.353	318.4	1.70E-20	0.356	318.6	1.24E-20	0.359	318.8	1.11E-20	0.362	319.0	7.70E-21	0.365

WL (nm)	Abs (cm^2)	QY	WL (nm)	Abs (cm^2)	QY	WL (nm)	Abs (cm^2)	QY	WL (nm)	Abs (cm^2)	QY	WL (nm)	Abs (cm^2)	QY
319.2	6.36E-21	0.368	319.4	5.36E-21	0.371	319.6	4.79E-21	0.374	319.8	6.48E-21	0.377	320.0	1.48E-20	0.380
320.2	1.47E-20	0.386	320.4	1.36E-20	0.392	320.6	1.69E-20	0.399	320.8	1.32E-20	0.405	321.0	1.49E-20	0.411
321.2	1.17E-20	0.417	321.4	1.15E-20	0.423	321.6	9.64E-21	0.430	321.8	7.26E-21	0.436	322.0	5.94E-21	0.442
322.2	4.13E-21	0.448	322.4	3.36E-21	0.454	322.6	2.39E-21	0.461	322.8	2.01E-21	0.467	323.0	1.76E-21	0.473
323.2	2.82E-21	0.479	323.4	4.65E-21	0.485	323.6	7.00E-21	0.492	323.8	7.80E-21	0.498	324.0	7.87E-21	0.504
324.2	6.59E-21	0.510	324.4	5.60E-21	0.516	324.6	4.66E-21	0.523	324.8	4.21E-21	0.529	325.0	7.77E-21	0.535
325.2	2.15E-20	0.541	325.4	3.75E-20	0.547	325.6	4.10E-20	0.554	325.8	6.47E-20	0.560	326.0	7.59E-20	0.566
326.2	6.51E-20	0.572	326.4	5.53E-20	0.578	326.6	5.76E-20	0.585	326.8	4.43E-20	0.591	327.0	3.44E-20	0.597
327.2	3.22E-20	0.603	327.4	2.13E-20	0.609	327.6	1.91E-20	0.616	327.8	1.42E-20	0.622	328.0	9.15E-21	0.628
328.2	6.79E-21	0.634	328.4	4.99E-21	0.640	328.6	4.77E-21	0.647	328.8	1.75E-20	0.653	329.0	3.27E-20	0.659
329.2	3.99E-20	0.665	329.4	5.13E-20	0.671	329.6	4.00E-20	0.678	329.8	3.61E-20	0.684	330.0	3.38E-20	0.690
330.2	3.08E-20	0.694	330.4	2.16E-20	0.699	330.6	2.09E-20	0.703	330.8	1.41E-20	0.708	331.0	9.95E-21	0.712
331.2	7.76E-21	0.717	331.4	6.16E-21	0.721	331.6	4.06E-21	0.726	331.8	3.03E-21	0.730	332.0	2.41E-21	0.735
332.2	1.74E-21	0.739	332.4	1.33E-21	0.744	332.6	2.70E-21	0.748	332.8	1.65E-21	0.753	333.0	1.17E-21	0.757
333.2	9.84E-22	0.762	333.4	8.52E-22	0.766	333.6	6.32E-22	0.771	333.8	5.21E-22	0.775	334.0	1.46E-21	0.780
334.2	1.80E-21	0.784	334.4	1.43E-21	0.789	334.6	1.03E-21	0.793	334.8	7.19E-22	0.798	335.0	4.84E-22	0.802
335.2	2.73E-22	0.798	335.4	1.34E-22	0.794	335.6	0.00E+00	0.790	335.8	1.25E-22	0.786	336.0	4.47E-22	0.782
336.2	1.23E-21	0.778	336.4	2.02E-21	0.773	336.6	3.00E-21	0.769	336.8	2.40E-21	0.764	337.0	3.07E-21	0.759
337.2	2.29E-21	0.754	337.4	2.46E-21	0.749	337.6	2.92E-21	0.745	337.8	8.10E-21	0.740	338.0	1.82E-20	0.734
338.2	3.10E-20	0.729	338.4	3.24E-20	0.724	338.6	4.79E-20	0.719	338.8	5.25E-20	0.714	339.0	5.85E-20	0.709
339.2	4.33E-20	0.703	339.4	4.20E-20	0.698	339.6	3.99E-20	0.693	339.8	3.11E-20	0.687	340.0	2.72E-20	0.682
340.2	1.99E-20	0.676	340.4	1.76E-20	0.671	340.6	1.39E-20	0.666	340.8	1.01E-20	0.660	341.0	6.57E-21	0.655
341.2	4.83E-21	0.649	341.4	3.47E-21	0.643	341.6	2.23E-21	0.638	341.8	1.55E-21	0.632	342.0	3.70E-21	0.627
342.2	4.64E-21	0.621	342.4	1.08E-20	0.616	342.6	1.14E-20	0.610	342.8	1.79E-20	0.604	343.0	2.33E-20	0.599
343.2	1.72E-20	0.593	343.4	1.55E-20	0.588	343.6	1.46E-20	0.582	343.8	1.38E-20	0.576	344.0	1.00E-20	0.571
344.2	8.26E-21	0.565	344.4	6.32E-21	0.559	344.6	4.28E-21	0.554	344.8	3.22E-21	0.548	345.0	2.54E-21	0.542
345.2	1.60E-21	0.537	345.4	1.15E-21	0.531	345.6	8.90E-22	0.525	345.8	6.50E-22	0.520	346.0	5.09E-22	0.514
346.2	5.15E-22	0.508	346.4	3.45E-22	0.503	346.6	3.18E-22	0.497	346.8	3.56E-22	0.491	347.0	3.24E-22	0.485
347.2	3.34E-22	0.480	347.4	2.88E-22	0.474	347.6	2.88E-22	0.468	347.8	9.37E-22	0.463	348.0	9.70E-22	0.457
348.2	7.60E-22	0.451	348.4	6.24E-22	0.446	348.6	4.99E-22	0.440	348.8	4.08E-22	0.434	349.0	3.39E-22	0.428
349.2	1.64E-22	0.423	349.4	1.49E-22	0.417	349.6	8.30E-23	0.411	349.8	2.52E-23	0.406	350.0	2.57E-23	0.400
350.2	0.00E+00	0.394	350.4	5.16E-23	0.389	350.6	0.00E+00	0.383	350.8	2.16E-23	0.377	351.0	7.07E-23	0.371
351.2	3.45E-23	0.366	351.4	1.97E-22	0.360	351.6	4.80E-22	0.354	351.8	3.13E-21	0.349	352.0	6.41E-21	0.343
352.2	8.38E-21	0.337	352.4	1.55E-20	0.331	352.6	1.86E-20	0.326	352.8	1.94E-20	0.320	353.0	2.78E-20	0.314
353.2	1.96E-20	0.309	353.4	1.67E-20	0.303	353.6	1.75E-20	0.297	353.8	1.63E-20	0.291	354.0	1.36E-20	0.286
354.2	1.07E-20	0.280	354.4	9.82E-21	0.274	354.6	8.66E-21	0.269	354.8	6.44E-21	0.263	355.0	4.84E-21	0.257
355.2	3.49E-21	0.251	355.4	2.41E-21	0.246	355.6	1.74E-21	0.240	355.8	1.11E-21	0.234	356.0	7.37E-22	0.229
356.2	4.17E-22	0.223	356.4	1.95E-22	0.217	356.6	1.50E-22	0.211	356.8	8.14E-23	0.206	357.0	0.00E+00	0.200

Photolysis File = CCHOR

WL (nm)	Abs (cm^2)	QY	WL (nm)	Abs (cm^2)	QY	WL (nm)	Abs (cm^2)	QY	WL (nm)	Abs (cm^2)	QY	WL (nm)	Abs (cm^2)	QY
260.0	2.00E-20	0.310	270.0	3.40E-20	0.390	280.0	4.50E-20	0.580	290.0	4.90E-20	0.530	295.0	4.50E-20	0.480
300.0	4.30E-20	0.430	305.0	3.40E-20	0.370	315.0	2.10E-20	0.170	320.0	1.80E-20	0.100	325.0	1.10E-20	0.040
330.0	6.90E-21	0.000												

Photolysis File = RCHO

WL (nm)	Abs (cm^2)	QY	WL (nm)	Abs (cm^2)	QY	WL (nm)	Abs (cm^2)	QY	WL (nm)	Abs (cm^2)	QY	WL (nm)	Abs (cm^2)	QY
280.0	5.26E-20	0.960	290.0	5.77E-20	0.910	300.0	5.05E-20	0.860	310.0	3.68E-20	0.600	320.0	1.66E-20	0.360
330.0	6.49E-21	0.200	340.0	1.44E-21	0.080	345.0	0.00E+00	0.020						

Photolysis File = ACET-93C

WL (nm)	Abs (cm^2)	QY	WL (nm)	Abs (cm^2)	QY	WL (nm)	Abs (cm^2)	QY	WL (nm)	Abs (cm^2)	QY	WL (nm)	Abs (cm^2)	QY
250.0	2.37E-20	0.760	260.0	3.66E-20	0.800	270.0	4.63E-20	0.640	280.0	5.05E-20	0.550	290.0	4.21E-20	0.300
300.0	2.78E-20	0.150	310.0	1.44E-20	0.050	320.0	4.80E-21	0.026	330.0	8.00E-22	0.017	340.0	1.00E-22	0.000
350.0	3.00E-23	0.000	360.0	0.00E+00	0.000									

Photolysis File = KETONE

WL (nm)	Abs (cm^2)	QY	WL (nm)	Abs (cm^2)	QY	WL (nm)	Abs (cm^2)	QY	WL (nm)	Abs (cm^2)	QY	WL (nm)	Abs (cm^2)	QY
210.0	1.10E-21	1.000	220.0	1.20E-21	1.000	230.0	4.60E-21	1.000	240.0	1.30E-20	1.000	250.0	2.68E-20	1.000
260.0	4.21E-20	1.000	270.0	5.54E-20	1.000	280.0	5.92E-20	1.000	290.0	5.16E-20	1.000	300.0	3.44E-20	1.000
310.0	1.53E-20	1.000	320.0	4.60E-21	1.000	330.0	1.10E-21	1.000	340.0	0.00E+00	1.000			

Photolysis File = GLYOXAL1

WL (nm)	Abs (cm^2)	QY	WL (nm)	Abs (cm^2)	QY	WL (nm)	Abs (cm^2)	QY	WL (nm)	Abs (cm^2)	QY	WL (nm)	Abs (cm^2)	QY
230.0	2.87E-21	1.000	235.0	2.87E-21	1.000	240.0	4.30E-21	1.000	245.0	5.73E-21	1.000	250.0	8.60E-21	1.000
255.0	1.15E-20	1.000	260.0	1.43E-20	1.000	265.0	1.86E-20	1.000	270.0	2.29E-20	1.000	275.0	2.58E-20	1.000
280.0	2.87E-20	1.000	285.0	3.30E-20	1.000	290.0	3.15E-20	1.000	295.0	3.30E-20	1.000	300.0	3.58E-20	1.000
305.0	2.72E-20	1.000	310.0	2.72E-20	1.000	312.5	2.87E-20	1.000	315.0	2.29E-20	1.000	320.0	1.43E-20	1.000
325.0	1.15E-20	1.000	327.5	1.43E-20	1.000	330.0	1.15E-20	1.000	335.0	2.87E-21	1.000	340.0	0.00E+00	1.000

Photolysis File = GLYOXAL2

WL (nm)	Abs (cm^2)	QY	WL (nm)	Abs (cm^2)	QY	WL (nm)	Abs (cm^2)	QY	WL (nm)	Abs (cm^2)	QY	WL (nm)	Abs (cm^2)	QY
355.0	0.00E+00	1.000	360.0	2.29E-21	1.000	365.0	2.87E-21	1.000	370.0	8.03E-21	1.000	375.0	1.00E-20	1.000
380.0	1.72E-20	1.000	382.0	1.58E-20	1.000	384.0	1.49E-20	1.000	386.0	1.49E-20	1.000	388.0	2.87E-20	1.000
390.0	3.15E-20	1.000	391.0	3.24E-20	1.000	392.0	3.04E-20	1.000	393.0	2.23E-20	1.000	394.0	2.63E-20	1.000
395.0	3.04E-20	1.000	396.0	2.63E-20	1.000	397.0	2.43E-20	1.000	398.0	3.24E-20	1.000	399.0	3.04E-20	1.000
400.0	2.84E-20	1.000	401.0	3.24E-20	1.000	402.0	4.46E-20	1.000	403.0	5.27E-20	1.000	404.0	4.26E-20	1.000
405.0	3.04E-20	1.000	406.0	3.04E-20	1.000	407.0	2.84E-20	1.000	408.0	2.43E-20	1.000	409.0	2.84E-20	1.000
410.0	6.08E-20	1.000	411.0	5.07E-20	1.000	411.5	6.08E-20	1.000	412.0	4.86E-20	1.000	413.0	8.31E-20	1.000
413.5	6.48E-20	1.000	414.0	7.50E-20	1.000	414.5	8.11E-20	1.000	415.0	8.11E-20	1.000	415.5	6.89E-20	1.000
416.0	4.26E-20	1.000	417.0	4.86E-20	1.000	418.0	5.88E-20	1.000	419.0	6.69E-20	1.000	420.0	3.85E-20	1.000
421.0	5.67E-20	1.000	421.5	4.46E-20	1.000	422.0	5.27E-20	1.000	422.5	1.05E-19	1.000	423.0	8.51E-20	1.000
424.0	6.08E-20	1.000	425.0	7.29E-20	1.000	426.0	1.18E-19	1.000	426.5	1.30E-19	1.000	427.0	1.07E-19	1.000
428.0	1.66E-19	1.000	429.0	4.05E-20	1.000	430.0	5.07E-20	1.000	431.0	4.86E-20	1.000	432.0	4.05E-20	1.000
433.0	3.65E-20	1.000	434.0	4.05E-20	1.000	434.5	6.08E-20	1.000	435.0	5.07E-20	1.000	436.0	8.11E-20	1.000
436.5	1.13E-19	1.000	437.0	5.27E-20	1.000	438.0	1.01E-19	1.000	438.5	1.38E-19	1.000	439.0	7.70E-20	1.000
440.0	2.47E-19	1.000	441.0	8.11E-20	1.000	442.0	6.08E-20	1.000	443.0	7.50E-20	1.000	444.0	9.32E-20	1.000
445.0	1.13E-19	1.000	446.0	5.27E-20	1.000	447.0	2.43E-20	1.000	448.0	2.84E-20	1.000	449.0	3.85E-20	1.000
450.0	6.08E-20	1.000	451.0	1.09E-19	1.000	451.5	9.32E-20	1.000	452.0	1.22E-19	1.000	453.0	2.39E-19	1.000
454.0	1.70E-19	1.000	455.0	3.40E-19	1.000	455.5	4.05E-19	1.000	456.0	1.01E-19	1.000	457.0	1.62E-20	1.000

Table A-3. (continued)

WL (nm)	Abs (cm^2)	QY	WL (nm)	Abs (cm^2)	QY	WL (nm)	Abs (cm^2)	QY	WL (nm)	Abs (cm^2)	QY	WL (nm)	Abs (cm^2)	QY
458.0	1.22E-20	1.000	458.5	1.42E-20	1.000	459.0	4.05E-21	1.000	460.0	4.05E-21	1.000	460.5	6.08E-21	1.000
461.0	2.03E-21	1.000	462.0	0.00E+00	1.000									

Photolysis File = MEGLYOX1

WL (nm)	Abs (cm^2)	QY	WL (nm)	Abs (cm^2)	QY	WL (nm)	Abs (cm^2)	QY	WL (nm)	Abs (cm^2)	QY	WL (nm)	Abs (cm^2)	QY
220.0	2.10E-21	1.000	225.0	2.10E-21	1.000	230.0	4.21E-21	1.000	235.0	7.57E-21	1.000	240.0	9.25E-21	1.000
245.0	8.41E-21	1.000	250.0	9.25E-21	1.000	255.0	9.25E-21	1.000	260.0	9.67E-21	1.000	265.0	1.05E-20	1.000
270.0	1.26E-20	1.000	275.0	1.43E-20	1.000	280.0	1.51E-20	1.000	285.0	1.43E-20	1.000	290.0	1.47E-20	1.000
295.0	1.18E-20	1.000	300.0	1.14E-20	1.000	305.0	9.25E-21	1.000	310.0	6.31E-21	1.000	315.0	5.47E-21	1.000
320.0	3.36E-21	1.000	325.0	1.68E-21	1.000	330.0	8.41E-22	1.000	335.0	0.00E+00	1.000			

Photolysis File = MEGLYOX2

WL (nm)	Abs (cm^2)	QY	WL (nm)	Abs (cm^2)	QY	WL (nm)	Abs (cm^2)	QY	WL (nm)	Abs (cm^2)	QY	WL (nm)	Abs (cm^2)	QY
350.0	0.00E+00	1.000	354.0	4.21E-22	1.000	358.0	1.26E-21	1.000	360.0	2.10E-21	1.000	362.0	2.10E-21	1.000
364.0	2.94E-21	1.000	366.0	3.36E-21	1.000	368.0	4.21E-21	1.000	370.0	5.47E-21	1.000	372.0	5.89E-21	1.000
374.0	7.57E-21	1.000	376.0	7.99E-21	1.000	378.0	8.83E-21	1.000	380.0	1.01E-20	1.000	382.0	1.09E-20	1.000
384.0	1.35E-20	1.000	386.0	1.51E-20	1.000	388.0	1.72E-20	1.000	390.0	2.06E-20	1.000	392.0	2.10E-20	1.000
394.0	2.31E-20	1.000	396.0	2.48E-20	1.000	398.0	2.61E-20	1.000	400.0	2.78E-20	1.000	402.0	2.99E-20	1.000
404.0	3.20E-20	1.000	406.0	3.79E-20	1.000	408.0	3.95E-20	1.000	410.0	4.33E-20	1.000	412.0	4.71E-20	1.000
414.0	4.79E-20	1.000	416.0	4.88E-20	1.000	418.0	5.05E-20	1.000	420.0	5.21E-20	1.000	422.0	5.30E-20	1.000
424.0	5.17E-20	1.000	426.0	5.30E-20	1.000	428.0	5.21E-20	1.000	430.0	5.55E-20	1.000	432.0	5.13E-20	1.000
434.0	5.68E-20	1.000	436.0	6.22E-20	1.000	438.0	6.06E-20	1.000	440.0	5.47E-20	1.000	441.0	6.14E-20	1.000
442.0	5.47E-20	1.000	443.0	5.55E-20	1.000	443.5	6.81E-20	1.000	444.0	5.97E-20	1.000	445.0	5.13E-20	1.000
446.0	4.88E-20	1.000	447.0	5.72E-20	1.000	448.0	5.47E-20	1.000	449.0	6.56E-20	1.000	450.0	5.05E-20	1.000
451.0	3.03E-20	1.000	452.0	4.29E-20	1.000	453.0	2.78E-20	1.000	454.0	2.27E-20	1.000	456.0	1.77E-20	1.000
458.0	8.41E-21	1.000	460.0	4.21E-21	1.000	464.0	1.68E-21	1.000	468.0	0.00E+00	1.000			

Photolysis File = BZCHO

WL (nm)	Abs (cm^2)	QY	WL (nm)	Abs (cm^2)	QY	WL (nm)	Abs (cm^2)	QY	WL (nm)	Abs (cm^2)	QY	WL (nm)	Abs (cm^2)	QY
299.0	1.78E-19	1.000	304.0	7.40E-20	1.000	306.0	6.91E-20	1.000	309.0	6.41E-20	1.000	313.0	6.91E-20	1.000
314.0	6.91E-20	1.000	318.0	6.41E-20	1.000	325.0	8.39E-20	1.000	332.0	7.65E-20	1.000	338.0	8.88E-20	1.000
342.0	8.88E-20	1.000	346.0	7.89E-20	1.000	349.0	7.89E-20	1.000	354.0	9.13E-20	1.000	355.0	8.14E-20	1.000
364.0	5.67E-20	1.000	368.0	6.66E-20	1.000	369.0	8.39E-20	1.000	370.0	8.39E-20	1.000	372.0	3.45E-20	1.000
374.0	3.21E-20	1.000	376.0	2.47E-20	1.000	377.0	2.47E-20	1.000	380.0	3.58E-20	1.000	382.0	9.90E-21	1.000
386.0	0.00E+00	1.000												

Photolysis File = ACROLEIN

WL (nm)	Abs (cm^2)	QY	WL (nm)	Abs (cm^2)	QY	WL (nm)	Abs (cm^2)	QY	WL (nm)	Abs (cm^2)	QY	WL (nm)	Abs (cm^2)	QY
250.0	1.80E-21	1.000	252.0	2.05E-21	1.000	253.0	2.20E-21	1.000	254.0	2.32E-21	1.000	255.0	2.45E-21	1.000
256.0	2.56E-21	1.000	257.0	2.65E-21	1.000	258.0	2.74E-21	1.000	259.0	2.83E-21	1.000	260.0	2.98E-21	1.000
261.0	3.24E-21	1.000	262.0	3.47E-21	1.000	263.0	3.58E-21	1.000	264.0	3.93E-21	1.000	265.0	4.67E-21	1.000
266.0	5.10E-21	1.000	267.0	5.38E-21	1.000	268.0	5.73E-21	1.000	269.0	6.13E-21	1.000	270.0	6.64E-21	1.000
271.0	7.20E-21	1.000	272.0	7.77E-21	1.000	273.0	8.37E-21	1.000	274.0	8.94E-21	1.000	275.0	9.55E-21	1.000
276.0	1.04E-20	1.000	277.0	1.12E-20	1.000	278.0	1.19E-20	1.000	279.0	1.27E-20	1.000	280.0	1.27E-20	1.000
281.0	1.26E-20	1.000	282.0	1.26E-20	1.000	283.0	1.28E-20	1.000	284.0	1.33E-20	1.000	285.0	1.38E-20	1.000
286.0	1.44E-20	1.000	287.0	1.50E-20	1.000	288.0	1.57E-20	1.000	289.0	1.63E-20	1.000	290.0	1.71E-20	1.000
291.0	1.78E-20	1.000	292.0	1.86E-20	1.000	293.0	1.95E-20	1.000	294.0	2.05E-20	1.000	295.0	2.15E-20	1.000
296.0	2.26E-20	1.000	297.0	2.37E-20	1.000	298.0	2.48E-20	1.000	299.0	2.60E-20	1.000	300.0	2.73E-20	1.000
301.0	2.85E-20	1.000	302.0	2.99E-20	1.000	303.0	3.13E-20	1.000	304.0	3.27E-20	1.000	305.0	3.39E-20	1.000
306.0	3.51E-20	1.000	307.0	3.63E-20	1.000	308.0	3.77E-20	1.000	309.0	3.91E-20	1.000	310.0	4.07E-20	1.000
311.0	4.25E-20	1.000	312.0	4.39E-20	1.000	313.0	4.44E-20	1.000	314.0	4.50E-20	1.000	315.0	4.59E-20	1.000
316.0	4.75E-20	1.000	317.0	4.90E-20	1.000	318.0	5.05E-20	1.000	319.0	5.19E-20	1.000	320.0	5.31E-20	1.000
321.0	5.43E-20	1.000	322.0	5.52E-20	1.000	323.0	5.60E-20	1.000	324.0	5.67E-20	1.000	325.0	5.67E-20	1.000
326.0	5.62E-20	1.000	327.0	5.63E-20	1.000	328.0	5.71E-20	1.000	329.0	5.76E-20	1.000	330.0	5.80E-20	1.000
331.0	5.95E-20	1.000	332.0	6.23E-20	1.000	333.0	6.39E-20	1.000	334.0	6.38E-20	1.000	335.0	6.24E-20	1.000
336.0	6.01E-20	1.000	337.0	5.79E-20	1.000	338.0	5.63E-20	1.000	339.0	5.56E-20	1.000	340.0	5.52E-20	1.000
341.0	5.54E-20	1.000	342.0	5.53E-20	1.000	343.0	5.47E-20	1.000	344.0	5.41E-20	1.000	345.0	5.40E-20	1.000
346.0	5.48E-20	1.000	347.0	5.90E-20	1.000	348.0	6.08E-20	1.000	349.0	6.00E-20	1.000	350.0	5.53E-20	1.000
351.0	5.03E-20	1.000	352.0	4.50E-20	1.000	353.0	4.03E-20	1.000	354.0	3.75E-20	1.000	355.0	3.55E-20	1.000
356.0	3.45E-20	1.000	357.0	3.46E-20	1.000	358.0	3.49E-20	1.000	359.0	3.41E-20	1.000	360.0	3.23E-20	1.000
361.0	2.95E-20	1.000	362.0	2.81E-20	1.000	363.0	2.91E-20	1.000	364.0	3.25E-20	1.000	365.0	3.54E-20	1.000
366.0	3.30E-20	1.000	367.0	2.78E-20	1.000	368.0	2.15E-20	1.000	369.0	1.59E-20	1.000	370.0	1.19E-20	1.000
371.0	8.99E-21	1.000	372.0	7.22E-21	1.000	373.0	5.86E-21	1.000	374.0	4.69E-21	1.000	375.0	3.72E-21	1.000
376.0	3.57E-21	1.000	377.0	3.55E-21	1.000	378.0	2.83E-21	1.000	379.0	1.69E-21	1.000	380.0	8.29E-24	1.000
381.0	0.00E+00	1.000												

Table A-4.   Values of chamber-dependent parameters used in the model simulations of the environmental chamber experiments for this study. [a]

_____

Parm.	Value(s)	Discussion
k(1)	<u>Phase 1</u> (DTC331-387) (min^{-1}): 0.233 - 0.000245 x RunNo <u>Phase 2</u> (DTC545-683) (min^{-1}) 0.367 - 0.000298 x RunNO	Derived from linear fit to results of quartz tube NO_2 actinometry measurements carried out around the time of the experiments as a function of run number. Apparently anomalous actinometry results between DTC600 and DTC646 were not used. See text.
RS/K1	<u>Phase 1</u>: DTC331-387: 0.078 ppb <u>Phase 2</u>: DTC545A-616A: 0.0091 ppb DTC545B-616B: 0.0068 ppb DTC624-683: 0.078 ppb	Based on averages of RS/K1 parameters which gave best fits to the data in model simulations of n-butane - NO_x experiments carried out around the times of the experiment. See by Carter et al (1995b,c). For runs DTC545-DTC616, side A appeared to have somewhat higher radical source than usual for this chamber. The radical source fit the data for the other runs were in the normal range, and were within the normal variability.
E-NO2/K1	Same as RS/K1	Results of pure air and acetaldehyde - air runs, which are sensitive to this parameter, indicate that RS/K1 and E-NO2/K1 tend to be within experimental variability of being the same. This would be expected if the radical source and NO_x offgasing are due to the same process, such as HONO offgasing. Therefore, it is assumed that E-NO2/K1 = RS/K1 unless there is evidence to the contrary.
k(O3W)	1.5×10^{-4} min^{-1}	The results of the O_3 dark decay experiments in this chamber are reasonably consistent with the recommended default of Carter et al (1995c) for Teflon bag chambers in general.
k(N25I) k(N25S)	2.8×10^{-3} min^{-1}, 1.5×10^{-6} - k_g ppm^{-1} min^{-1}	Based on the N_2O_5 decay rate measurements in a similar chamber reported by Tuazon et al. (1983). Although we previously estimated there rate constants were lower in the larger Teflon bag chambers (Carter and Lurmann, 1990, 1991), we now consider it more reasonable to use the same rate constants for all such chambers (Carter et al., 1995c).
k(NO2W) yHONO	1.6×10^{-4} min^{-1} 0.2	Based on dark NO_2 decay and HONO formation measured in a similar chamber by Pitts et al. (1984). Assumed to be the same in all Teflon bag chambers (Carter et al, 1995c).
k(XSHC)	250 min^{-1}	Estimated by modeling pure air irradiations. Not important om affecting model predictions except for pure air or NO_x-air runs.

_____

[a] See Table A-2 for definitions of the parameters.

APPENDIX B
RESULTS OF DETAILED SPECIATED ANALYSES

      The results of the detailed hydrocarbon and oxygenate speciation analyses of the exhausts used in this program are given in Tables B-1 and B-2. Table B-1 gives the results of the analyses made during the FTP tests, weighed appropriately for each mode, with the data given in units of mg/mile. Table B-2 gives the results of the analyses of the transfer bag made during the second phase of the program, given in units of ppm VOC in the transfer bag.

Table B-1. Results of speciation measurements during the FTP baseline tests.

Method / Compound	FTP Emissions (mg/mile)					
	LPG		M100	M85	Rep Car	Suburban
Test No.	9605005	9605011	9711077	9712005	9711030	9803005
Total Measured NMHC	804.0	826.6	385.5	157.3	136.0	296.8
Total Unknowns			4.1	3.6	27.3	57.2
Total NMHC	804.0	826.6	389.6	160.9	163.3	354.0
Percent Unknowns			1%	2%	17%	16%
GC-FID Analysis						
Methane	166.5	160.0	10.85	12.57	42.56	80.26
Ethane	29.2	8.3	0.14	0.39	3.03	7.98
Propane	695.1	702.9	0.01	0.24	0.10	0.47
Butane	3.56	26.8	0.32	2.09	1.17	12.94
Pentane	-	-	0.54	0.48	0.69	8.83
Hexane	-	-	-	0.20	0.23	5.53
Heptane	-	-	-	0.51	1.67	2.97
Octane	-	-	-	0.11	0.57	1.68
Nonane	-	-	0.27	0.31	0.13	0.63
Decane	-	-	-	0.04	0.10	0.25
Undecane	-	-	0.41	0.06	0.18	0.33
Dodecane	-	-	0.87	0.22	0.11	0.32
2-Methylpropane	0.40	0.04	-	0.40	0.12	1.75
2,2-Dimethylpropane	0.23	1.00	0.47	0.16	-	1.28
2-Methylbutane	0.46	0.81	1.37	1.26	-	19.36
2,2-Dimethylbutane	-	-	-	0.11	0.27	1.77
2,3-Dimethylbutane	-	-	-	0.08	0.24	2.58
2-Methylpentane	-	-	-	0.46	0.09	9.72
3-Methylpentane	-	-	0.07	0.31	2.44	5.85
2,2,3-Trimethylbutane	-	-	-	-	0.03	0.09
2,2-Dimethylpentane	-	-	-	-	-	6.80
2,3-Dimethylpentane	0.04	0.53	0.06	0.25	3.83	4.18
2,4-Dimethylpentane	-	-	0.07	0.11	2.21	2.64
3,3-Dimethylpentane	-	-	-	-	0.21	0.37
2-Methylhexane	-	-	-	0.51	2.55	3.90
3-Methylhexane	-	-	-	0.26	2.86	4.05
2,2,4-Trimethylpentane	-	-	0.05	0.38	8.38	5.38
2,3,3-Trimethylpentane	-	-	-	-	0.34	-
2,3,4-Trimethylpentane	-	-	0.09	0.65	1.99	1.84
3-Ethylpentane	-	-	0.12	0.14	0.72	1.46
2,2-Dimethylhexane	0.27	0.20	-	-	0.10	0.24
2,3-Dimethylhexane	-	-	0.29	0.11	0.76	0.94
2,4-Dimethylhexane	-	-	-	0.07	1.24	1.23
2,5-Dimethylhexane	-	-	-	0.14	0.97	1.50
3,3-Dimethylhexane	-	-	-	-	0.23	0.66
2-Methylheptane	-	-	-	0.13	0.79	1.97
3-Methylheptane	-	-	0.08	0.02	1.01	2.30
4-Methylheptane	-	-	-	0.06	0.27	0.81
2,3-Dimethylheptane	-	-	-	0.18	0.06	0.19
2,4-Dimethylheptane	-	-	-	-	0.12	0.52

Table B-1 (continued)

Method / Compound	FTP Emissions (mg/mile)				
	LPG	M100	M85	Rep Car	Suburban
3,5-Dimethylheptane	-	-	-	0.47	0.77
2,2,5-Trimethylhexane	-	-	0.09	0.90	0.80
2,3,5-Trimethylhexane	-	-	-	0.13	0.34
2-Methyloctane	-	-	0.07	0.37	1.04
3-Methyloctane	-	-	0.07	0.27	1.01
2,2-Dimethyloctane	-	-	-	0.07	0.06
2,4-Dimethyloctane	0.15	0.56	0.11	0.07	0.45	1.33
Cyclopentane	-	-	0.08	0.39	1.06
Methylcyclopentane	-	-	0.23	0.43	0.21	0.05
Cyclohexane	-	-	0.60	0.14	0.39	2.82
t-1,2-Dimethylcyclopentane	-	-	-	-	-	-
c-1,3-Dimethylcyclopentane	-	-	-	0.12	0.48	1.09
Methylcyclohexane	-	-	-	0.17	0.97	2.56
1c,2t,3-Trimethylcyclopentane	-	-	-	-	-	-
c-1,2-Dimethylcyclohexane	8.03	0.70	-	-	0.12	0.50
c-1,3-Dimethylcyclohexane	-	-	-	0.07	0.21	0.82
t-1,3-Dimethylcyclohexane	-	-	-	-	0.13	0.61
t-1,4-Dimethylcyclohexane	-	-	-	-	0.07	0.35
Ethylcyclohexane	0.68	2.08	4.11	-	0.07	-
Ethene	59.61	76.69	0.74	1.64	6.03	23.80
Propene	-	-	-	-	-	11.24
1-Butene	-	-	0.23	-	-	13.21
c-2-Butene	-	-	-	-	-	-
t-2-Butene	-	-	-	-	-	1.07
2-Methylpropene	-	-	-	0.68	4.21	0.87
1-Pentene	-	-	-	0.33	0.20	0.04
c-2-Pentene	0.66	0.28	-	-	-	0.04
t-2-Pentene	0.17	0.83	-	0.05	0.62	0.62
2-Methyl-1-Butene	1.00	0.33	-	0.11	-	0.73
3-Methyl-1-Butene	-	-	-	0.04	0.05	-
2-Methyl-2-Butene	-	-	-	0.06	0.19	1.24
1-Hexene	-	-	-	0.09	0.11	0.14
c-2-Hexene	-	-	-	-	0.09	-
t-2-Hexene	-	-	-	-	-	0.21
c-3-Hexene	-	-	-	-	0.11	0.05
t-3-Hexene	-	-	0.05	-	1.06	-
2-Methyl-1-Pentene	-	-	-	-	-	-
3-Methyl-1-Pentene	-	-	-	-	-	0.21
4-Methyl-1-Pentene	-	-	-	-	0.07	0.15
2-Methyl-2-Pentene	-	-	-	0.19	0.17	0.26
3-Methyl-c-2-Pentene	0.53	-	-	-	0.19	0.33
3-Methyl-t-2-Pentene	-	-	-	0.04	0.18	0.44
4-Methyl-c-2-Pentene	-	-	-	0.78	5.14	-
4-Methyl-t-2-Pentene	-	-	0.38	-	3.88	-
3,3-Dimethyl-1-Butene	-	-	-	-	0.34	0.14
1-Heptene	-	-	-	-	-	-
c-2-Heptene	-	-	-	-	0.07	0.08
t-2-Heptene	-	-	-	-	0.07	-

Table B-1 (continued)

Method / Compound	FTP Emissions (mg/mile)				
	LPG	M100	M85	Rep Car	Suburban
t-3-Heptene	-	-	-	-	0.07	-
2,3-Dimethyl-2-Pentene	-	-	-	-	-	-
3,4-Dimethyl-1-Pentene	-	-	0.08	-	-	0.04
3-Methyl-1-Hexene	0.45	-	-	-	-	-
2-Methyl-2-Hexene	-	-	-	-	0.19	0.18
3-Methyl-t-3-Hexene	-	-	-	-	-	-
1-Octene	-	-	-	-	0.11	0.60
c-2-Octene	-	-	-	-	0.03	0.35
t-2-Octene	-	-	-	-	0.04	0.05
t-4-Octene	-	-	-	0.28	0.07	0.07
2,4,4-Trimethyl-1-Pentene	-	-	-	-	0.06	0.08
2,4,4-Trimethyl-2-Pentene	-	-	-	-	-	-
3-Ethyl-c-2-Pentene	-	-	-	-	0.04	0.02
1-Nonene	-	-	-	-	0.25	0.66
Propadiene	-	-	-	-	-	0.38
1,3-Butadiene	-	-	0.01	0.12	0.65	1.23
2-Methyl-1,3-Butadiene	0.42	0.68	0.18	-	1.55	0.62
Cyclopentadiene	-	-	-	0.05	-	-
Cyclopentene	-	-	-	0.05	0.03	0.31
1-Methylcyclopentene	-	-	-	-	5.02	-
3-Methylcyclopentene	-	-	0.15	-	-	0.15
Cyclohexene	-	-	-	-	0.05	0.18
Ethyne	-	-	0.28	0.59	5.02	10.63
Propyne	-	-	-	-	-	-
1-Butyne	-	-	2.59	-	-	0.30
2-Butyne	-	-	-	-	0.03	-
Benzene	1.31	2.14	0.20	0.98	3.90	11.34
Toluene	0.37	0.45	0.35	1.69	10.45	18.63
Ethylbenzene	-	-	-	0.25	2.70	3.39
o-Xylene	-	-	0.10	0.49	2.28	4.22
m&p-Xylene	-	-	0.10	1.35	6.93	11.29
n-Propylbenzene	-	-	-	0.09	0.33	0.70
i-Propylbenzene	-	-	-	-	0.07	0.23
1-Methyl-2-ethylbenzene	-	-	-	0.17	0.53	1.24
1-Methyl-3-ethylbenzene	-	-	0.05	0.49	1.73	3.05
1-Methyl-4-ethylbenzene	-	-	-	0.24	0.78	1.47
1,2-Dimethyl-3-ethylbenzene	-	-	-	-	0.04	0.09
1,2-Dimethyl-4-ethylbenzene	-	-	-	0.07	0.19	0.42
1,3-Dimethyl-2-ethylbenzene	-	-	-	-	0.04	0.06
1,3-Dimethyl-4-ethylbenzene	-	-	-	0.05	-	0.23
1,4-Dimethyl-2-ethylbenzene	-	-	-	0.05	0.12	0.51
1,2,3-Trimethylbenzene	-	-	-	0.17	0.31	0.75
1,2,4-Trimethylbenzene	-	-	0.35	0.57	1.84	3.67
1,3,5-Trimethylbenzene	-	-	-	0.25	0.76	1.61
Indan	-	-	-	0.02	0.13	0.35
i-Butylbenzene	-	-	-	-	-	0.05
s-Butylbenzene	-	-	-	-	0.03	0.07
2-Methyl-Butylbenzene	-	-	-	-	0.13	-

Table B-1 (continued)

Method / Compound	FTP Emissions (mg/mile)					
	LPG		M100	M85	Rep Car	Suburban
tert-1-Butyl-2-Methyl-Benzene	-	-	-	-	0.03	-
tert-1-Butyl-3,5-Dimethyl-Ben:	-	-	0.08	0.00	0.03	0.05
1,2-Diethylbenzene	-	-	-	0.08	0.06	0.12
1,3-Diethylbenzene	-	-	-	0.05	0.04	0.17
1,4-Diethylbenzene	0.27	0.10	-	-	0.11	0.23
1-Methyl-2-n-Propylbenzene	0.07	0.53	-	-	0.10	0.28
1-Methyl-3-n-Propylbenzene	-	-	-	0.09	0.24	0.46
1-Methyl-4-n-Propylbenzene	-	-	-	0.21	0.59	1.26
1-Methyl-2-i-Propylbenzene	-	-	-	-	-	-
1-Methyl-3-i-Propylbenzene	-	-	-	-	0.03	0.15
1-Methyl-4-i-Propylbenzene	-	-	-	-	-	-
1,2,3,4-Tetramethylbenzene	-	-	-	-	0.11	0.13
1,2,3,5-Tetramethylbenzene	-	-	-	0.07	-	0.28
1,2,4,5-Tetramethylbenzene	1.03	0.56	-	0.07	0.19	0.34
n-Pent-Benzene	-	-	0.10	0.03	0.12	0.25
Styrene	-	-	-	0.06	0.51	1.19
Naphthalene	-	-	0.36	0.19	0.15	0.50
Methyl-t-Butyl-Ether	-	-	-	-	1.61	9.39
Ethyl-t-Butyl-Ether	-	-	2.82	-	-	-
Results of Oxygenate Analysis						
Formaldehyde	(No data)		20.86	9.72	3.12	3.14
Acetaldehyde			1.79	1.34	0.97	0.52
Propionaldehyde			-	-	-	-
Acrolein			2.69	2.57	1.64	3.04
Methacrolein			-	-	0.05	0.45
n-Butyraldehyde			-	-	-	-
Crotonaldehyde			-	-	-	-
Pentanaldehyde			-	-	-	-
Hexanaldehyde			2.26	3.52	-	-
Benzaldehyde			0.25	0.49	0.20	0.15
p-Tolualdehyde			0.83	-	0.19	0.13
Acetone			-	-	-	-
Butanone			-	-	0.12	-
Results of Impinger Analysis						
Methanol	(No data)		337.30	114.96	11.04	-
GC-FID Unknowns						
Unknown (C1-C4)			2.60	3.62	5.81	41.97
Unknown (C4-C12)			1.48	-	21.45	15.21

Table B-2. Results of detailed speciation analysis of transfer bag in Phase 2 exhaust runs.

Method / Compound	Transfer Bag Concentration (ppm) [a]													
Chamber Run Number	DTC588	DTC589	DTC591	DTC592	DTC593	DTC594	DTC595	DTC596	DTC572	DTC575	DTC574	DTC576	DTC581	DTC577
Vehicle or Fuel	M100	M100	M85	M85	M85	M85	M85 [b]	M85	CNG	CNG	Rep	Rep	Rep	Rep
Total Measured NMHC (ppmC)	1.82	70.49	32.52	19.99	37.62	35.38	33.54	44.81	1.13	1.39	16.35	21.98	17.57	17.11
Total Unknowns (ppmC)									0.21			3.56		2.61
Total NMHC (ppmC)	1.82	70.49	32.52	19.99	37.62	35.38	33.54	44.81	1.33	1.39	16.35	25.55	17.57	19.71
Percent Unknowns (ppmC)									15%			14%		13%
GC-FID Analysis (ppm)														
Methane	0.080	0.873	0.355	0.814	0.752	0.349	0.908	0.922	28.160	37.139	2.806	3.361	3.363	3.096
Ethane	-	-	0.004	0.008	0.012	0.008	0.024	0.016	0.289	0.568	0.324	0.359	0.278	0.369
Propane	-	-	-	-	-	-	-	-	-	-	-	-	0.001	-
Butane	-	-	-	-	-	-	3.360	-	0.001	-	-	0.035	0.026	0.031
Pentane	0.000	0.002	0.003	-	0.001	-	0.003	0.002	-	-	0.031	0.040	0.031	0.030
Hexane	-	0.002	0.003	-	0.000	-	-	-	-	-	0.032	0.023	0.022	0.017
Heptane	-	-	-	-	0.000	-	-	-	-	-	0.024	0.033	0.026	0.025
Octane	-	-	-	-	-	-	-	-	-	-	0.009	0.011	0.009	0.008
Nonane	0.002	-	-	0.005	-	-	-	0.002	-	-	0.002	0.003	0.003	0.002
Decane	-	-	-	-	-	-	-	0.002	-	-	0.001	0.002	-	0.002
Undecane	0.020	0.007	-	-	0.003	0.012	-	0.014	-	-	0.006	0.011	-	0.007
Dodecane	0.060	-	-	-	-	-	-	-	-	-	-	-	-	-
2-Methylpropane	-	-	-	-	-	-	-	-	-	-	0.002	0.005	0.005	0.007
2,2-Dimethylpropane	-	-	-	-	-	-	-	-	-	-	0.003	-	0.141	-
2-Methylbutane	-	0.012	0.026	-	0.003	-	0.003	0.008	-	-	0.189	0.228	0.169	0.176
2,2-Dimethylbutane	0.003	0.002	0.001	-	-	-	-	-	-	-	0.007	0.007	0.007	0.007
2,3-Dimethylbutane	0.002	0.004	0.004	-	0.003	0.004	-	0.002	0.003	-	0.023	0.027	0.023	0.020
2-Methylpentane	0.002	0.008	0.006	-	0.003	0.002	-	0.002	-	-	0.070	0.084	0.073	0.064
3-Methylpentane	0.000	0.004	0.004	-	0.000	-	0.001	0.001	-	-	0.037	0.044	0.036	0.030
2,2,3-Trimethylbutane	-	-	-	-	-	-	-	-	-	-	0.002	0.002	0.002	0.002
2,2-Dimethylpentane	-	-	-	-	-	-	-	-	-	-	0.003	-	0.002	0.002
2,3-Dimethylpentane	-	0.002	0.003	-	0.000	-	-	-	-	-	0.055	0.066	0.052	0.049
2,4-Dimethylpentane	-	0.002	-	-	-	0.004	-	-	-	-	0.032	0.040	0.031	0.029
3,3-Dimethylpentane	-	-	-	-	-	-	-	-	-	-	-	-	0.004	-
2-Methylhexane	-	0.002	0.002	-	0.002	-	-	-	-	-	0.038	0.046	0.036	0.035
3-Methylhexane	0.000	0.002	0.002	-	0.000	-	-	-	-	-	0.042	0.050	0.040	0.037
2,2,4-Trimethylpentane	-	0.003	0.003	-	0.000	-	-	-	-	-	0.111	0.134	0.105	0.099
2,3,3-Trimethylpentane	-	-	-	-	-	-	-	-	-	-	-	-	-	-
2,3,4-Trimethylpentane	-	0.001	-	-	-	-	-	-	-	-	0.026	0.032	0.026	0.024
3-Ethylpentane	-	-	0.003	-	-	-	-	-	-	-	0.011	0.013	0.010	0.010
2,2-Dimethylhexane	-	-	-	-	-	-	-	-	-	-	0.002	0.003	0.001	0.002
2,3-Dimethylhexane	-	-	-	-	-	-	-	-	-	-	0.009	0.012	0.011	0.012
2,4-Dimethylhexane	-	-	-	-	-	-	-	-	-	-	0.017	0.021	0.015	0.015
2,5-Dimethylhexane	-	-	-	-	-	-	-	-	-	-	0.013	0.016	0.012	0.012
3,3-Dimethylhexane	-	-	-	-	-	-	-	-	-	-	0.004	0.004	0.004	0.003
2-Methylheptane	-	-	-	-	-	-	-	-	-	-	0.011	0.014	0.012	0.014
3-Methylheptane	-	0.002	-	-	-	-	-	-	-	-	0.004	0.005	0.016	0.005
4-Methylheptane	-	0.002	-	-	-	-	-	-	-	-	0.004	0.005	0.005	0.005
2,3-Dimethylheptane	-	-	-	-	-	-	-	-	-	-	0.001	0.001	0.001	-
2,4-Dimethylheptane	-	-	-	-	-	-	0.008	0.008	-	-	0.003	0.002	0.002	0.002

Table B-2 (continued)

Method / Compound	Transfer Bag Concentration (ppm) [a]													
Chamber Run Number	DTC588	DTC589	DTC591	DTC592	DTC593	DTC594	DTC595	DTC596	DTC572	DTC575	DTC574	DTC576	DTC581	DTC577
Vehicle or Fuel	M100	M100	M85	M85	M85	M85	M85	M85	CNG	Rep	Rep	Rep	Rep	Rep
3,5-Dimethylheptane	-	-	-	-	-	-	-	-	-	-	0.003	-	0.003	-
2,2,5-Trimethylhexane	-	-	-	-	-	-	-	-	-	-	0.012	0.015	0.012	0.011
2,3,5-Trimethylhexane	-	-	-	-	-	-	-	-	-	-	0.002	0.002	0.002	0.002
2-Methyloctane	-	-	-	-	-	-	-	-	-	-	0.001	0.001	0.006	-
3-Methyloctane	-	-	-	-	-	-	-	-	-	-	0.004	0.005	0.004	0.004
2,2-Dimethyloctane	-	-	0.008	-	-	-	-	-	-	-	-	0.001	-	0.001
2,4-Dimethyloctane	0.001	0.001	0.001	0.001	-	0.002	-	0.002	-	-	0.018	0.023	0.017	0.017
Cyclopentane	0.004	0.007	0.006	-	-	-	-	-	-	-	0.003	0.004	0.003	0.002
Methylcyclopentane	-	0.004	0.005	-	0.001	-	-	0.002	-	-	0.023	0.029	0.020	0.021
Cyclohexane	-	0.006	-	-	0.002	-	-	-	-	-	0.004	0.004	0.004	-
t-1,2-Dimethylcyclopentane	-	-	-	-	-	-	-	-	-	-	-	-	-	-
c-1,3-Dimethylcyclopentane	-	-	-	-	-	-	-	-	-	-	0.007	0.008	0.007	0.007
Methylcyclohexane	-	-	-	-	0.002	-	-	-	-	-	0.014	0.020	0.014	0.014
1c,2t,3-Trimethylcyclopentane	-	-	-	-	-	-	-	-	-	-	-	-	-	-
c-1,2-Dimethylcyclohexane	-	0.003	-	-	-	-	0.002	-	-	-	0.003	0.003	0.002	0.002
c-1,3-Dimethylcyclohexane	0.003	0.004	-	-	0.002	-	-	0.003	0.007	-	0.004	0.004	0.004	0.004
t-1,3-Dimethylcyclohexane	-	-	-	-	-	-	-	0.002	-	-	0.002	0.002	0.002	0.002
t-1,4-Dimethylcyclohexane	-	0.002	-	-	-	-	-	-	-	-	0.001	0.002	0.002	0.002
Ethylcyclohexane	-	-	-	-	-	-	-	-	-	-	-	-	-	0.002
Ethene	-	0.000	0.025	0.007	0.034	-	0.023	0.018	0.004	0.033	0.377	0.531	0.352	0.522
Propene	-	-	-	-	-	-	-	-	-	-	-	-	0.003	-
1-Butene	-	-	0.008	0.006	0.013	-	-	-	-	-	0.031	-	-	-
c-2-Butene	-	-	-	-	-	0.005	-	-	-	-	0.010	0.014	-	0.009
t-2-Butene	-	-	-	-	-	-	-	-	-	-	0.032	0.019	-	0.107
2-Methylpropene	0.005	0.007	-	-	-	-	-	-	-	-	-	0.274	0.197	0.186
1-Pentene	-	-	-	-	-	-	0.006	0.006	-	-	0.003	0.005	0.004	0.003
c-2-Pentene	-	-	-	-	-	-	-	-	-	-	0.003	0.004	0.003	0.003
t-2-Pentene	-	0.005	-	-	-	-	-	-	-	-	0.004	0.007	0.007	0.005
2-Methyl-1-Butene	-	-	-	-	-	-	-	-	-	-	0.011	0.014	0.011	0.010
3-Methyl-1-Butene	-	-	-	-	-	-	-	-	-	-	0.004	0.005	0.003	0.003
2-Methyl-2-Butene	-	-	-	-	-	-	-	-	-	-	0.013	0.018	0.013	0.012
1-Hexene	-	-	-	-	-	-	-	-	-	-	-	0.003	-	0.002
c-2-Hexene	-	-	-	0.003	-	-	-	0.003	-	-	-	0.002	-	-
t-2-Hexene	-	-	-	-	-	-	-	-	-	-	0.003	0.003	0.002	0.002
c-3-Hexene	-	-	-	-	-	-	-	-	-	-	-	-	-	-
t-3-Hexene	-	-	-	-	-	-	-	-	-	-	-	0.002	0.002	-
2-Methyl-1-Pentene	-	-	-	-	-	-	-	-	-	-	-	0.002	0.002	0.002
3-Methyl-1-Pentene	-	-	-	-	-	-	-	-	-	-	-	-	-	-
4-Methyl-1-Pentene	-	-	-	-	-	-	-	-	-	-	-	0.002	-	-
2-Methyl-2-Pentene	-	-	-	-	-	-	-	-	-	-	0.004	0.004	0.005	0.006
3-Methyl-c-2-Pentene	0.003	-	-	-	-	-	-	-	-	-	0.004	0.004	0.003	0.003
3-Methyl-t-2-Pentene	-	-	0.002	-	-	-	-	-	-	-	0.020	0.003	0.003	0.003
4-Methyl-c-2-Pentene	-	-	-	-	-	-	-	-	-	-	-	0.024	0.003	0.018
4-Methyl-t-2-Pentene	-	-	-	-	-	-	0.003	-	-	-	-	-	-	-
3,3-Dimethyl-1-Butene	-	-	-	-	-	-	-	-	-	-	-	-	0.001	-
1-Heptene	-	-	-	-	-	-	-	-	-	-	-	-	-	-

Table B-2 (continued)

Method / Compound	Transfer Bag Concentration (ppm) [a]													
Chamber Run Number	DTC588	DTC589	DTC591	DTC592	DTC593	DTC594	DTC595	DTC596	DTC572	DTC575	DTC574	DTC576	DTC581	DTC577
Vehicle or Fuel	M100	M100	M85	M85	M85	M85	M85	M85	CNG	Rep	Rep	Rep	Rep	Rep
c-2-Heptene	-	-	-	-	-	-	-	-	-	-	-	-	-	-
t-2-Heptene	-	-	-	-	-	-	-	-	-	-	-	-	-	-
t-3-Heptene	0.002	-	-	-	-	-	-	-	-	-	-	-	-	-
2,3-Dimethyl-2-Pentene	-	-	-	-	-	0.002	-	-	-	-	-	-	-	-
3,4-Dimethyl-1-Pentene	-	-	-	-	-	-	-	-	-	-	-	-	-	-
3-Methyl-1-Hexene	-	-	-	-	-	-	-	-	-	-	-	-	-	-
2-Methyl-2-Hexene	-	-	-	-	-	-	-	-	-	-	-	0.002	0.001	-
3-Methyl-t-3-Hexene	-	-	-	-	-	-	0.001	-	-	-	-	-	-	-
1-Octene	-	-	-	-	-	-	-	-	-	-	0.001	0.002	0.002	0.002
c-2-Octene	-	0.002	-	-	-	-	-	-	0.001	-	-	0.002	0.002	0.002
t-2-Octene	-	-	-	-	-	0.002	-	-	-	-	-	-	-	-
t-4-Octene	-	-	-	-	-	-	-	-	-	-	-	0.001	0.001	-
2,4,4-Trimethyl-1-Pentene	-	0.002	-	-	-	-	-	-	-	-	-	-	-	-
2,4,4-Trimethyl-2-Pentene	-	-	-	-	-	-	-	-	-	-	-	-	-	-
3-Ethyl-c-2-Pentene	-	-	-	-	-	-	-	0.001	-	-	-	-	-	-
1-Nonene	-	0.003	0.001	0.002	-	-	0.004	0.005	0.001	-	0.002	0.004	0.004	0.003
Propadiene	-	-	-	-	-	-	-	-	-	-	-	-	-	-
1,3-Butadiene	-	-	-	-	-	-	-	-	-	-	0.031	0.037	0.032	0.028
2-Methyl-1,3-Butadiene	-	-	-	-	-	-	-	-	-	-	0.013	0.017	0.014	0.006
Cyclopentadiene	-	-	-	-	-	-	-	-	-	-	0.009	0.011	0.009	0.009
Cyclopentene	-	-	-	-	-	-	-	-	-	-	0.003	0.003	0.003	0.007
1-Methylcyclopentene	-	-	-	-	-	-	-	-	-	-	-	-	-	-
3-Methylcyclopentene	-	-	0.005	-	-	-	-	-	-	-	-	-	-	-
Cyclohexene	-	-	-	-	-	-	-	-	-	-	-	0.002	-	-
Ethyne	-	-	-	-	-	-	-	-	-	-	0.033	0.066	0.060	0.060
Propyne	-	-	-	-	-	-	-	-	-	-	-	-	-	-
1-Butyne	-	-	-	-	-	-	-	-	-	-	-	-	-	-
2-Butyne	-	-	-	-	-	-	-	-	-	-	-	-	-	0.005
Benzene	0.003	0.012	0.013	0.007	0.021	0.008	0.014	0.011	-	-	0.097	0.141	0.095	0.091
Toluene	-	0.009	0.012	0.004	0.016	0.004	0.010	0.010	-	-	0.197	0.273	0.203	0.188
Ethylbenzene	-	0.002	0.002	0.002	0.003	0.001	0.002	0.003	-	-	0.053	0.070	0.049	0.049
o-Xylene	-	0.002	0.002	0.001	0.004	0.001	0.005	0.003	-	-	0.049	0.065	0.047	0.043
m&p-Xylene	-	0.005	0.006	0.003	0.011	0.006	0.013	0.014	-	-	0.144	0.195	0.145	0.134
n-Propylbenzene	-	-	0.001	-	-	-	-	-	-	-	0.006	0.009	0.007	0.007
i-Propylbenzene	-	-	-	-	-	-	-	-	-	-	0.001	0.001	0.002	0.001
1-Methyl-2-ethylbenzene	0.002	-	0.001	-	-	-	-	-	-	-	0.013	0.016	0.013	0.012
1-Methyl-3-ethylbenzene	0.001	0.001	0.002	0.002	-	0.002	0.002	0.003	-	-	0.039	0.052	0.036	0.039
1-Methyl-4-ethylbenzene	-	-	0.001	0.001	0.001	-	0.002	0.002	0.000	-	0.014	0.021	0.015	0.016
1,2-Dimethyl-3-ethylbenzene	-	-	0.029	-	-	-	-	-	-	-	0.001	0.002	0.001	0.001
1,2-Dimethyl-4-ethylbenzene	0.001	-	0.002	-	-	-	-	0.001	-	-	0.007	0.008	0.006	0.005
1,3-Dimethyl-2-ethylbenzene	-	-	0.049	-	-	-	-	-	-	-	0.002	0.002	-	0.001
1,3-Dimethyl-4-ethylbenzene	0.003	0.003	0.001	0.004	-	0.005	-	0.007	-	-	0.004	0.005	0.004	0.003
1,4-Dimethyl-2-ethylbenzene	-	0.001	0.001	-	-	-	0.007	-	-	-	0.005	0.007	0.005	0.004
1,2,3-Trimethylbenzene	0.003	-	0.001	0.001	0.001	0.002	0.001	0.002	-	-	0.009	0.012	0.009	0.011
1,2,4-Trimethylbenzene	0.001	0.003	0.005	0.001	0.004	0.003	0.001	0.003	-	-	0.048	0.067	0.049	0.046
1,3,5-Trimethylbenzene	0.001	-	0.002	0.001	0.002	0.001	0.001	0.001	-	-	0.017	0.024	0.018	0.017

Table B-2 (continued)

Method / Compound	Transfer Bag Concentration (ppm) [a]													
Chamber Run Number	DTC588	DTC589	DTC591	DTC592	DTC593	DTC594	DTC595	DTC596	DTC572	DTC575	DTC574	DTC576	DTC581	DTC577
Vehicle or Fuel	M100	M100	M85	M85	M85	M85	M85	M85	CNG	Rep	Rep	Rep	Rep	Rep
Indan	0.030	-	-	-	-	-	-	-	-	-	0.003	0.005	0.004	0.003
i-Butylbenzene	-	-	-	-	-	-	-	0.001	-	-	-	-	-	-
s-Butylbenzene	-	-	-	-	-	-	-	-	-	-	-	-	-	-
2-Methyl-Butylbenzene	-	-	-	-	-	-	-	-	-	-	-	-	-	-
tert-1-Butyl-2-Methyl-Benzene	-	-	-	-	-	-	-	-	-	-	-	-	-	-
tert-1-Butyl-3,5-Dimethyl-Benzene	0.004	0.017	0.008	0.012	-	0.031	0.038	0.041	-	-	0.001	0.001	0.001	0.001
1,2-Diethylbenzene	-	-	-	-	-	-	-	-	-	-	0.005	0.008	0.006	0.005
1,3-Diethylbenzene	-	-	-	-	-	-	-	-	-	-	0.003	0.005	0.003	0.003
1,4-Diethylbenzene	-	-	-	-	-	-	-	-	-	-	0.005	0.007	0.006	0.005
1-Methyl-2-n-Propylbenzene	-	-	-	-	-	-	-	-	-	-	0.005	0.006	0.006	0.004
1-Methyl-3-n-Propylbenzene	-	-	0.001	-	-	-	0.014	0.001	-	-	-	-	-	-
1-Methyl-4-n-Propylbenzene	0.022	0.007	-	0.005	0.003	0.013	-	0.015	0.002	-	0.006	0.012	0.009	0.008
1-Methyl-2-i-Propylbenzene	-	-	-	-	-	-	-	-	-	-	0.001	0.001	0.001	-
1-Methyl-3-i-Propylbenzene	-	-	-	-	-	-	-	-	-	-	-	-	-	-
1-Methyl-4-i-Propylbenzene	-	-	-	-	-	0.025	0.032	0.028	-	-	-	-	-	-
1,2,3,4-Tetramethylbenzene	-	-	-	-	-	-	-	-	0.003	-	0.002	0.003	0.002	0.002
1,2,3,5-Tetramethylbenzene	-	-	-	-	-	-	-	-	-	-	0.005	0.004	0.005	0.004
1,2,4,5-Tetramethylbenzene	-	-	-	-	-	-	-	-	-	-	0.003	-	0.003	0.002
n-Pent-Benzene	-	0.035	0.016	0.020	-	0.064	0.089	0.082	-	-	0.001	0.006	0.003	0.004
Styrene	-	-	0.022	-	-	-	-	-	0.003	-	0.019	0.023	0.018	0.019
Naphthalene	0.005	0.013	0.008	0.010	0.002	0.021	0.030	0.027	0.009	-	0.002	0.015	0.011	0.008
Methyl-t-Butyl-Ether	-	-	-	-	-	-	-	-	-	-	0.025	0.028	0.030	0.022
Ethyl-t-Butyl-Ether	-	-	-	-	-	-	-	-	-	-	0.002	-	-	-
Results of Oxygenate Analysis (ppm)														
Formaldehyde	-	3.512	1.258	0.930	1.252	0.949	0.797	1.174	0.283	0.192	0.443	0.491	0.422	0.378
Acetaldehyde	-	0.002	0.003	0.000	0.001	-	0.001	-	-	-	0.030	0.037	0.030	0.025
Propionaldehyde	-	-	-	-	-	-	-	-	-	-	0.001	-	-	-
Acrolein	-	-	0.001	-	-	-	-	0.017	-	-	0.023	-	0.019	0.025
Methacrolein	-	-	-	-	-	-	-	-	-	-	-	-	0.010	-
n-Butyraldehyde	-	-	-	-	-	-	-	-	-	-	0.007	0.004	-	0.007
Crotonaldehyde	-	-	-	-	-	-	-	-	-	-	-	-	-	-
Pentanaldehyde	-	-	-	-	-	-	-	-	-	-	-	-	-	0.031
Hexanaldehyde	-	-	0.013	0.012	-	-	-	-	-	-	-	0.009	0.004	0.006
Benzaldehyde	-	-	-	-	-	-	-	-	-	-	0.028	0.030	0.028	-
p-Tolualdehyde	-	-	-	0.012	0.003	-	0.002	-	-	-	0.029	0.031	0.026	-
Acetone	-	-	-	-	-	-	-	-	-	-	-	-	-	0.004
Butanone	-	-	-	-	-	-	-	-	-	-	-	-	-	-
Results of Impinger Analysis (ppm)														
Methanol	65.223	28.815	18.029	35.547	32.304	16.427	40.522	-	-	0.496	0.771	0.636	0.831	
GC-FID Unknowns (ppmC)														
Unknown (C1-C4)	-								-			2.641	-	2.025
Unknown (C4-C12)	0.206											0.921	-	0.582

[b] Aborted Experiments

B-9

Table B-2 (continued)

Method / Compound	Transfer Bag Concentration (ppm) [a]										
Chamber Run Number	DTC584	DTC585	DTC586	DTC582	DTC583	DTC661	DTC662	DTC663	DTC665	DTC666	DTC667
Vehicle or Fuel [b]	Sub'n	Sub'n	Sub'n	Taurus	Taurus	Toyota	Toyota	Toyota	Accord	Accord	Accord
Total Measured NMHC (ppmC)	88.57	45.51	63.20	1.33	4.56	93.00	109.15	103.84	8.45	13.42	13.33
Total Unknowns (ppmC)						18.49	20.57	22.06	1.35	1.70	2.43
Total NMHC (ppmC)	88.57	45.51	63.20	1.33	4.56	111.49	129.72	125.90	9.80	15.12	15.76
Percent Unknowns (ppmC)						17%	16%	18%	14%	11%	15%
GC-FID Analysis (ppm)											
Methane	8.416	4.577	5.787	1.136	2.517	7.691	7.841	7.760	3.235	3.311	3.234
Ethane	0.576	0.414	0.501	0.112	0.212	0.452	0.568	0.491	0.116	0.158	0.174
Propane	0.015	0.009	0.017	-	0.002	0.029	0.026	0.023	0.006	0.008	0.006
Butane	0.095	0.053	0.061	0.016	0.033	0.167	0.208	0.195	0.017	0.020	0.021
Pentane	0.308	0.172	0.216	0.013	0.027	0.431	0.523	0.506	0.029	0.038	0.038
Hexane	0.222	0.120	0.154	0.004	0.011	0.224	0.258	0.254	0.020	0.028	0.028
Heptane	0.125	0.065	0.083	0.002	0.004	0.125	0.163	0.156	0.008	0.009	0.009
Octane	0.062	0.031	0.043	0.001	0.002	0.064	0.074	0.072	0.004	0.005	0.005
Nonane	0.020	0.011	0.016	-	0.001	0.025	0.029	0.028	0.002	0.002	0.002
Decane	0.006	0.002	0.004	-	-	0.013	0.015	0.015	0.001	0.001	0.001
Undecane	0.025	0.012	0.020	-	0.004	0.006	0.006	0.007	-	-	-
Dodecane	0.002	-	-	-	-	0.040	0.005	0.004	0.002	0.001	0.001
2-Methylpropane	0.019	0.013	0.017	-	0.006	0.030	0.037	0.035	-	-	-
2,2-Dimethylpropane	-	-	-	0.005	-	-	-	-	0.101	-	0.032
2-Methylbutane	0.622	0.355	0.439	0.022	0.047	1.021	1.250	1.189	0.044	0.061	0.065
2,2-Dimethylbutane	0.025	0.016	0.020	0.002	0.005	0.150	0.178	0.168	0.002	0.003	0.003
2,3-Dimethylbutane	0.084	0.048	0.061	0.002	0.005	0.128	0.150	0.142	0.005	0.010	0.010
2-Methylpentane	0.274	0.168	0.183	0.012	0.026	0.462	0.537	0.518	0.033	0.048	0.048
3-Methylpentane	0.174	0.097	0.119	0.005	0.010	0.283	0.327	0.320	-	0.022	0.022
2,2,3-Trimethylbutane	0.004	0.003	0.004	-	-	0.007	0.008	0.008	0.003	0.002	0.002
2,2-Dimethylpentane	-	-	0.005	-	-	0.010	-	-	-	-	-
2,3-Dimethylpentane	0.190	0.099	0.128	0.003	0.007	0.119	0.137	0.133	0.008	0.011	0.011
2,4-Dimethylpentane	0.106	0.058	0.075	0.002	0.004	0.074	0.084	0.084	0.005	0.006	0.006
3,3-Dimethylpentane	0.003	0.002	0.003	-	-	0.015	0.018	0.016	-	-	-
2-Methylhexane	0.127	0.067	0.086	0.002	0.005	0.163	0.189	0.184	0.009	0.014	0.014
3-Methylhexane	0.139	0.072	0.093	0.003	0.006	0.168	0.194	0.188	0.010	0.014	0.014
2,2,4-Trimethylpentane	0.217	0.113	0.146	0.005	0.011	0.108	0.170	0.161	0.006	0.009	0.009
2,3,3-Trimethylpentane	0.002	0.002	0.002	-	-	-	-	-	-	-	-
2,3,4-Trimethylpentane	0.081	0.040	0.051	0.001	0.003	0.052	0.062	0.059	0.003	0.004	0.004
3-Ethylpentane	0.047	0.025	0.034	-	0.002	0.069	0.080	0.077	0.004	0.005	0.005
2,2-Dimethylhexane	0.008	0.004	0.006	-	-	0.012	0.020	0.016	-	-	-
2,3-Dimethylhexane	0.043	0.019	0.026	-	0.002	0.029	0.037	0.035	0.002	0.001	0.001
2,4-Dimethylhexane	0.055	0.026	0.035	-	0.002	0.042	0.049	0.047	0.002	0.003	0.003
2,5-Dimethylhexane	0.051	0.025	0.034	-	0.003	0.055	0.064	0.062	0.002	0.004	0.004
3,3-Dimethylhexane	0.018	0.009	0.012	-	0.002	0.027	0.032	0.031	0.002	0.001	0.001
2-Methylheptane	0.065	0.032	0.043	-	0.002	0.074	0.086	0.084	0.004	0.005	0.005
3-Methylheptane	0.024	0.012	0.016	-	-	0.075	0.106	0.103	0.004	0.004	0.004
4-Methylheptane	0.024	0.012	0.016	-	-	0.026	0.031	0.030	0.001	0.002	0.002
2,3-Dimethylheptane	0.006	0.004	0.005	-	-	0.008	0.010	0.010	-	-	-
2,4-Dimethylheptane	0.011	0.006	0.009	-	-	0.018	0.021	0.020	-	-	-

Table B-2 (continued)

Method / Compound	Transfer Bag Concentration (ppm) [a]										
Chamber Run Number	DTC584	DTC585	DTC586	DTC582	DTC583	DTC661	DTC662	DTC663	DTC665	DTC666	DTC667
Vehicle or Fuel	Sub'n	Sub'n	Sub'n	Taurus	Taurus	Toyota	Toyota	Toyota	Accord	Accord	Accord
3,5-Dimethylheptane	-	0.007	0.014	-	-	0.023	-	0.026	-	-	-
2,2,5-Trimethylhexane	0.047	0.023	0.032	-	0.002	0.022	0.026	0.025	0.002	0.003	0.003
2,3,5-Trimethylhexane	0.010	-	-	-	-	-	-	0.010	-	-	-
2-Methyloctane	0.006	0.004	0.005	-	-	0.044	0.051	0.051	0.002	0.003	0.003
3-Methyloctane	0.028	0.015	0.022	-	0.002	0.036	0.041	0.041	0.002	0.002	0.002
2,2-Dimethyloctane	0.005	0.003	0.004	-	-	-	-	-	-	0.001	0.001
2,4-Dimethyloctane	0.041	0.024	0.031	-	0.001	0.055	0.071	0.059	0.006	0.008	0.008
Cyclopentane	0.044	0.025	0.032	-	0.003	0.071	0.082	0.080	0.003	0.005	0.005
Methylcyclopentane	0.227	0.121	0.151	-	0.011	0.327	0.389	0.383	0.015	0.020	0.020
Cyclohexane	0.081	0.042	0.055	0.002	0.005	0.185	0.211	0.209	0.008	0.012	0.012
t-1,2-Dimethylcyclopentane	-	-	-	-	-	-	-	-	0.002	0.004	0.004
c-1,3-Dimethylcyclopentane	0.036	0.019	0.025	-	0.002	0.056	0.065	0.063	0.003	0.004	0.004
Methylcyclohexane	0.081	0.039	0.053	0.001	0.004	0.139	0.163	0.159	0.007	0.007	0.007
1c,2t,3-Trimethylcyclopentane	-	-	-	-	-	-	-	-	-	-	-
c-1,2-Dimethylcyclohexane	0.014	0.007	0.010	-	-	0.025	0.029	0.028	-	-	-
c-1,3-Dimethylcyclohexane	0.019	0.009	0.012	-	-	0.043	0.051	0.049	0.001	0.002	0.002
t-1,3-Dimethylcyclohexane	0.015	0.007	0.009	-	-	0.032	0.042	0.041	0.003	0.001	0.001
t-1,4-Dimethylcyclohexane	0.006	0.003	0.004	-	-	0.015	0.018	0.018	-	-	-
Ethylcyclohexane	0.006	0.004	0.006	-	-	0.020	0.023	0.023	0.001	-	-
Ethene	5.036	2.874	4.099	0.024	0.124	3.480	4.341	3.954	0.763	1.158	1.247
Propene	1.615	-	-	-	0.044	1.429	1.796	1.592	0.246	0.370	0.398
1-Butene	-	-	-	-	-	-	-	-	-	-	-
c-2-Butene	0.109	0.053	0.079	-	0.004	-	-	-	-	0.015	0.015
t-2-Butene	0.198	0.146	0.182	-	0.040	-	-	-	-	-	-
2-Methylpropene	1.626	0.980	1.297	-	0.037	0.983	1.186	1.168	-	0.184	-
1-Pentene	0.034	0.019	0.026	-	0.006	0.046	0.057	0.051	0.003	0.004	0.004
c-2-Pentene	0.021	0.013	0.017	-	-	0.034	0.041	0.039	0.003	0.003	0.003
t-2-Pentene	0.033	0.023	0.028	-	-	0.062	0.074	0.069	0.004	0.005	0.005
2-Methyl-1-Butene	0.047	0.028	0.037	-	0.002	0.086	0.103	0.097	0.009	0.013	0.013
3-Methyl-1-Butene	0.023	0.016	0.022	-	-	0.033	0.040	0.035	0.002	0.003	0.003
2-Methyl-2-Butene	0.092	0.058	0.077	-	0.003	0.098	0.115	0.112	0.010	0.014	0.014
1-Hexene	0.022	0.008	0.012	-	-	0.020	0.024	0.021	-	-	-
c-2-Hexene	0.006	0.003	0.005	-	-	0.010	0.011	-	-	-	-
t-2-Hexene	0.012	0.007	0.009	-	-	0.020	0.023	0.023	0.001	0.002	0.002
c-3-Hexene	0.008	-	-	-	-	-	-	-	-	-	-
t-3-Hexene	-	0.005	0.006	-	-	-	-	-	-	-	-
2-Methyl-1-Pentene	-	0.004	0.005	-	-	0.016	0.018	0.018	-	-	-
3-Methyl-1-Pentene	0.009	0.006	0.009	-	-	0.014	0.017	0.017	-	-	-
4-Methyl-1-Pentene	-	-	-	-	-	-	-	-	-	0.007	0.007
2-Methyl-2-Pentene	0.018	0.006	0.007	-	-	0.011	0.033	0.032	0.002	0.002	0.002
3-Methyl-c-2-Pentene	0.016	0.008	0.012	-	-	0.021	0.023	0.026	0.003	0.002	0.002
3-Methyl-t-2-Pentene	0.080	0.041	0.065	-	0.005	0.040	0.046	0.045	0.003	0.003	0.003
4-Methyl-c-2-Pentene	-	-	-	-	-	0.015	0.016	0.014	-	-	-
4-Methyl-t-2-Pentene	0.005	0.007	0.009	-	-	0.015	0.016	0.014	-	0.002	-
3,3-Dimethyl-1-Butene	0.003	0.002	0.003	-	-	0.004	0.004	0.003	-	-	-
1-Heptene	-	-	-	-	-	0.040	-	-	-	-	-

Table B-2 (continued)

Method / Compound	Transfer Bag Concentration (ppm) [a]										
Chamber Run Number	DTC584	DTC585	DTC586	DTC582	DTC583	DTC661	DTC662	DTC663	DTC665	DTC666	DTC667
Vehicle or Fuel	Sub'n	Sub'n	Sub'n	Taurus	Taurus	Toyota	Toyota	Toyota	Accord	Accord	Accord
c-2-Heptene	0.005	0.003	0.004	-	-	0.005	0.008	0.006	-	-	-
t-2-Heptene	0.003	0.002	0.003	-	-	-	-	-	-	-	-
t-3-Heptene	-	-	-	-	-	-	-	-	-	-	-
2,3-Dimethyl-2-Pentene	-	-	-	-	-	-	-	-	-	-	-
3,4-Dimethyl-1-Pentene	0.003	0.003	0.003	-	-	0.004	0.005	0.005	-	-	-
3-Methyl-1-Hexene	-	0.001	-	-	-	-	-	-	-	-	-
2-Methyl-2-Hexene	0.009	0.005	0.007	-	-	0.010	-	-	-	-	-
3-Methyl-t-3-Hexene	-	-	-	-	-	-	-	-	-	-	-
1-Octene	0.014	0.007	0.010	-	-	0.027	0.032	0.030	-	0.001	0.001
c-2-Octene	0.004	0.003	0.001	-	-	-	0.013	0.013	-	-	-
t-2-Octene	0.002	0.002	0.003	-	-	-	-	-	-	-	-
t-4-Octene	0.002	0.003	0.004	-	-	-	-	-	-	-	-
2,4,4-Trimethyl-1-Pentene	0.003	0.002	0.002	-	-	0.006	0.008	0.007	-	-	-
2,4,4-Trimethyl-2-Pentene	0.001	-	0.002	-	-	-	0.003	0.002	-	-	-
3-Ethyl-c-2-Pentene	0.001	-	-	-	-	0.005	0.007	0.005	-	-	-
1-Nonene	0.015	0.008	0.012	-	-	0.022	0.025	0.025	-	0.001	0.001
Propadiene	-	0.027	0.047	-	-	0.071	-	-	-	-	-
1,3-Butadiene	0.214	0.117	0.179	-	0.004	0.198	0.259	0.214	0.040	0.068	0.073
2-Methyl-1,3-Butadiene	0.067	0.043	0.054	-	-	0.060	0.075	0.066	0.010	0.019	0.019
Cyclopentadiene	0.069	0.035	0.049	-	0.002	0.069	0.085	0.072	0.016	-	0.029
Cyclopentene	0.027	0.018	0.023	-	-	0.048	0.058	0.053	0.003	-	0.005
1-Methylcyclopentene	-	-	-	-	-	-	-	-	-	-	-
3-Methylcyclopentene	-	-	-	-	-	-	-	-	-	-	-
Cyclohexene	0.009	0.006	0.009	-	-	0.031	0.036	0.033	-	0.003	0.003
Ethyne	1.404	0.265	0.619	-	-	1.320	1.662	1.464	0.030	0.333	0.326
Propyne	-	-	-	-	-	-	-	-	-	-	-
1-Butyne	-	-	-	-	-	0.005	0.007	0.005	-	-	-
2-Butyne	0.003	0.003	0.003	-	-	0.002	0.003	0.003	-	-	-
Benzene	0.513	0.297	0.426	0.010	0.027	0.503	0.581	0.553	0.079	0.125	0.125
Toluene	0.989	0.544	0.754	0.005	0.035	1.159	1.347	1.292	0.116	0.190	0.190
Ethylbenzene	0.186	0.100	0.143	0.003	0.005	0.202	0.237	0.229	0.019	0.031	0.031
o-Xylene	0.246	0.132	0.193	0.003	0.011	0.264	0.305	0.291	0.025	0.041	0.041
m&p-Xylene	0.669	0.356	0.516	0.007	0.027	0.721	0.834	0.798	0.068	0.114	0.114
n-Propylbenzene	0.030	0.015	0.024	-	0.001	0.042	-	0.047	0.003	0.004	0.004
i-Propylbenzene	0.009	0.005	0.008	-	-	0.010	0.011	0.011	-	-	-
1-Methyl-2-ethylbenzene	0.053	0.027	0.043	0.002	0.003	0.063	0.074	0.070	0.006	0.009	0.009
1-Methyl-3-ethylbenzene	0.142	0.073	0.112	0.003	0.009	0.160	0.179	0.168	0.017	0.025	0.025
1-Methyl-4-ethylbenzene	0.060	0.032	0.049	0.002	0.004	0.071	0.082	0.078	0.007	0.011	0.011
1,2-Dimethyl-3-ethylbenzene	0.005	0.003	0.004	-	-	0.006	0.005	0.007	-	-	-
1,2-Dimethyl-4-ethylbenzene	0.021	0.010	0.017	-	0.002	0.024	0.025	0.024	0.002	0.003	0.003
1,3-Dimethyl-2-ethylbenzene	0.003	0.002	0.003	-	-	0.005	0.005	0.005	-	-	-
1,3-Dimethyl-4-ethylbenzene	0.012	0.006	0.010	-	0.001	0.013	0.014	0.013	0.001	0.002	0.002
1,4-Dimethyl-2-ethylbenzene	0.015	0.010	0.012	-	0.002	0.018	0.018	0.018	0.002	0.002	0.002
1,2,3-Trimethylbenzene	0.046	0.023	0.037	0.001	0.005	0.046	0.052	0.049	0.005	0.006	0.006
1,2,4-Trimethylbenzene	0.217	0.106	0.172	0.003	0.015	0.231	0.265	0.246	0.024	0.039	0.039
1,3,5-Trimethylbenzene	0.069	0.035	0.055	0.002	0.005	0.087	0.099	0.095	0.007	0.011	0.011

Table B-2 (continued)

Method / Compound				Transfer Bag Concentration (ppm) [a]							
Chamber Run Number	DTC584	DTC585	DTC586	DTC582	DTC583	DTC661	DTC662	DTC663	DTC665	DTC666	DTC667
Vehicle or Fuel	Sub'n	Sub'n	Sub'n	Taurus	Taurus	Toyota	Toyota	Toyota	Accord	Accord	Accord
Indan	0.020	0.010	0.015	-	0.002	0.023	0.026	0.025	0.002	0.002	0.002
i-Butylbenzene	0.001	-	0.001	-	-	0.004	0.005	-	-	-	-
s-Butylbenzene	-	-	0.002	-	-	0.006	0.006	0.007	-	-	-
2-Methyl-Butylbenzene	-	-	0.007	-	-	-	0.009	-	-	-	-
tert-1-Butyl-2-Methyl-Benzene	0.002	0.001	0.002	-	-	-	-	-	-	-	-
tert-1-Butyl-3,5-Dimethyl-Benzene	0.002	0.001	0.002	-	-	0.002	0.002	0.002	-	-	-
1,2-Diethylbenzene	0.003	0.002	0.002	-	-	0.007	0.006	0.007	-	-	-
1,3-Diethylbenzene	0.022	0.001	0.002	-	0.001	0.003	0.003	0.004	-	-	-
1,4-Diethylbenzene	0.009	0.005	0.007	-	-	0.013	0.014	0.012	0.001	0.001	0.001
1-Methyl-2-n-Propylbenzene	0.017	0.008	0.010	-	0.001	0.018	0.020	0.018	-	0.002	0.002
1-Methyl-3-n-Propylbenzene	0.019	0.009	0.013	-	0.002	0.022	0.025	0.024	0.001	0.002	0.002
1-Methyl-4-n-Propylbenzene	0.028	0.013	0.023	-	0.005	0.036	0.040	0.039	0.007	0.005	0.005
1-Methyl-2-i-Propylbenzene	-	-	-	-	-	-	-	-	-	-	-
1-Methyl-3-i-Propylbenzene	0.004	0.003	0.003	-	-	0.006	0.008	0.007	-	-	-
1-Methyl-4-i-Propylbenzene	-	-	-	-	-	0.003	0.003	0.004	-	-	-
1,2,3,4-Tetramethylbenzene	0.009	0.004	0.006	-	0.001	0.007	0.007	0.008	-	-	-
1,2,3,5-Tetramethylbenzene	0.017	0.007	0.012	-	0.002	0.017	0.017	0.016	0.002	0.002	0.002
1,2,4,5-Tetramethylbenzene	0.011	0.005	-	-	0.001	0.010	-	0.012	0.001	0.001	0.001
n-Pent-Benzene	-	0.001	0.004	-	-	0.010	0.011	0.010	0.001	0.001	0.001
Styrene	0.062	0.035	0.056	-	0.002	0.066	0.080	0.082	0.011	0.020	0.020
Naphthalene	0.025	0.012	0.020	-	0.004	0.023	0.019	0.019	-	0.003	0.003
Methyl-t-Butyl-Ether	0.059	-	0.073	-	-	0.832	0.983	0.893	-	-	-
Ethyl-t-Butyl-Ether	0.002	-	-	-	-	-	-	-	-	-	-
Results of Oxygenate Analysis (ppm)											
Formaldehyde	0.933	0.649	0.848	0.070	0.125						
Acetaldehyde	0.324	0.195	0.253	0.001	0.005						
Propionaldehyde	0.017	0.004	0.003	-	-						
Acrolein	0.160	0.097	0.112	-	0.015						
Methacrolein	0.009	0.004	0.003	-	-						
n-Butyraldehyde	-	0.009	0.013	-	-						
Crotonaldehyde	0.006	-	-	-	-						
Pentanaldehyde	-	0.001	0.004	-	-						
Hexanaldehyde	-	-	-	-	-						
Benzaldehyde	0.059	0.032	0.048	0.000	-						
p-Tolualdehyde	0.054	0.037	0.038	-	-						
Acetone	0.025	0.011	0.016	-	-						
Butanone	0.020	0.005	0.006	-	0.002						
Results of Impinger Analysis (ppm)											
Methanol	1.001	0.681	0.786	0.090	0.200						
GC-FID Unknowns (ppmC)											
Unknown (C1-C4)						14.267	15.756	16.752	1.206	1.349	2.068
Unknown (C4-C12)						4.227	4.811	5.307	0.142	0.352	0.363

[a] "-" means that compound was not detected; (blank) means that analysis was not carried out.

B-13

APPENDIX C
CHRONOLOGICAL RUN LISTING

A chronological listing of all the environmental chamber experiments carried out for this program is given in Table C-1. For each experiment, this gives the run number, the date the run was carried out, the run title, a description and indication of the purpose of the experiment, and a brief summary of the results of the experiment, including the results of model simulations, where applicable. In most cases, detailed data from the experiments can be obtained from the authors in computer readable format (see Carter et al, 1995c).

Table C-1. Chronological listing of the environmental chamber experiments carried out for this program.

RunID	Date	Title	Description / Purpose	Results / Comments
DTC331	4/3/96	Propene - NOx	Standard 1 ppm propene, 0.5 ppm NOx run.	Control experiment for comparison with similar runs. Results as expected.
DTC333	4/11/96	Pure Air Irradiation	No injections	Control run to test for chamber contamination and evaluate chamber effects model. Approximately 30 ppb of ozone formed in each side after 6 hours irriadiation. Results as expected and consistent with chamber effects model.
DTC334	4/12/96	CO + NOx	~50 ppm CO and ~0.15 ppm NOx injected in both sides.	Control run to evaluate chamber radical source. Results consistent with predictions of chamber effects model.
DTC339	4/23/96	Mini-Surrogate + Warm Stabilized LPG Exhaust (Both sides)	Mini-surrogate VOC components and LPG exhaust (warm stabilized), and supplemental NOx injected into both sides of chamber.	Run primarily for testing methods. Low levels of propane only significant VOC found in exhaust. Results similar to standard mini-surrogate run. Good side equivalency. Results consistent with model predictions.
DTC340	4/24/96	Mini-Surrogate + Warm Stabilized LPG Exhaust (A)	Mini-surrogate VOC components injected into both sides of chamber. Exhaust from warm stabilized LPG vehicle injected into side A. NOx injected separately in each side to equalize amount of NOx.	Reactivity experiment to determine the effect of adding LPG exhaust to a standard mini-surrogate - NOx experiment. Small but measurable effect of exhaust. Small amounts of propane and ethene present. Results consistent with model predictions.
DTC341	4/25/96	n-Butane + Chlorine Actinometry	Run started in the afternoon after an aborted LPG exhaust run. ~0.8 ppm n-butane and 0.3 ppm chlorine irriadiated for 1.75 hours, with n-butane decay monitored.	Run to measure light intensity from rate of photolysis of Cl2 as measured by n-butane consumption due to reaction with Cl. Rate of n-butane consumption corresponded to an NO_2 photolysis rate of 0.216 min^{-1}.

Table C-1, Continued

RunID	Date	Title	Description / Purpose	Results / Comments [a]
DTC342	4/26/96	Mini-surrogate and LPG Emissions + Formaldehyde (A)	Mini-surrogate, LPG exhaust (warm stabilized) and NOx injected into both sides, then formaldehyde injected into side A.	This run was intended to look at the effect of adding formaldehyde to LPG exhaust, but the mini-surrogate VOCs were also injected due to a misunderstanding. Looked like a mini-surrogate + formaldehyde reactivity experiments. Results as expected.
DTC343	4/29/96	NO$_2$ Actinometry	Quartz tube actinometry method used.	Run to measure light intensity from NO$_2$ photolysis rate measurement. Measured NO$_2$ photolysis rate was 0.209 min^{-1}.
DTC344	4/30/96	LPG Exhaust + Formaldehyde (A)	LPG exhaust injected into both sides of chamber, and formaldehyde injected into side A. No supplemental NOx injections (all NOx came from exhaust).	Run for mechanism evaluation of a low reactivity exhaust mixture. Model calculations indicate that difference between effect of adding formaldehyde is sensitive to reactivity characteristics of low-reactivity mixtures. Again, ~1 ppm propane only significant VOC exhaust component measured. Only minor amounts of O3 formed on both sides, but NO consumption much faster on added formaldehyde side. Model predictions consistent with experimental results in side with exhaust only, but overpredicted, by a factor of ~2, the NO oxidation and O3 formation rates on the added formaldehyde side.
DTC346	5/2/96	Propene + NOx	Standard 1 ppm propene, 0.5 ppm NOx run.	Control experiment for comparison with similar runs. Results as expected.

Table C-1, Continued

RunID	Date	Title	Description / Purpose	Results / Comments [a]
DTC347	5/3/96	n-Butane + NOx (RH~5%)	4 ppm n-butane and 0.25 ppm NOx injected in both sides. Air humidified to 5% using water bubbler.	Run to measure chamber radical source under humidified conditions of added LPG runs. NO oxidation rate only slightly faster than predicted by standard chamber effects model for dry conditions. Good side equivalency.
DTC348	5/7/96	Cold Start LPG Exhaust + Formaldehyde (A)	Similar experimental conditions as run DTC-344 except LPG exhaust from cold start.	Cold start LPG exhaust found to have non-negligible amounts of ethene and propene, unlike previous runs. Much more rapid rate of NO oxidation and O3 formation than observed in run DTC-344, with ozone being formed on both sides. Ozone formation and NO oxidation faster on formaldehyde side. Results on both sides consistent with model predictions.
DTC349	5/8/96	Cold Start LPG Exhaust + Formaldehyde (B)	Repeat of DTC348, except formaldehyde injected into side B.	Slightly more exhaust VOCs than run DTC-348, but generally results were very similar. Consistent with model predictions on both sides.
DTC350	5/9/96	Synthetic LPG Exhaust + Formaldehyde (B)	Repeat of previous two runs except that synthetic exhaust (propane, ethene, etc. + NO) used instead of real exhaust.	Results are similar to runs with real exhaust and consistent with model predictions.
DTC351	5/10/96	Mini-Surrogate + Cold Start LPG Exhaust (B)	Similar procedures as run DTC-340 except cold start exhaust used instead of warm stabilized.	Exhaust addition had significant effect on NO oxidation and ozone formation. Consistent with model predictions.
DTC352	5/14/96	Mini Surrogate + Synthetic LPG Exhaust (A)	Repeat of previous run except synthetic LPG exhaust used instead of real exhaust.	Similar results as previous run. Synthetic LPG has same reactivity characteristics as real LPG exhausts. Results consistent with model predictions.

Table C-1, Continued

RunID	Date	Title	Description / Purpose	Results / Comments [a]
DTC353	5/15/96	Aborted Mini Surrogate + LPG Exhaust	Aborted due to problem with vehicle emissions lab.	
DTC354	5/16/96	Mini Surrogate + LPG Exhaust (A)	Repeat of DTC351 except lower amounts of exhaust added.	Similar results as previous mini-surrogate + LPG exhaust or synthetic exhaust runs. Consistent with model predictions.
DTC355	5/17/96	Bag Transfer Cold Start LPG Exhaust + Formaldehyde (B)	Exhaust injected using a transfer bag rather than the transfer line to determine if transfer method has any effects. Exhaust injected into both sides, formaldehyde injected into side B.	Run with exhaust alone consistent with previous runs and with model predictions. Run with added formaldehyde formed somewhat less O_3 and NO oxidation than model predicted, but consistent with range of results of previous runs.
DTC356	5/20/96	n-Butane + CL2 Actinometry	Same as DTC-341	See comments for DTC341. Rate of n-butane consumption corresponded to an NO_2 photolysis rate of 0.209 min-1.
DTC357	5/21/96	n-Butane - NOx (RH=10%)	4 ppm n-butane and 0.25 ppm NOx injected in both sides. Air humidified to 10% using water bubbler.	Control run to measure chamber radical source under higher humidity conditions characteristic of added LPG runs. NO oxidation rate slightly faster than predicted by standard "dry" chamber model, as expected. Similar result as DTC-347.
	5/22/96 - 6/7/96		Runs for other programs were carried out	
DTC367	6/8/96	NO_2 Actinometry	Quartz tube actinometry method used.	Measured NO_2 photolysis rate was 0.198 min^{-1}.
DTC371	6/17/96	Propene + NOX	Standard 1 ppm propene, 0.5 ppm NOx run.	Control experiment for comparison with similar runs. Experimental results are consistent with previous runs, but measured propene levels are only half what was injected. Probable problem with propene analysis. This is being investigated.

Table C-1, Continued

RunID	Date	Title	Description / Purpose	Results / Comments [a]
DTC372	6/18/96	M100 Exhaust (Cold Start) + NOx	Cold start emissions collected after 100 seconds running, collected for 5 minutes. Injected into both sides, and NOx injected.	No methanol data. Only 30 ppb initial formaldehyde. Only slow NO oxidation and no ozone formation. Because of lack of methanol data, run is not considered to be sufficiently well characterized for modeling.
DTC373	6/21/96	n-Butane + NOx	4 ppm n-butane and 0.25 ppm NOx injected in both sides	NO oxidation rate slightly slower than predicted by standard chamber effects model, but within normal range.
DTC374	6/24/96	M100 Exhaust (Cold Start	Cold start M100 emissions collected into both sides of the chamber during first 5 minutes of running. NO additional NOx injected.	Measured initial formaldehyde, NOx, = 10.06 ppm and 0.1 ppm, respectively. 0.2 ppm O_3 formed at end of 6 hours. Methanol data subsequently judged to be unreliable, so run not sufficiently well characterized for modeling.
DTC375	6/25/96	Mini Surrogate + M100 Exhaust (A)	Mini-surrogate VOCs injected into both sides. Cold start M100 exhaust injected into side A for 3 minutes. NOx injected to equalize NOx on both sides.	NO oxidation and ozone formation rate much faster on side with added exhaust. Model somewhat underpredicted effect of added M100. Good fits to formaldehyde formation.
DTC376	6/26/96	Aborted Mini Surrogate + M100 Exhaust run	Aborted due to problems with vehicle emissions laboratory.	
DTC377	6/27/96	Mini surrogate + M100 Exhaust (B)	Mini-surrogate VOCs injected into both sides. Cold start M100 exhaust injected into side A for 3 minutes, with flow rate into chamber reduced by a factor of 2 compared to run DTC-375. NOx injected to equalize NOx on both sides.	Effect on NO oxidation and ozone formation on exhaust side about half that for run DTC-375, as expected. Model underpredicted effect of added M100 to a somewhat greater extent than for DTC-375.
DTC378	6/28/96	Full surrogate + M100 Exhaust (B)	Similar procedures as run DTC-377 except full surrogate used.	The addition of the M100 exhaust approximately doubled the amount of ozone formed. Results consistent with model predictions.

Table C-1, Continued

RunID	Date	Title	Description / Purpose	Results / Comments [a]
DTC379	7/9/96	Synthetic M100 exhaust (to duplicate DTC-374)	Methanol and formaldehyde, in amounts similar to those believed to be present in run DTC-374 injected into both sides of chamber. Subsequently it was concluded that the initial methanol was too high because of problems with methanol analysis in that run.	About twice as much ozone formed in this run as in run DTC-374, which is consistent with inappropriately high amounts of methanol being injected in this run. Ozone formation was somewhat less than model predicted.
DTC380	7/10/96	Mini Surrogate + Synthetic M100 Exhaust (to duplicate DTC-377)	Mini-surrogate VOCs and NOx injected into both sides. Methanol and formaldehyde injected to levels similar to those in run DTC-377. Initial formaldehyde somewhat lower.	Effect on NO oxidation and ozone formation somewhat less than observed in run DTC-377, which can be attributed to somewhat lower initial formaldehyde levels. Model underpredicted effects of M100 on NO oxidation and ozone formation.
DTC381	7/11/96	Full Surrogate + Synthetic M100 Exhaust (to duplicate DTC-378) (B)	Full surrogate VOCs and NOx injected into both sides. Methanol and formaldehyde injected to levels similar to those in run DTC-378.	Slightly less formaldehyde and methanol than run DTC-378, but results were very consistent. Model gave good fits to observed effects on NO oxidation and ozone formation.
DTC382	7/12/96	Methanol - NOx (A) and Formaldehyde - NOx (B)	Methanol - NOx run on side A and formaldehyde - NOx run on side B.	Run to test model for the single M100 compounds. Formaldeyde monitor malfunctioned, so only added methanol run could be modeled. Model somewhat overpredicted ozone formation in methanol run.
DTC383	7/16/96	CO + NOx	Control run to measure chamber radical source and chamber dilution.	NO oxidation rate somewhat faster than predicted by standard chamber model, but results within normal variability.
DTC384	7/19/96	n-Butane + NOx	Control run to measure chamber radical source and for comparison with other n-butane runs.	No n-butane data available, so initial n-butane had to be estimated. Results consistent with predictions of standard chamber model.

Table C-1, Continued

RunID	Date	Title	Description / Purpose	Results / Comments [a]
DTC387	7/25/96	formaldehyde (A) & acetaldehyde (B) + NOx	Control run for mechanism and analytical evaluation for aldehydes.	Acetaldehyde data are of low quality because of GC problems and that run was not modeled. For formaldehyde run, model slightly underpredicted ozone yield, but gave good fits to OH tracer consumption rates.
	7/26/96 - 8/26/97		Reaction bags replaced. Light banks changed. Runs for other programs were carried out. Method for transferring exahust into the chamber was modified.	
DTC545	8/26/97	n-Butane + NOx	Characterization run to measure the chamber radical source.	The results were in the normal range and consistent with the predictions of the standard chamber model. The NO oxidation rate was slightly higher on side A.
DTC546	8/27/97	Acetaldehyde + air	Test for NOx offgasing from the chamber walls by measuring O3 and PAN formation in the absence of added NOx.	Run turned out not to be useful for NOx offgasing measurement because of slight NO contamination in the pure air system. Results were consistent with model predictions.
DTC555	9/16/97	n-Butane + NOx	Characterization run to measure the chamber radical source	The results were in the normal range and consistent with the predictions of the standard chamber model. Good side equivalency observed.
DTC561	9/26/97	Methanol + Formaldehyde (A)	0.2 ppm NOx and 5 ppm methanol on both sides, with 0.2 ppm formaldehyde on Side A.	Ozone formation on formaldehyde side only. Model simulated NO oxidation rate on methanol only side, but overpredicted O3 on the formaldehyde side by about 50%.

Table C-1, Continued

RunID	Date	Title	Description / Purpose	Results / Comments [a]
DTC562	9/29/97	NO2 Actinometry	Measure light intensity using quartz tube NO2 actinometry method.	NO2 photolysis rate was 0.218 min^{-1}, in excellent agreement with trend from previous runs.
DTC563	9/30/97	M100 Exhaust (A) & Synthetic Exhaust (B)	M100 exhaust in side A, methanol, formaldehyde, NOx mixture in the other. Initial NOx and formaldehyde were not well matched; Side B had more methanol and less NOx.	As expected based on unequal injections, Side B and formed more O3,. Model somewhat overpredicted ozone on Side A and significantly overpredicted it on Side B.
DTC564	10/1/97	M100 Exhaust (A) & Synthetic Exhaust (B)	M100 exhaust in side A, methanol, formaldehyde, NOx mixture in the other. Reactants much better matched.	Very similar O3 formation on both sides. Model somewhat overpredicted O3 equally on both sides.
DTC565	10/2/97	Mini Surrogate + M100 Exhaust (A)	Standard mini-surrogate mixture on both sides, M100 exhaust on Side A. NOx injected to yield equal amounts on both sides, for standard level in mini-surrogate runs.	As expected, greater rate of NO oxidation and O3 formation on added M100 side. Model slightly overpredicted NO oxidation and O3 formation on both sides.
DTC566	10/3/97	n-Butane + NOx	Characterization run to measure the chamber radical source.	NO oxidation rate was somewhat greater on Side A than Side B. Side A results in good agreement with predictions of standard chamber model, but Side B results in normal range.

Table C-1, Continued

RunID	Date	Title	Description / Purpose	Results / Comments [a]
DTC567	10/16/97	CNG Exhaust (A) & Synthetic Exhaust (B)	CNG exhaust injected in Side A and CO and NOx, the only significant components measured in the CNG, injected in Side B. Initial concentrations matched well.	Only slow NO oxidation observed, with rate slightly faster on Side A, but slower than model predictions. Model somewhat overpredicted NO oxidation rates about equally on both sides. Side differences consistent with inequavalency observed in DTC566.
DTC568	10/17/97	Mini Surrogate + CNG Exhaust (A)	Standard mini-surrogate mixture on both sides, CNG exhaust on Side A. NOx injected to yield equal amounts on both sides, for standard level in mini-surrogate runs.	Only slightly faster O3 formation and NO oxidation on added CNG side, which may be due to chamber side inequality and not CNG effect. Model slightly overpredicted reactivity on side B.
DTC569	10/20/97	Mini Surrogate + CNG Exhaust (A)	Standard mini-surrogate mixture on both sides, CNG exhaust on Side A. NOx injected to yield equal amounts on both sides, for standard level in mini-surrogate runs. Larger amounts of exhaust CO present in this run than DTC568.	higher NO oxidation and O3 formation rate on added CNG side compared to base case. Model simulation underpredicted effect of added CNG.
DTC570	10/21/97	Mini Surrogate Side Equivalency Test	Standard mini-surrogate run on both sides, to test for side equavalency.	Very slightly faster O3 formation and NO oxidation on Side A. Results reasonably well simulated by the model.
DTC571	10/24/97	n-Butane - NOx	Characterization run to measure the chamber radical source.	NO oxidation rate was somewhat greater on Side A than Side B. Chamber model adjusted to be consistent with this.

Table C-1, Continued

RunID	Date	Title	Description / Purpose	Results / Comments [a]
DTC572	10/28/97	Mini Surrogate + CNG Exhaust (A)	Standard mini-surrogate mixture on both sides, CNG exhaust on Side A. NOx injected to yield equal amounts on both sides, for standard level in mini-surrogate runs. Lower amounts of exhaust CO present in this run than DTC569.	higher NO oxidation and O3 formation rate on added CNG side compared to base case. Model gave good fit to data on both sides.
DTC573	10/29/97	Low NOx Full Surrogate + CNG Exhaust (A)	Standard full surrogate mixture on both sides, CNG exhaust on Side A. NOx injected to yield equal amounts on both sides, for standard level in low NOx full surrogate runs. Similar amounts of exhaust CO present in this run than DTC572.	Slightly faster O3 formation and slightly higher O3 yield on added CNG side. Model gave good prediction of changes caused by added CNG exhaust. Some high molecular weight compounds observed by GC may be due to syringe contamination.
DTC574	10/30/97	Rep Car Exhaust	Equal amounts of exhaust from the CE-CERT reproducibility study vehicle ("rep car") was added to both sides of the chamber. Major pollutant was CO, small amounts of ethene, propene, toluene, m-xylene and formaldehyde also detected.	Essentially no ozone formation, about 2/3 the NO oxidized. Good side equivalency. Model overpredicted O3 formation rates.
DTC575	10/31/97	CNG Exhaust (A) & CO (B)	CNG exhaust added to Side A, and equal amounts of CO and NOx added to Side B. Some formaldehyde (~20 ppb) observed in CNG side.	Essentially no ozone formation and only slow NO oxidation on side B; faster NO oxidation and some O3 formation on Side B. Model overpredicted NO oxidation rates in both sides, with the overprediction being greatest for the CNG side.

C-11

Table C-1, Continued

RunID	Date	Title	Description / Purpose	Results / Comments [a]
DTC576	11/4/97	Mini Surrogate + Rep Car Exhaust (A)	Standard mini-surrogate mixture on both sides, rep car exhaust on Side A. NOx injected to yield equal amounts on both sides, for standard level in mini-surrogate runs.	Somewhat faster NO oxidation and O3 formation observed on added exhaust side. Model gives reasonably good fits to data.
DTC577	11/5/97	Full Surrogate + Rep Car Exhaust (A)	Standard full surrogate mixture on both sides, rep car exhaust on Side A. NOx injected to yield equal amounts on both sides, for standard level in full surrogate runs. Exhaust levels similar to DTC576.	Faster NO oxidation and O3 formation observed on added exhaust side. Model slightly underpredicts O3 on both sides, but otherwise is reasonably consistent with results.
DTC578	11/6/97	Propene + NOx	Standard control run for comparison with previous propene - NOx runs and side equivalency test run.	Results comparable with other propene runs in this chamber and good side equivalency observed. Model somewhat overpredicted O3 formation rate.
DTC579	11/7/97	Methanol + Formaldehyde (B)	Methanol and NOx injected in both sides, formaldehyde in Side B.	Only slow NO oxidation on Side A, much faster NO oxidation and some O3 formation on added formaldehyde side. Model consistent with Side A data, but somewhat overpredicted NO oxidation and O3 formation on added formaldehyde side.
DTC580	11/11/97	NO2 Actinometry	Measure light intensity using quartz tube NO2 actinometry method.	NO2 photolysis rate was 0.204 min^{-1}, suggesting a slight downward trend in light intensity due to ageing of the lights.

Table C-1, Continued

RunID	Date	Title	Description / Purpose	Results / Comments [a]
DTC581	11/12/97	Mini Surrogate + Rep Car Exhaust (A)	Standard mini-surrogate mixture on both sides, rep car exhaust on Side A. NOx injected to yield equal amounts on both sides, for standard level in mini-surrogate runs. Similar exhaust pollutant levels as DTC576.	Faster NO oxidation and O3 formation observed on added exhaust side. Model slightly underpredicted effect of added exhaust.
DTC582	11/13/97	97 Taurus Exhaust	Exhaust from RFG-fueled 97 Taurus injected in both sides of the chamber. No significant pollutants detected other than CO and NOx.	Only slow NO oxidation observed; no O3 formation. Model overpredicted NO oxidation rate in middle of run, suggesting problems with the chamber model.
DTC583	11/14/97	Mini Surrogate + Taurus Exhaust (A)	Standard mini-surrogate mixture on both sides, Taurus exhaust on Side A. NOx injected to yield equal amounts on both sides, for standard level in mini-surrogate runs.	Slightly faster O3 formation observed in Side A, but some of difference may be due to side inequivalency. Model prediction consistent with experimental results.
DTC584	11/18/97	Suburban Exhaust	Exhaust from UCR-owned RFG-fueled Suburban injected into both sides of chamber. CO and various VOCs detected, with relatively high levels of NOx (0.6 ppm).	Approximately 1/2 the initial NO oxidized; no O3 formation. Model slightly overpredicted NO oxidation rate during last period of run..
DTC585	11/19/97	Mini Surrogate + Suburban Exhaust (A)	Standard mini-surrogate mixture on both sides, Suburban exhaust on Side A. NOx injected to yield equal amounts on both sides. Because of high NOx in exhaust, NOx was ~50% higher than in standard mini-surrogate run.	No ozone formation on base case side, but significant O3 on exhaust side. Model slightly overpredicted NO oxidation and/or O3 formation on both sides, bug gave reasonably good simulation of effect of added exhaust.

Table C-1, Continued

RunID	Date	Title	Description / Purpose	Results / Comments [a]
DTC586	11/20/97	Full Surrogate + Suburban Exhaust (A)	Standard full surrogate mixture on both sides, Suburban exhaust on Side A. NOx injected to yield equal amounts on both sides, for standard level in full surrogate runs. Exhaust levels similar to DTC576.	Added exhaust caused faster NO oxidation and higher O3 yields. Model somewhat overpredicted initial NO oxidation rates but gave reasonably good fits to ozone formation, and correctly simulated relative effects of exhaust addition.
DTC587	11/21/97	n-Butane + NOx	Characterization run to measure the chamber radical source.	NO oxidation rate was somewhat greater on Side A than Side B. Side A results in good agreement with predictions of standard chamber model. Side B results lower than normal range. Difference greater than observed in previous n-butane run.
DTC588	11/24/97	M100 Exhaust (A) & Synthetic M100 Exhaust (B)	M100 exhaust injected in Side A, and equal amounts of CO, methanol, formaldehyde, and NOx injected into Side B.	Results on both sides almost equivalent, despite slightly higher initial formaldehyde in Side B. Some O3 formation occurred. Model overpredicted NO oxidation and O3 formation rates on both sides, approximately equally.
DTC589	11/25/97	Mini Surrogate + M100 Exhaust (A)	Standard mini-surrogate mixture on both sides, M100 exhaust on Side A. NOx injected to yield equal amounts on both sides. Because of higher NOx in exhaust, NOx was somewhat higher than in standard mini-surrogate run.	Significantly faster NO oxidation and more O3 formed on added M100 side. Model gave reasonably good simulation of data.
DTC590	11/26/97	Mini Surrogate Side Equivalency Test	Standard mini-surrogate run on both sides, to test for side equavalency.	Slightly faster ozone formation and NO oxidation on Side A, but difference not great. Results reasonably consistent with model.

Table C-1, Continued

RunID	Date	Title	Description / Purpose	Results / Comments [a]
DTC591	12/2/97	Full Surrogate + M85 Exhaust (A)	Standard full surrogate mixture on both sides, M85 exhaust on Side A. NOx injected to yield equal amounts on both sides. NOx was only slightly higher than that in standard full surrogate runs.	Somewhat faster NO oxidation and more O3 formation on added M100 side. Model somewhat overpredicts initial NO oxidation rates on both sides, but gives good simulation of O3 and the relative effect of added M100.
DTC592	12/3/97	M85 Exhaust	M85 exhaust injected in both sides of the chamber.	No O3 formation. Similar results on both sides. Model slightly overpredicted the NO oxidation rates.
DTC593	12/4/97	Mini Surrogate + M85 Exhaust (A)	Standard mini-surrogate mixture on both sides, M85 exhaust on Side A. NOx injected to yield equal amounts on both sides. Because of higher NOx in exhaust, NOx was somewhat higher than in standard mini-surrogate run.	Somewhat faster NO oxidation and ozone formation on added M85 side. Model gave reasonably good simulations to both sides.
DTC594	12/5/97	Full Surrogate + M85 Exhaust (A)	Standard full surrogate mixture on both sides, M85 exhaust on Side A. NOx injected to yield equal amounts on both sides. NOx was only slightly higher than that in standard full surrogate runs.	Somewhat faster NO oxidation and O3 formation on added M85 side. Model slightly overpredicted NO oxidation rates on both sides, but gave good fits to ozone and to effects of added exhaust.
DTC595	12/9/97	Aborted M85 run	Run aborted due to injection problems.	GC data available from transfer bag.
DTC596	12/10/97	Mini Surrogate + M85 Exhaust	Standard mini-surrogate mixture on both sides, M85 exhaust on Side A. NOx injected to yield equal amounts on both sides. NOx was similar to levels in standard mini-surrogate run.	M85 caused faster NO oxidation and O3 formation. Model somewhat underpredicts O3 on both sides, but gives good simulation of effect of exhaust addition.

Table C-1, Continued

RunID	Date	Title	Description / Purpose	Results / Comments [a]
DTC597	12/11/97	Propene - NOx	Standard control run for comparison with previous propene - NOx runs and side equivalency test run.	Results comparable with other propene runs. Model gives good simulation of data. Slightly faster O3 formation rate on Side A. Formaldehyde data at end of run appear to be anomalously high.
	1/12/98 - 2/10/98	Experiments for another program.	Experiments were carried out for another program involving injecting isocyanates into the chamber.	Isocyanate exposure was shown to cause higher chamber radical source in Side A. The chamber model was modified to account for the side differences, which primarily affected low ROG/NOx experiments.
DTC612	2/11/98	Formaldehyde + NOx	Experiments for evaluating formaldehyde mechanism and chamber model for current conditions of chamber. Equal amounts of formaldehyde and NOx injected on both sides.	Approximately 77 ppb O3 formed on Side A and 67 on Side B. Model predicted over 200 ppb O3. This overprediction is consistent with results of previous formaldehyde - NOx runs.
DTC614	2/13/98	O3 and CO dark decay	Ozone and CO were monitored in the chamber with the lights out to measure both dilution and ozone dark decay.	The CO data indicated no significant dilution. The O3 decay rates were 1.1 and 0.8%/hour on Sides A and B, respectively, somewhat higher than average for this chamber.
DTC615	2/18/98	Full Surrogate + Diesel Exhaust	Standard full surrogate VOCs injected into both sides of the chamber, exhaust from a 1984 Mercedes Diesel sedan injected into side B, and NOx was injected into Side A to yield the same level on both sides.	Because of high NOx only low levels of O3 formed. NO oxidation and ozone formation was higher on the added diesel side. The model predicted much less of an effect of the Diesel exhaust than observed experimentally.

Table C-1, Continued

RunID	Date	Title	Description / Purpose	Results / Comments [a]
DTC616	2/19/98	Full Surrogate + NOx	Full surrogate VOCs and NOx injected into both sides of the chamber at levels equal to the base case side in run DTC615.	Because of high NOx only low levels of O3 formed. Slightly more ozone formed on Side A due to chamber effects attributed to isocyanate exposure. Results in excellent agreement with model predictions with appropriate chamber model.
DTC617	2/20/98	NO2 actinometry	The NO2 photolysis rate was measured using the quartz tube method.	The results were consistent with DTC613 and confirmed a decrease in the light intensity in the chamber. The chamber effects model was updated to take this into account.
DTC619 - DTC621	2/26/98 - 3/2/98	NO2 Actinometry	Characterize outputs of other light banks.	The results were consistent with previous actinometry results and indicated a decrease in total light intensity in the chamber.
			New Reaction bags were installed. The total light intensity was increased by using 75% maximum rather than 50% maximum as used previously. Light intensity uncertain (see text). This configuration used until run DTC648.	
DTC622 - DTC623	3/6/98 - 3/13/98	NO2 Actinometry	Measure light intensity using various lighting configurations and combinations using quartz tube method.	It was determined that the best way to approximate the light intensity range of the previous exhaust runs is to use 3/4 maximum lights. This gives an NO_2 photolysis rate of about 0.22 min^{-1}.
DTC624	3/23/98	Pure Air Irradiation	Characterize background effects in new reaction bags.	Around 26 ppb O3 formed after 6 hours, which is about half the level generally observed after reaction bags have been extensively used.

Table C-1, Continued

RunID	Date	Title	Description / Purpose	Results / Comments [a]
DTC625	3/25/98	Propene + NOx	Standard control run for comparison with previous propene - NOx runs and side equivalency test run.	Good side equivalency. Results reasonably consistent with model predictions.
DTC626	3/26/98	NO2 Actinometry	Measure light intensity with new lighting configuration.	The NO2 photolysis rate was ~0.2 min^{-1}, which is lower than expected. Subsequent analysis of data led to conclusion that this value is probably low. See text.
DTC627	3/27/98	Mini Surrogate + NOx	Standard mini-surrogate run to test for side equivalency and for comparison with previous runs.	Good side equivalency observed. Somewht more ozone formed than model predicted.
DTC628	3/30/98	n-Butane + NOx	Characterization run to measure the chamber radical source.	NO oxidation rate somewhat higher on Side B than Side A. Standard chamber model prediction between Side A and Side B results.
DTC629	4/1/98	Aborted run	Run aborted due to leak in chamber.	
DTC630	4/2/98	Formaldehyde - NOx (A) and Acetaldehyde - NOx (B)	Approximately 0.5 ppm formaldehyde (Side A) and ~1 ppm acetaldehyde (Side B) irriadiated in the presence of ~0.25 ppm NOx. Control run for testing chamber and light model for these aldehydes.	Comparable amount of ozone formation (~0.15 ppm) on both sides. Ozone formation somewhat greater than model prediction on both sides.
DTC631	4/3/98	Mini Surrogate + Formaldehyde (A)	Approximately 0.25 ppm formaldehyde added to a standard mini-surrogate - NOx mixture. Run for comparison with M100 reactivity experiments.	Results reasonably consistent with model predictions.

Table C-1, Continued

RunID	Date	Title	Description / Purpose	Results / Comments [a]
DTC632	4/10/98	CNG Surrogate (A) + CO - NOx (B)	CO, formaldehyde and NOx injected into Side A to duplicate CNG run DTC575A, CO and NOx injected into Side B to duplicate CO - NOx run DTC575B.	100 ppb O3 formed on CNG Surrogate side, 50 ppb on Side B. Results of CNG surrogate run in very good agreement with model predictions, model slightly overpredicted NO oxidation rate on CO - NOx side, but results in expected range.
DTC633	4/14/98	Mini Surrogate + CNG Surrogate (B)	CNG surrogate (CO + formaldehyde) added to a standard mini-surrogate run, for approximate duplicate of previous mini-surrogate + CNG runs.	Added CNG surrogate increased O3 formation on Side B. Model slightly underpredicted maximum O3 on both sides, and slightly underpredicted relative effect of added surrogate.
DTC634	4/15/98	Mini Surrogate + M100 Surrogate (A)	M100 surrogate (methanol + formaldehyde) added to a mini-surrogate - NOx mixture to approximately duplicate conditions of DTC565 and DTC589.	Surrogate M100 caused a significant increase in O3 formation and NO oxidation rates. Model slightly underprediced O3 on both sides, but was reasonably consistent with the effect of the added M100 surrogate.
DTC635	4/16/98	n-Butane + NOx	Characterization run to measure the chamber radical source.	NO oxidation rates about the same on both sides. Model slightly overpredicted NO oxidation rates, but results in normal range.
DTC636	4/17/98	Mini Surrogate + M85 Surrogate (B)	M85 surrogate (methanol + formaldehyde) added to a mini-surrogate - NOx mixture to approximately duplicate conditions of DTC593.	Added M85 surrogate increased O3 formation on Side B. Model slightly underpredicted maximum O3 on both sides, and very slightly underpredicted relative effect of added surrogate.

Table C-1, Continued

RunID	Date	Title	Description / Purpose	Results / Comments [a]
DTC637	4/21/98	Full Surrogate + methanol + formaldehyde	M85 surrogate (methanol + formaldehyde) added to a full surrogate - NOx mixture to approximately duplicate conditions of DTC591.	Surrogate M85 caused an increase in O3 formation and NO oxidation rates. The model slightly underpredicted O3 on both sides, but it was consistent with the effect of the added M85 surrogate.
DTC639	4/23/98	Rep Car RFG Surrogate - Varied NOx	A mixture of NOx, CO and 8 hydrocarbons representing the exhaust components measured in run DTC574 was injected into Side A. Side B had the same CO and organics, but half the NOx.	Run DTC574A seemed to have reactant concentrations comparable to run DTC574, but had much higher NO oxidation rates and some O3 formation. More O3 formation occurred on Side B. Model signficantly underpredicted NO oxidation and O3 formation rates on both sides.
DTC640	4/24/98	Suburban RFG Surrogate - Varied NOx	A mixture of NOx, CO and 8 hydrocarbons representing the exhaust components measured in run DTC584 was injected into Side B. Side A had the same CO and organics, but lower NOx.	No ozone formation on side B, significant ozone formation on lower NOx side. Results on both sides in good agreement with model predictions.
DTC641	4/27/98	Mini Surrogate + RFG Surrogate (A)	A mixture of CO and hydrocarbons to replicate the exhaust components measured in RFG exhaust was added to a mini-surrogate - NOx mixture to replicate run DTC585.	More O3 formed on both sides than in run DTC585, but relative effect of RFG addition approximately the same. Model slightly underpredicted maximum O3 on both sides, and slightly underpredicted effect of added surrogate.
DTC642	4/28/98	Mini Surrogate + RFG Surrogate (B)	A mixture of CO and hydrocarbons to replicate the exhaust components measured in RFG exhaust was added to a mini-surrogate - NOx mixture to replicate run DTC576.	More O3 formed on both sides than in run DTC576, and relative effect of RFG addition was somewhat larger. Model underpredicted O3 on both sides, but gave reasonably good prediction of effect of added surrogate.

C-20

Table C-1, Continued

RunID	Date	Title	Description / Purpose	Results / Comments [a]
DTC643	4/29/98	Full Surrogate + RFG Surrogate (A)	A mixture of CO and hydrocarbons to replicate the exhaust components measured in RFG exhaust was added to a mini-surrogate - NOx mixture to replicate run DTC577.	More O3 formed on both sides than in run DTC577, and relative effect of RFG addition was somewhat larger. Model underpredicted O3 on both sides, and somewhat underpredicted effect of added surrogate.
DTC644	4/30/98	n-Butane + NOx	Characterization run to measure the chamber radical source.	Slightly faster NO oxidation rate on Side B than Side A, but difference small and results in normal range and consistent with model predictions.
DTC645	5/5/98	Mini Surrogate + NOx	Determine side equivalency using mini-surrogate mixture.	Good side equivalency. Model somewhat underpredicted ozone formation.
DTC646	5/6/98	NO2 Actinometry		The NO2 photolysis rate was ~0.2 min^{-1}, which is lower than expected. Subsequent analysis of data led to conclusion that this value is probably low. See text.
			Lights cleaned. Actinometry tube repositioned. Subsequent runs carried out using 50% lights unless indicated otherwise. Light intensity less uncertain.	
DTC648	5/11/98	NO2 Actinometry (50% and 100% Lights)	Measure light intensity with 100% lights on and at standard 50% lights.	The NO2 photolysis rate was 0.174 min-1 at 50% lights and 0.345 min-1 at 100%. These are higher than expected based on the previous determinations, but consistent with results of subsequent actinometry runs. See text.
DTC649	5/12/98	Mini Surrogate + NOx	Standard mini-surrogate run and side equivalency test with new lighting configuration.	Good side equivalency. Results in good agreement with model predictions.
DTC651	5/15/98	NO2 Actinometry (100% Lights)	Measure light intensity with 100% lights on.	NO2 photolysis rate is 0.341 min-1, in good agreement with previous actinometry run.

Table C-1, Continued

RunID	Date	Title	Description / Purpose	Results / Comments [a]
DTC652	5/18/98	NO2 Actinometry (steady state method)	Evaluate standard actinometry results by measuring NO2 photolysis rate using steady state method.	Initial NO2 photolysis rate measurements gave 0.16 - 0.17 min-1, in good agreement with quartz tube results.
DTC653	5/19/98	Mini Surrogate + formaldehyde (100% LIghts)	Determine effect of light intensity on mini-surrogate and formaldehyde reactivity results. Evaluate ability of model to predict effects of varying light intensity.	Faster NO oxidation and more O3 formation on base case side than mini-surrogate run with standard light intensity. Formaldehyde caused increased O3 formation and increased m-xylene . Model gave good simulation of base case run but somewhat underpredicted effect of added formaldehyde.
DTC654	5/20/98	CO - NOx (A) and CNG Surrogate (B)	CO, formaldehyde and NOx injected into side B to duplicate CNG run DTC575A. CO and NOx injected into Side A.	Approximately 17 ppb O3 formed on CO side and ~46 ppb on CNG surrogate side. CNG surrogate run reasonablly good duplicate of CNG run DTC575A. Results reasonably consistent with model predictions.
DTC655	5/21/98	Mini Surrogate + CNG Surrogate (A)	CO and formaldehyde added to a mini-surrogate mixture to duplicate conditions of added CNG exhaust experiment DTC572.	Effect of CNG surrogate addition similar to results of CNG exhaust run. Results reasonably consistent with model predictions, though effect of added surrogate somewhat underpredicted.
DTC656	5/22/98	Full Surrogate + M85 Surrogate (B)	Methanol and formaldehyde added to a full surrogate mixture to duplicate conditions of added M85 exhaust experiment DTC591	Effect of surrogate addition similar to results of corresponding exhaust run. Model underpredicted effect of added surrogate.
DTC657	5/26/98	NO2 Actinomerty	Measure light intensity	NO2 photolysis rate is 0.173 min-1, reasonably consistent with results of other actinometry runs during this period.

Table C-1, Continued

RunID	Date	Title	Description / Purpose	Results / Comments [a]
DTC658	5/27/98	Mini Surrogate + M100 Surrogate (A)	Methanol and formaldehyde added to a mini-surrogate mixture to duplicate conditions of added M100 exhaust experiment DTC589.	Relative effect of M100 surrogate addition similar to exhaust run, except that O3 formation and NO oxidation faster on both sides. Model somewhat underpredicted reactivities on both sides, but gave good prediction of effect of surrogate addition.
DTC659	5/28/98	N-Butane - NOx	Characterization run to measure the chamber radical source.	Approximately the same NO oxidation rate on both sides. Model somewhat overpredicted NO oxidation rate, but result in normal range.
DTC660	5/29/98	Suburban RFG Surrogate - Varied NOx	Mixture of VOCs and NOx added to Side B to duplicate conditions of Suburban exhaust run DTC584. Side A had same VOCs but lower NOx.	Results in side B reasonably similar to run DTC584. More O3 formed on Side A due to lower NOx levels. Side B results in good agreement with model predictions, but model somewhat underpredicted O3 on Side A.
DTC661	6/2/98	1983 Toyota Truck Exhaust	Exhaust from a high-mileage 1983 Toyota mini-truck owned by a CE-CERT staff member introduced into both sides of the chamber.	Exhaust had relatively high VOC levels; ~400 ppb O3 formed. Model somewhat underpredicted initial NO oxidation rate and final O3 yield.
DTC662	6/3/98	Mini Surrogate + Toyota Truck Exhaust (A)	Exhaust from Toyota truck added to standard mini-surrogate mixture, with NOx equalized on both sides.	Exhaust addition caused large increase in O3. Model underpredicted effect of added exhaust by a factor of 1.5 - 2.
DTC663	6/4/98	Full Surrogate + Toyota Truck Exhaust (B)	Exhaust from Toyota truck added to standard full surrogate mixture, with NOx equalized on both sides.	Exhaust addition caused moderate to large increase in O3. Model underpredicted O3 on both sides, but was reasonably consistent with effect of exhaust addition.

Table C-1, Continued

RunID	Date	Title	Description / Purpose	Results / Comments [a]
DTC664	6/5/98	Mini Surrogate + Suburban Surrogate (B)	Mixture of VOCs to duplicate exhaust in DTC585 added to Side B.	Effect of exaust surrogate addition similar to results of added exhaust run, except that faster NO oxidation and more O3 formation occurred on both sides. Model underpredicted effect of added surrogate by a factor of 1.5 - 2.
DTC665	6/9/98	1988 Honda Accord exhasut	Exhaust from a relatively high-mileage 1988 Honda Accord sedan owned by a CE-CERT staff member introduced into both sides of the chamber.	VOCs relatively low and no O3 formation occurred. NO oxidation rate in agreement with model predictions. Good side equivalency.
DTC666	6/10/98	Mini Surrogate + Honda Accord Exhaust (A)	Exhaust from the Honda Accord added to a standard mini-surrogate mixture. NOx equalized on both sides.	Added exhaust caused moderate increase in NO oxidation and O3 formation rates. Model somewhat underpredicted effect of added exhaust.
DTC667	6/11/98	Full Surrogate + Honda Accord Exhaust (B)	Exhaust from the Honda Accord added to a standard full surrogate mixture. NOx equalized on both sides.	Added exhaust caused moderate increase in O3 formation. Model somewhat underpredicted O3 on both sides, but was reasonably consistent with effect of added exhaust.
DTC668	6/12/98	Mini Surrogate + NOx	Side equivalency test with standard mini-surrogate run.	Good side equivalency observed. Model somewhat underpredicted O3 formation.
DTC669	6/16/98	Full Surrogate + Rep Car RFG Surrogate (A)	Mixture of VOCs to duplicate those observed in the added Rep Car exhaust run DTC577 was added to a standard full surrogate - NOx mixture.	More O3 formation on both sides than in exhaust run, and exhaust surrogate had a somewhat smaller effect on O3 formation. Model underpredicted O3 on both sides but was reasonably consistent with effect of added surrogate.

C-24

Table C-1, Continued

RunID	Date	Title	Description / Purpose	Results / Comments [a]
DTC670	6/17/98	Mini Surrogate + M85 Surrogate (B)	Methanol and formaldehyde added to a standard mini-surrogate run to duplicate added M85 exhaust run DTC593.	Effect of added surrogate similar to effect of added exahust in run DTC593, though more O3 formation occurred on both sides. Results consistent with model predictions.
DTC671	6/18/98	Rep Car RFG Surrogate + Varied NOx	Mixture of VOCs and NOx added to side A to duplicate Rep Car exhaust run DTC574. Less NO added to Side B.	Side A results good match to DTC574, with only small amounts of O3 formed. 60 ppb O3 formed on Side B. Model somewhat overpredicted NO oxidation and O3 formation rates, by the same amouns on both sides.
DTC672	6/19/98	Mini Surrogate + Rep Car RFG Surrogate (B)	Mixture of VOCs added to standard mini-surrogate mixture to reproduce Rep Car exhaust run DTC576.	Results gave reasonably good duplicate of corresponding exhaust run. Model somewhat overpredicted effect of added surrogate.
DTC673	6/22/98	NO2 Actinomerty	Measure light intensity	NO2 photolysis rate is 0.156 min-1, reasonably consistent with results of other actinometry runs during this period.
DTC674	6/23/98	Propene - NOx	Standard propene run with comparison with other such runs in this chamber.	Leak in sample line affected validity of NOx, O3 and CO data. Run not modelable. Good side equivalency observed.
DTC677	6/26/98	Toyota Exhaust Surrogate + NOx	VOC and NOx mixture added to chamber in attempt to duplicate Toyota truck exhaust run DTC661. Additional NO injected because it was believed that the NO level was lower than desired. Subsequently concluded that NOx data were invalid.	Leak in sample line affected validity of NOx, O3 and CO data. Run not modelable. Run also not duplicate of exhaust run because of the additional NO which was added. Therefore, data not useable.

Table C-1, Continued

RunID	Date	Title	Description / Purpose	Results / Comments [a]
DTC678	6/30/98	Mini Surrogate + Toyota Exhaust Surrogate (A)	VOC mixture added to mini-surrogate mixture in attempt to duplicate Toyota truck exhaust run DTC662. Additional NO injected because of mistaken belief that NO levels were lower than desired.	Leak in sample line affected validity of NOx, O3 and CO data. Run not useable. See comments above.
DTC679	7/1/98	Full Surrogate + Toyota Exhaust Surrogate (B)	VOC mixture added to full surrogate mixture in attempt to duplicate Toyota truck exhaust run DTC663. Additional NO injected because of mistaken belief that NO levels were lower than desired.	Leak in sample line affected validity of NOx, O3 and CO data. Run not useable. See comments above.
DTC680	7/2/98	n-Butane + NOx	Characterization run to measure chamber radical source. Additional NO injected in the mistaken belief that the NO in the chamber was lower than desired.	Leak in sample line affected validity of NOx, O3 and CO data. Run not modelable.
DTC681	7/7/98	Mini Surrogate + Honda Exhaust Surrogate (A)	Sample line fixed. VOC mixture added to standard mini-surrogate mixture to duplicate honda exhaust run DTC666. NOx injected to be equal on both sides.	Run did not closely duplicate DTC666 because of lower NOx levels, but amount of d(O3-NO) formed on both sides and effect of exhaust surrogate was similar. Results reasonably consistent with model predictions.
DTC682	7/8/98	Ozone and CO dark decay	Measure ozone dark decay and dilution for characterization purposes.	The O3 decay rate in Sides A and B were 0.8 and 1.0 %/hour, respectively, in good agreement with the 0.9%/hour assumed in the standard chamber model. Dilution was less than 0.1%/hour.
DTC683	7/9/98	Propene - NOx	Standard propene - NOx run for control purposes and comparisoin with comparable runs in this chamber, and side equivalency test.	Results comparable to other propene - NOx runs in this chamber and consistent with model predictions. Good side equivalency.
DTC684	7/13/98	NO2 Actinomerty	Measure light intensity	NO2 photolysis rate is 0.160 min-1, consistent with results of other actinometry runs.

Table C-1, Continued

RunID	Date	Title	Description / Purpose	Results / Comments [a]
DTC704	8/31/98	NO2 Actinomerty	Measure light intensity	NO2 photolysis rate is 0.165 min-1, consistent with results of other actinometry runs.